THE STRUCTURAL AND METAMORPHIC GEOLOGY OF THE VAL PIORA REGION, TICINO, SWITZERLAND

by

THOMAS IAN INGLIS SIBBALD

A thesis submitted for the
Diploma of Imperial College

Imperial College
April, 1971

ABSTRACT

The Val Piora area lies in central southern Switzerland at the junction of the Lower Pennine and Helvetic zones of the Swiss Alps. It is comprised by pre-Mesozoic crystalline rocks of the southern Gotthard Massif and western Lucomagno or Lukmanier Massif, together with Mesozoic metasediments of the authochthonous cover of the Gotthard Massif and of the allochthonous Pennine series. These two distinct metasediment series are separated by the Frontal Pennine Thrust.

Four episodes of Alpine deformation are recognised in the Mesozoic rocks. During the first deformation the allochthonous Pennine series was thrust over the residual authochthonous cover of the Gotthard Massif. These movements led to folding, thrusting, and the development of a penetrative foliation in both metasediment series. Structures of this age are absent in the basement, where the first structures are pre-Alpine (Hercynian). Both basement and cover were complexly folded and thrust during the second deformation. North-south trending linear mineral (stretching) fabrics show that the rocks suffered a uniaxial constrictional strain ($k = \infty$) during the third deformation. Rotated porphyroblasts with S. trails of inclusions demonstrate the rotational nature of this strain. The fourth deformation resulted in folding and boudinage of the earlier formed planar and linear structures. The relationship between the third and fourth episode strain axes suggests that the third and fourth deformations were intimately related if not continuous.

The relationship between deformation and metamorphic mineral growth indicates lower almandine-amphibolite facies metamorphism between the end of the third and the fourth deformations. The Alpine metamorphism was progressive, increasing in grade from lower greenschist conditions after the first Alpine deformation. Pre-Alpine relict minerals in the basement suggest a Hercynian greenschist facies metamorphism.

The significance of certain metamorphic microstructures, snowball garnets, hornblende garbenschiefer and garnet crystal size distributions apparent in the rocks of the Val Piora area has been investigated in detail.

TABLE OF CONTENTS

LIST OF SYMBOLS (not defined in text)

N - North
S - South
E - East
W - West
L - Lower
M - Middle
U - Upper
2D - Two dimensional
3D - Three dimensional
R.I. - Refractive index

m. - Metre(s)
cm. - Centimetre(s)
mm. - Millimetre(s)
c.c. - Cubic centimetre(s)
^{o}C - Degrees centigrade
$\mathring{A}$ - Ångström units
m.y. - Million years
(x 15) - Magnification of photomicrograph

M.R. 6969015580 - Map reference (Landeskarte der Schweiz)

X, Y, Z - Principal (3D) strain axes. $X > Y > Z$ (or where applicable, light vibration directions in a biaxial mineral).

X', Z' - Principal (2D) directions of strain within a plane. $X' > Z'$

$2V_x$ - Angle between the circular sections of the strain ellipsoid, measured across the Z axis.

$k = \infty > 1 > 0$ - Flinn's (1962) k values (cf. Fig. 3.12)

$$k = \frac{Z(X - Y)}{Y(Y - Z)}$$

a, b, c - Crystallographic axes

$D_{p.A.}$ - The pre-Alpine episode(s) of deformation.
D_1 - The first episode of Alpine deformation.
D_2 - The second episode of Alpine deformation.
D_3 - The third episode of Alpine deformation.
D_4 - The fourth episode of Alpine deformation.

CHAPTER I

INTRODUCTION

1.1) The geographical setting

The Val Piora area, some 50 square kilometres in extent, lies to the east of the St. Gotthard Pass in the Canton of Ticino, S. Switzerland. The area is bounded by Val Leventina in the south, Airolo and Val Canaria in the west, Val Cadlimo in the north and Val Termine, Passo del Uomo, Passo Sole and Pizzo Pecian in the east.

Val Leventina, the deepest of the valleys, is an important line of communication and contains road and rail links between the industrial centres of Switzerland and N. Italy. The small town of Airolo at the head of the valley owes its importance to its position at the foot of the Gotthard Pass and the entrance to the Gotthard rail tunnel, which re-emerges further north at Göschenen in Reusstal. Some 6 kilometres east of Airolo, down Val Leventina, the lowest point within the area is marked by the small village of Piotta (1005 m.). Access to Val Piora by road, (via Altanca), or by funicular is most easily gained from Piotta. As a whole the area is well served by minor roads, tracks and footpaths.

The Val Piora area lies on the watershed between the Rhine and Po river systems. The Ticino in Val Leventina flows first east and then south via Lago Maggiore to the Po valley. The rivers in Val Canaria and Val Piora are tributaries of the Ticino. By contrast the Rhein de Medel in Val Cadlimo flows first east and then northwards down Val Medel to join the Vorderrhein at Disentis. The evolution of the drainage pattern in the Val Piora area has been discussed by Garwood (1906) and Krige (1918, pp. 539-541). Both authors conclude that Val Piora itself originally belonged to the Rhine river system and drained eastwards and north through Val Termine. This situation was reversed by the capture of the headwaters of the early Val Piora drainage by the Foss, the present overflow from Lago Ritom.

The east-west trending Val Piora, with Lago Ritom (1850 m.) at its foot, dominates the area. The valley, cut along the junction

of the Mesozoic metasediments and the pre-Mesozoic basement, as Val Leventina, is surrounded by mountains. To the north the line of peaks, Pizzo Tom, (2361 m.), Punta Negra (2688 m.), Pizzo Taneda (2667 m.), Pizzo Corandoni (2659 m.) and Shenadui (2678 m.), formed by gneisses of the Gotthard Massif, separate Val Piora from Val Cadlimo. To the south the ridge Pizzo del Sole, (2773 m.), (Molare of older maps), Pizzo Pecian (2764 m.), and Poncione Pro do Roduc (2507 m.), formed by gneisses of the Lukmanier Massif, lies between the Piora and Leventina valleys. Val Piora is bounded in the west by the Mesozoic metasediment peaks of Camoghe (2357 m.) and Föisc (2208 m.), (Fongio of older maps), and in the east by the spectacularly jagged Pizzo Colombe (2545 m.) formed by vertical beds of white Triassic marble.

Val Piora is notable for its abundant lakes many of which have been described and bathymetrically charted by Garwood (1906). In considering the origin of the lakes, Garwood (1906), and later Krige (1918, pp. 534-539), find no single explanation for their formation, but emphasise the importance of solution of the underlying rocks as an agent in the development of those which overlie Triassic marbles and gypsum, (e.g. Lago Ritom, Lago Tom and Lago Cadagno). Garwood suggested the role of ice erosion to be of minor importance in the formation of these natural rock basins.

The action of ice has been suggested to be the primary cause of the overdeepening of the Val Leventina with respect to its lateral hanging valleys (e.g. Val Piora), (Davis, 1900). Garwood (1902, 1932) has objected to this proposition on the basis that the present geomorphological features of the valley to the north of Biasca are inconsistent with such an origin (e.g. overlapping spurs, river gorges). The presence of benches at different levels on the valley sides, Garwood suggests, points to a complex evolution which involved several alternating stages of deepening by water action and widening by glacial action, corresponding with different glacial recessions and advances.

The natural drainage pattern has been somewhat modified in recent years to make the best use of water and relief in the production of

electricity. Lago Ritom has been dammed at Piora and its level raised by some 10 metres. Capture of the headwaters of the Rhein de Medel in Val Cadlimo and of the Garegna in Val Canaria has been effected by tunnels, so that these streams add to the volume of water flowing into Lago Ritom. A more recent project will make use of the energy gained by the Ticino itself in its fall between Airolo and Piotta.

1.2) The geological setting

The Western Alps form an arcuate mountain chain which is convex towards the European Foreland in the northwest. The chain may be subdivided into two main longitudinal structural zones, an outer and an inner zone separated by a major thrust plane, the Frontal Pennine Thrust. These zones are known respectively as the Dauphinois and Pennine zones in the French Alps and the Helvetic and Pennine zones in the Swiss Alps. The zones may be further subdivided into the separate thrust slices or nappes which comprise them.

The tectonic subdivisions of the Swiss Alps (Fig. 1.1) are described briefly below. For more detailed general descriptions the works of Collet (1935), Bailey (1935), Cadisch (1953), Trümpy (1960), and the classic of Heim (1920) are recommended.

1) The Foreland

a) The Jura - The Folded Jura or southern Jura forms a crescent shaped range well in front of the Alps. The Mesozoic and Tertiary cover is flexure folded and locally thrust over the underlying Permo-Carboniferous and crystalline Hercynian basement. To the northwest, the locally faulted flat lying cover rocks which extend over the Central Plateau of France are known as the Tabular Jura.

b) The Swiss Plain or Molasse Trough - This low lying area to the south of the Jura is formed by Middle Oligocene - Upper Miocene clastic sediments, (Molasse), derived from the rising Alpine mountain chain in the south. The sediments are generally undeformed, except near the Alpine front, where they are overridden by the Helvetic nappes, and near the folded Jura where they are thrust and folded.

2) The Helvetic Zone

a) The Helvetic and Ultrahelvetic Nappes - These nappes are formed by sediments of Permian to Tertiary age, which slid under the influence of gravity or were pushed northwards off the External Massifs as recumbant folds and thrust slices. The Ultrahelvetic lie structurally above the Helvetic nappes and have their roots further to the south on the Gotthard and southern side of the Gotthard Massif (Trümpy, 1960).

b) The External Massifs - The External Massifs, together with the sedimentary cover which was not stripped off during the formation of the Helvetic and Ultrahelvetic nappes, form the authochthonous and parauthochthonous region of the Helvetic Zone. The External Massifs lie in a broken line to the south of the Helvetic and Ultrahelvetic nappes. They are brought to the surface in the cores of a series of gentle culminations which cross cut the axis of the mountain chain at a high angle. The Massifs are composed of Permo-Carboniferous sediments and older crystalline pre-Hercynian and Hercynian rocks. The basement rocks show the effects of both the Alpine and Hercynian and possibly earlier orogenies. In the French Alps the Hercynian and Alpine effects are clearly distinguished as their respective structural trends are markedly oblique, (e.g. in the Aiguilles Rouges Massif (Oulianoff, 1934; Ramsay, 1963)). In the Swiss Alps in the Aar and Gotthard Massifs the trends are often sub-parallel and less easily separated. Passing from north to south across the Massifs, the Alpine fabrics become more intense in company with the increasing grade of the Alpine metamorphism.

3) The Pennine Zone

The Pennine Zone contains the largest of the Alpine nappes. The nappes are formed by sheets of basement rock separated by eugeosynclinal Mesozoic sediments and volcanics. Argand (1916) interpreted these as gigantic recumbant anticlines, the Mesozoic sediments representing the corresponding intervening synclines. It seems more likely however that they are thrust slices of basement. The lowest levels of the Pennine Zone are brought to the surface in the cores of the Toce and Ticino culminations. Over much of the zone the nappes are flat lying, but in the south they turn downwards and form a region of steeply dipping rocks known as the Root Zone. The Root Zone is bounded to the south by a large steeply inclined fault, the Insubric Fault, which brings strongly deformed and metamorphosed rocks of the Pennine Zone in contact with undeformed and unmetamorphosed rocks of the Hinterland to the south.

In the frontal region of the Helvetic Zone, between the Arve and Aare rivers and elsewhere as Klippes (e.g. Mythen and Sulen), an isolated pile of nappes, the Prealps, is found. The Prealps lie structurally above the Ultrahelvetic nappes and have stratigraphic affinities with the Upper Pennine and Lower Austro-Alpine nappes. They possibly represent the detached frontal parts of these nappes.

The intensity and structural complexity of the Alpine deformation increases from north to south across the fold belt. In the Pennine Zone and along the internal part of the Helvetic Zone at least three generations of post-nappe tectonic structures are recognised. The grade of metamorphism also increases from north to south. In the outer Helvetic Zone the rocks are unmetamorphosed whereas in the deepest exposed levels of the orogenic belt, the Lower Pennine Zone, they have undergone almandine-amphibolite facies regional metamorphism. The highest grade of metamorphism, (upper almandine-amphibolite facies), is recorded in the south of the Lower Pennine region which is also a centre of late Alpine igneous activity, (e.g. the Bergeller granite).

Trümpy (1960) has suggested from stratigraphic evidence that the compressive phase of the Alpine orogeny was initiated at the end of the Cretaceous (65 m.y.), reached a climax in the Eocene - Lower Oligocene ($\pm$ 38 m.y., the Eocene - Oligocene boundary), and lasted at least into the Miocene (26-7 m.y.). He considers the Alpine metamorphism to have been approximately synchronous with the period of maximum compression. Radiometric age dates of phengites and muscovites from a zone surrounding the Lower Pennine region (Hunziker, 1970; Jäger, 1970), together with stratigraphic and radiometric dating of the "syn-metamorphic" Bergeller granite (Jäger et al, 1967; Milnes, 1969) lends support to Trümpy's age interpretation of the Alpine metamorphism. However, studies of the attitude of the metamorphic isograds, (Wenk, 1962), and of the relationships between deformation and metamorphic mineral growth, (e.g. Chatterjee, 1961; Higgins, 1964b), have shown quite clearly that the metamorphic climax occurred not only after the emplacement of the nappes, but at a late stage in the deformation history in

the Lower Pennine region. Here the main phase of crustal compression took place earlier than envisaged by Trümpy (cf. Trümpy, 1960 p. 879). Recent Rb/Sr whole rock age determinations in the range 110-125 m.y. from the fronts of the Pennine nappes (Hunziker, 1970; Jäger, 1970) place the earliest Alpine movements in the Lower Cretaceous.

By the time the Alps became a high mountain chain, and the source of the clastic sediments of the marginal Molasse basins and before the Helvetic and overlying nappes had taken up their final positions and overridden the Molasse along the Alpine front, the deformation in the deepest levels of the orogenic belt which are exposed today had virtually if not completely ceased. The belt of crustal instability had migrated further north. Ramsay's (1963) suggestion that the belt of instability migrated back to the Pennine Zone after the thrusting of the Helvetic nappes seems unlikely.

THE TECTONIC SUBDIVISIONS OF THE SWISS ALPS AND THE STRUCTURAL SETTING OF THE VAL PIORA AREA.

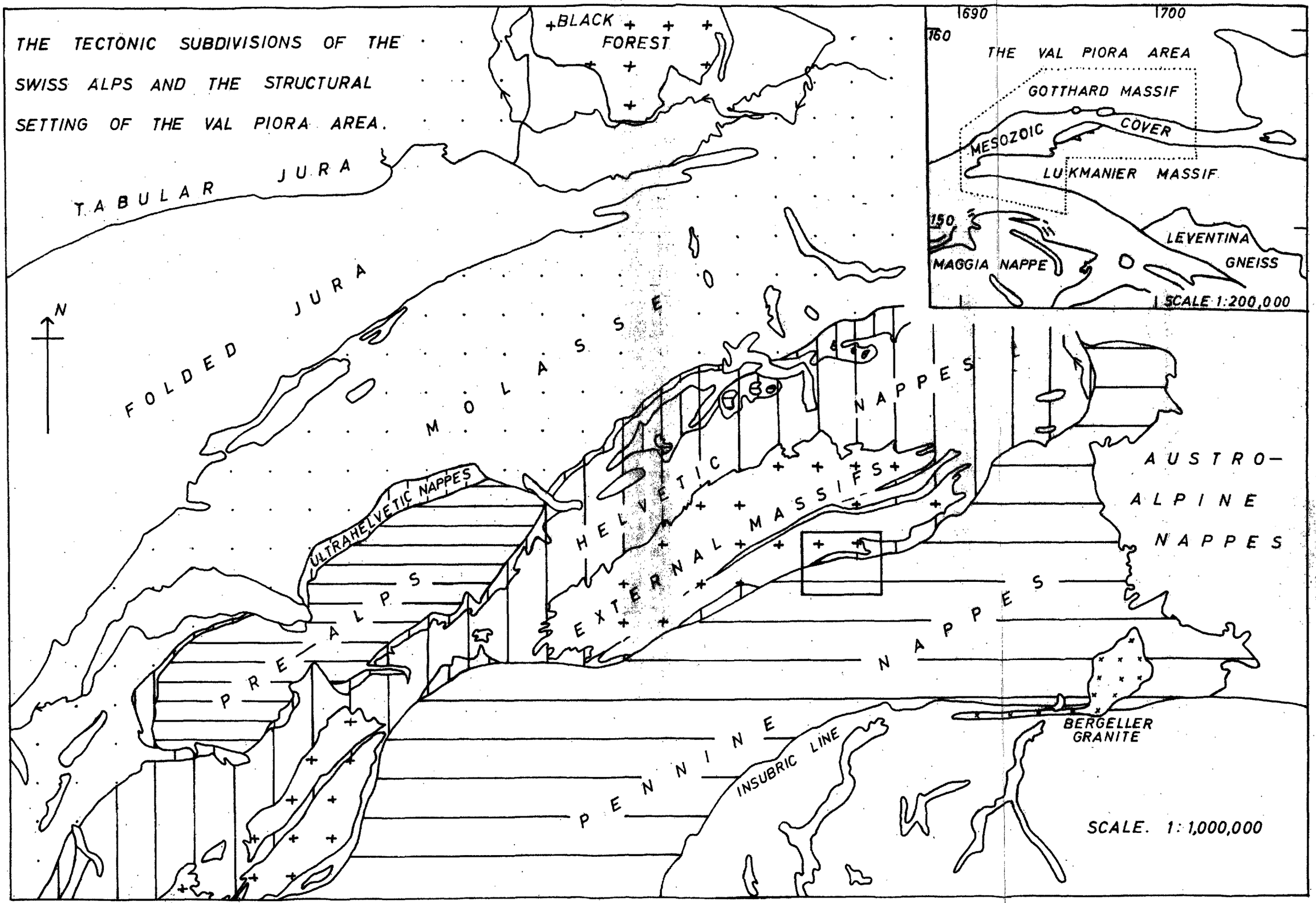

Fig. 1·1

1.3) Resumé of the geology of the Val Piora area

The rocks of the Val Piora area form three structural units (Fig. 1.1):-

1) The Mesozoic cover.
2) The Gotthard Massif.
3) The Lukmanier Massif.

1) The Mesozoic cover

The Mesozoic metasediments present in the area belong in part to the authochthonous cover of the Gotthard Massif and in part to the allochthonous Pennine series. These two distinct sedimentary facies are separated by the Frontal Pennine Thrust. The authochthonous cover may be shown by lithological comparisons with adjacent areas in which index fossils are found, to range from Lower Trias, to Lower Jurassic, (Lower Lias) in age. The poorly fossiliferous Pennine metasediments (Higgins,1964a; Bianconi,1965), are of probable Triassic and Jurassic age. The authochthonous metasediments are more closely comparable to the miogeosynclinal Helvetic sediments than to the adjacent eugeosynclinal Pennine series. They represent a continuation of the Helvetic series deposited in the southern part of the Helvetic miogeosyncline. From a structural viewpoint the authochthonous metasediments can be treated as Ultrahelvetic, as they lie to the south of the roots of the Helvetic nappes but to the north of the roots of the Pennine nappes. They are the remnants left behind when the overlying cover slid or was pushed northwards to form the Ultrahelvetic nappes.

2) The Gotthard Massif

The Gotthard Massif is one of the External Massifs and together with its cover rocks forms part of the authochthon of the Helvetic Zone. In the Val Piora area it is comprised by pre-Hercynian granite gneiss, (Streifengneiss), and metasediments possibly of Precambrian age. A number of Hercynian lamprophyre dyke intrusions are also recognised.

3) The Lukmanier Massif

The Lukmanier Massif is formed by pre-Mesozoic granite and sedimentary gneisses together with amphibolites of uncertain origin. In terms of Bossard's (1936, pp. 51-57) stratigraphic classification of the gneisses of the Lukmanier Massif the metasediments are possibly Devonian or Silurian and the granitic gneisses Hercynian in age. Observations in the Val Piora area suggest that there are at least two generations of acid intrusives the latest of which is thought to be of late Hercynian age, (Section 2.3). Bossard's stratigraphic classification is based on the very limited evidence available and must be accepted in this light.

The structural position of the Lukmanier Massif is also uncertain. The Massif has been interpreted both as a nappe, as part of a nappe and as part of the relatively unmoved Hercynian basement,(i.e. a southern extension of the Zone of External Massifs). The various structural interpretations of the Lukmanier Massif up to the year 1936, have been summarised by Kundig, (in Niggli et al, 1936). Even in recent years there has been no agreement as to the origin of the Massif. Dal Vesco (1964) considers it to be a slice of basement joined at depth to the southern side of the Gotthard Massif whereas Chadwick (1965) suggests that it is more closely related to the Pennine nappe cores, and is a basement slice caught up in the base of the Pennine nappe pile but not transported very far. In the present work evidence is given in favour of Dal Vesco's interpretation.

The area has a complex history of deformation. In the Mesozoic cover four discrete episodes of Alpine deformation are distinguished. The latter three of these may be recognised in the basement Massifs but the earliest is found to be absent. The earliest generation of structures in the Massifs is Hercynian.

The area underwent lower almandine-amphibolite facies metamorphism after the third episode of Alpine deformation. The Alpine metamorphism was progressive, the grade increasing from lower greenschist conditions during the first episode of Alpine deformation.

1.4) The literature and previous research

Geological studies were initiated in the Val Piora area by K. von Fritsch (1873), during mapping of the Gotthard region. He distinguished and described a number of rock types within the Mesozoic cover and basement and recognised the broadly synclinal nature of the Mesozoic rocks in Val Piora. Shortly after this the area became known to English geologists through papers given to the Geological Society of London by Bonney, in which he set out to disprove Heim's allegation, made at the International Geological Congress meeting of 1888, that fossiliferous Mesozoic rocks which had suffered metamorphism were to be found in the Swiss Alps. Bonney (1890, 1894) described sections in Val Piora and a section in Val Canaria, (earlier described by Grübenmann (1888)), in evidence against Heim's allegation. Bailey (1935) gives a lucid account of the controversy and its background. Garwood (1902, 1906) in two later papers given to the Geological Society, discussed aspects of the geomorphology of the Val Piora area and of the surrounding region.

The first work of importance was undertaken by Krige (1918). Although he discussed the structure and structural evolution of the area, his study was essentially petrological and included detailed descriptions of rocks, minerals and mineral textures and a number of chemical analyses. He recognised the Mesozoic rocks of Val Piora to be a complex synclinal zone, formed by a number of folds and in the south Schuppen, between two masses of dissimilar basement, the authochthonous Gotthard Massif and the allochthonous Lukmanier Massif, (the equivalent of the Adula nappe in the east and the Simplon nappes in the west).

Bossard (1929, and in Niggli et al, 1936) published the results of similar work in the area between the Valle di Lucomagno and Val Leventina east of Val Piora. The work was supported by a number of whole rock chemical analyses (Niggli, 1929). Bossard's lithological and stratigraphic subdivision of the Lukmanier Massif gneisses was adopted in Spezialkarte No. 116 (Geologische Karte der Tessiner Alpen zwischen Maggia - und Bleniotal, Preiswerk et al, 1934), and Krige's map

of the Massif to the west of Bossard's area is reproduced in this work slightly modified to accommodate this subdivision.

In succeeding years geological investigations of this type continued in adjacent areas, e.g. Huber (1943) in the Gotthard Massif and cover to the north and northeast, Hasler (1949) in the Maggia nappe and cover to the south, and Günthert (1954) in the Maggia nappe and cover to the southeast.

Kvale (1957, 1966) and Wunderlich (1958) in the course of more widespread investigations made observations in the Val Piora area about the tectonic structures and the time relationships between structures and metamorphic mineral growth.

Steiger's (1962) account of the sedimentary gneisses which form the southern part of the Gotthard Massif between the St. Gotthard and Lukmanier passes, is the next important work in the Val Piora area. As well as making detailed petrological observations, he deduced within these rocks a complex history of deformation and metamorphic mineral growth which compares closely with that outlined in this thesis. Radiometric age dating of different generations of hornblende crystals formed during the Alpine metamorphism was carried out with a view to dating different phases of the Alpine orogeny (Steiger 1963a, 1963b, 1964).

Dal Vesco (1964) undertook an investigation of the structure of the Val Piora area in connexion with the geological survey for the new Gotthard tunnel (Amsteg - Giornico, Basistunnel). As Krige, he recognised that the Mesozoic rocks in Val Piora formed a complex synclinal zone determined by folds and thrusts, however in contrast to Krige, he considered the basement masses on either side of this zone to be similar and connected at depth. In a short report on a geological excursion in the Piora, Lukmanier and Blenio valleys, Gansser and Dal Vesco (1964) refer for the first time to the allochthonous Pennine metasediments which form the core of the Val Piora structure west of Lago Ritom. (These had previously been interpreted as part of the authochthonous cover.)

An analysis of the structural and metamorphic history of the Lukmanier area, to the east of Val Piora, was completed by Chadwick in 1965 and forms the prelude to the present work.

In the last decade the Zürich school of geologists have completed a detailed stratigraphic study of the authochthonous and parauthochthonous cover rocks of the eastern Gotthard Massif, in an attempt to unravel the structure of this region. At an early stage a new stratigraphic classification, based on fossil evidence and lithological comparisons with the Mesozoic rocks of the Helvetic nappes, was proposed (Baumer et al, 1961). Detailed studies of individual areas followed (e.g. Jung,1963; Baumer, 1964; Frey, 1967). Of these Frey's work deserves particular mention, not only on account of the excellence of his geological analysis of the Greina area, but also because of his summary and synthesis of the new work in surrounding areas. It is encouraging to record that the interpretation of the geological history of the region as a whole, which follows from the structural observations made in this thesis, accords well with the history which has emerged from the detailed stratigraphic work of the Zürich school of geologists.

There is of course a large amount of literature of more general relevance to the geology of the Val Piora area. The most important of this is mentioned in the following chapters.

1.5) Aims and methods

The present research is aimed at attaining a greater understanding of the structural and metamorphic history of the rocks of the Val Piora area. The research forms part of a programme, whose objective must be regarded as the elucidation of the structure of the Alps themselves, through detailed mapping and the application of modern structural mapping techniques. This programme owes its conception and promotion to Prof. J.G. Ramsay.

In the region surrounding Val Piora detailed work has been completed or is in progress in the following areas:-

1)	Nufenen pass - Basodino area	- Higgins (1964).
2)	Lukmanier pass area	- Chadwick (1965).
3)	Cristallina area	- Ramsay (in progress).
4)	Pizzo Molare area	- Thakur (in progress).
5)	Bosco - Gurin area	- Hall (in progress).

Smaller scale, B.Sc. mapping projects have also been completed in:-

1)	Greina pass area	- Cobbold (1969).
2)	Sambuco - Massari area	- Rossetti (1970).
		- Mountenay (1970).
		- Davies (1971).
3)	Pizzo Rotondo area	- Lewis (1970).

Geological mapping has been carried out on a scale 1 : 10,000 on photographic enlargements of the 1 : 50,000 scale topographic map, Landeskarte der Schweiz, Sheet 266, Val Leventina (1961). The more detailed 1 : 25,000 scale topographic map, Carta nazionale della Svizzera, Sheet 1252, Ambri - Piotta (1965), was used in conjunction with the enlargements.

The area was exposure mapped. In the less well exposed regions an attempt was made to visit every visible exposure, whereas in the better exposed areas localities were chosen in accord with accessibility and complexity of the geology. Approximately 2,500 localities are recorded at which structural observations have been made. Exposure is generally good and clean above 2000 metres, however below this level

much of the area is thickly wooded. This feature combines with the steep valley sides to hinder mapping of lower lying parts.

Slumping, a common phenomenon in the Alps, is fairly widespread throughout the area. It is particularly marked on the flanks of Val Canaria and in parts of the cliffs along the southern margin of the Gotthard Massif, north of Val Piora. Steiger (1962, pp.382-383) has suggested that slumping of the Gotthard Massif gneisses contributes to the fan structure of the Massif, as surface dips are generally less than those taken below ground. Slumping of the Lukmanier Massif gneisses on the north side of Val Leventina is also often observed. It is noticable that the feature is most marked on south facing slopes, on which downward movement is facilitated by the orientation of the late Alpine fractures (Section 3.56).

In conjunction with the field work laboratory studies of the rock forming metamorphic mineral assemblages, the mineral fabrics, the relationships between mineral growth and deformation and of the metamorphic microstructures, snowball garnets, garnet crystal size distributions, and hornblende garbenschiefer have been undertaken.

The results of this research are presented in the following chapters, and where appropriate, summary and discussion provided at the end of each chapter.

CHAPTER II

STRATIGRAPHY

2.1) Introduction

The rocks of the Val Piora area can be divided into three distinct structural units. These are:-

1) The Mesozoic cover.
2) The Gotthard Massif.
3) The Lukmanier Massif.

In this chapter the stratigraphy of the different structural units is discussed.

2.2) The Mesozoic cover

The Mesozoic cover in the Val Piora area is formed by metasediments belonging to the authochthonous cover of the Gotthard Massif, and to the allochthonous series of the Pennine nappes. The presence within Val Piora itself of these two distinct metasediment facies has only recently been appreciated (Gansser and Dal Vesco, 1964). Previous investigations had concluded that all the Mesozoic rocks in Val Piora and their western extension in Val Canaria were a part of the Mesozoic cover of the Gotthard Massif (Krige, 1918; Bossard, 1929b; Niggli et al, 1936). Krige's stratigraphic classification of the Mesozoic metasediments, which is given below, and his geological map show however that in his lithological subdivision of the Upper Bünderschiefer he essentially distinguished the two metasediment facies.

4) Black-grey garnet schists, Calcareous mica schists, Marbles — Upper Bünderschiefer = Lias.

3) Quartenschiefer = L. Bünderschiefer

2) Rauhwacke and gypsum

1) Sericite quartzite

3), 2), 1) — Trias.

The black-grey garnet schists and marble are now thought to be Liassic rocks of the authochthonous cover of the Gotthard Massif and the calcareous mica schists to be allochthonous Pennine Bünderschiefer* (Gansser and Dal Vesco, 1964; Frey, 1967; p.71).

In terms of the new stratigraphic classification of the authochthonous and parauthochthonous cover of the Gotthard Massif proposed by Baumer et al (1961), the black-grey garnet schists have been correlated with the basal and lower Stgir series and the marbles with the upper Stgir series, Gelbsandfacies (yellow sand facies), (Frey, 1967, p. 71).

In the present work the former correlation is accepted; however the marbles are interpreted as part of the Pennine Bünderschiefer

---

* The term Bünderschiefer is used in the presently accepted sense suggested by Bolli and Nabholz (1959), i.e. Pennine post Triassic rocks, and not in the wider sense as in Krige's classification above.

Table 2.1 The stratigraphic classification and correlation of the Mesozoic cover of the S. Gotthard Massif.

a) The authochthonous/parauthochthonous cover.

Val Piora area (authochthonous)	Eastern Gotthard region (authochthonous/parauthochthonous)	Nufenenpass region (authochthonous)	
Younger Mesozoic sheared out	Coroi series	Younger Mesozoic sheared out	Middle Jurassic
	Upper Inferno series		
	Middle Inferno series		
	Lower Inferno series	Knotenschiefer series	Lower Jurassic (Lias)
	Upper Stgir series	Sandstone series	
Black garnet schist series	Lower Stgir series	Upper garnet schist series	
	Basal Stgir series	Middle garnet schist series	
	Lias basal quartzite	Lower garnet schist series	
Quartenschiefer	Quarten series	Quartenschiefer	Upper Triassic
Rauhwacke, Dolomite & Gypsum	Röti series	Rauhwacke & Dolomite	Lower Triassic
Quartzite	Melser series	Quartzite	

b) The allochthonous cover

Calcareous mica schist series	Lugnezerschiefer	Bünderschiefer	Jurassic
Rauhwacke, Dolomite & Gypsum	Quartenschiefer) Grenztrias Rauhwacke & Dolomite)	(Quartenschiefer) Rauhwacke & Dolomite	Triassic

sequence. In defence of this interpretation the analogy between these rocks and the Gelbsandfacies of the Upper Stgir series, which has been drawn by Frey (1967, p. 71) is questioned. The Gelbsandfacies is typified by yellow weathering sandy limestones interbanded with green quartzites, with a few intercalated black pelitic schists and occasionally calcareous schists (Frey 1967, p. 61). The marbles on the other hand are extremely pure (Krige, 1918, pp. 647-648) and are hence unlike the sandy limestones of the Gelbsandfacies. Furthermore the marbles are intercalated with calcareous mica schists typical of the Pennine Bünderschiefer and not quartzites, etc., as the sandy limestones of the Gelbsandfacies.

The proposed classification of the Mesozoic metasediments in the Val Piora area is summarised in Table (2.1), where it is also correlated with the sedimentary sequences in the Eastern Gotthard (Baumer et al, 1961; Jung, 1963; Baumer, 1964) and Nufenenpass (Liszkay, 1965) regions.

2.21) The authochthonous cover of the Gotthard Massif

The Triassic rocks.

a) The basal quartzite

The basal Triassic quartzite shows a considerable variation in thickness in the Val Piora area. At some basement contacts the quartzite is either absent or found as thin slivers included by Triassic marble, (e.g. the northern contact of the Lukmanier Massif and cover between Valle and Madrano). Along others it is well foliated, micaceous, and forms a horizon 1-5 metres thick between the basement gneisses and the Triassic marbles, (e.g. the southern contact of the Gotthard Massif and cover (see also Hafner, 1958, pp. 396-397; Steiger, 1962, pp. 344-345), and at the northern contact of the Lukmanier Massif and cover east of Lago Ritom). In the vicinity of Piora the quartzite reaches a thickness of 15-20 metres, is more massive though still micaceous and contains occasional large prismatic tourmaline crystals. Here it is sometimes pebbly at its lower, stratigraphic, margin. On the south side of Lago Ritom the quartzite is even thicker, extremely micaceous,

contains tourmaline crystals, and is often strongly rodded parallel to the hinges of folds formed during the second episode of Alpine deformation (Sections 3.22, 3.42). In this area a part of the micaceous quartzite, which has been assigned to the basal Trias, may represent a strongly sheared facies of the augen gneiss in which felspar has broken down to white mica and quartz (cf. Krige, 1918, p. 574). Krige (1918, p. 523) has expressed similar reservations about the Triassic age of all the quartzite in this particular area.

b) The Rauhwacke, dolomite and gypsum

The main mass of Triassic marble in the Val Piora area is a pale yellow, cavernous weathering, micaceous Rauhwacke (or marble breccia). Layered dolomite is also occasionally observed. A large mass of gypsum surrounded by Rauhwacke is found on the east side of Val Canaria and gypsum is interbanded with Rauhwacke on the west side of the valley (Bonney, 1890, pp. 204-213; Krige, 1918, p. 520, pp. 590-591, and Plate $\overline{X}$; Dal Vesco, 1964, pp. 37-40). In the present study these rocks have been mapped as a single lithological unit which varies enormously in thickness, and at some localities (e.g. at the northern contact of the Lukmanier Massif and cover between Valle and Madrano), is even absent, so that Quartenschiefer lies in direct contact with the basement. The thickness variation is in large part a tectonically induced variation.

Other than in the immediate vicinity of the basement contact, where a good schistosity is often developed, the Triassic marbles and gypsum tend to be rather structureless and show at most a poor, generally large scale compositional banding and/or a weak schistosity. A number of sections through the Val Piora marbles have been described by Dal Vesco (1964, pp. 19-29).

Although Triassic marbles of both the authochthonous and allochthonous cover are certainly present in the Val Piora area no clear distinction can be drawn between them. As such they have been treated as a single lithological unit and discussed together.

c) The Quartenschiefer

The Quartenschiefer, Quarten-Series of Baumer et al (1961), Frodalera - Series of Dal Vesco (1964, pp. 19 and 41), and Gansser and Dal Vesco (1964, p. 620), Lower Bünderschiefer or Quartenschiefer of Krige (1918, pp. 522-523), is thickly formed in Val Piora. It is comprised chiefly of grey-green mica schists containing irregular calcareous, (dolomitic), intercalations. The thickness of the intercalations may vary from a centimetre to a few metres. The micaceous layers generally contain both white mica and biotite, the muscovite showing a tendency to occur as small crystals oriented in the schistosity and the biotite to form porphyroblasts which are either lineated or random in orientation. These layers are often rich in kyanite and epidote and occasionally contain quartz kyanite segregations. Within this sequence rather pure white quartzite layers and lenses up to a few metres thick are found.

Together with these rocks garnet mica schists, garnet hornblende mica schists and garnet staurolite kyanite mica schists, like those exposed at Frodalera (Bossard, 1929b, pp. 119-120) form a small part of the Quartenschiefer in Val Piora.

The Jurassic rocks.

The black garnet schist series

The series is typified by the occurrence of well foliated grey-black garnet mica schists. The garnets generally form euhedral porphyroblasts up to a centimetre in diameter which are set in a fine grained matrix of quartz, white mica and rarely calcite. Small porphyroblasts of plagioclase, staurolite, biotite and kyanite are also found in these rocks but are not often identifiable in hand specimen. The dark colour of the schists is attributed to the presence of finely divided carbonaceous material (Krige, 1918, p. 522). In contrast to the Quartenschiefer, the black garnet schists are regularly banded. Individual layers are more continuous and remain relatively constant in thickness, taking into account thickness variations due to folding. They range from a few millimetres to a few metres thick and are often separated by thin calcareous and less commonly siliceous layers and segregations. The black garnet schists

are interbanded on a much larger scale with red brown weathering, dominantly calcareous rocks, marbles, siliceous marbles, calcareous mica schists and occasional quartzites. These rocks often contain carbonate and quartz-carbonate segregations elongate in the plane of the foliation.

It is these calcareous rocks that have yielded the only fossils found in Val Piora. Krige (1918, p. 522) discovered echinoderm remains and Dal Vesco (1964, pp. 29-31) crinoid fragments. In the present study crinoid fragments were observed at a single locality, some 300 metres due south of the summit of Föisc, in a blue-grey, brown weathering marble.

2.22) The allochthonous cover

The calcareous mica schist series.

The Bünderschiefer is represented in the Val Piora area by the calcareous mica schist series. This series is exclusively found together with Triassic marbles of uncertain affinity (Section 2.21) in Val Leventina and Val Canaria. In Val Piora itself it is present only in the region to the west of Alpe Ritom. It is formed by a monotonous succession of light brown weathering rocks, ranging in composition from pure marble, (the "Mamore" of Krige (1918 pp.647-648) and Section 2.2), to carbonate free quartz mica schists. The mica schists contain a wide range of porphyroblast minerals, of which biotite and plagioclase are almost ubiquitous, garnet, staurolite and kyanite are common and hornblende is rare. The rocks show a well developed compositional banding, pelitic layers alternating with carbonate layers on a scale that varies from a millimetre or less to several tens of metres. The compositional banding is particularly well displayed because the pelitic layers are picked out in relation to the carbonate layers by differential weathering. Carbonate and quartz-carbonate segregations are typically present in the plane of the foliation.

On a small scale the distinction between the Bünderschiefer and the rocks of the black garnet schist series of the authochthonous cover of the Gotthard Massif is not always clear cut. Overall the

Bünderschiefer are more calcareous, less carbonaceous and correspondingly lighter in colour and they contain no quartzites (cf. Bossard, 1929b, pp. 110-113).

In the areas to the east and west of Val Piora the tectonic contact between the Pennine and Gotthard Massif metasediments is marked by a generally well developed zone of Triassic rocks, the Grenztrias (Oberholzer, 1955, pp. 382-384; Baumer, 1964, p. 51; Liszkay, 1965, p. 931; Frey, 1967, p. 88). In the Val Piora area, although it is probable that Triassic marbles of Pennine affinity are in contact with the authochthonous cover in the region to the west of Föisc, there is no regularly developed zone of Triassic rocks comparable to the Grenztrias at the base of the Bünderschiefer sequence. For example in the Alpe di Lago, Alpe Ritom area only one isolated exposure of Rauchwacke is found at the junction of the Bünderschiefer and the Black garnet schist series. The metre thick lens of Rauhwacke at 2260 metres on the southwest ridge of Camoghe interpreted by Frey (1967, p. 71) as Grenztrias is thought to represent the line of a tectonic discontinuity within the Bünderschiefer itself (Section 3.21).

2.3) The Gotthard Massif

The gneisses of the Gotthard Massif can be divided into three distinct groups.

1) The Hercynian and Alpine? instrusive rocks.
2) The pre-Hercynian granite gneiss (Streifengneiss).
3) The pre-Hercynian sedimentary and mixed gneisses.

2.31) The Hercynian and Alpine? intrusive rocks

Four major intrusions, ranging from granite to diorite in composition, are recognised in the Gotthard Massif. These are, the Gamsboden granite gneiss, the Fibbia granite gneiss, the Medelser granite/Cristallinia granodiorite/Ufiern diorite, and the Rotondo granite, which includes the Lucendro, Tremola and Prosa granites. The petrology and structure of the individual intrusions has been described by various authors (Sonder, 1921; Ambühl, 1929; Winterhalter, 1930; Huber, 1943; Hafner, 1958; Hofmänner, 1964). The Gamsboden, Fibbia and Medelser/Cristallina/Ufiern intrusions are clearly deformed, as they show both planar and linear tectonic fabrics. By contrast, in the Rotondo granite these fabrics are absent and there is evidence only of a weak late Alpine deformation of the granite (Hafner, 1958; Kvale, 1957, 1966). To explain the differences in fabric between the Fibbia and Rotondo granites Sonder (1921) suggested the following sequence of events:-

1) Intrusion of the Fibbia granite.
2) Stress period.
3) Intrusion of the Rotondo granite.

Both intrusions were thought to be of Hercynian age and the stress period to be a late Hercynian event. Kvale (1957, 1966) however has pointed out that the linear and planar fabrics are comparable to those in the adjacent gneisses and Mesozoic cover. On this basis, he has presented a case for accepting a late, (post-tectonic), Hercynian age for the Fibbia, Gamsboden and Medelser/Cristallina/Ufiern intrusions and a late Alpine age for the Rotondo granite. A more detailed account of the age problem is given by Grünenfelder and Hafner (1962).

Radioactive age determinations of zircons (Grünenfelder, 1962), have shown that zircons from the Fibbia, Gamsboden, and Medelser granite gneisses give Hercynian ages (approx. 300 m.y.), while those from the Rotondo granite give an ambiguous age (approx. 140 m.y.), which gives no immediate support to either of the proposed ages, Hercynian or Alpine, for this intrusion. To explain this anomalous zircon age Grünenfelder and Hafner (1962) have suggested that the Rotondo granite is a remobilised Hercynian granite which was intruded into its present position, possibly during Alpine times, taking with it its older but now altered zircon population. The Rb/Sr. whole rock isochron for the Rotondo granite, (approx. 260 m.y.), suggests a primary Hercynian age (Jäger and Niggli, 1964). Thus if remobilisation took place, then it did so without isotopic homogenisation.

Minor intrusive bodies, lamprophyres, quartz porphries, aplites and pegmatites are recognised to be related to the granite plutons. The same problems that beset the age determination of the major intrusions are present in the interpretation of the minor intrusives. Some of the bodies are clearly deformed and show the development of planar and linear fabrics (Huber, 1943; Hafner, 1958, p. 270; Chadwick, 1965), as the Fibbia granite gneiss, etc. Others show original igneous minerals and textures (Hafner, 1958, p. 271) as the Rotondo granite.

Three lamprophyre dykes are found in the Gotthard Massif in the Val Piora area. The intrusions are steep sided and in sharp contact with the adjacent gneisses (Fig. 2.1). Petrologically the rocks are comparable to the metamorphosed kersantites and kersantite-spessartites described by Huber (1943, pp. 119-120). The dykes are clearly deformed as they are folded (Section 3.32). Though axial planar biotite fabrics are absent or poorly developed, linear biotite fabrics (L. tectonite fabrics, Section 3.23) are commonly observed. The linear fabrics compare in orientation with the mica lineations in the adjacent gneisses and Mesozoic cover (Sections 3.23, 3.33). In view of these observations about the state of deformation, a probably Hercynian age for the dykes may be inferred.

Fig. 2.1. The contact between a lamprophyre dyke and the Streifengneiss. The strongly developed foliation in the Streifengneiss contrasts with the lack of visible structure in the lamprophyre. The dyke in fact shows a weak linear fabric (Section 2.31). Punta Negra, M.R. 6961815766.

Fig. 2.2. Deformed quartzo-felspathic layers (aplites?) in the Sorescia gneiss. The foliation is axial planar to these folded layers. Lago di Dentro, M.R. 6992515670.

2.32) The pre-Hercynian granite gneiss (Streifengneiss)

The pre-Hercynian granite gneiss, or Streifengneiss, a term suggested by Krige (1918, p. 541) in view of the "conspicuous streaked appearance" of the rock, occurs extensively along the middle of the Gotthard Massif (Winterhalter, 1930, Tafel. I). The Streifengneiss to the north of the Val Piora area has been investigated by Huber (1943). He concludes (pp. 186-190 and pp. 206-208), that the rock formed through crystallisation of a homogeneous magma, which was of granitic composition but for a slight excess of alumina possibly derived by assimilation. The rock subsequently underwent tectonic and metamorphic modifications to form the Streifengneiss. A similar conclusion is reached by Oberholzer (1955) in considering the origin of the Streifengneiss in the Western Gotthard Massif. Zircon age determinations, ($^{Pb207}/Pb_{206} = 560 \pm 90$, $^{U238}/Pb_{206} = 485 \pm 20$, $U_{235}/Pb_{207} = 520 \pm 25$ m.y. (Grünenfelder, 1962)), suggest that the Streifengneiss magma was intruded at the latest in the Lower Palaeozoic.

The Streifengneiss in the Val Piora area, (Krige, 1918, pp. 541-545) is a generally well foliated quartzo-felspathic augen gneiss. The augen are formed by aggregates of quartz and felspar grains in varying states of recrystallisation (Section 4.3) and are surrounded by a matrix rich in muscovite and biotite. They are generally elongate in the plane of the foliation and give rise to the rodding structure which is so characteristic of the Streifengneiss. The origin of this structure is discussed in Section 3.31. The intensity with which rodding is developed varies. Sometimes the structure is so strong that the rock fabric is more nearly linear than planar. At other times rodding is absent and the augen form discs several centimetres in diameter lying in the plane of the foliation. Both small and large scale variations in the intensity of rodding are observed.

2.33) The pre-Hercynian sedimentary and mixed gneisses

A number of east-west extending zones of sedimentary and mixed gneisses, described as "Muldenzonen" by Huber (1943, p. 93) can be recognised in the Streifengneiss. On the basis of whether or not

the rocks of these sedimentary gneiss zones were metasomatised or intruded by aplites and pegmatites related to the Streifengneiss magma, Huber was able to distinguish zones of two different ages. The Motta Naira, Paradis and Ravetsch Nordgrates zones (Ambühl, 1929) were thought to predate the emplacement of the Streifengneiss magma, whereas the Boreal, Tenelin and Tremola zones were thought to postdate this event but to be earlier than the emplacement of the Hercynian granites, etc.. Subsequent investigations have shown Huber's Tremola zone to be more complex (e.g. Hafner, 1958; Steiger, 1962). In the areas to the west (Hafner) and east (Steiger) of the Gotthard Pass the zone has been divided into the following gneiss units:-

	West (Hafner, 1958)		East (Steiger, 1962)
Cavanna series	Hühnerstock gneiss	-	Streifengneiss ?
	Sorescia gneiss	-	Sorescia gneiss
	Prato series	-	Prato series and Corandoni zone
	Tremola series	-	Tremola series
	absent	-	Giubine series

The gneisses of the Cavanna series and their equivalents to the east of the Gotthard Pass show indications of ultrametamorphism, in contrast to Tremola and Giubine series gneisses which do not. Of the relationship between the Cavanna series and the Tremola series, Hafner (1958, p. 358) concludes, that at the time of the ultrametamorphism of the Cavanna series the Tremola series had not been deposited. The Sorescia, Prato series and Corandoni zone gneisses may be assigned to the group of sedimentary gneisses which predate the intrusion of the Streifengneiss, the Tremola and Giubine series gneisses to the group that postdate it (Steiger, 1962, p. 454).

As the Streifengneiss zircon ages give a minimum age for the intrusion of the Streifengneiss magma, and as Lower Palaeozoic rocks are apparently absent in the Swiss Alps, Steiger (1962, pp. 484-485) has suggested that both the Streifengneiss and Tremola series are of Precambrian age.

In the Val Piora area all of the gneiss series described by Steiger, except the Prato series are observed. The Prato series is confined to the area to the west of Val Canaria (Steiger, 1962, p. 475 and Tafel IV). The gneiss series proposed by Steiger have been adopted in the mapping of the part of the Gotthard Massif exposed in the Val Piora area. The lithological map presented here (Encl. 1) is essentially identical to that produced by Steiger (1962, Tafel IV). Where differences in the interpretation of the position of lithological boundaries exist, they are small and occur in areas in which boundaries are transitional. The various gneiss series have been described in great detail by Steiger, and accordingly only the briefest outline of their structure and petrology is given below.

a) The Tremola series

The Tremola series has been divided into three zones, the northerly Pontino zone, the middle Sasso Rosso zone, and the southerly Nelva zone. The zones wedge out successively towards the east against the tectonically determined southern margin of Gotthard Massif (Sections 3.22, 3.32) and only the Pontino zone is extensively developed east of Val Canaria (Steiger, 1962, p. 448, Fig. 2 and Tafel IV). The Pontino zone is comprised of mica gneisses, often garnetiferous, and subordinate hornblende gneisses, together with a few amphibolites, calc-silicate rocks and quartzites. The rocks of the Sasso Rosso zone are similar but often chlorite bearing whereas the Nelva zone is rather richer in mica gneisses and poorer in hornblende bearing rocks than the Pontino zone.

b) The Sorescia gneiss

The Sorescia gneiss forms two distinct zones, one on either side of the Corandoni zone gneisses. On Pizzo Taneda the northerly zone is interleaved with Giubine series gneisses which throughout the rest of the area separate the Sorescia from the Streifengneiss. Typically, the Sorescia gneiss is a well foliated quartzo-felspathic two mica gneiss which contains quartz-alkali felspar augen with a maximum dimension up to a few centimetres. Sub-concordant pegmatites and quartzo-felspathic layers, (aplites?), are common. The foliation is

axial planar to the earliest generation of folds which deform these bodies (Fig. 3.22).

The northern zone is formed by typical Sorescia gneiss, which remains remarkably uniform in composition throughout and is in fairly sharp contact, (transitional over a metre or two), with the garnet mica gneisses of the Giubine series to the north and the amphibolites and garnet mica gneisses of the Corandoni zone to the south.

The southern zone is less uniform in composition. The typical Sorescia gneiss described above is found throughout the zone in the west of the area. In the east, particularly south of Lago di Dentro, the gneiss contains muscovite porphyroblasts; biotite is less regularly distributed and is concentrated in biotite rich bands and lenses and layers of garnet mica gneiss and amphibolite are found within the sequence. Contacts with the Tremola series and Corandoni zone are fairly well defined in the west of the area, but in the east are often uncertain in view of the presence of gneisses typical of the Tremola series and Corandoni zone within the Sorescia gneiss.

c) Corandoni zone

The Corandoni zone is formed by amphibolites, hornblende mica gneisses and mica gneisses. The rocks are often garnetiferous and characteristically show a well developed banding of light and dark mineral layers. The thickness of individual layers is variable.

d) The Giubine series

Of the subdivisions of the Giubine series recognised by Steiger (1962, Tafel IV), only the Granat(quer)glimmerschieferzone is represented in the Val Piora area. The other two zones, the Schmitzengneis- and Stromatische zones are found west of Val Canaria. The gneisses of the Granat(quer)glimmerschieferzone are, as the zone name might suggest, dominantly garnet mica gneisses. In these rocks biotite typically forms prophyroblasts which often show a well developed L. tectonite fabric (Section 3.33) and hornblende, forming garben (Chapter 6) is a fairly common minor constituent. Amphibolites and well banded biotite rich gneisses are also found in this zone. The Giubine series gneisses are in centimetre sharp contact with the more northerly lying Streifengneiss.

2.4) The Lukmanier Massif

In contrast to the Gotthard Massif the Lukmanier Massif has received the attention of few workers. Bossard's work (1929a, and in Niggli et al, 1936) represents the most comprehensive study yet available. Krige (1918) and Chadwick (1965) have mapped parts of the Lukmanier Massif in the course of their investigations in the Val Piora and Lukmanier areas respectively. Both Krige (1918, p. 530) and Bossard (1929, pp. 52 and 72) have emphasised the problems of mapping the Massif. Bossard (1929, p. 72) writes:-

"The rocks of the Lukmanier Massif are petrographically very variable. No rock series shows the same picture over a great distance; petrographically similar beds merge quickly into one another." (My translation.)

In much of the Val Piora area the problems are magnified by poor and tree covered exposure.

The lithological subdivision of the gneisses of the Lukmanier Massif proposed in the present study, summarised below, is essentially the same as that made by Krige (1918).

Augen gneisses (Piora type) - Quartzo-felspathic gneisses which contain large felspar augen.

Orange Group gneisses - Orange coloured, micaceous gneisses which contain porphyroblasts of garnet, staurolite, kyanite, tourmaline and hornblende.

Mixed Group gneisses - Interbanded quartzo-felspathic gneisses, (the Older Granite gneisses) and micaceous gneisses.

Amphibolites - Hornblende rich rocks, typically with plagioclase, biotite, quartz, calcite and epidote and often garnet. Interbanded calcareous horizons.

The Younger Granite gneisses - Small granitic intrusions of probable sheet form which cross cut compositional banding in the Mixed and Orange Group gneisses.

The Orange Group gneisses are comparable to Krige's paragneiss and the Mixed Group gneisses together with the Augen gneisses (Piora type) and the Younger Granite gneisses to his ortho- and mixed zone gneisses. Many of the gneisses to the east of Lago Ritom, which Krige has mapped as ortho- and mixed zone rocks, I have assigned to the Orange Group. Otherwise the positioning of lithological boundaries is similar.

Bossard (in Preiswerk et al,Spezialkarte No. 116, 1934) and Chadwick (1965) mapped discrete orthogneiss horizons within the gneisses of the Lukmanier Massif. Chadwick distinguished White Group granite gneisses from Bronich (conglomeratic), and Orange (garnetiferous micaceous, as above), Group paragneisses and amphibolites. In the Val Piora area Spezialkarte No. 116 shows the Lukmanier Massif to be formed by pre-Carboniferous para- and mixed gneisses and amphibolites, which have been intruded by "granite gneisses of Lucomagno type". Examination of areas shown on this map as granite gneiss of Lucomagno type has revealed that these areas are formed by both Younger and Older Granite gneisses. There are however many granite gneisses which are not depicted on the map, so that it seems probable that an attempt has been made to distinguish the Younger Granite gneisses as "granite gneisses of Lucomagno type", but this has resulted in the inclusion of some of the Older Granite gneisses in this subdivision. In the present study it was considered impractical, because of poor exposure and in the case of the Older Granite gneisses because they are so complexly interbanded with the other gneisses of the Mixed Group, to map either the Older or the Younger Granite gneisses as distinct lithological units.

The relative ages of the granite gneisses were determined from structural observations; the Older Granite gneisses were deformed before the intrusion of the Younger Granite gneisses (Section 3.42). The dating of Older and Younger Granite gneisses which are differentiated in time by the first recognisable episode of deformation in the gneisses of the Lukmanier Massif is important to the interpretation of the history of the Massif. As the Younger Granite gneisses

contain only Alpine tectonic structures they are either of late Hercynian or early Alpine age, (they predate the second episode of Alpine deformation (Section 3.42)). A late Hercynian age seems most likely as there is abundant evidence of the intrusion of granitic magma into the basement during this period, whereas, to the best of the authors knowledge there is no record of this type of igneous activity during early Alpine times. The implications of this age are, that the earliest recognisable generation of tectonic structures in the Lukmanier Massif must also be of Hercynian age and that the Older Granite gneisses must be of pre-Hercynian or syntectonic Hercynian age. The solution of this age problem awaits more radioactive age determinations.

2.41) The Augen gneisses (Piora type)

These augen gneisses are found on the south side of Lago Ritom and in the Madrano region. They are characterised by the occurrance of augen composed dominantly of felspar and with a maximum dimension ranging up to 10 cm. In general the augen are, as the term implies, eye shaped when viewed in planes at right angles to the schistosity. In the plane of the schistosity they either form discs or are elongate (rodded) parallel to the hinges of folds formed during the second episode of Alpine deformation. Quartz rich layers in the matrix are similarly rodded in this direction (Section 3.42 and Fig. 3.43). More angular ideomorphic felspar shaped augen are also observed. Krige (1918, pp. 570-574) found that the more ideomorphic augen were formed by microperthite and orthoclase porphyroclasts, whereas the more rounded augen were composed of grain aggregates of sodic plagioclase, orthoclase, sericite and quartz. He suggested that these aggregates were the products of unmixing of original microperthite and breakdown of some of the orthoclase to sericite and quartz in response to deformation and metamorphism. The augen are set in a matrix of quartz, acid plagioolase, white mica and biotite in which white mica is present in excess of biotite. Tourmaline occurs sporadically throughout the rock as large single crystals several centimetres long or as groups of crystals.

The gneiss is relatively homogeneous in composition except in the vicinity of Hotel Piora where biotite rich and quartzo-felspathic, (aplitic?), layers and lenses and other indications of compositional banding are observed. Gansser and Dal Vesco (1964) report the presence of quartzite pebbles up to 20 cm. long in the gneiss here and suggest that the rock is sedimentary in origin. Krige (1918, pp. 570-574) on the other hand considers the rock to be an orthogneiss. I have been unable to find any conclusive field evidence in favour of one or other of these two hypotheses.

The contact of the Augen gneisses with the Orange Group gneisses is generally transitional over several metres from typical augen bearing gneiss to typical augen free micaceous garnet gneiss.

2.42) The Orange Group gneisses

The term Orange Group was coined by Chadwick (1965) to apply to a group of orange coloured gneisses which occur along the northern margin of the Lukmanier Massif south of the Valle di Lucomagno. These gneisses clearly extend into the Val Piora area and here are found in the north of the Massif along its exposed length.

The Orange Group gneisses are quartz rich micaceous gneisses in which white mica occurs as small crystals and biotite tends to form porphyroblasts. Small garnet prophyroblasts up to 5 mm. diameter are almost always present and porphyroblasts of staurolite, plagioclase and less commonly kyanite, hornblende and tourmaline have also been observed.

Compositional banding, formed by the interbanding of more quartzose and more micaceous layers is generally poorly developed. Where present segregations of quartz run parallel to the plane of the banding. These segregations are almost ubiquitous in the Orange Group rocks and in areas in which compositional banding is very poor or absent their relationships to the schistosity, (i.e. whether they are parallel to it or cross cut it), often provide the only clue for the interpretation of the age of this structure.

2.43) The Mixed Group gneisses

The Mixed Group gneisses form the central and southern part of the Lukmanier Massif to the south and west of Piora and outcrop again south of the Orange Group east of Passo Comasnengo. The group is composed largely of grey coloured quartzo-felspathic gneisses interbanded with micaceous gneisses often garnetiferous and similar to those that typify the Orange Group.

The quartzo-felspathic gneisses show a wide range of appearance. Some are well banded, quartz felspar layers alternating with more micaceous layers on a variety of scales, whereas others are rather homogeneous in composition (the Older Granite gneisses). These latter gneisses sometimes contain quartz felspar augen. The augen bearing varieties are generally irregularly distributed throughout the group. In the central part of the Lukmanier Massif along the eastern margin of the area augen gneiss is common however and forms the western extension of a large mass of this rock.

2.44) The Amphibolites

Amphibolites are found in both the Orange and Mixed Group gneisses as layers and lenses which are parallel to compositional banding in the adjacent rocks. They occur as isolated single horizons and particularly in the Orange Group in zones in which a number of horizons are interbanded with the host gneisses. The amphibolite layers themselves often display a fine scale interbanding of light and dark constituents (Fig. 2.3). Individual layers vary from a few centimetres to a few tens of metres in thickness.

Major constituents include hornblende, plagioclase, biotite, quartz, calcite and epidotes. Garnet is found in some horizons. Rocks composed largely of calcite, quartz, biotite and epidote are found interbanded with many of the amphibolites. They are especially common in the west of the Massif.

The greater number of the amphibolites in the Lukmanier Massif have been interpreted by both Krige (1918, pp. 584-586) and Bossard (1929a,p. 88; 1936, p. 54) as para-amphibolites. Both authors point

Fig. 2.3.

Banded amphibolite, showing two generations of coaxial fold structures. The earliest folds are the first generation of structures recognised in the Lukmanier Massif gneisses. The weaker later set are second generation fold structures (Sections 3.41, 3.42). Road section, Altanca-Piora, M.R. 6943615354.

Fig. 2.4.

An intrustion of Younger Granite gneiss, of sheet form and discordant to compositional banding in the surrounding Mixed Group gneisses. Note the coarse fracturing parallel to the weak second generation cleavage in the Mixed Group gneisses. Road section, Altanca-Piora, M.R. 6950415335.

to the association with carbonate rocks as an important argument in favour of a sedimentary origin. This argument is however not always valid. A case in point is the striped amphibolites of Connemara, Western Ireland, which are often associated with marbles but which have been shown from their chemical trend to be ortho-amphibolites (Evans and Leake, 1960). Only the recognition of sedimentary or igneous chemical trends within a group of amphibolites confirms beyond doubt the origin of these bodies (Leake, 1964; Van de Kamp, 1969).

2.45) The Younger Granite gneisses

In the central part of the Lukmanier Massif to the south and west of Piora a few small intrusions of granitic composition are found cross cutting the compositional banding in the surrounding gneisses (Fig. 2.4). Their discordant relationship is most clearly seen in the exposures along the lower part of the road from Altanca to Piora. Contacts with the host gneisses are sharp and often sub-parallel and planar suggesting that the intrusions in these places have sheet form. Elsewhere however the geometry of the contacts is less regular and the form of the intrusions uncertain.

Quartz, microcline, sodic plagioclase, muscovite and biotite are the major mineralogical constituents of these rocks. But for the appearance of a few felspar porphyroclasts the original igneous textures have been completely destroyed by recrystallisation and new mineral growth. The felspar porphyroclasts are composed of coarsely intergrown microcline and sodic plagioclase and probably represent igneous perthites further unmixed by deformation and metamorphism.

Individual granite gneiss sheets have not been mapped, as they are, in volumetric terms, of little importance and because of the difficulties involved in attempting to trace them in the poor and wooded exposure of this region.

CHAPTER III

THE STRUCTURAL GEOLOGY

3.1) Introduction

The structural analysis of the Val Piora area is presented in the following manner. Firstly, the geometry and time relations of major and minor structures within the individual structural units, the Mesozoic cover, the Gotthard Massif, and the Lukmanier Massif are discussed (Sections 3.2, 3.3, 3.4). Their deformation histories are compared, the important aspects of different deformation episodes emphasised and the structural relationships between basement and cover outlined (Section 3.5). The significance, in terms of fold mechanism, of certain features of the geometry of natural folds is discussed (Section 3.6), and brief note is made (Section 3.7) of the apparent simplicity of the structural patterns produced during the third and fourth episodes of Alpine deformation. In conclusion, the history of deformation deduced in the Val Piora area is compared with that found in adjacent areas by other workers and an attempt is made to clarify the regional tectonic picture (Sections 3.8, 3.9).

The general techniques used in this analysis are as those outlined in standard texts (e.g. Turner and Weiss, 1963). The rather more specialised techniques applied in the study of fold geometry, isogon techniques, have been described by Ramsay (1967). The nomenclature is that used or recommended in Ramsay (1967), unless otherwise stated.

3.2) The Mesozoic cover

Although the fabric in the basement rocks of the Lower Pennine nappes is thought to be of Alpine age (Wenk, 1955), pre-Alpine structures have been described in the rocks of the Gotthard Massif (Steiger, 1962; Kvale, 1966). It is in order to appreciate the effects of the Alpine deformation alone that the deformation history of the cover is considered first.

Four episodes of deformation are recognised in the cover rocks. The structures which have arisen during these deformation episodes and their significance in elucidating the deformational history are discussed below.

3.21) The first episode of Alpine deformation

The metasediments of the cover show a well developed foliation*. As this structure is usually found to be parallel to compositional banding, the question of its origin naturally arises. Does it represent original bedding or is it tectonic? The tectonic nature of the foliation is convincingly demonstrated by the presence of tight to isoclinal folds (Fleuty, 1964a) in compositional banding to which it is axial planar (Fig. 3.1). Folds whose limbs are strongly attenuated or even ruptured indicate that original compositional banding or bedding has not only been repeated by folding, thickened or thinned, but also disrupted by planes of discontinuity (Fig. 3.2). Compositional banding has in fact been transposed from one dominant orientation to another to form a transposition foliation (Turner and Weiss, 1963, p. 92).

The foliation is characterised by:-

1) A preferred crystallographic orientation in the plane of the foliation of both white mica, which forms the dominant element of the planar structure, and biotite. The micas are also dimensionally oriented within the plane of the foliation, and hence lineated. Minerals of prismatic habit (e.g. kyanite

---

* Foliation as used in this text means a planar structure. It does not imply a compositional layering, (cf. Ragan, 1967).

Fig. 3.1. Isoclinal first generation fold. Black garnet schist series; Val Piora, M.R. 6969815568.

Fig. 3.2. First generation folds with strongly attenuated or ruptured limbs. Bünderschiefer; Alpe di Lago, M.R. 6937515575.

and epidote) often show a preferred orientation of their longest axes in the foliation. In some cases these are also observed to be lineated.

2) A dimensional orientation of non-platy minerals in the plane of the foliation. Quartz and calcite exhibit this feature, but in most cases the dimensional fabric of these minerals has been determined by later deformation and/or recrystallisation (Section 4.2).

Folds of first deformation age are uncommon and often distinguished with difficulty from coaxial structures of second deformation age (Figs. 3.3, 3.4). The folds are tight to isoclinal and appear on a variety of scales, wavelengths varying from a few centimetres to hundreds of metres.

The geometry of the folded layers is often close to that of pure similar or Class 2 folds (Ramsay, 1967, p. 369 and Table 7.3), especially in rocks in which compositional differences reflecting ductility contrast between layers are slight. Fig. 3.5 shows the isogon plot (Ramsay, 1967, pp. 363-372) for three layers of a first generation fold, which may be seen (Fig. 3.3) to be folded coaxially by a second generation structure. The layers show little if any compositional difference and the isogon patterns for the layers exhibit parallel to weakly convergent isogons corresponding to Class 2 to 1.C. geometry (Ramsay, 1967, p. 36 and Table 7.3). The slight departure from similar geometry, (Class 2 geometry, parallel isogons), may be equated with non-passive (Donath and Parker, 1964) layer behaviour. This is most marked in layers which have a marked compositional and probably also a large ductility contrast with the matrix (Fig. 3.6).

The well defined stratigraphic units of the authochthonous cover of the Gotthard Massif (Section 2.21) allow the effects of the first deformation episode to be recognised. The present distribution of these stratigraphic units cannot be interpreted as the product of folding alone. The isolated occurrences of black garnet schist series rocks in the Quartenschiefer, and of Rauhwacke in both the black garnet schist series and the Quartenschiefer, indicate that extensive slicing

Fig. 3·3 Coaxial second generation folds folding first generation structures. Black garnet schist series, Alpe Ritom MR.6957715556.

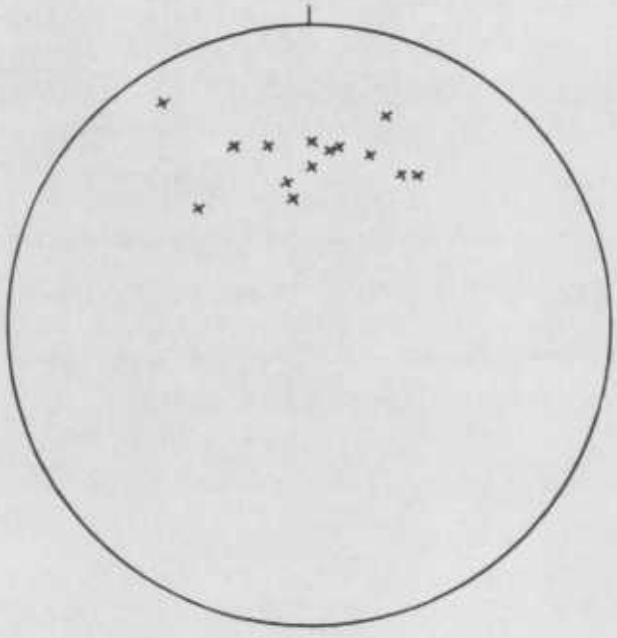

Fig. 3·4 First generation fold axes. Alpe Ritom, Alpe Piora area.

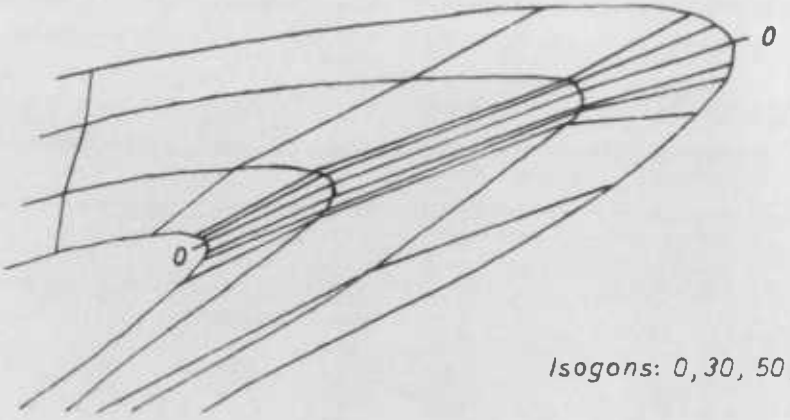

Fig. 3·5 First generation fold with Class 2-1C layer geometry. The fold is part of the refolded structure shown in Fig. 3·3.

Fig. 3·6 Isoclinal first generation fold with buckled quartz-carbonate layers in the fold core. Note the shape of the buckled layers, pinched inner and rounded outer arcs (Class 1C geometry). Black garnet schist series; Val Piora, MR.6969215569.

of the cover must also have taken place. This view is further justified by the disrupted fold structures already mentioned.

The contact between the allochthonous Pennine and authochthonous Gotthard Massif metasediments, which represents the line of a major tectonic discontinuity (Jung, 1963; Baumer, 1964; Frey, 1967), is found in the Val Piora area to be approximately parallel to the first foliation and therefore appears to be related to this structure. The interpretation of this relationship is that the overthrusting of the Pennine metasediments onto the authochthonous cover of the Gotthard Massif was accompanied in both metasediment series by intensive folding and slicing, a new foliation developing parallel to the plane of the major discontinuity.

In the region east of Lukmanier the junction of the two metasediment facies is marked by a thin zone of Triassic rocks (Grenztrias (Frey, 1967, p. 88)). The Grenztrias is absent in the Val Piora area (Section 2.22) except for one isolated exposure of Rauhwacke on Alpe di Lago. Within the Pennine metasediments themselves however Rauhwacke horizons are found, some of which may be interpreted to mark tectonic discontinuities of first deformation age. Others are clearly related to discontinuities of second deformation age (Section 3.22). The prominent Rauhwacke horizon crossing Alpe di Lago and Pso. di Camoghe and a Rauhwacke sliver which appears on the south ridge of Camoghe at 2260 metres (cf. Frey, 1967, p. 71), probably mark discontinuities of first deformation age. These horizons are traced with difficulty in the southeast face of Camoghe, partly because they appear here only as lenses, the southern horizon being much reduced in thickness, and partly because they are folded by second generation structures. Further to the east the contact between allochthonous Pennine and authochthonous Gotthard Massif metasediments is also seen to be folded by second structures (Encls. 1 and 2).

3.22) The second episode of Alpine deformation

Folds formed during the second episode of deformation (Fig. 3.7) are found on a variety of scales, wavelengths vary from less than a

millimetre to hundreds of metres. The folds have interlimb angles which are close to tight, axial surfaces which are moderately inclined to upright and fold hinges which are moderately plunging to vertical. A rodding structure which parallels the fold hinges is often developed in the cores of second generation folds.

A feature of these folds, and probably of folds in general, is their changing geometry. When traced along their axial surfaces they change their amplitude and eventually die out. Folds showing this feature have been noted before (Ramsay, 1962, Fig. 8; 1967, Fig. 7.12). The implications of this variable geometry are that fold axes and axial surfaces converge and can be curved. This is discussed further in Section 3.6.

A cleavage is often found sub-parallel to the axial surfaces of the second folds. In many cases it is formed by a preferred crystallographic orientation of both white mica and biotite, which are also dimensionally oriented within the cleavage plane and hence lineated. The axial plane growth of micas is most clearly seen in thin section and can appear relatively poor in the field because of overprinting by later mineral growth. In other cases, especially in rocks which are rich in mica, a strain slip cleavage is developed or the first foliation is merely crenulated with little sign even in thin section of an axial plane orientation of mica. Undoubtedly composition exercises a strong control on the type of structure that forms, a feature observed in the other tectonic units (Sections 3.32, 3.42). There is little tendency for non-platy minerals to be flattened in the axial plane. In the main the quartz and calcite dimensional fabrics in folded layers and segregations are equidimensional polygonal grain aggregates typical of annealing recrystallisation (Voll, 1960; Rast, 1965). Rarely segregations or veins appear parallel to, or fanning about, the axial surfaces of folded calcareous layers and lenses. The segregations are either of calcite and of coarser grain size than the matrix or of quartz (Fig. 3.8).

The overall geometry of the second generation folds closely approaches that of the similar fold model, however detailed examination

Fig. 3.7. Second generation folds. Black garnet schist series. Alpe Ritom, M.R. 6956515552.

Fig. 3.8. Carbonate segregations in the axial planes of second generation folds. Black garnet schist series; Alpe Ritom, M.R. 6956415552.

of the individual folded layers, both visually and using isogon techniques, indicates that these often show either distinct Class 3 or 1.C. geometry (Figs. 3.9, 3.10). Fanning of the axial surfaces of both harmonic and disharmonic high order folds about lower order structures and less commonly weakly convergent cleavage fans in Class 1.C. layers give further evidence for buckling or non-passive layer behaviour during the folding process (Ramsay, 1967, p. 404).

The attitude of second fold axes and axial surfaces has been recorded where possible in the cover rocks. Despite the variable geometry of second folds both these structural elements are relatively constant in attitude within a given sub-area. The direction of plunge of the fold axes varies between northwest and northeast, except in Val Leventina where plunges become irregular as the axial surfaces become vertical. The axial surfaces dip in a north to northwesterly direction. The relevant structural data is summarised in Encl.3, in the sub-area stereograms and axial surface/cleavage trend map.

By recording the symmetry of second folds, together with the attitude of the first foliation, the geometry of the major structures of second deformation age has been established. Over most of the area mapped fold symmetry remains constant. In Val Leventina northerly dipping second fold axial surfaces cut consistently across a northeasterly dipping first foliation. In Val Canaria the same second fold symmetry is observed and found to remain constant across the thin strip of Bünderschiefer, which is sandwiched between thick Triassic marbles. There is therefore no evidence that this structure, which has been interpreted both as a synform (Grünbenmann, 1888; Krige, 1918) and as a fault bounded slice (Bonney, 1890) represents a synform of second deformation age.

The broadly synformal nature of the metasediments of Val Piora is generally accepted (Krige, 1918; Gansser and Dal Vesco, 1964). It is proposed to examine the form of this synformal structure more closely. Only in the region north and west of Lago Ritom do significant changes in second fold symmetry occur. The interpretation of structure in this region is shown by the first foliation trend map (Encl. 2).

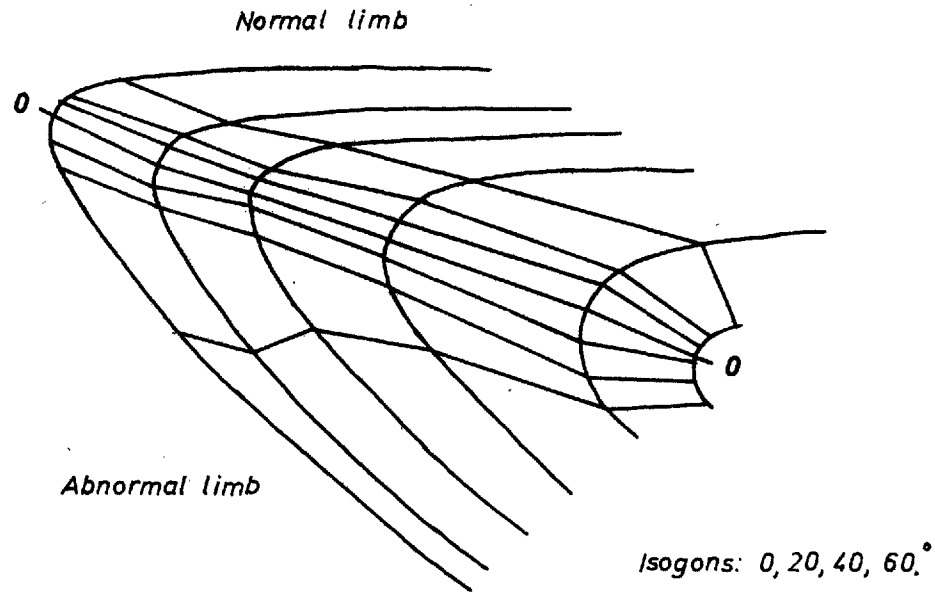

Fig. 3·9 Second generation fold with Class 1C-2 layer geometry.
Quartenschiefer; west end of Lago Ritom, MR. 6947315468.

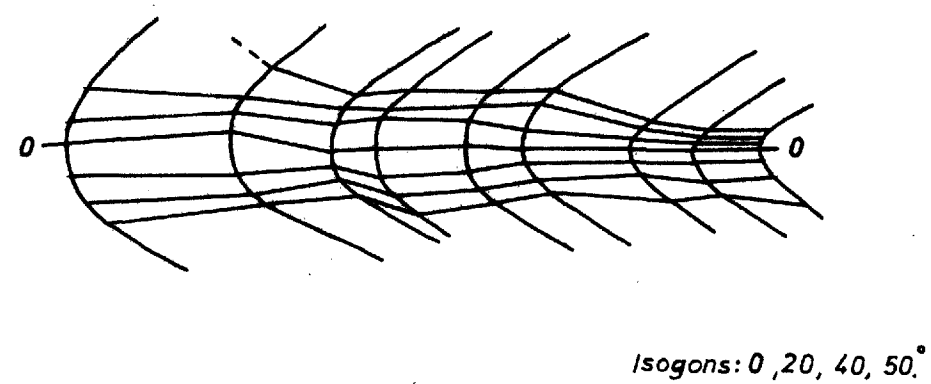

Fig. 3·10 Second generation fold with Class 1C-2-3 layer geometry.
Black garnet schist series; Alpe Ritom, MR. 6956515552.

Considering first the area immediately east of Lago Ritom; there is no change in second fold symmetry in the metasediments lying between the Triassic marbles bounding the southern margin of the Gotthard Massif and the northern margin of the Lukmanier Massif. The symmetry of the second folds is the same as that observed in Val Leventina and Val Canaria. This situation is also though less obviously the case in the much thinned continuation of these metasediments in eastern Val Piora. Towards the east second folds become tighter and the angle between first foliation and second generation cleavage correspondingly reduced, so that the symmetry of structures becomes difficult to recognise. Chadwick's interpretation of the metasediments as a Phase B (Section 3.8) synformal fold core is however not supported by field observations. The lithological and first foliation trend maps (Encls. 1 and 2) show the metasediments in the region north of Lago Ritom to be complexly folded. Although changes in second fold symmetry occur, nowhere here is the southern limb of a major synform seen. Apparent from the trend map is the changing geometry of the second folds when traced along their axial surfaces, a feature noted in the description of the minor structures.

Only in the region west of Lago Ritom are traces of the southern limb of a major structure found. Passing southwards across the prominent Rauhwacke horizon which crosses the Btta. di Föisc, the symmetry of the second folds changes sharply (Encl. 2). Somewhat further to the south in the cliffs above the western end of Lago Ritom the fold symmetry changes once more, again on crossing a thin Rauhwacke horizon, which dies out to the southwest (Encl. 2). These sharp changes in fold symmetry across Rauhwacke horizons are significant. Some Rauhwacke horizons have been shown to mark tectonic discontinuities formed during the first deformation; it seems probable that others represent similar structures related to the second. This interpretation is strengthened by the fact that the latter horizons are not folded by second folds and the fact that they are in many instances oblique to first foliation. They appear to closely parallel the second cleavage, which suggests that they can be interpreted as marking tectonic slides (Fleuty, 1964b).

Having established the general pattern of the second deformation other structural features lend themselves to interpretation in the same way. A number of different slides are recognised both between cover and cover and basement and cover. The relevant characteristics of the individual structures are summarised below, and in Enclosures 2 and 3. These structures which are best seen in the relatively well exposed region west and south of Lago Ritom cannot all be traced with certainty in the poorly exposed ground further west.

Cover - cover slides.

Slide AA' - This slide zone is marked by a Rauhwacke marble horizon across which fold symmetry changes. Rocks lying to the north belong to the northern limb of the Piora structure.

Slide BB' - Some few metres below the Rauhwacke horizon marking AA' another parallel but thinner horizon is seen (Encl. 1). This presumably represents the line of another discordance. There is no change in fold symmetry across this latter structure.

Slide CC' - As the previously described slides this structure is marked by a Rauhwacke horizon, though only locally. Otherwise it coincides with a change in fold symmetry.

Slide DD' - Although there is no change in fold symmetry, this structure is suggested, by the flat lying Rauhwacke Quartenschiefer contact in the cliffs forming the west face of Föisc, and the form of the isolated exposures of black garnet schist series rocks south of the summit of Föisc. This slide appears to cut across EE' (Encl. 2) and itself to be cut off in the east, as the slides AA', BB' and CC', by slide FF'.

Basement - cover slides

The attitude of the basement - cover slides differs from that of the cover - cover slides in that it is determined by the second cleavage in the basement. This is seen to be significantly oblique to that in the cover in the region southwest of Lago Ritom (Encl. 3).

Slide EE' - Along the line of slide EE' a thin slice of cover rocks, Rauhwacke marble and basal Triassic quartzite, is found. The arrangement of cover rocks within this slice is not symmetric (Encl. 1) as

expected in a fold and the lithologies of the basement not only change across the slice but also show minor second folds of the same symmetry.

Slide FF' - South of the slide DD' the cover rocks appear to be folded as a synform in the gneisses of the Lukmanier Massif (Krige, 1918; Gansser and Dal Vesco, 1964). Closer analysis of the second fold symmetry in the cover rocks of this structure show that there is no change across it. A change occurs at the cover-basement contact and at the continuation of this contact within the basement. This relationship can be interpreted by a slide at the cover-basement contact.

Slide GG' - In the area east of Lago Ritom the contact of the Lukmanier Massif with the cover has been interpreted as a slide. The slide zone is marked by the Rauhwacke marble horizon (Encls. 1, 2 and 3). This interpretation is based on the following observations. The contact is closely parallel to the second cleavage in the basement (Encl. 3) and is not folded along this part of its length by second structures (cf. Chadwick, 1965, 1968). The overall symmetry of the second folds appears to change on passing from cover to basement. This slide is probably continuous with AA'.

Other slide structures observed between the Lukmanier Massif and the cover at the western termination of the Massif are discussed later (Section 3.42).

Slide HH' - The contact between the Gotthard Massif and the cover is interpreted as a slide in the same way as that between Lukmanier Massif and cover. The slide zone is in this instance marked by a thick Triassic marble horizon, which is noticably discordant to foliation in the Quartenschiefer and black garnet schist series rocks in the region to the north of Lago Ritom, and is not folded by second folds (Encl. 2). East of Alpe Piora the marble marking the slide zone is probably in contact with marble, hence the increase in thickness to the east, and the contact between marble and Quartenschiefer is probably stratigraphic (Encl. 3).

Two wedges of cover rocks are found in the Lukmanier gneisses on the south side of Lago Ritom. These are not clearly interpreted

as infolds of cover in folded basement, as folds of cover in basement determined by block movements in the basement or as slices of cover in basement arising from sliding of basement and cover. In view of the discussion above, it seems likely that sliding has played an important part in their development, and also probably accounts for much of the lithological complexity of the basement rocks surrounding them (Encls. 1 and 2).

The effects of the second episode of deformation on the cover rocks can be summarised. The metasediments in Val Piora cannot be considered to form a simple reclined synform between the Gotthard and Lukmanier basement gneisses. The southern limb of such a structure is either missing (east of Lago Ritom), or intensely modified by tectonic sliding (south and west of Lago Ritom), which involves both basement and cover. In the eastern extension of this structure in Val Canaria only elements belonging to the northern limb are recognised. The northern contact of the Piora structure with the Gotthard Massif has also been shown to be determined by a slide. Second folds in the metasediments of Val Leventina have consistently the same sense as those on the northern limb of the Val Piora structure.

3.23) The third episode of Alpine deformation

Linear mineral fabrics are well developed in both the cover and basement rocks of the Val Piora and adjacent areas (Steiger, 1962; Higgins, 1964b; Chadwick, 1965; Kvale, 1966). In sections 3.21 and 3.22 it has already been noted that micas lying within the first and second generation foliation planes are dimensionally oriented and hence lineated. These lineations are sub-parallel to one another, but generally oblique to second fold axes and cannot be explained by intersection of the two foliations. Other micas, which grow across first and second planar structures, are also lineated; they show a complete girdle or L. tectonite fabric (Flinn, 1965) and are dimensionally oriented parallel to the girdle fabric axis. This axis is also generally oblique to the second fold axis but is close in orientation to the other lineations and therefore to the first and second foliation planes. The complete girdle fabric is often well demonstrated

by porphyroblastic biotite crystals and can usually be identified in the field. In the case of white mica it can only clearly be recognised in oriented thin sections.

The development of the L. tectonite fabric is variable, even on the scale of a thin section, and depends on the degree to which pre-existing fabrics have been destroyed by recrystallisation and the growth of new minerals. The linear fabrics are not confined to micas. Ilmenite, which is of platy habit, shows an L. tectonite fabric and kyanite a preferred orientation of c axes.

There is good evidence that these lineations represent extension directions. Quartz pressure shadows are elongate and mineral aggregates streaked out parallel to them. In areas adjacent to Val Piora they have been shown to record the X axis of deformed objects (Higgins, 1964b, Chadwick, 1965).

With due regard to the effects of later folding and slumping all the linear mineral fabrics have a remarkably constant north-south orientation throughout the area (Encl. 6).

Flinn (1965) has argued that the shape of the deformation ellipsoid should be reflected in the mineral fabric. Thus, rocks which have suffered pure constrictional deformation ($k = \infty$) can be expected to have complete girdle mica fabrics (L. tectonite fabrics), rocks which have undergone pure flattening ($k = 0$), planar mica fabrics (S. tectonite fabrics) and rocks which have suffered an intermediate type of deformation ($\infty > k > 0$), partial girdle fabrics (LS. tectonite fabrics). These fabrics appear in the field as the structural elements: lineation, schistosity, and lineation together with schistosity. Flinn's analysis becomes more complicated in naturally deformed rocks which have suffered polyphase deformation. In this case the total tectonic mica fabric (this excludes elements of the total fabric resulting from static growth and/or recrystallisation) is in general made up of a number of part fabrics, developed to varying degrees and formed during separate episodes or increments of deformation (e.g. in the Val Piora area, first foliation, second foliation and the L. tectonite mica fabric). Early part fabrics are of course modified and

in some instances destroyed by later episodes of deformation which have been accompanied by recrystallisation and/or new mineral growth.

How then are the mica lineations within the first and second foliations in the Val Piora rocks to be interpreted. Are they features of the original first and second part fabrics or have they arisen through modification of these original part fabrics by later episodes of deformation? There are three possible interpretations that can be made:-

1) The mica lineations within the first and second foliations, formed at the same time as their respective planar structures, are of different ages. Both first and second foliation lineated micas are older than the L. tectonite mica fabric.

2) The mica lineations within the first and second foliations are modifications of these foliations, arising from a later episode of pure constrictional deformation which gave rise to the L. tectonite mica fabric. Thus they record the (2D) principal extension directions, X' directions, within the first and second foliation planes.

3) The mica lineations within the first and second foliations were formed at the same time, during the second episode of deformation. The L. tectonite mica fabric developed during a later, third, episode of deformation. In this case, the second foliation can be assumed to represent the XY plane of the second episode strain ellipsoid and the mica lineation within this plane therefore records X (the 3D principal extension direction of this ellipsoid). The lineation within the first foliation represents the (2D) principal extension direction X' within this second generation folded surface.

The first of these possibilities requires that folds of second deformation age should fold an earlier linear mica fabric. There is no evidence for this and therefore the hypothesis is rejected. The other two hypotheses will now be examined by considering the geometric consequences of imposing a strain on a set of earlier planar structures.

Flinn (1962) has shown that the (2D) principal directions of strain within a plane of any orientation in relation to the (3D) principal axes of the strain ellipsoid may be found simply by the Fresnel construction. For a set of planes of differing orientation related to a common axis the loci of the (2D) principal directions within these planes give rise to (2D) principal direction curves. In Fig. 3.11a (2D) principal direction curves have been constructed for values of $2V_X$ = 0 degrees and $2V_X$ = 140 degrees for a set of planes related to a common axis, which lies at 60 degrees to X in the XY plane of the strain ellipsoid. The choice of these particular values will be justified in the further discussion. It is seen from the loci of X' (the polar (2D) principal direction curve, which also contains X and the common axis of the planes), that in the case where $2V_X$ = 140 degrees, X' rotates in planes of increasing angular departure from X or the XY plane, initially rapidly towards the common axis. In the case where $2V_X$ = 0 degrees the angular difference between the common axis and X' is initially retained. This observation forms the basis for the further interpretation of the origin of the mica lineations observed in the Val Piora rocks.

The magnitude of X' (also Z', X'/Z') depends both on the shape of the ellipsoid (X/Y, Y/Z) and the orientation of the plane containing X' (and Z') within the ellipsoid. Thus, as X' rotates towards the fold axis in successive planes (Fig. 3.11a), it changes its magnitude. Though at X it is a direction of extension it may become a direction of contraction. The behaviour of X' (and Z') is determined by the lines of no finite and no infinitesimal strain of the strain ellipsoid (Flinn, 1962, p. 403-407). In the following discussion X' is considered always as the direction of greatest extension. This is not unreasonable in planes with small angular difference to X and the XY plane.

It has been noted that the mica lineations (X' principal directions) within the first and second foliation planes, which may be considered to form a set of planes of restricted orientation about the second fold axis, do not differ greatly in orientation from one

Fig. 3.11a. (2D) principal direction curves (X', polar principle direction curve and Z', equatorial principle direction curve) for a set of planes, related to an axis at 60 degrees to X in the XY plane of the ellipsoid, constructed for values of $2V_X$ = 0 degrees and $2V_X$ = 140 degrees. The curves are symmetrical across the XY plane and are only illustrated for half the possible planar orientations in each case.

Fig. 3.11b. Partial X' (2D) principle direction curves for values of $2V_X$ = 0 degrees and $2V_X$ = 140 degrees, reconstructed to 'fit' the Piora situation. The second generation fold axis (F.A.) lies at 30 degrees to Y in the XY plane of the ellipsoid. X' principle directions in planes covering the general range of planar orientations observed in much of the Val Piora area are illustrated. If these directions determine the orientations of the mica lineation observed in the plane of the first foliation, then in the case $2V_X$ = 0 degrees the measured orientations of the mica lineation should plot as a group distinct from the second fold axis, whereas in the case $2V_X$ = 140 degrees they will plot as a group spreading between X and the second fold axis. Comparison of this Fig. with Encls. 3 and 6 shows that the former case, $2V_X$ = 0 degrees, is realised.

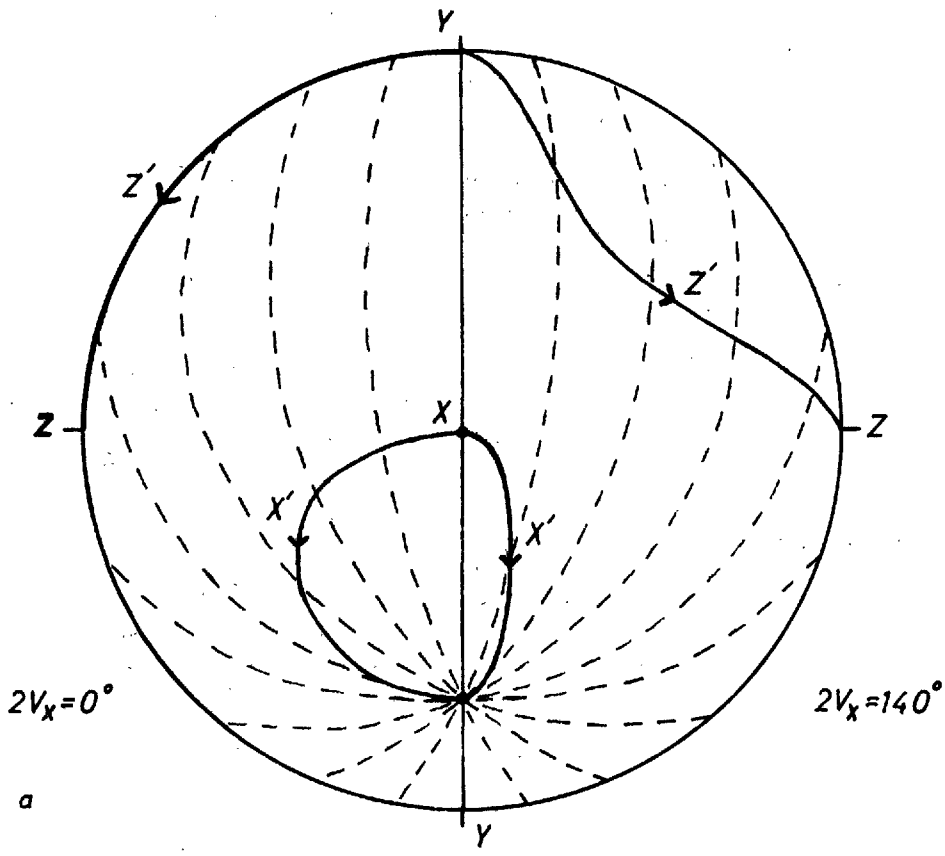

Fig. 3·11 a

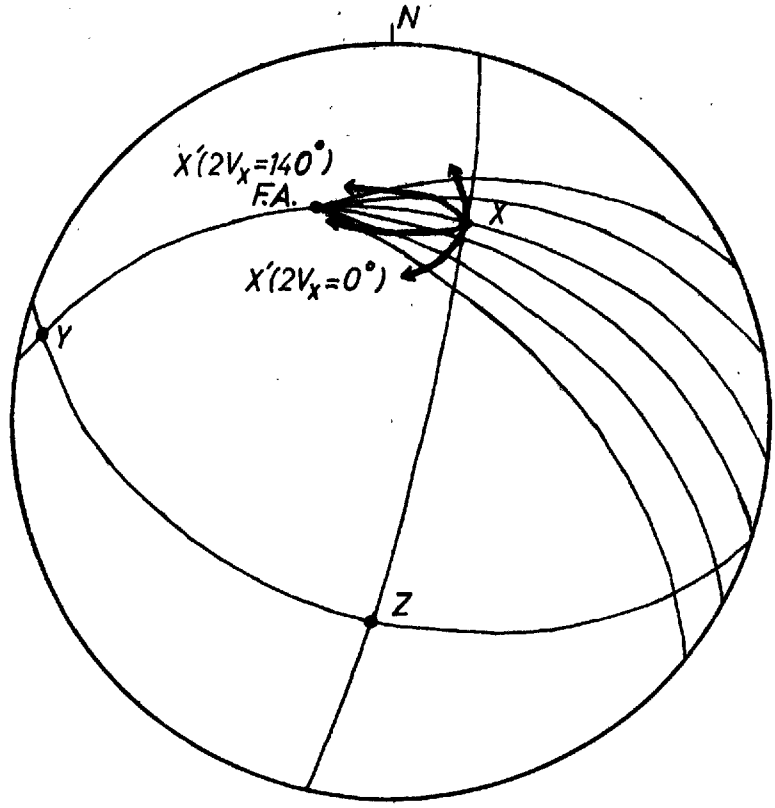

Fig. 3·11 b

another or from the axis of the L. tectonite mica fabric. Angular differences between the lineations and the second fold axis are retained. This pattern of X' (2D) principal directions conforms with that predicted when the axis of the L. tectonite mica fabric is interpreted as the X axis of a strain ellipsoid whose $2V_X = 0$ (Fig. 3.11a and b) and hence an ellipsoid of pure constrictional ($k = \infty$), type (cf. Fig. 3.12). The second of the hypotheses outlined above, that the mica lineations within the first and second foliations are modifications of these foliations produced by a later episode of pure constrictional deformation, is therefore a geometric possibility.

The third hypothesis outlined above, that the mica lineations within the first and second foliations were formed at the same time during the second episode of deformation, will now be examined. If the second foliation represents the XY plane of the second episode strain ellipsoid and the mica lineation within this surface defines the X direction of this strain, the orientations of the X' (2D) principal directions in folded first foliation surfaces can be determined for different values of $2V_X$. The formation of a foliation with a lineation (LS. tectonite fabric) during the second episode of deformation suggests that the strain ellipsoid, which gave rise to this fabric, had an intermediate k value (Flinn, 1965) and hence for a moderate amount of strain a large $2V_X$, (Fig. 3.12). The case $2V_X = 140$ degrees has been discussed and the rapid rotation towards the common axis of the X' (2D) principal directions in planes of increasing angular difference to the XY plane of the ellipsoid noted (Fig. 3.11a and b). A marked divergence is then to be expected between the X (3D) principal direction in the second foliation (second fold axial plane) and the X' (2D) principal directions in the first foliation (second fold limbs), where an angular difference exists between these surfaces and where their common axis (second fold axis) lies oblique to X. No such divergence is observed in the Val Piora rocks and on this basis this interpretation of the mica lineations is considered to be untenable.

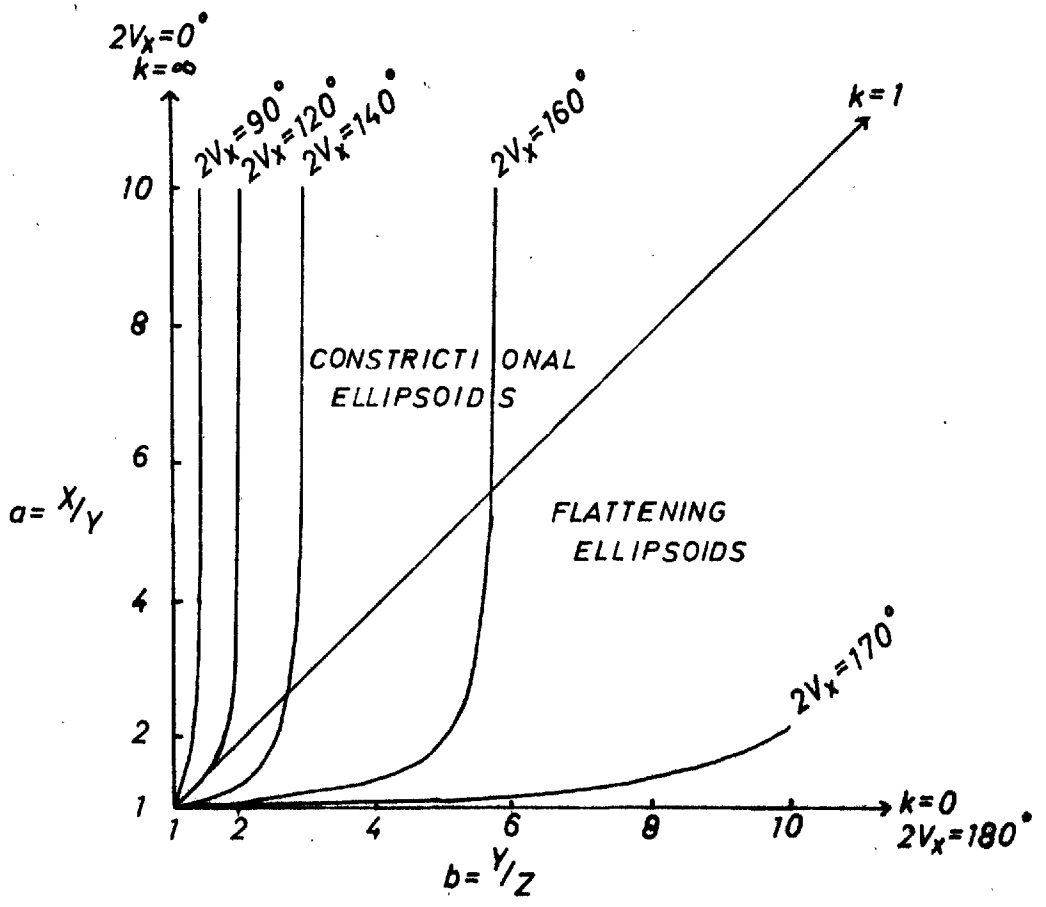

Fig. 3·12 *Flinn's deformation plot. Note the modified terminology; ellipsoid axes, X>Y>Z. V_x = angle between X and the pole to a circular section.*

Flinn (1962, p. 404) has pointed out that the principal directions within a plane are directions of potential fold hinges or boudinage axes. If the hypothesis of pure constrictional deformation ($k = \infty$) is accepted, then the X' (2D) principal direction will be an axis of folding during progressive deformation and the Z' (2D) principal direction either an axis of folding or boudinage (Flinn, 1962, p. 408). For planes containing X or at a low angle to X (as in the rocks of the Val Piora area) the Z' (2D) principal direction will be an axis of boudinage.

Folds whose axes are parallel to the mica lineations are found within the area. Their occurrence is rare; they are confined to rocks rich in mica with a well developed planar structure. Wavelengths and amplitudes are in the centimetre to millimetre range and axial surfaces are sub-vertical and sub-perpendicular to first foliation. Boudinage structures with axes sub-perpendicular to the mineral lineation (i.e. sub-parallel to Z') also exist. However, these appear in most cases to be later than the mineral lineation, (Section 3.24). There is therefore evidence for the fold if not the boudinage structures which might be expected to result from a pure constrictional deformation.

In the analysis of the mica lineations only the total strain relating to the third (L. tectonite mica fabric forming) episode of deformation has until now been considered. There has been no discussion of the strain history. It is possible to develop a strain ellipsoid by a multitude of different strain paths and it is certain that rotational strain is an important quantity in natural deformation. In general the determination of the rotational component in naturally deformed material is impossible as initial orientations are unknown (Chapple, 1968). Evidence for a rotational component may however be obtained where rotations* shown by rigid particles, for instance snowball garnets, exceed 90 degrees (Section 5.8).

---

* Differential rotations of particles and their matrix.

Study of the relationships between deformation and mineral growth (Section 4.2) has shown that snowball garnets grew and rotated during the third episode deformation, which also gave rise to the mica lineations. Rotation axes appear to have remained constant during growth and sub-perpendicular to the mica lineations. Rotations of up to 160 degrees are observed. In some cases rotation has taken place after growth and can be attributed to the effects of the fourth episode of deformation (Section 3.24). The sense of rotation is constant throughout the area both in the cover and basement rocks.

Certain observations have been made which place restrictions on the third episode rotational strain path.

In the discussion above reference has been made to the role of (2D) principal directions in different planes, in determining the directions along which structures are generated. During progressive deformation these directions in general change as the plane containing them changes in attitude. The structural movement paths* of the principal directions and those of the structures (fold hinges and boudinage axes) generated at them in general diverge (Flinn, 1962, p. 408; Ramsay, 1967, pp. 174-177). However, poles to planes and structural directions contained by symmetry planes of the ellipsoid will remain in these symmetry planes during progressive irrotational deformation. Under these conditions structural movement paths of principal directions and structures will coincide. (For uniaxial ellipsoids, $k = \infty$ and $k = 0$, all planes containing the unique symmetry axis are planes of symmetry (Flinn, 1962, p. 407)). Where the strain is rotational the structural movement paths only coincide when the plane containing the principal directions also contains the axis relating successive increments of rotational strain. This axis must in turn be coincident with one of the principal axes of both the finite and all the incremental strain ellipsoids. This point may be

---

* The paths taken by planar (foliations) and linear elements (fold hinges, boudinage axes and (2D) principal directions) in moving from their initial to their final orientations during progressive deformation.

illustrated by considering (3D) simple shear, in which successive increments of rotational strain are related by a rotation about the Y principal strain axis. The structural movement paths will be coincident only in planes which contain the Y principal strain axis of the finite and all the incremental strain ellipsoids.

The fact that the crystal rotation axes remain constant, that the form of the pressure shadows is not sigmoidal, and that fold axes are found parallel to the mineral lineation, suggests that the structural movement paths were approximately coincident during the third episode of deformation (i.e. the principal directions remained constant in attitude within the planes throughout deformation).

The restriction placed on the deformation path therefore is that structural movement paths should be approximately coincident and that the third episode strain ellipsoid should be of pure constrictional ($k = \infty$) type. For the perfect coincidence of structural movement paths during rotational deformation the possible orientations of planes in relation to finite and incremental strain axes is extremely limited (i.e. in the case of 3D simple shear, described above). However, where orientations are less specific, it is probable that structural movement paths will coincide approximately for certain conditions of strain. Thus where successive increments of rotational strain are of a pure constrictional type and related by an axis of rotation in the ZY plane of the ellipsoid, structural movement paths will be approximately coincident for planes whose intersection with the ZY plane is close to the axis of rotation. The superposition of strain increments of this type in the manner outlined above does not lead to a finite strain ellipsoid of pure constrictional type ($k = \infty$) (Fig. 3.13a). To achieve a pure constrictional finite strain successive increments are necessarily constrictional strains, of the type, $\infty > k > 1$, and the Y axis is the axis of rotation relating these increments. It should also be noted, that as the angle between the finite and incremental strain axes diverges successive increments must necessarily have progressively decreasing k values (Fig. 3.13b). The postulated relationships between the third episode total strain and incremental

Fig. 3.13. The Flinn plot (Fig. 3.12), is used diagrammatically to illustrate how superposition of different strain increments during progressive rotational deformation can influence the strain path. Successive increments are related by a rotation about the Y principal strain axis. In 3.13a increments are of pure constrictional type ($k = \infty$), whereas in 3.13b though the initial increment is pure constriction and the finite strain is pure constriction successive increments are dissimilar and show progressively decreasing k values.

Fig. 3.14. Postulated relationship between the third deformation finite and incremental strain axes (X_f, Y_f, Z_f and X_i, Y_i, Z_i), the principal directions of strain in the plane of the first foliation (X' and Z'), the mineral lineation, the crystal rotation axes and the sense of crystal rotation, the pressure shadows and the third generation folds which parallel the mineral lineation.

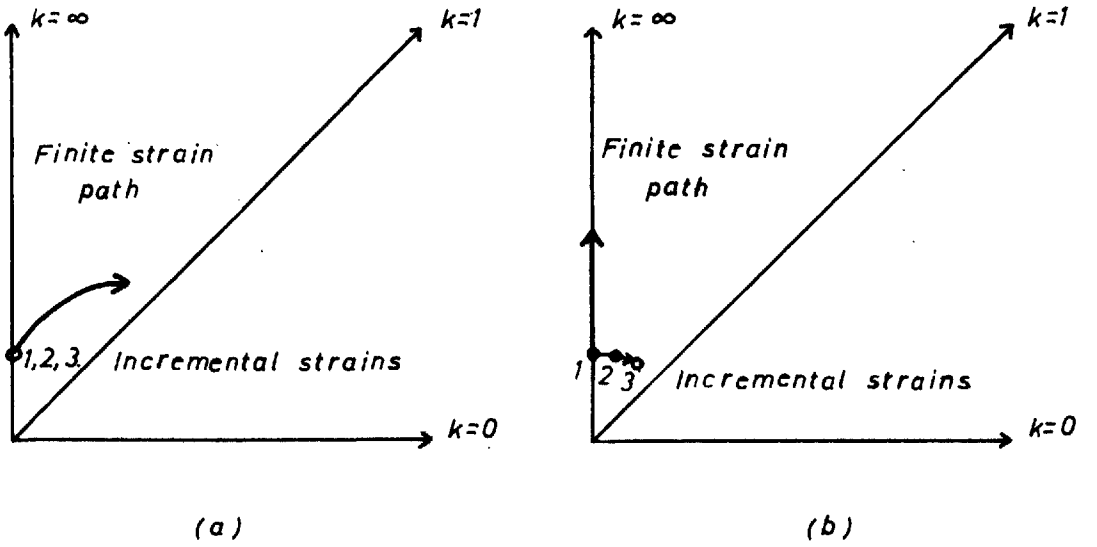

Fig. 3·13

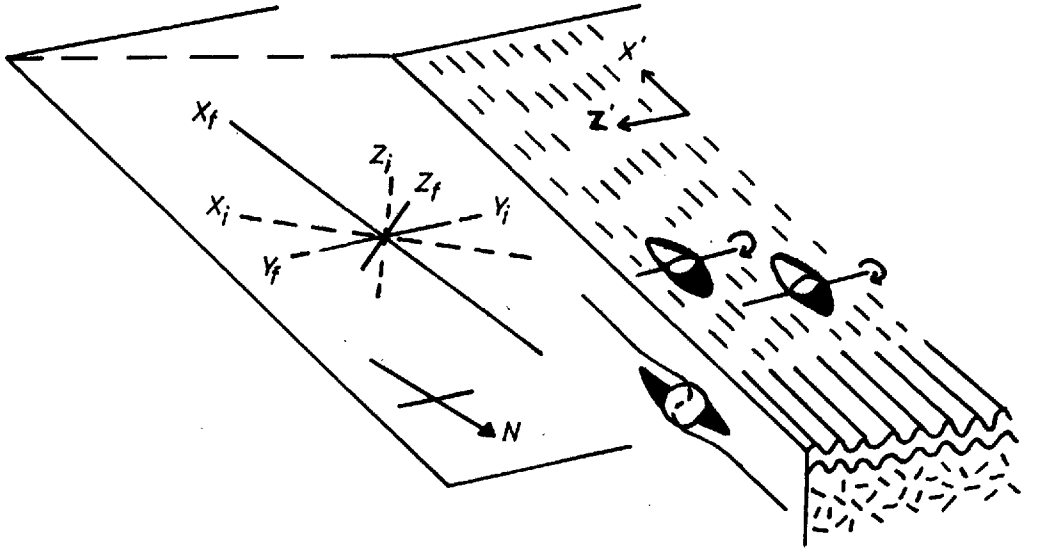

Fig. 3·14

strain axes and the different structures produced during the third deformation are summarised in Fig. 3.14.

The general absence of structures of third deformation age (folds are rare and boudinage structures which are indisputably of this age absent) suggests that while the body rotation component of the third episode strain may have been large, the distortional component may have been small. This apart, the conditions of rising temperature under which deformation took place (Section 4.5) may have had the effect of reducing ductility contrasts so that significant amounts of strain were accommodated homogeneously.

3.24) The fourth episode of Alpine deformation

Only minor fourth generation folds, with wavelengths varying from less than a millimetre to a few metres are found in the cover rocks (Fig. 3.15). These folds are typified by interlimb angles which are close to open, axial surfaces which are moderately to gently inclined in a north-northeasterly direction and fold hinges which are sub-horizontal to gently plunging east or west (Encl. 6). Fourth folds show changing geometry, when traced along their axial surfaces; fold hinges and axial surfaces often appear gently curved.

There is seldom an axial plane cleavage associated with these folds; however, in those cases where there is, it is always of strain slip type. Rast (1965, p. 89, Fig. 4) has suggested that the compositional variation of quartz and mica which reflects this type of structure arises from the preferred regeneration of mica in the zones of maximum flexure of crenulations. Rickard (1961) and Nicholson (1966) on the other hand consider that the basis for this compositional variation is the solution of quartz and preferred migration of silica as opposed to alumina (or more strictly mica forming components) from the crenulation limbs to the crenulation hinges. It is possible in the rocks of the Val Piora area to observe strain slip cleavage at all stages of development and it is apparent that little if any new mica has been generated (Fig. 3.16). The structure, in this case at least, has arisen in the manner suggested by Rickard and Nicholson. A thermodynamic basis for preferred migration has been established

Fig. 3.15.

Fourth generation folds. Quartenschiefer, Costa Giubin, Val Piora; M.R. 6985215543.

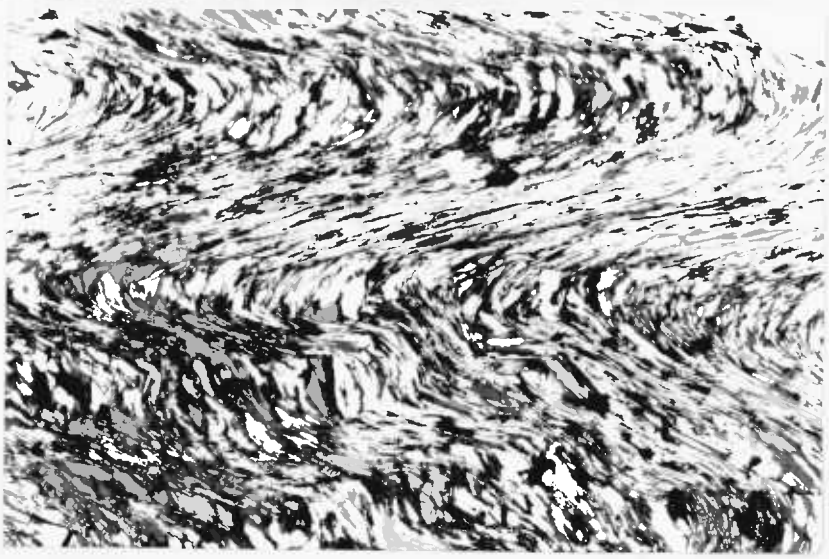

Fig. 3.16. Photomicrograph of fourth generation crenulations. Note the concentration of quartz in the crenulation cores. There is no evidence of the formation of new mica. Quartenschiefer, La Motta. (x 12).

(Gresens, 1966a) and Carmichael (1969) has put forward convincing arguments for the relative immobility of alumina in relation to silica. The zones of alumina concentration which arise on the crenulation limbs may subsequently form the loci for recrystallisation of mica and for the preferred nucleation of alumina rich minerals (Section 4.2, Fig. 4.3). Ramsay (1967, p. 388) has suggested that the spacing of the crenulations is controlled by the initial wavelength of buckled competent layers in the sequence and the amount to which this wavelength has been modified by later compressive strain. The positions of crenulations may also be governed by porphyroblast minerals and in this case the spacing is dependent on the size and concentration of these minerals (Fig. 3.17).

Although the overall geometry of fourth folds approaches the similar fold model the geometry of individual layers departs from true similar more obviously than with those making up second folds. The fourth folds are made up of Class 1.C. and 3 layer associations. The geometry of folded pelitic layers, (kyanite-epidote rich layers) in the Quartenschiefer rocks is particularly close to that of pure buckle folds (Fig. 3.18). The buckles are often disharmonic and have shapes which are reminiscent of the elasticas, frequently shown by ptygmatic veins, indicating a large wavelength/thickness ratio and hence a large ductility contrast between the layer and its matrix (Ramberg, 1960, 1961). The more obvious buckling behaviour of these layers during the fourth episode of deformation, relative to that during the second episode of deformation, reflects an increasing ductility contrast between the layers and their matrix arising from metamorphic mineral changes within the layers (growth of kyanite and epidote) between the episodes of deformation.

Fourth folds deform the third episode mineral lineations. Measurements of the locus of this folded lineation show that it approximates to a great circle (Fig. 3.19). Ramsay (1960; 1967, pp. 469-482) has shown the great circle type of locus to be a characteristic of similar folding. Where a non-similar or buckling component is present in the fold formation departures from a great

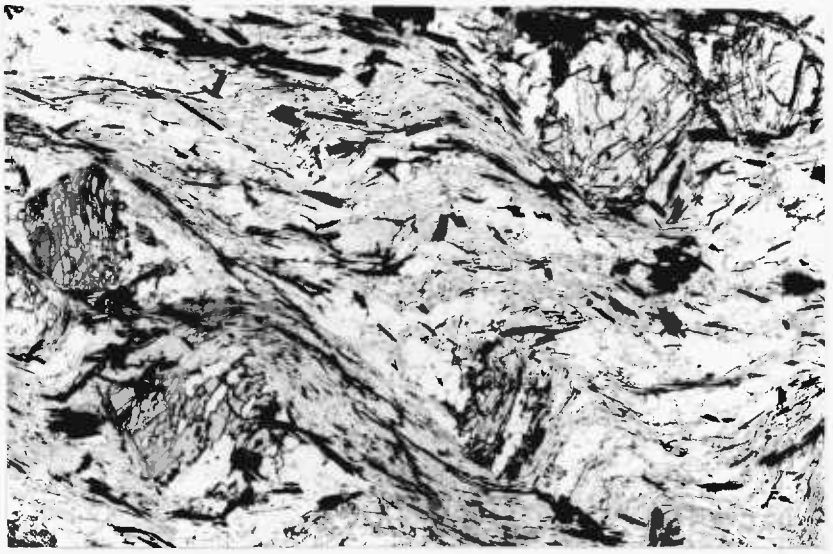

Fig. 3.17. Photomicrograph of pre-tectonic garnet prophyroblasts influencing the positions of crenulations. The example is taken from Lukmanier Massif and the crenulations are probably of second deformation age. Orange Group gneiss Sotto Nante, M.R. 6906215310. (x 15).

Fig. 3.18. Fourth generation structures showing disharmonically buckled kyanite-epidote layers. Quartenschiefer, Costa Giubin, Val Piora; M.R. 6981315541.

Fig. 3.19. Relationship between the deformed lineation locus, the fourth generation fold axis and axial plane and the 'a' direction. If the fourth fold axial plane represents the XY plane of the ellipsoid and the fold axis coincides with the Y principal strain axis then X is found to be approximately coincident with 'a'. Also apparent is the small angular difference, α, between the Z axis and the lineation locus plane. Typical example of lineation deformed by a fourth generation fold. Bünderschiefer. Val Leventina, M.R. 6947515172.

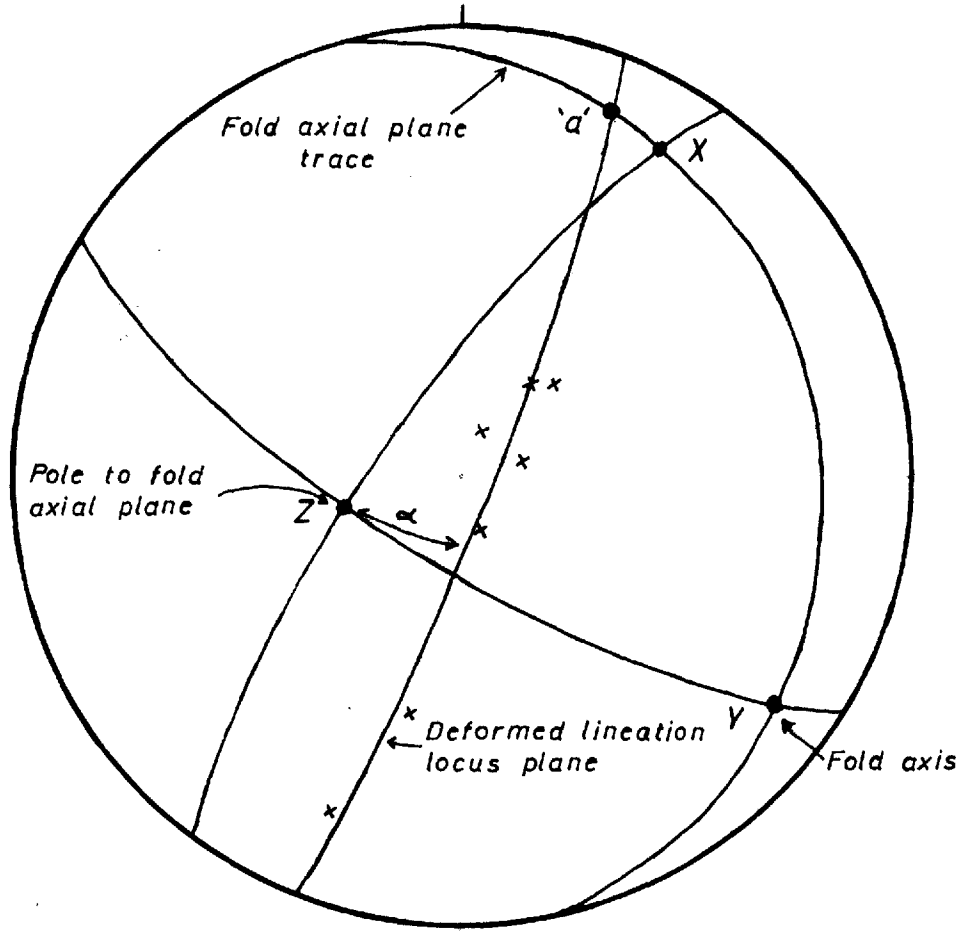
Fold axial plane trace
'a'
X
Pole to fold axial plane
Z
α
Deformed lineation locus plane
Y
Fold axis

Fig. 3·19.

circle locus are to be expected. The recognition of non-similar layer geometry above is indicative of such a component in some layers at least. 'a' shear directions (Ramsay, 1960; 1967, p. 472) have been calculated from a small number of folds by finding the great circle plane of best fit to the deformed lineation locus. The calculated 'a' directions plunge gently north-northeast or south-southwest (Encl. 6). There is some difficulty in equating the non-similar layer geometry of fourth folds with the great circle lineation pattern which is a characteristic of lineations deformed by pure similar folds. This observation is not unique to the fourth generation folds in the Val Piora area, but seems to be a general one in the sense that in many areas great circle loci appear to be associated with folds which are not truely similar. In these circumstances the exact meaning of 'a' becomes uncertain. It is probably also the case that the tendency exists to 'fit' lineations to great circle patterns, where in fact they show departures from this pattern, because methods of field analysis are inadequate to demonstrate such departures.

The aerial distribution of fourth folds is of interest. They are well developed in regions in which first and second foliations are steeply dipping. In regions where dips are less than 50 degrees they are uncommon. The significance of this observation is discussed below.

Both symmetrical and asymmetrical boudinage structures are found in the cover rocks. They are however not particularly common. Whereas the formation of symmetrical structures can be explained by tensional failure on planes at approximately 90 degrees to layering asymmetric structures appear to be caused by shear failure on planes inclined to layering (Section 3.44). The age of the boudins clearly postdates both the first and second episodes of deformation, as structures of these ages are boudinaged (Fig. 3.20). The axes of boudinage structures plunge gently east or west and are sub-perpendicular to the third episode mineral lineation (Encl. 6). Although this might suggest that the two structures are related, especially as the lineation is interpreted as an extension direction, the lineation is found to be deformed by the boudinage structures.

Fig. 3.20. Boudins of fourth deformation age deforming first generation isoclinal folds. Bünderschiefer; western end of Lago Ritom, M.R. 6945515468.

The character of cavity fillings of boudins can be a useful indicator of age. Apart from quartz, carbonate, white mica, chlorite fillings indicative of late metamorphic conditions, quartz-kyanite fillings are observed. Although kyanite occurs as a lineated mineral most kyanite growth appears to have taken place after the third episode of deformation (Section 4.2). Therefore the boudinage structures probably also formed after the third and during the fourth episode of deformation.

Because of the progressive nature of deformation both planes and lines rotate. Directions within planes which are initially shortened may suffer later elongation (Flinn, 1962, p. 402-403). Within the finite strain ellipsoid three distinct fields of behaviour can be recognised:

1) The field of continuous shortening.
2) The field of continous elongation.
3) The field of shortening and later elongation.

These three fields of behaviour represent different structural regimes corresponding to:

1) The field of folding only.
2) The field of boudinage only.
3) The field of initial folding and later boudinage.

This has been illustrated for the simple irrotational and rotational strains, pure shear and simple shear (Ramsay, 1967, pp. 114-120).

Fourth folds are best developed in regions where the first and second foliations are steeply dipping (e.g. in Val Leventina and eastern Val Piora). Boudinage structures, though found in association with fourth folds, are found only where the earlier planar structures are moderately dipping. These observations suggest that, with respect to the fields of behaviour discussed above, the steeply dipping planar structures fall in the field of continuous shortening and the moderately dipping planar structures in the field of initial shortening and later elongation. This interpretation is supported, when the attitude of the planar structures is considered in relation

to the orientation and nature of the fourth episode strain ellipsoid.

There is no direct evidence (fabric) which allows determination of the orientation and shape of the fourth episode strain ellipsoid. Any deductions about these features must be based on the interpretation placed on the fold and boudinage structures.

If the axial surfaces of the fourth folds are considered to define the orientation of the XY plane of this ellipsoid (cf. Cloos, 1947) then to define the orientation of the ellipsoid fully the X axis within this plane must be known.

The observation that fourth fold axes in the cover rocks are often sub-parallel to fourth generation boudinage axes (this is much more clearly seen in the Lukmanier Massif in eastern Val Piora) suggests that the layering had a specialised orientation to the (3D) principal strain axes during the fourth episode of deformation. Flinn (1962, p. 407) has shown that an axis of folding may become an axis of boudinage during progressive irrotational deformation, where the structural movement paths of the (2D) principal directions within a plane and the structures generated at them remain coincident (i.e. where the pole to the plane is contained by a symmetry plane of the ellipsoid). For a general type of strain ($0 < k < \infty$) this implies that the plane contains one of the (3D) principal strain axes Z, Y or X. With regard to the development of potential structures, if Z or X lie in the plane of the layering and are axes of folding which become axes of boudinage, then the (2D) principal direction at right angles to Z or X in the layering will be respectively either an axis of continuous shortening or an axis of continuous elongation during progressive deformation. If however Y lies in the plane of the layering the (2D) principal direction at right angles to Y in the layering will be an axis of continuous shortening, where $k > 1$, an axis of continuous elongation, where $k < 1$, or an axis of no structure, where $k = 1$. The absence of structures parallel to this potential structural axis suggests the last of these possibilities, and hence that the strain during the fourth episode of deformation if irrotational, approximated to pure shear ($k = 1$).

'a' directions determined from mineral lineations deformed by fourth folds in the Val Leventina area show a mean orientation approximately at right angles to the fourth fold axes, the postulated Y axis of the fourth episode strain ellipsoid. They are hence approximately coincident with the X axis of the ellipsoid (Fig. 3.19).

Where a homogeneous flattening component is involved in the folding process the deformed lineation locus will rotate towards the YZ plane of the ellipsoid irrespective of the manner in which the lineation locus is generated (cf. Ramsay, 1967, Chapter 8). In the case of fourth folds, over which the plane containing the lineation locus has been determined, the angular difference between Z (normal to axial surface) and the locus plane is small as is the angle between X and the locus plane ('a' and X are approximately coincident (Fig. 3.19)). Therefore with due regard to the possible effect of a homogeneous flattening component, the initial position of the locus plane and hence of X during the third episode of deformation (seen as the deformed mineral lineation) must have been close to the XZ plane of the fourth episode strain ellipsoid. The high angle between the fourth episode Y axis and the deformed lineation locus and hence between the fourth fold axis and the lineation before deformation, goes some way to explaining how an approximate great circle locus can be produced by folds which are not truely similar. As the lineation before deformation approaches a position at right angles to the fold axis, so the deformed lineation pattern produced by a pure buckle fold (small circle pattern) approaches more closely that produced by a pure similar fold (great circle pattern). In the limit, where the lineation is at right angles to the fold axis, the deformed lineation pattern is an identical great circle for both fold mechanisms (Ramsay, 1967, Figs. 8.4 and 8.8).

From the manner in which increments of rotational strain were added during the third episode of deformation (Fig. 3.14), it is apparent that successive increments of rotational strain will have approached more closely both in orientation and relative shape (k value) the fourth episode strain ellipsoid. This suggests that the third and fourth episodes of deformation were intimately related, if not continuous.

3.3) The Gotthard Massif

The history of deformation of the Gotthard Massif has features which are similar to that of the cover. Four episodes of deformation are recognised of which the latter three have equivalents in the cover. The first episode of deformation is considered to be of pre-Alpine (Hercynian) age. There is no equivalent in the Gotthard gneisses of the first episode of Alpine deformation in the Mesozoic cover.

The basis for this interpretation of the relationship between the deformation history of basement and cover rests essentially on two points. Firstly in terms of the major tectonic subdivisions of the Alps, the Gotthard Massif belongs to the Zone of External Massifs, which are recognised to be relatively unmoved blocks of basement in comparison to the basement and cover rocks in the Lower Pennine Zone to the south. The Gotthard Massif has not therefore suffered the major translative nappe forming movements characteristic of the first episode of Alpine deformation. Secondly, the most important tectonic structures which involve Gotthard basement and cover correlate with the second deformation of the cover. Indeed, where the authochthonous cover (Baumer et al, 1961) is found unconformably in contact with the Gotthard Massif there is no evidence of movements earlier than second episode of Alpine deformation, which affect this unconformity. From the observations of Baumer et al (1961), Baumer (1964) and Frey (1967) it is apparent that a décollement exists in the Mesozoic cover and that below this décollement the effects of the first episode of Alpine deformation are not observed.

3.31) The pre-Alpine (Hercynian) episode of deformation

The most striking structural element in the rocks of the Gotthard Massif is a penetrative foliation. This planar structure is presumably of tectonic origin as it is axial planar to folds in compositional banding. These folds are tight to isoclinal (Figs. 3.21, 3.22) so that in general foliation is observed both on a small and a large scale to be sub-parallel to compositional banding (Encls. 1 and 4).

The geometry of folded layers in minor folds of this age often approaches that expected in similar or Class 2 folds (Figs. 3.21, 3.22). Some layers, which in view of their composition are probably markedly

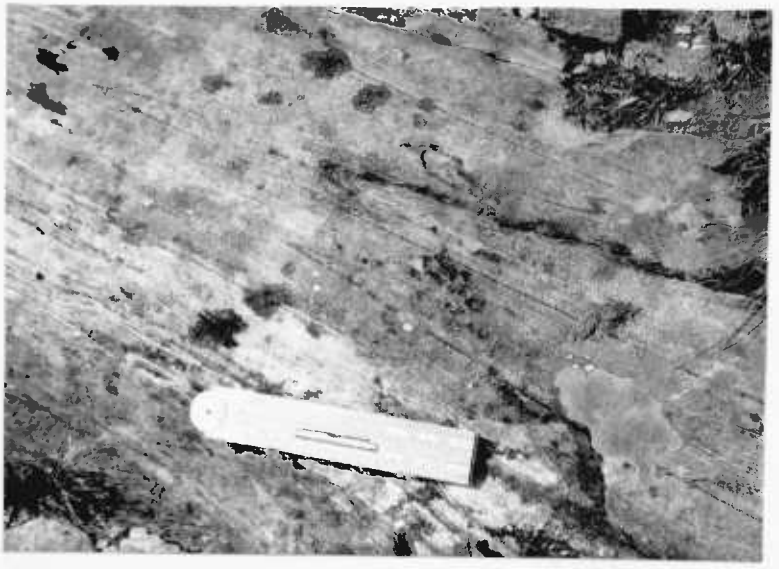

Fig. 3.21. First generation isoclines in the banded amphibolites of the Corandoni zone. Lago dello Stabbio, M.R. 6979815715.

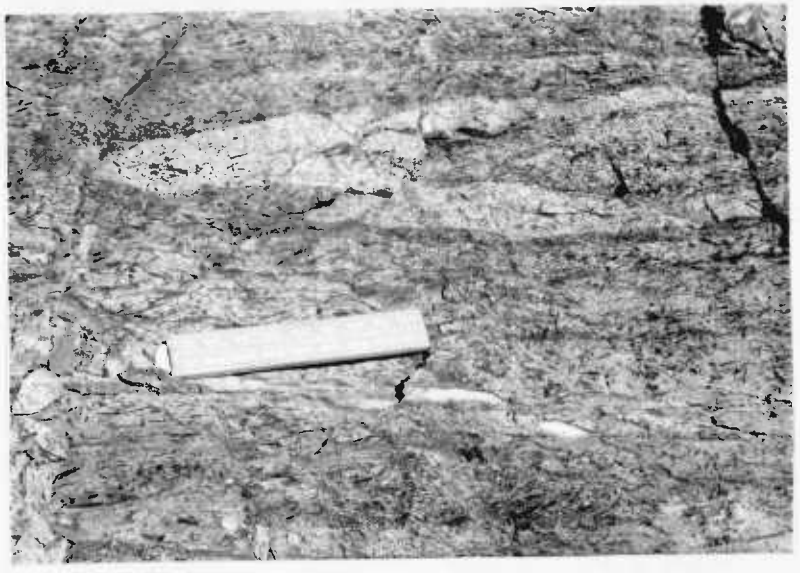

Fig. 3.22. First generation isocline in a banded amphibolite of the Corandoni zone. Note the random orientation and size of the hornblende porphyroblasts (scale = inches). Basso del Lago Oscuro, M.R. 6965315723.

Fig. 3·23 First generation folding of quartzo-felspathic layers in the Sorescia gneiss. The Class 1C geometry of these folded layers is clear (Fig. 3·23b). Lago di Dentro, M.R. 6992515670.

(a)

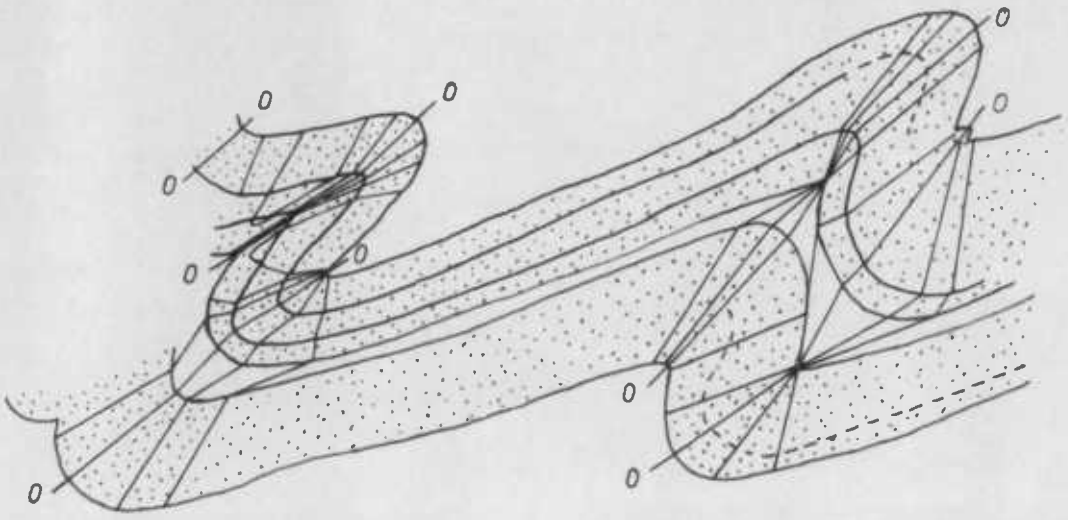

Isogons: 0, 40, 60, 80°.

(b)

less ductile than their matrix, show clearly Class 1.C. geometry (Figs. 3.23a and b).

The first foliation is characterised by a preferred orientation of micas, white mica usually being the dominant element of the planar structure and better oriented than biotite. Micas lying within the foliation plane are non-equant and lineated. Quartz grains are often "flattened" or dimensionally oriented in the plane of the foliation (Section 4.3).

A pronounced rodding in the Streifengneiss has been described by many authors (Krige, 1918; Huber, 1943; Steiger, 1962; Chadwick, 1965; Kvale, 1966). Huber (1943, p. 135) describes it as a b - tectonite fabric, Steiger (1962, p. 577) infers that it is an intersection lineation as it is parallel to fold axes in the Prato series and Corandoni zone and Kvale (1966, p. 68) describes it as the B axis of quartz and mica fabrics in rocks unaffected by the Alpine movements. The rodding (Fig. 3.24), which is an elongation of quartzo-felspathic material, has been found in this area to occur at the intersection of the first foliation described above and an earlier planar structure. Exposures in which both planar structures are developed are few, as the earlier one has been largely transposed. This interpretation of the rodding in the Streifengneiss is supported by the parallelism of the rodding to fold axes and intersection lineations (Fig. 3.25) in the adjacent Guibine series and Corandoni zone gneisses. A rodding structure, which is similar but rather less clearly developed, is sometimes found in the Soresoia series gneisses.

The attitude of the first foliation, and fold axis, rodding or intersection lineation has been recorded (Encl. 4). The foliation is found to be extremely constant in attitude throughout the area mapped, particularly in the Streifengneiss. In the other gneiss series the greater local variation is both a function of their inhomogeneity and the fact that the gneisses forming the cliffs marking the southern margin of the Gotthard Massif are to some extent slumped, dips being generally less than in underground workings (Steiger 1962,

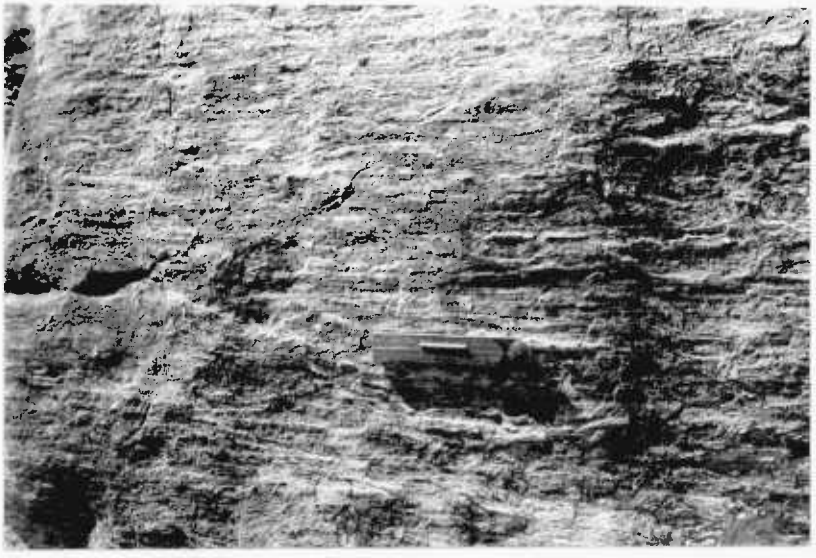

Fig. 3.24. Quartz-felspar rodding in the Streifengneiss. Val Cadlimo, M.R. 7019069790.

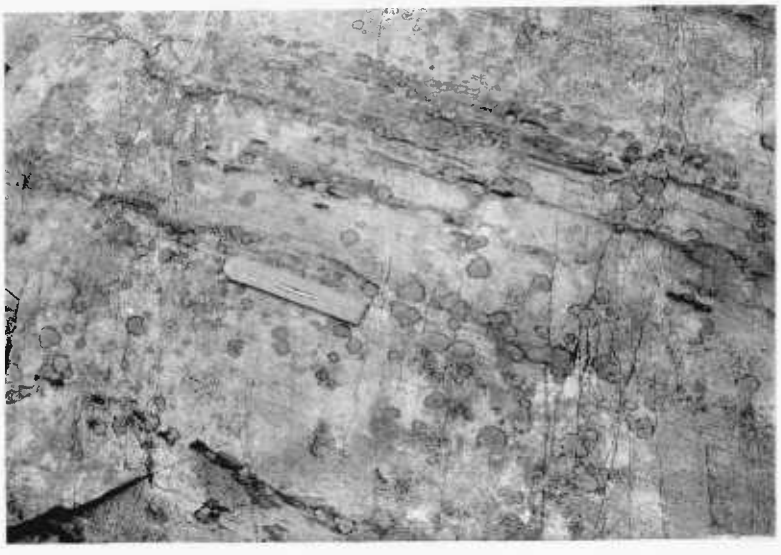

Fig. 3.25. First generation intersection lineation shown by compositional striping in the plane of the foliation. The traces of mineralised fractures, containing biotite and garnet are visible cross cutting the intersection lineation at approximately 90 degrees. The fractures are of third deformation age. Giubine series. Lago dell'Isra, M.R. 6982415734.

p. 576). The foliation is noticably oblique to the southern margin of the Massif (Encls. 1 and 4) and successive lithological units are seen to wedge out to the east. In the region east of Val Canaria the foliation changes sharply from an east-west to a northeast-southwest trend (Steiger, 1962, Tafel V). The parameter, which has been used to describe the orientation of the linear structures in the plane of the foliation, is rake. The advantages of using this parameter have been discussed by Elliot (1965, pp. 872-874). In the Streifengneiss sufficient data was available and the rodding was found to be sufficiently constant on a small scale to allow a rake isogon map (Elliot, 1965, p. 871 and pp. 874-879) to be constructed (Encl. 4). In the other gneiss series data was too limited and variable to allow this and measurements from different localities are recorded separately.

The point which arises from this analysis, particularly in the Streifengneiss, is that, although the foliation is constant in attitude, that of the rodding shows a wide variation throughout the area. Chadwick (1965, p. 85 and Fig. 17) has suggested that the variation in attitude of the rodding, in the Lukmanier area, can be explained by inhomogeneous strain in the plane of the foliation (differential strain in X, in Y, or in both X and Y). This seems unlikely to have occurred in the compositionally homogeneous Streifengneiss in which strains might also be expected to be homogeneous. Also, if Chadwick's hypothesis is correct, it is to be expected that strain trajectories, as recorded by the foliation (XY plane of the strain ellipsoid) will show convergence or divergence in sympathy with the change in attitude of the rodding. There is no evidence that this occurs, in fact the constant attitude of the foliation throughout the area suggests that the strain was relatively homogeneous.

An alternative hypothesis is that the deformation, which gave rise to the first foliation and rodding, was superimposed on a planar structure already irregular in attitude. The geometry of the early planar structure has not been determined, however it is appropriate to point out that the existence of an early planar structure and irregularities of this structure in the Streifengneiss, which initially

crystallised from a granitic magma (Huber, 1943, pp. 186-190) and was assumedly structureless is evidence for a complex history of deformation prior to the pre-Alpine (Hercynian) deformation discussed above.

Because all structures were rotated into near parallelism during the latest pre-Alpine episode of deformation and earlier planar structures largely transposed, the recognition of major and minor structures formed during this latest episode of pre-Alpine deformation, as distinct from structures which may have been produced during earlier episodes, has not been possible. Collectively considered, the structures which have resulted from these deformations are the interleaving of Giubine and Sorescia series gneisses within the area and on a regional scale, the east-west striking zones of paragneiss within the Streifengneiss (Muldenzonen of Huber (1943, pp. 92-97 and Fig. 6)).

3.32) The second episode of Alpine deformation

Only minor folds of second deformation age (Figs. 3.26, 3.27) with wavelengths up to a few metres and interlimb angles which are open to close are found in the Gotthard Massif. These folds typically show variable geometry when traced along their axial surfaces, like folds of the second and fourth generations seen in the cover rocks. Axial surfaces are gently to moderately inclined to the north and fold hinges are gently to moderately plunging in a northwesterly to northeasterly direction. The orientation data for these structures is summarised in Enclosure 3.

A poor axial plane cleavage (second foliation) is often associated with the folds. The structure arises from a weak preferred orientation of white mica, biotite and in some instances chlorite. Axial plane structure is generally only evident where first foliation is at a high angle to the second fold axial plane. On the normal limbs of second folds, where first foliation lies at a small angle to the second fold axial plane, new micas tend to grow mimetically in the earlier planar structure. Quartz grains in the cores of second folds are characteristically equant and contrast with the "flattened" quartz grains lying in the plane of the first foliation on the fold limbs (Section 3.21). Axial plane structure in rocks rich in white mica

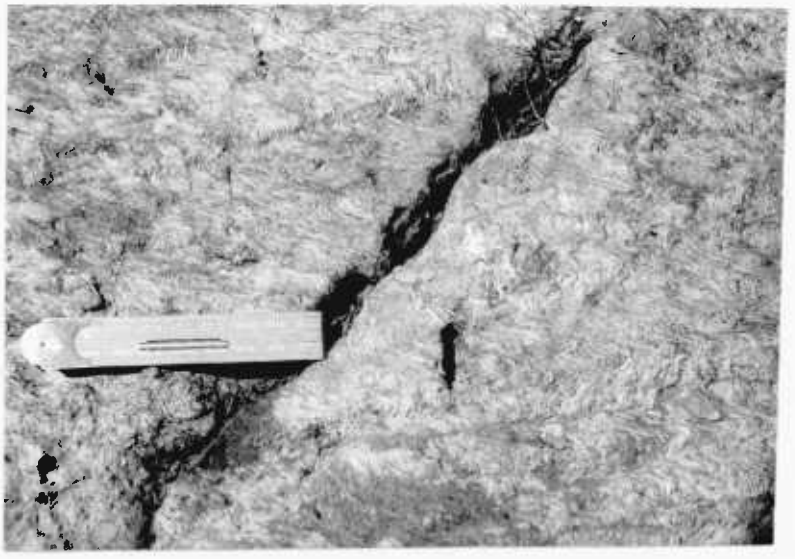

Fig. 3.26. Second generation folds, Sorescia gneiss. Bassa del Lago Oscuro, M.R. 6964715737.

Fig. 3.27. Second generation folds, Giubine series. Lago dello Stabbio, M.R. 6976715746.

is of strain slip type or the mica layers are crenulated on a micro scale.

Because of the rather poorly defined compositional layering in the Gotthard gneisses, examples of second folds from which layer geometry can be analysed are uncommon and largely confined to the well banded gneisses of the Corandoni series. Although their overall geometry approaches that of true similar folds, analysis of individual layers using isogon techniques shows departure of the geometry of these layers from that expected of true similar folds. There is therefore evidence that the layers did not behave passively during deformation.

The intensity of second folding decreases passing northwards from the southern margin of the Gotthard Massif. In the Streifengneiss itself minor second generation folds and second foliation appear to be absent. Some lamprophyre dykes however are folded (Encl. 1). The well developed first foliation in the Streifengneiss is found to be approximately axial planar to these structures, but in the lamprophyres themselves there is little evidence of an axial planar mica fabric (Fig. 3.28). In view of this it is unreasonable to accept the obvious interpretation, that the folding of the lamprophyres occurred during the pre-Alpine (Hercynian) deformation. This is also an unreasonable interpretation in view of the probable late Hercynian age of the dykes (Section 2.31). The lack of an axial planar mica fabric, particularly in the folded dyke rocks which are compositionally suitable for the development of such a fabric, suggests that the deformation which gave rise to the folds was rather weak and more in keeping with the second episode of Alpine deformation. The approximate orientation of the first foliation in the axial plane of the folds reflects the small angle between first foliation and the second fold axial plane.

The tectonic nature of the contact between the Gotthard Massif and the cover rocks in Val Piora and the region to the west has been recognised by many authors (Oberholzer, 1955; Hafner, 1958; Steiger, 1962; Higgins, 1964b). In the region to the east of Val Piora the northern contacts of the Scopi and Valle del Lucomagno zones with the Massif are also recognised as tectonic and of Phase B (equivalent to the second episode of Alpine deformation) age (Chadwick, 1965; Frey, 1967).

Fig. 3.28. Contact between the Streifengneiss and a lamprophyre dyke. Note how the strongly developed pre-Alpine foliation in the Streifengneiss contrasts with the lack of visible structure in the lamprophyre. Punta Negra, M.R. 6961815766.

In the analysis of the cover deformation evidence was given to suggest that the Gotthard Massif-cover contact could be interpreted as a slide zone of second deformation age (Section 3.22). This interpretation is strengthened by the observed sub-parallelism to the contact of second foliation in the Gotthard gneisses (Encl. 3), and by the fact that this structure appears more intensely developed closer to the contact. The decrease in the intensity of second folding and second foliation northwards from the southern margin of the Gotthard Massif can be related to a decrease in the intensity of deformation away from this slide zone.

Two factors appear to have influenced the intensity of development of second foliation. Firstly there is an obvious dependence on the intensity of deformation and secondly, there is a tendency for micas to grow mimetically in the first foliation rather than form a new planar structure, particularly where the angle between these two structures is small. Thus, it is probable that in some cases first foliation was reworked during the second Alpine deformation, in the sense that new mica growth took place in the plane of the first foliation rather than in a new orientation.

Block movements in the basement on planes sub-parallel to second foliation appear to have determined the geometry of the southern margin of the Gotthard Massif, at least as far east as Val Camadra (cf. Frey, 1967, Figs. 23 and 24). The positions of the movement zones or slides can be related to the older, pre-Alpine structures. The northern boundary of the Scopi zone coincides with the paragneisses of the Boreal zone and that of the Valle del Lucomagno and Val Piora zone with the Tremola zone (Chadwick, 1968, p. 1134).

3.33) The third episode of Alpine deformation

Linear mineral fabrics, which are closely comparable to those in the cover rocks, are observed in the gneisses of the Gotthard Massif. These fabrics have been described by many authors and Kvale (1966) provides a summary of their observations together with new fabric data.

In the Gotthard gneisses of the Val Piora region two distinct types of linear mica fabric are recognised. The first of these is seen as a dimensional orientation of non-equant micas in the planes of the first and second foliations. In practice the second foliation is seldom of sufficient intensity for a lineation of micas to be observed within it. The second type of mica fabric is an L. tectonite fabric (Section 3.23) and is formed by micas, which grow across the first and second foliations. The two distinct linear mica fabric types are recognisable, in the field in the case of biotite and in thin section in the case of white mica. The degree to which one linear fabric type is developed at the expense of the other varies. Hornblende, though generally displaying a random growth fabric, sometimes shows a preferred orientation of crystallographic c axes parallel to the mica lineations described above. The linear fabrics have a constant north-south orientation which parallels that observed in the cover rocks (Encl. 6).

Syntectonic snowball garnets are found rarely in the Tremola series gneisses. The rotation axes of these crystals are sub-perpendicular to the mineral lineation and the sense of rotation conforms with that observed in the cover rocks (cf. Steiger, 1962, pp. 462-463, Tafel I, Fig. 2, and Tafel III, Fig. I).

In view of the compatability of the linear mineral fabrics in both the cover and Gotthard Massif, the same mechanism of deformation can be envisaged to have acted in their formation (Section 3.23).

Folds formed during the third episode of Alpine deformation in the Gotthard Massif are not, as in the cover rocks, confined to crenulations whose axes parallel the linear mineral fabric, and which are only found in well foliated micaceous rocks. Although these exist (cf. Steiger, 1962 (Kleinfältelungen)) structures which have many of the features of kink bands (Dewey, 1965) are also recognised. Thin planar fold zones or kink bands (Figs. 3.29, 3.30) generally from a few millimetres to a few centimetres wide are found transecting first foliation. These are often arranged in conjugate pairs, which are usually asymmetrically disposed to the foliation plane (Figs. 3.31,

Fig. 3.29. Kink band of third deformation age in the Streifengneiss. Note the curved trace of the kinked first foliation. Lago Oscuro, M.R. 6965515781.

Fig. 3.30. Kink band of third deformation age in the Streifengneiss. Note the angular style of the structure and the irregularly developed fractures bounding the kink band. Piatto della Miniera, M.R. 6991515706.

Fig. 3.31. Asymmetric conjugate kink fold, Streifengneiss. Pizzo Corandoni, M.R. 6987015790.

Fig. 3.32.

Asymmetric conjugate kink fold, Giubine series. Lago della Stabbio, M.R. 6975515749.

3.32). Poles to kink bands are distributed on a great circle whose pole approximately coincides in orientation with the mineral lineation. The intersection axes of conjugate kink planes are likewise approximately coincident with the mineral lineation and lie in or near the first foliation plane (Figs. 3.33, 3.34). The great circle distribution of poles to kink planes observed in measurements from the area as a whole is also apparent on the scale of a single outcrop. The angle between conjugate kink planes varies. Angles measured across the foliation plane perpendicular to the intersection axes of conjugate pairs vary from 40 - 140 degrees.

Both normal and reversed structures (Dewey, 1965, p. 460, Fig. 1) are recognised (Fig. 3.35). Style changes from angular (Fig. 3.30), the kinked foliation being bounded by sharp planes, which are sometimes planes of fracture, to curved (Fig. 3.29), in which the kinked foliation follows a curved trace. Often within these latter structures a multiplication of folds occurs within the kink zone. In general, kink bands lying at a high angle to foliation are geniculate and those at a low angle to foliation, curved. The angle between external and internal foliation is seldom bisected by the kink plane and usually changes along the length of the kink band, so that the structure dies out. Thickness measurements indicate that though the orthogonal thicknesses, t, t', of external and internal foliation differ the thicknesses measured parallel to the kink plane, T, T', remain constant (Fig. 3.35). Examples of these measurements are recorded below (Table 3.1).

Differences in texture between internal and external foliation are observed. Within the kink zones quartz grains are equant rather than "flattened" in the plane of the first foliation and micas grow across the foliation, often with a weak preferred orientation in the axial plane of the kink, rather than in the foliation.

Conjugate folds and kink bands are usually thought to develop at a late stage during the deformational history of an area (Dewey 1965), and have been considered by some authors (Johnson, 1956; Ramsay, 1962c) probably incorrectly (Ramsay 1967, p. 453), to be indicative of brittle

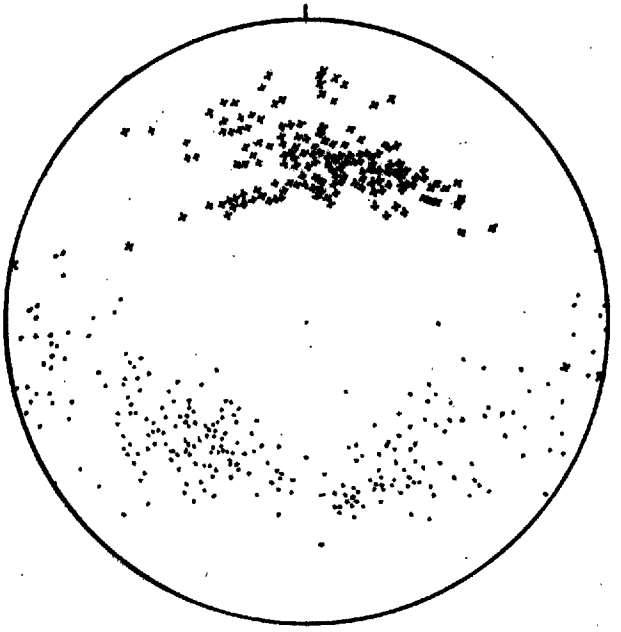

Fig. 3·33 Poles to axial planes (·) and axes (×) of kink bands.

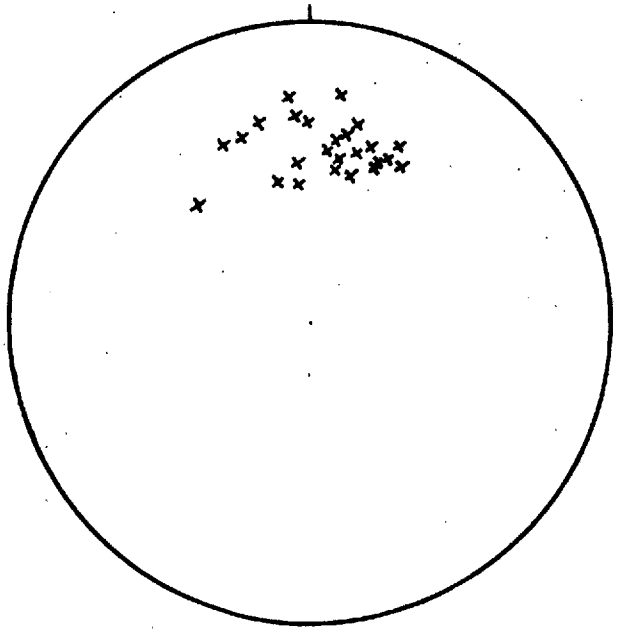

Fig. 3·34 Intersection axes of conjugate pairs of kink bands.

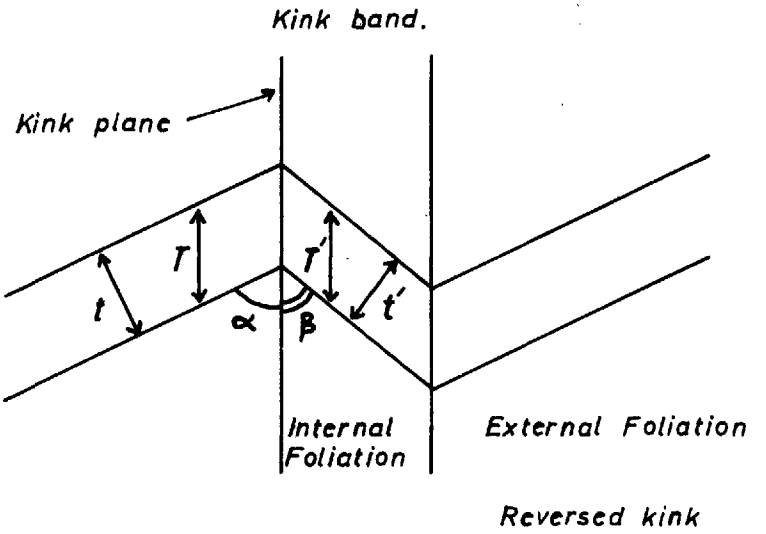

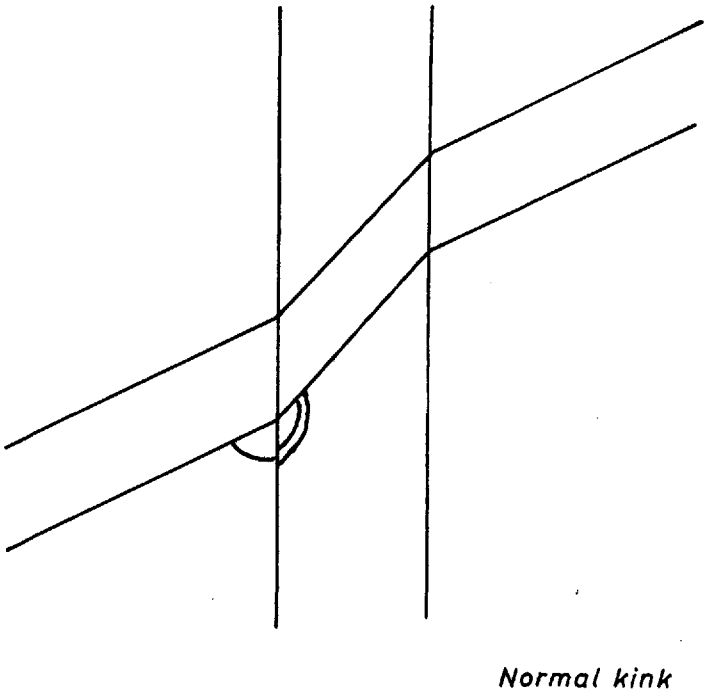

Fig. 3·35 Kink band geometry.

Table 3.1

t	t'	T	T'	α degrees	β degrees
1.3	2.4	2.3	2.4	30	50
0.50	0.9	1.0	0.9	30	60
0.70	1.3	1.5	1.3	15	70
0.9	1.5	1.7	1.6	30	50
2.8	4.5	4.7	4.5	40	90
1.2	3.6	3.4	3.6	25	75

deformation. The preferred development of these structures in well foliated rocks suggests that slip on the foliation is the fundamental method of deformation (Ramsay, 1967, pp. 438-440). Indeed conjugate kink bands have been produced experimentally in this way (Patterson and Weiss, 1966). This mechanism of deformation places restrictions on the geometry of the resultant structures. The kink plane bisects the angle between the internal and external foliation and the orthogonal thickness of foliation remains constant throughout the structures. Dewey (1965, pp. 459-464) has questioned the feasibility of explaining all kink band formation by foliation slip and has suggested that some kink bands may be produced by continuous simple shear. In these the kink plane parallels the shear plane and the foliation deforms passively (Dewey, 1965, Fig. 2). Geometrically these latter structures differ from the former, in that kink planes do not generally bisect the angle between internal and external foliation and the orthogonal thickness of foliation changes throughout the structure. The thickness measured parallel to the kink plane remains constant however, as this is a plane of no strain (Dewey, 1965, Fig. 12A). The geometry of the structures described from the Gotthard Massif is closely related to that of kinks produced by this latter deformation mechanism.

The evidence that the kink bands were formed during the deformation which gave rise to the linear mineral fabrics has not yet been discussed. Interference criteria of the type outlined by Ramsay (1962b;

1967, Chapter 10), which might be used to interpret the age of these structures in relation to others, are not found. As the style of second generation folds is similar to that shown by the kinks, these two ages of structures are often differentiated with difficulty. However, second generation structures are usually more penetrative. There are two lines of evidence which suggest a relationship between the kink bands and the linear mineral fabrics; firstly, the analysis of the age of the kinks in terms of the growth periods of different metamorphic minerals indicates that the structures formed during a period of rising temperature, just as the linear mineral fabrics (Section 4.3); secondly, a geometrical relationship between the kink planes and the mineral lineation is observed (the kink planes intersect in the mineral lineation).

Although most kink structures are reversed, normal structures are also found, particularly in the Streifengneiss. The normal kinks are often seen to degenerate into shear planes along which apparent extension in the plane of the first foliation has taken place. Normal shears (Fig. 3.36), showing no obvious relation to kink structures as above, are common in the well banded Tremola series gneisses. They occur singly, or in conjugate pairs with no fixed angular relationship to one another, and have orientations broadly coincident with the kink planes. Particularly the axes of intersection of conjugate shears are similar to those of conjugate kinks (Fig. 3.37). It seems probable that the shears were formed during the deformation which gave rise to the linear mineral fabrics. This is suggested by their orientation in relation to the linear mineral fabrics, and by their age in relation to second generation folds and the growth periods of metamorphic minerals. With respect to this latter point, both hornblende and biotite are concentrated along the shear planes and show either a random or a northerly plunging linear fabric.

One other structural feature should be mentioned in the context of the third episode of Alpine deformation. In the Tremola and Giubine series gneisses thin planar zones, which are enriched in the mafic minerals, hornblende, biotite and garnet and on which no obvious

Fig. 3.36. Normal shear plane. The sense of shear is shown by the displaced compositional banding. Note the concentration of hornblende along the shear plane. In some layers, (top of photo.), fractures enriched in hornblende and oriented sub-perpendicular to banding are visible. There is seldom any obvious displacement on these latter structures. Tremola series. Alpe Stabiello, M.R. 6947715660.

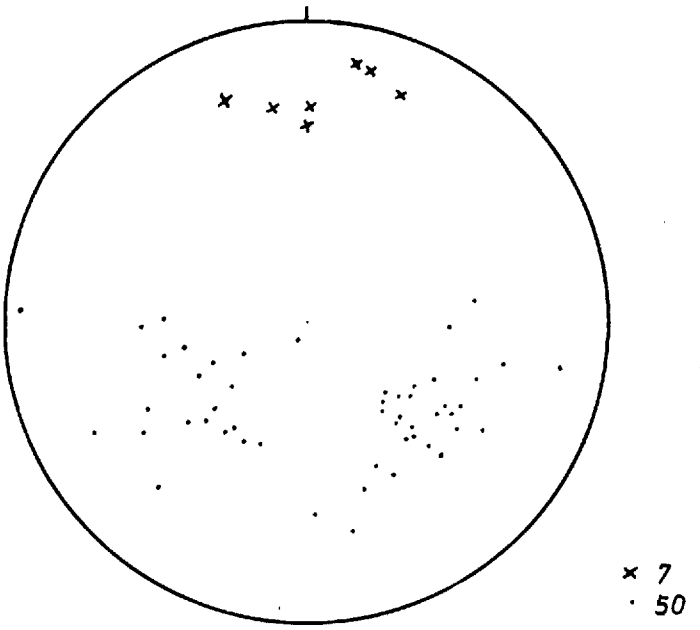

Fig. 3·37 Poles to normal shear planes (·), and intersection axes of conjugate pairs of shears (×).

displacement has taken place, are observed (Figs. 3.25 and 3.36). Though the orientation of these zones has not been recorded in detail, field observations indicate that they show a preferred orientation similar to that of the kink bands and normal shears.

Kink bands of the type produced by Patterson and Weiss (1966) represent zones of permanent deformation within an elastically strained specimen and are analogous to Luders bands in plastically deformed metal specimens. They can be regarded as deformational instabilities. The concentration of deformation in particular zones arises from the presence of stress concentrations at which yielding begins, and the phenomena of strain softening (Orowan, 1960, p. 340 and Fig. 7). Instabilities also occur during low speed high temperature deformation of viscous materials (viscous creep) and are likewise seen as zones in which deformation is concentrated (Orowan, 1960, p. 341). In view of the penetrative nature of the linear fabric and the metamorphic conditions that existed during the third episode of Alpine deformation, the structural features, kink bands, normal shears and planes of mineral concentration are interpreted as instabilities which have arisen during viscous creep. It is significant that the symmetry of distribution of these instabilities reflects the symmetry of the third episode constrictional strain.

3.34) The fourth episode of Alpine deformation

Folds of fourth deformation age are absent in the Gotthard gneisses of the Val Piora area and are only rarely seen in those of the adjacent Lukmanier area (Chadwick, 1965). Further east in Val Camadra, folds of this age are well developed in the paragneisses bounding the southern margin of the Massif (Cobbold, 1969).

Boundinage structures, usually symmetrical, with gently westerly or easterly plunging axes (Encl. 6) are common in the banded paragneisses but rare in the Streifengneiss. The relationships of the boudins to other structures, the character of the mineralogical fillings in the boudin necks (combinations of quartz, felspar, white mica, chlorite and rarely kyanite) and often the presence of unfilled necks (voids) indicates that boudinage was active during the fourth episode

of Alpine deformation. From the attitude of the boudinage axes a north-south extension in the plane of the compositional layering can be inferred. Further evidence of this extension is provided by the limited occurrence, sub-perpendicular to layering, of southward dipping quartz veins, some of which contain kyanite. In the cover, the type of structure formed during this episode of deformation has been shown to be dependent on the attitude and hence relation of earlier planar structures to the fourth episode strain ellipsoid (Section 3.24). The occurrence of boudinage structures alone, suggests that the first foliation in the Gotthard Massif lay within the field of continuous elongation of this ellipsoid.

3.4) The Lukmanier Massif

The structural analysis of the Lukmanier Massif has been hindered by the poor lithological layering in many of the gneisses, the lack of well defined lithological units (Section 2.4), the transposition of first foliation during the second episode of Alpine deformation and, over a part of the area, the poor and wooded exposure.

Throughout much of the Massif the geometry of second generation structures is not clear, because second foliation forms the dominant planar structure, and neither the absolute attitude of first foliation nor its relation to second foliation (sense of second folds) can be determined. Thus the interpetation of the Lukmanier Massif as a major structure of second deformation age and the nature of this structure, must be judged with regard to the limitations of the data available for this interpretation.

The sequence of deformation episodes is however clear. Four episodes of deformation are recognised of which the latter three have equivalents in the cover rocks. The first episode of deformation is considered to be of pre-Alpine age. There is no equivalent in the Lukmanier Massif gneisses of the first episode of Alpine deformation in the Mesozoic cover.

3.41) The pre-Alpine (Hercynian) episode of deformation

The gneisses of the Lukmanier Massif show a foliation which in general is parallel to compositional banding and is characterised by a preferred crystallographic orientation of dominantly white mica but also biotite. These micas are oftennon-equant and lineated. Isoclinal folds in compositional banding to which this foliation is axial planar (Fig. 3.38) indicate a tectonic origin for the structure. These folds are uncommon and the few observed examples plunged steeply to the north and were coaxial with second generation folds (Figs. 2.3, 3.38).

The attitude of first foliation has been recorded where possible throughout the Massif. Only in the gneisses to the south and west of Piora is sufficient data (measurements of the absolute attitude of first foliation or evidence of the relation of first to second foliation

Fig. 3.38.

First generation folds refolded by coaxial second generation structures. The trace of the second foliation lies approximately parallel to the length of the ruler. Mixed Group gneiss; road section, Altanca-Piora, M.R. 6940215325.

Fig. 3.39.

Second generation folds. Orange Group gneiss; road section, Altanca-Piora, M.R. 6940915347.

(second fold sense)) available to enable a first foliation trend map to be constructed (Encl. 5). Three significant features emerge from this map; firstly, the first foliation is discordant to both the upper and lower margins of the Massif, secondly, the first foliation is discordant to the junction between the Orange and Mixed Group gneisses in this region, and thirdly, the first foliation has been folded to form a westward closing reclined second fold. The significance of these features is best discussed in the context of the second episode of Alpine deformation.

3.42) The second episode of Alpine deformation

Folds of second deformation age (Fig. 3.39) are the most commonly observed fold structures in the Lukmanier Massif. Their axial surfaces are moderately to steeply inclined to the north, fold hinges are moderately to steeply plunging, and both structural elements are extremely constant in attitude throughout most of the area (Encl. 3). Interlimb angles of second folds are usually close to open and wavelengths variable from a few millimetres to a few hundreds of metres. Though the style of the folds approaches similar, Class 3 and 1.C. layer associations are generally recognisable. Layering is seldom sufficiently well developed or sufficiently regular to allow detailed geometrical analysis. The geometry of largerfolds of this age is seen in Enclosure 5 in near profile section, because of the relationship of the second fold axes to the topographic surface. As the minor folds, they change their geometry when traced along their axial surfaces; the fold amplitude varies and the structure eventually dies out. As a consequence axial surfaces converge and diverge and in places are obviously oblique to axial plane cleavage (cf. Encl. 3).

An axial plane cleavage (second foliation) of variable style is usually associated with the second folds. In most cases it is a preferred crystallographic orientation of non-equant lineated white mica and biotite. Quartz grains show a tendency to be "flattened" in the plane of the cleavage, even in mica free layers (Section 4.4). This type of structure is particularly well developed in rocks containing intermediate amounts of mica, whereas in rocks rich in white

mica axial plane structure is of strain slip type or the micaceous layering is merely crenulated on a micro scale. In the mica poor Mixed Group gneisses a coarse fracturing is often found parallel to a weak preferred orientation of micas (Fig. 2.4). The variation with composition in the style of axial plane structure is a feature of second folds in the other tectonic units (Sections 3.22, 3.32). Shear discontinuities, which are generally sub-parallel to the axial surfaces of the second folds, are common. The displacements appear to have no consistent sense within the scale of observation, as adjacent shears frequently show displacements which are opposed (Fig. 3.40). The spacing of the discontinuities is usually irregular except in some well foliated quartzo-felspathic gneisses in which a regular spacing of discrete mica rich planes is observed (Fig. 3.41).

In regions where first foliation is transposed by second foliation evidence of the earlier planar structure is afforded by isolated second generation minor folds, in rocks in which compositional banding is well developed, and by the almost ubiquitous development of intersection lineation phenomena, such as rodding of quartz lenses, rodding of augen and compositional stripping, in the plane of the second foliation (Figs. 3.42, 3.43).

The appearance of second foliation as the dominant planar structure, particularly in the regions bounding the northern margin of the Massif, can be interpreted as a reflection of the greater intensity of second deformation in these regions. Thus, the intensity of the second deformation appears to increase northwards towards the northern margin of the Massif, which has been shown (Section 3.22, Encls. 2 and 3) to be determined by a series of folds and tectonic slides of second deformation age. The variation in intensity of the second deformation is somewhat similar to that observed in the Gotthard gneisses (Section 3.32).

In the region to the south and east of Lago Ritom, analysis of second generation structures within and at the margin of the Lukmanier Massif is hindered by the lack of available first foliation orientation data. There is little which can be usefully added to the

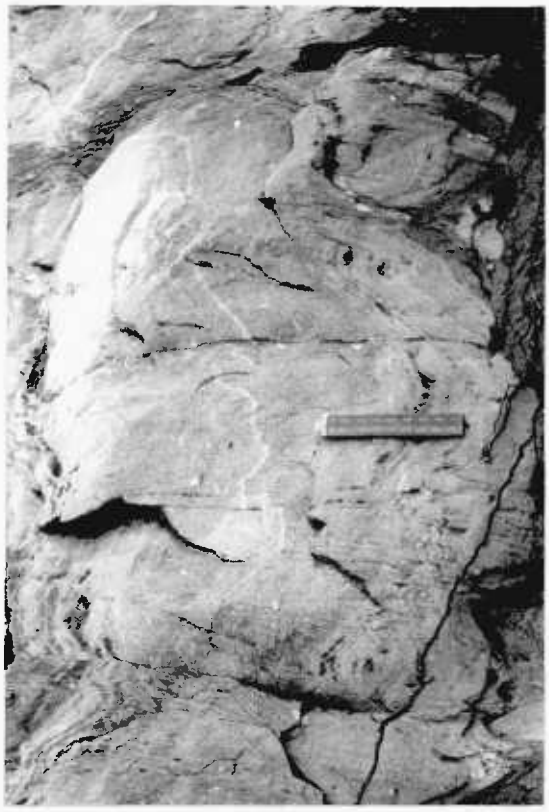

Fig. 3.40

Second fold axial planar discontinuities along which visible displacements have occurred. There is no consistent sense of displacement. Orange Group gneiss; road section, Altanca-Piora, M.R. 6940915347

Fig. 3.41.

Regularly spaced second fold axial planar discontinuities represented by discrete mica rich planes. Mixed Group gneiss; road section, Piotta-Altanca, M.R. 6950615283.

Fig. 3.42. Second generation intersection lineation formed by quartz rods in the plane of the second foliation. Orange Group gneiss; Valle, M.R. 6951115440.

Fig. 3.43. Second generation intersection lineation formed by a rodding of quartz-felspar augen in the plane of the second foliation. Augen gneiss (Piora type); Piora, M.R. 6951615439.

comments already made about the structure of this region (Section 3.22, Encl. 2). The first foliation trend map in the region to the west of Lago Ritom shows the structure of the Massif here to be a westward closing reclined second fold (Section 3.41, Encl. 5). The first foliation is discordant to both the upper and lower margins of the Massif and to the junction between the Orange and Mixed Group gneisses. The discordance at the upper margin of the Massif arises from the presence of a slide of second deformation age at the basement-cover contact. The same interpretation cannot however be applied to the lower margin, which is oblique to the second foliation in basement and cover, but sub-parallel to first foliation in the cover. In this case the discordance appears to reflect an original unconformity between basement and cover. This implies that first foliation in the Lukmanier Massif is of pre-Alpine age.

Indirect evidence for this hypothesis is provided by the presence within the Lukmanier Massif of a number of sheet intrusions of granitic composition (the Younger Granite gneisses (Section 2.4)), which are only deformed by structures of the second and later episodes of Alpine deformation. If the first foliation in the Lukmanier Massif gneisses is considered to be of the same age as the first foliation in the cover rocks, then these intrusions must have been emplaced between the nappe forming movements and the second episode of Alpine deformation. This seems to be unlikely (Section 2.4), however a pre-Alpine age for both the first foliation and the intrusions in the Lukmanier Massif is in accord with the interpetation placed on the age of similar features in the Gotthard Massif (Section 2.31).

The discordance between first foliation and the contact between the Orange and Mixed Group gneisses can be considered to be either earlier or the same age as the second episode of Alpine deformation. If earlier, the discordance may have been present in the original layered complex, and somewhat analogous to a facies change, or it may have been produced by folding during the pre-Alpine deformation. If the same age as the second episode of Alpine deformation, sliding

in the plane of the second cleavage, of which there is ample evidence, could give rise to a discordance of this nature. Because the junction between the two gneiss series is poorly defined (Section 2.4), it is difficult to decide which of these three interpretations is most likely.

The structural relationship between the Lukmanier Massif and the cover at its western termination near Madrano (Encl. 5) is not unlike that observed in the region south and west of Piora (Encl. 2). In the Piora area it has been shown that the attitude of second foliation differs between basement and cover and that this difference is reflected in the attitude of the second slides (Section 3.22). Because of this the slides interfere with one another (e.g. slide EE' is cut off by slide DD' (Encl. 2)). By analogy, the observation that second foliation in the cover rocks of Val Canaria is oblique to that in the Lukmanier gneisses of the Madrano region (Encl. 3), suggests the possibility that the east-west trending basement-cover slides here are also cut off to the west by a slide structure, whose attitude is related to that of the second foliation in the cover. As the overall trend of the western margin of the Massif is sub-parallel to the second foliation in the cover it is probable that the basement-cover contact is in part determined by this latter slide structure (Encl. 5). A weak later cleavage, whose attitude is coincident with that observed in the cover rocks of Val Canaria (Encl. 3) is found locally to cut the second foliation in the Lukmanier Massif gneisses of this western margin. The structure is characterised by a weak preferred orientation of lineated non-equant white mica and biotite or is of strain slip type. Associated minor folds to which the cleavage is axial planar have steeply plunging hinges, interlimb angles which are generally open to close and wavelengths that are seldom greater than a few centimetres. As the cleavage is parallel to the cover oriented slide structure postulated above (Encl. 5) a genetic relationship is inferred. Thus in the Lukmanier gneisses of the Madrano area two generations of fold structures of second deformation age are observed, the first formed during the major folding and associated sliding of the Lukmanier basement and

cover and the second during the later sliding of the cover over the basement. In the Piora area although a similar situation is realised minor structures of the later generation are not found in the basement gneisses. The factors which have led to these relationships are discussed in Section 3.5.

3.43) The third episode of Alpine deformation

The linear mineral fabrics observed in the gneisses of the Lukmanier Massif are closely comparable both in orientation (Encl. 6) and type to those formed in the cover and Gotthard Massif during the third episode of Alpine deformation. Biotite and white mica crystals lying within the first and second generation planar structures are often found to be lineated (Sections 3.41, 3.42) and in some rocks biotite has a pronounced L. tectonite fabric (cf. Section 3.23). Hornblende occasionally shows a preferred orientation of c axes parallel to the mica lineations. The attitude of the linear fabrics is constant (Encl. 6) and generally oblique to the intersection linear structures of the first and second foliations (second fold axes).

Rare synkinematic or snowball garnets have rotation axes which are approximately perpendicular to the mineral lineation and the sense of rotation corresponds to that of rotated garnets observed in the other structural units.

Fold structures of this generation are absent in the Lukmanier gneisses.

As the linear mineral fabrics and associated features are so similar in the cover, the Gotthard Massif and the Lukmanier Massif, it is reasonable to place the same interpretation upon them (Section 3.23).

3.44) The fourth episode of Alpine deformation

Both folds and boudinage structures of fourth deformation age are found in the Lukmanier Massif. Fourth folds are not well developed and are largely confined to finely banded micaceous rocks in regions of steeply dipping planar structures. Fold geometry changes rapidly parallel to fold axial surfaces and fold wavelengths are seldom greater than a metre. A poor axial plane structure sometimes observed in the

field is seen in thin section to be due to a weak preferred orientation of white mica. Fold hinges plunge gently west or east and fold axial surfaces dip moderately to gently in a north to northwesterly direction (Encl. 6). Fourth generation folds are most common in the Lukmanier Massif in the region east of Val Piora.

Both symmetrical and asymmetrical boudinage structures (Figs. 3.44a and b) with gently westerly or easterly plunging axis (Encl. 6) are observed throughout the Massif and are particularly common in the region east of Piora. As in the other structural units the boundinage structures can be shown to postdate the mineral lineation, as they deform it and as they contain mineral fillings or voids characteristic of the late stages of metamorphism (cf. Section 3.24).

Whereas symmetrical boudins can be ascribed to necking (pinch and swell structures) or, where sharp separation has occurred, extension fracturing (Griggs and Handin, 1960) of a competent layer contained by a more ductile matrix (Ramberg, 1955; Rast, 1956; Ramsay, 1967, pp. 103-109), asymmetric structures appear to be caused by faulting of the competent layer on planes inclined to the layer boundaries (Fig. 3.44b). The reasons for this difference in behaviour are not immediately apparent from field observations, however if a comparison can be drawn with experimental work (Griggs and Handin, 1960) failure of the competent layer by faulting is a behaviour which is transitional between brittle and ductile. In contrast failure by extension fracturing indicates brittle behaviour of the boudinaged layer and the development of pinch and swell structure, ductile behaviour. Thus, where a marked ductility contrast exists between the boudinaged layer and the matrix, brittle behaviour of the layer is more likely than in the case where this contrast is reduced. Field observations suggest that symmetrical boudins in which separation has occurred are generally associated with a more marked ductility contrast than asymmetric structures. Coe (1958) for instance has also described possible asymmetric boudins in a layer which is not noticably different from the matrix. The inference which must be drawn is that the type of structure which is formed depends on the ductility of the boudinaged

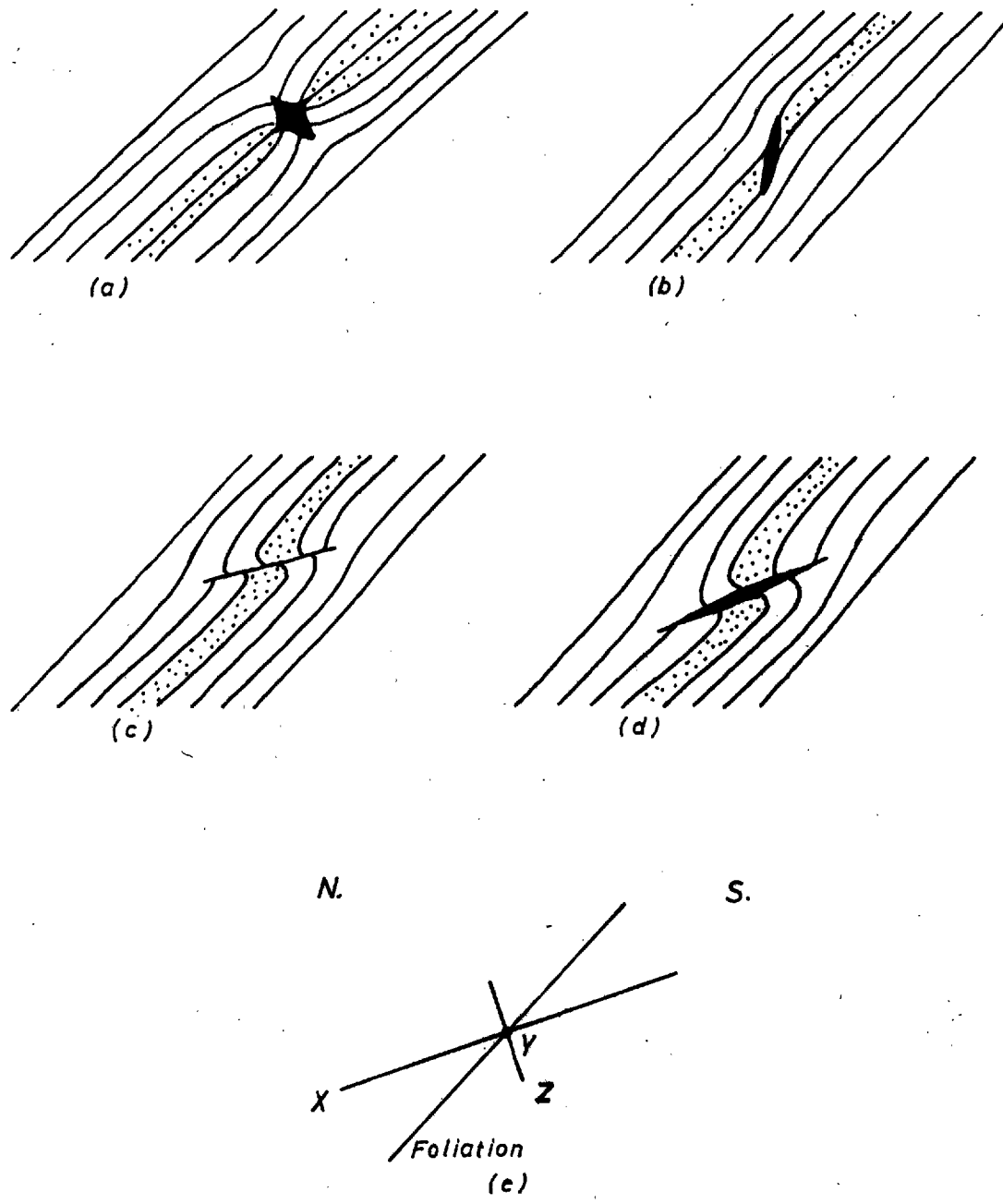

Fig. 3·44 Fourth generation boudinage structures. (a)Symmetrical boudin with mineralised neck. (b)Asymmetrical boudin with mineralised fracture region. (c)Boudinaged fourth fold. (d)Boudinaged fourth fold with mineralised fracture region. (e)Relationship between fourth episode strain axes and boudinaged foliation.

layer. Where the boudinaged layer contains the principal stress and strain axes, as in the experimental work (Griggs and Handin, 1960), faulting can occur on conjugate planes of high shear stress. The asymmetric boudins, throughout the Val Piora area all show the same sense (Fig. 3.44b) and hence only one of the two possible fault planes is developed. This presumably reflects the fact that the fourth deformation strain axes (Section 3.24) (Fig. 3.44e) and probably also stress axes were oblique to layering, so that one of the two possible planes of faulting was preferred.

The time relationship between folding and boudinage is clear as fourth folds are found to be boudinaged (Figs. 3.44c and d). In these structures the abnormal fold limb is cut by a shear discontinuity (Fig. 3.44c) often associated with late mineralisation (Fig. 3.44d).

As in the cover, a relationship between type of fourth generation structure (fold or boudin) and dip of the earlier planar structures appears to exist. In steeply dipping regions folds only are found, whereas in moderately dipping regions folds, boudinaged folds and boudins are observed. The reasons for this relationship have been discussed (Section 3.24). With respect to the fourth episode deformation ellipsoid, the observed association of structures suggests that the steeply dipping planar structures in the Lukmanier gneisses lie within the field of continuous shortening and the moderately dipping planar structures in the field of initial shortening and later elongation.

3.5) Synthesis

The purpose of this section is to summarise the suggested correlations between successive deformation episodes in the different structural units, to emphasise the important features of each episode of deformation and to examine the structural relationships between basement and cover. The first part of this proposal is carried out simply in Table 3.2. The reasons for the suggested correlations (Table 3.2) have been discussed in the preceding sections.

The important features of each of the episodes of deformation are considered below.

Table 3.2 Correlation of deformation episodes

	Mesozoic cover	Gotthard Massif	Lukmanier Massif
Pre-Alpine (Hercynian)		$D_{p.A.}$ Intrusion of granites and lamprophyres	$D_{p.A.}$
Alpine	D_1	-	-
	D_2	D_2	D_2
	D_3	D_3	D_3
	D_4	D_4	D_4
	← Late Alpine structures →		

3.51) The pre-Alpine deformation

In the Gotthard Massif the pre-Alpine deformation has been shown to be polyphase (Section 3.31). During the last of the pre-Alpine deformation episodes the most striking of the structural elements (first foliation and rodding) observed in the Gotthard Massif gneisses were produced. Major structures, the zones of paragneiss in the Streifengneiss (Muldenzonen of Huber (1943)) are recognised to be the product of the general period of pre-Alpine deformation but cannot, for the reasons outlined in Section 3.31, be shown to be the product of any particular one of the deformation episodes.

Minor structures (e.g. first foliation), which are interpreted to be of pre-Alpine age (Section 3.41), are found in the Lukmanier Massif, however no major structures of this age are apparent.

Igneous intrusions, the lamprophyres in the Gotthard Massif and the granite sheets (the Younger Granite gneisses) in the Lukmanier Massif were emplaced after the pre-Alpine deformation (Sections 3.32, 3.42). The intimate relation of similar lamprophyre intrusions to granitic bodies of known pre-Alpine age in the Gotthard Massif (Huber, 1943, pp. 113-127 and Section 2.31) strongly suggests that the intrusions in the Val Piora area also belong to this period of magmatic activity.

3.52) The first episode of Alpine deformation

Major translative, nappe forming movements led to the thrusting of Pennine Mesozoic metasediments over the authochthonous Mesozoic cover of the Gotthard Massif during the first episode of Alpine deformation. As a consequence stratigraphic relationships in both metasediment series were disrupted by folding and sliding and a penetrative foliation was formed parallel to the planes of discontinuity. The major tectonic discontinuity which marks the base of the Pennine metasediment series is discordant to the deformed stratigraphy in the authochthonous cover. In Val Piora the discontinuity transgresses from the black garnet schist to the Quartenschiefer series and in Val Leventina it probably lies in the Triassic marbles bounding the southern margin of the Lukmanier Massif. Major and minor structures formed by the first Alpine deformation are absent in both the Gotthard and Lukmanier Massifs. In the Gotthard Massif their absence is consistent with the recognition that the Massif, in belonging to the Zone of External Massifs, probably did not undergo during the first episode of Alpine deformation the major translations and internal distortions suffered by the basement nappes in the Lower Pennine region to the south. The absence of structures of nappe movement age in the Lukmanier Massif, which has been interpreted both as a Lower Pennine nappe and as a southern extension of the Gotthard Massif (Sections 1.3, 1.4), suggests that it may be more closely related to the Gotthard Massif than to the Lower Pennine nappes.

3.53) The second episode of Alpine deformation

The disposition of the different structural units, the Gotthard Massif, the Lukmanier Massif and the cover, was determined largely by the second episode of Alpine deformation. The cover rocks were folded and in Val Piora and Val Canaria also affected by sliding. It has been shown (Section 3.22) that the metasediments lying between the basement gneisses of the Gotthard and Lukmanier Massifs cannot be considered to form a simple westward closing reclined second generation synform, as the southern limb of such a structure is either missing (east of Lago Ritom), or intensely modified by tectonic sliding (south and west of Lago Ritom). The northern limb of the Val Piora structure is cut by a tectonic slide or slide zone which bounds the southern margin of the Gotthard Massif.

In the Gotthard Massif itself the intensity of development of second structures and of the second deformation decreases northwards from the southern margin of the Massif. In the Streifengneiss the absence of second generation structures can be ascribed to both the weakness of the second deformation and to the reworking of the first (pre-Alpine) foliation in preference to the formation of a new planar structure (Section 3.32). This process of reworking was probably an important feature of the second deformation in the Gotthard Massif gneisses of the Lukmanier (Chadwick, 1965, p. 106) and Val Camadra areas (Cobbold, personal communication).

The gneisses of the Lukmanier Massif suffered both major folding and sliding during the second episode of Alpine deformation. The structure of the Lukmanier Massif is a westward closing reclined second generation antiform, whose northern limb has been modified by sliding with the southern limb of the synformal complement in the cover (Sections 3.22, 3.42, Encls. 2, 3 and 5). The northern contact of the Lukmanier Massif with the cover is thus determined by a complex association of folds and slides of second deformation age. The extremely strongly developed second foliation along the northern margin of the Massif, suggests that the deformation was most intense in this structurally complex region.

The second slide structures, which occur in the Lukmanier Massif, at the junction of the Lukmanier Massif and the cover and in the cover itself, can be divided into two sets:

1) Slides that are parallel to second foliation in the Lukmanier Massif.

2) Slides that are parallel to second foliation in the cover.

The relationship between these two sets of slide structures is discussed below.

Although the attitude of the second foliation (and slides) in both basement and cover has been influenced by subsequent episodes of Alpine deformation, it is thought probable that differences in attitude existed at the end of the second episode of Alpine deformation. These resulted from a ductility contrast between basement and cover which in turn led to an inhomogeneous resolution of the second episode strain by the two units. (The analogy may be drawn with the variation observed in the attitude of axial plane cleavage in layers of different competence within a fold.) The geometric form of most basement-cover contacts suggests that the assumption of a ductility contrast is usually justified. For example, in the Pennine Zone the lobate basement nappe sheets are separated by tightly pinched synclinal zones of Mesozoic cover rocks and in the Zone of External Massifs the Mesozoic cover appears in tightly pinched synclines separated by broad anticlinal zones of basement (Ramsay, 1967, p. 383 and Fig. 7.43). Such features arise from the deformation of a more ductile cover sequence overlying a less ductile basement (Ramsay, 1967, pp. 382-386). A ductility contrast of this nature might also be inferred from contrasting compositions of the basement and cover in the Val Piora area. Thus, during the second episode of Alpine deformation the more ductile cover would have accommodated itself to the changing shape of the basement units.

The processes by which the basement changed shape and by which the cover accommodated itself to this change were complex, as were the resultant second generation structures, as neither the basement nor the cover themselves behaved homogeneously during this episode of

deformation. An attempt is made below to explain some of the observed relationships between basement and cover although it is clear from the preceding remarks that a rigorous analysis of the deformation pattern which gave rise to the second generation structures is likely to be impossible.

As the east-west trending second slides at the margin of the Lukmanier Massif are continuous with northeast-southwest trending second slides in the Mesozoic cover (e.g. GG' and AA'), movement appears to have taken place simultaneously on surfaces of varying orientation during the second episode of Alpine deformation For movement without a continuous change in shape of one side of a slide structure in relation to the other, the movement direction must be parallel to the axis of the curved slide surface or, in the case of two oblique planar surfaces, must be parallel to the line of intersection of these surfaces. For a displacement of the cover-basement contact to be apparent the movement direction must also be oblique to the line of intersection of the cover-basement contact and the slide (Fig. 3.45a). The present line of intersection of the east-west trending second slides at the margin of the Lukmanier Massif and the northeast-southwest trending second slides in the cover, appears to plunge in a more westerly direction on the second slide surface than the line of intersection of the cover-basement contact. If the line of intersection of the second slide surfaces determines the movement direction on these surfaces then a northwest-southeast movement direction is indicated. The sense of movement on the slides is shown by the relative displacement of basement and cover at the southern margin of the Gotthard Massif (i.e. the northern limb of the Val Piora synform and the Gotthard Massif moved upward in relation to the southern limb and to the Lukmanier Massif). Accepting these qualifications the observed overthrusting of the Lukmanier Massif by the cover on slides parallel to second cleavage in the cover in the Piora and Madrano areas (Figs. 3.45b and c) and the part or complete absence of the southern limb of the Piora synform (Section 3.22) may be explained. The cross cutting relationship or interference of slides (Sections

Fig. 3.45. a The relationship, on the second slide surface (S_2) between the movement direction (M.D.) the line of intersection of the cover-basement contact (C.B.I.) the actual displacement (d) and the apparent displacement (d) is illustrated.

b and c Cut away block diagrams illustrating suggested structural relationships between the Lukmanier Massif and the cover in the Piora and Madrano areas. The overthrusting of the basement by the cover and the interference of the slide structures arises because of the initial difference in attitude, in the two structural units, of these structures. The slides are lettered as in Encls. 2, 3 and 5.

Fig. 3·45

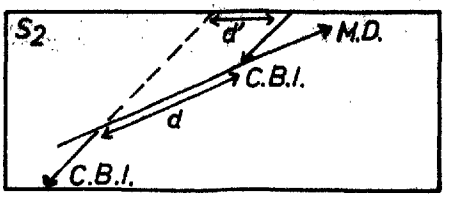

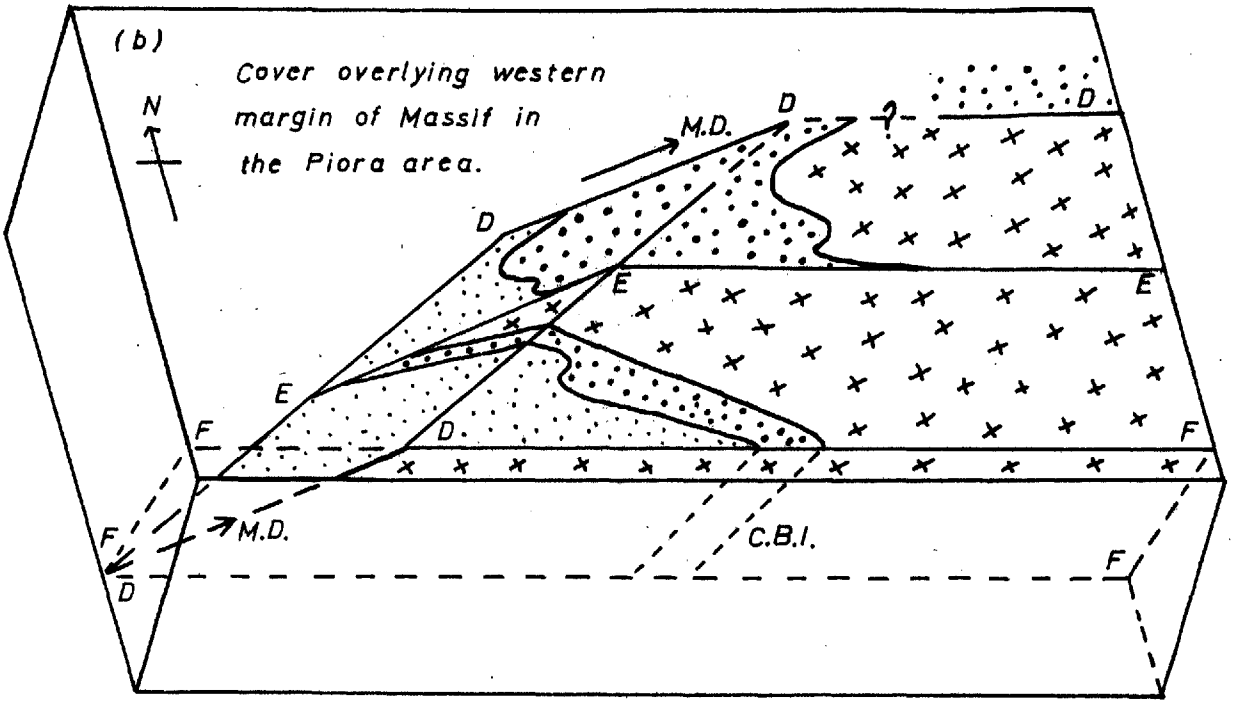

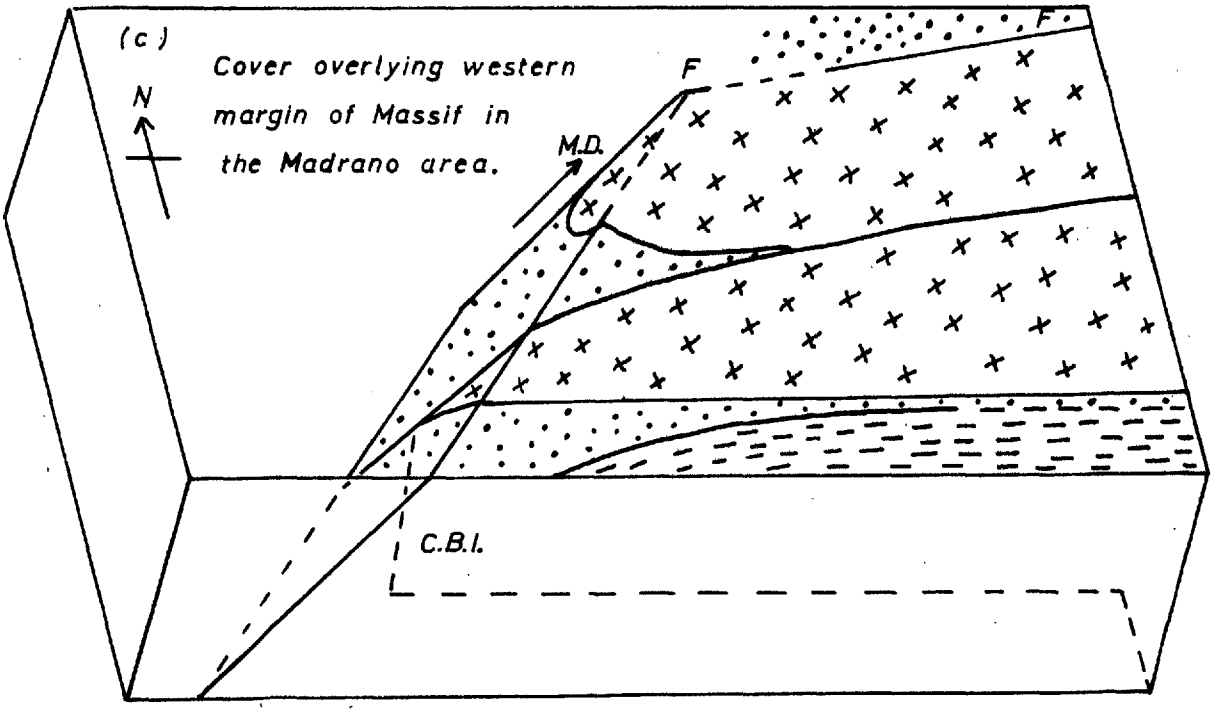

Rauhwacke and quartzite

Quartenschiefer

Bünderschifer

Lukmanier Massif

3.22, 3.42, Encl. 2, 3 and 5) need not imply different ages for the individual structures, merely different amounts of movement on them caused by differential movement of the basement blocks of the Lukmanier Massif. In the event of a northwest-southeast direction of movement on the slides, the amount of movement on individual slides required to produce the observed displacements of the cover-basement contact (Fig. 3.45a) must amount to several kilometres (cf. Section 3.9).

3.54) The third episode of Alpine deformation

The significance of the linear mineral fabrics and associated structures produced in the cover rocks by the third episode of Alpine deformation has already been discussed (Section 3.23). In both the Gotthard and Lukmanier Massifs similar linear mineral fabrics are observed and it is therefore probable that these were produced by a similar condition of deformation. In the Gotthard Massif kink bands, normal shears and planes of mafic mineral concentration (Section 3.33) have been interpreted as deformational instabilities arising during the high temperature viscous creep of the rocks during this episode of deformation. Overall however, features indicative of inhomogeneous strain (folds and boudins) are uncommon, suggesting that while the body rotation component of the third episode strain may have been large the distortional component may have been small. The conditions of rising temperature under which the third episode of Alpine deformation took place may also have aided, by the reduction of ductility contrasts, the homogeneous accommodation of greater amounts of distortional strain (Section 3.23).

On the basis of the interpretation of the fabrics and the associated structures, the third episode strain ellipsoid is suggested to approximate to pure constriction ($k = \infty$). The deformation which gave rise to this type of strain ellipsoid has been shown to be of a general rotational nature. In order to satisfy restrictions placed on the third episode deformation path by the structures, successive increments of rotational strain necessary to produce an overall pure constriction are constrictional strains of the form $1 < k < \infty$ which have progressively decreasing k values as deformation proceeds and which are related by a simple rotation about their Y axes (Section 3.23).

3.55) The fourth episode of Alpine deformation

Both fold and boudinage structures were produced during the fourth episode of Alpine deformation. The association of fourth episode structures, folds alone, boudins alone and folds and boudins or boudinaged folds, has been found to be determined by the attitude of the deformed planar structures in relation to the different fields of behaviour of directions within the fourth episode strain ellipsoid. Thus the presence of boudins alone (e.g. in the Gotthard Massif) suggests that the deformed planar structure falls within the field of continuous elongation, of folds alone (e.g. in the regions of steeply dipping planar structures in the cover and Lukmanier Massif), that it falls within the field of continuous shortening and the association of fold and boudinage structures (e.g. in regions of moderately dipping planar structures in the cover and Lukmanier Massif), within the field of initial shortening and later elongation. The premise is made above that structures once formed are unlikely to be destroyed, merely modified. In this context it can be argued that if this were not the case then the presence of parasitic folds (De Sitter, 1958) on the flanks of tightly oppressed larger structures would be enigmatic.

As the mean attitude of the fourth episode strain ellipsoid remains relatively constant throughout the area the different behaviours of the deformed planar structures, as recorded by the associations of structures produced, must arise from the superposition of the fourth episode strain on a set of structures of differing initial orientation. In part this difference stems from the fact that the deformed planar structures are not all of the same age (e.g. pre-Alpine age in the Gotthard Massif, first Alpine deformation age in the cover and pre-Alpine and second Alpine deformation age in the Lukmanier Massif), in part from inhomogeneous strain during earlier episodes of deformation.

The fourth episode strain ellipsoid is thought to have an intermediate k value ($k \simeq 1$) (Section 3.24). The orientation and shape of this ellipsoid when considered in relation to the

addition of successive increments of rotational strain during the third episode of Alpine deformation suggests that these deformations were intimately related if not continuous.

3.56) Late Alpine structures

a) Kink bands

Kink bands form structures of very minor importance in the Lukmanier Massif and in well banded Triassic marbles of the cover. Unlike the kinks in the Gotthard Massif they show features which allow them to be interpreted as structures developed at a late stage during the deformational history. The kink planes dip steeply to the south and the kink axes plunge gently in an easterly or westerly direction.

b) Breccia bands

Thin bands of Rauhwacke rich in angular fragments of Quartenschiefer are found particularly in the Quartenschiefer rocks east of Alpe Carorescio. These bands, which appear to be sub-parallel to first foliation, are clearly of tectonic origin (Krige, 1918, p. 527; Dal Vesco, 1964, pp. 56-57), though originally mistaken for conglomerate horizons, (Königsberger, 1909, p. 854). The age of these phenomena is less clear.

Linear mineral fabrics are observed in many of the schist fragments of the breccia bands. As these linear fabrics have no particular orientation in space, it can be deduced that the schists were brecciated after the linear fabrics were imposed (i.e. after the third episode of Alpine deformation). By a similar argument in relation to fourth generation structures it can be demonstrated that brecciation occurred after the fourth episode of Alpine deformation.

In the Rauhwacke directly underlying the Gotthard Massif in the Riale di Nelva, Bonney (1890, p. 209) reported the presence of schist fragments, which though similar in many respects to members of the Mesozoic succession in fact were probably derived from the Gotthard Massif. These fragments likewise show linear mineral fabrics with no particular orientation in space. It appears that at a late stage in the Alpine deformation some of the old structural lines were reactivated. In view of the lack of fabric within these breccia

bands the effects of this deformation are considered to be of minor importance.

c) Joints

No attempt has been made to make a detailed study of the joints in the rocks of the Val Piora area. Two dominant joint orientations are recognised however. Joints belonging to the first of these strike approximately east-west and dip steeply to moderately south, and those belonging to the second strike approximately north-south and dip at high angles to east or west. Typically east-west joints contain late mineral fillings, quartz, calcite, adularia, white mica and chlorite in various combinations. The north-south joints are usually barren.

3.6) Fold geometry and fold mechanism

Though the overall shape of the fold structures produced by the different episodes of deformation often closely approaches that of a pure similar fold, analysis of the layer geometry shows that the folds are in general made up of Class 1.C. and 3 layer associations. The presence of layers of Class 1.C. geometry indicates that buckling was a factor in fold development and the association of layers of Class 1.C. and 3 geometry conforms with the structural pattern produced by buckling of a multilayer complex with some modification of the fold shape by superimposed strain, as in flattened flexural folds (Ramsay, 1967, p. 432 and pp. 411-415). Though for the purposes of analysis the folds can be treated as initially buckled multilayers which have suffered a later homogeneous compressive strain (Ramsay, 1967, p. 433 and Fig. 7.102), in the general case shortening of the layer system by buckling occurs simultaneously with shortening by homogeneous compressive strain (homogeneous layer shortening) (Ramberg, 1964; Flinn, 1962, pp. 402-403). The rate of buckle shortening in relation to homogeneous layer shortening depends among other factors on the ductility contrast that exists between the layers (Ramberg, 1964, Equations 7 and 15). Where this contrast is large shortening takes place largely by buckling, where small, largely by homogeneous layer shortening. The greater the component of homogeneous layer shortening after the initiation of buckling the more closely the layer geometry approaches that expected in a pure similar fold. This conforms with the observation that Class 1.C. and 3 layer geometry is most pronounced where a marked compositional difference reflecting a large ductility contrast exists between the layers.

In a multilayer sequence consisting of a large number of layers of differing thickness and ductility, in view of the dependence of fold wavelength on layer thickness and ductility contrast between layers, several orders or wavelengths of folds can be expected to develop (Ramberg, 1963a, 1964). It is extremely probable that the variation in wavelength shown by each generation of folds in the Val Piora area is a direct result of this dependence.

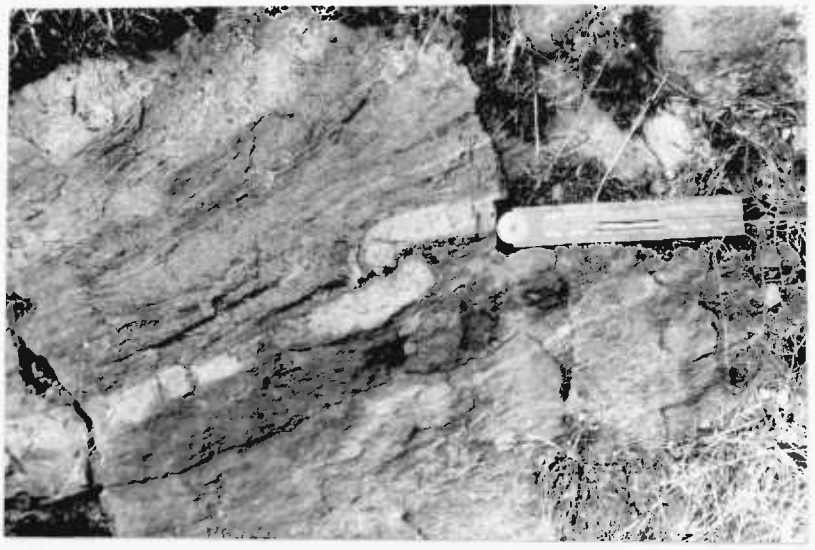

Fig. 3.46. Buckled quartzo-felspathic layer in a quartz-felspar mica gneiss. The folding of the surrounding banding dies out rapidly away from the buckled layer. Second generation fold, Mixed Group gneiss; road section, Piotta-Altanca, M.R. 6953815286.

Fig. 3.47. Second generation fold in the Quartenschiefer showing changing geometry and dying out when traced along the axial surface. South of Föisc, M.R. 6943615389.

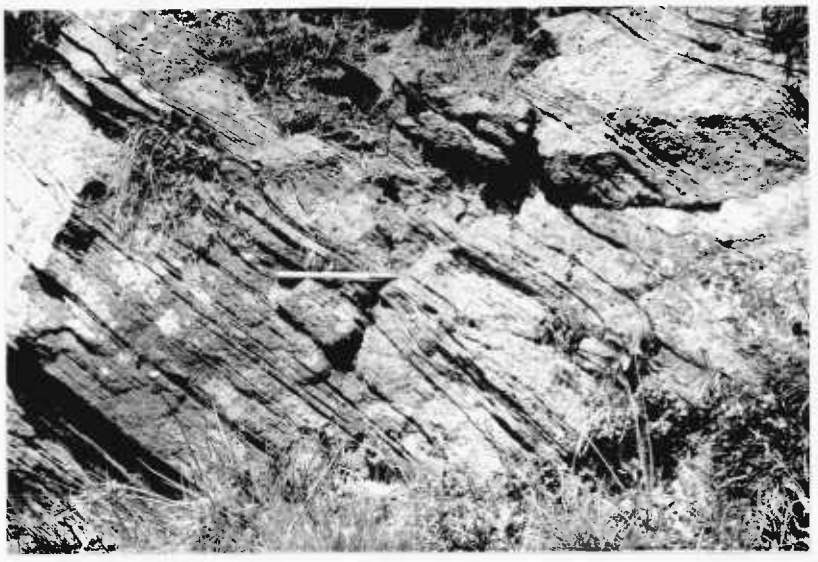

Fig. 3.48. Second generation fold showing changing geometry and dying out in both directions from a central maximum amplitude layer. Two other folds of comparable geometry equal distances on either side of this structure are also visible. Black garnet schist series; La Motta, M.R. 6959715569.

Invariably folds show changing geometry when traced perpendicular to their axes along their axial surfaces. They change their amplitude and eventually die out (Figs. 3.46, 3.47, 3.48). The variation in fold amplitude is often approximated by a simple fold model in which the amplitude of the folded layers decreases away from a single maximum amplitude layer at the centre of the fold. Geometrically the fold may be divided into two parts characterised by the style of variation in layer thickness, T, measured parallel to the fold axial surface, on either side of the maximum amplitude layer. On the convex sides of the maximum amplitude layer T decreases towards the fold hinge (Class 1.C. layer geometry), whereas on the concave sides it increases (Class 3 layer geometry) (Fig. 3.49).

This pattern of variation in T is characteristic of that observed in the zones of contact strain surrounding buckled layers (Ramsay, 1967, p. 416 and Fig. 7.82); it is also a consequence of any attempt to construct an idealised concentric or parallel fold over a sufficient thickness of strata (Hills, 1953, Fig. 48a; Ramberg, 1963b, Fig. 10) (Fig. 3.50a). Where the shape of the buckled layer and the zone of contact strain or the idealised concentric fold have been modified by a component of homogeneous compressive strain (e.g. as in Fig. 3.50b where the homogeneous strain component has been superimposed at 45 degrees) the pattern is retained, but becomes less clear, particularly for large values of superimposed strain.

Examples of natural folds which have a geometry which is not unlike the model are illustrated (Figs. 3.46, 3.47, 3.48). In Fig. 3.47 both the geometry (Class 1.C.) and contrasting ductility (suggested by the markedly different composition compared to the matrix) of the maximum amplitude layer suggest that in this case the changing geometry of the fold can be sensibly equated with the pattern of contact strain surrounding a single layer buckle. This is less obviously the case in Fig. 3.48, where the maximum amplitude layer is not clearly of contrasting ductility to the matrix nor does it display such marked Class 1.C. geometry. Observations such as this have led Ramsay to the conclusion (Ramsay, 1967, pp. 434-435 and Fig. 7.104) that fold patterns

Fig. 3.49. Regimes of differing layer geometry in a fold whose amplitude decreases away from a central maximum amplitude layer. T is the thickness measured parallel to the axial surface and is related in layers on either side of the maximum amplitude layer:- $T_1 > T_2 > T_3$.

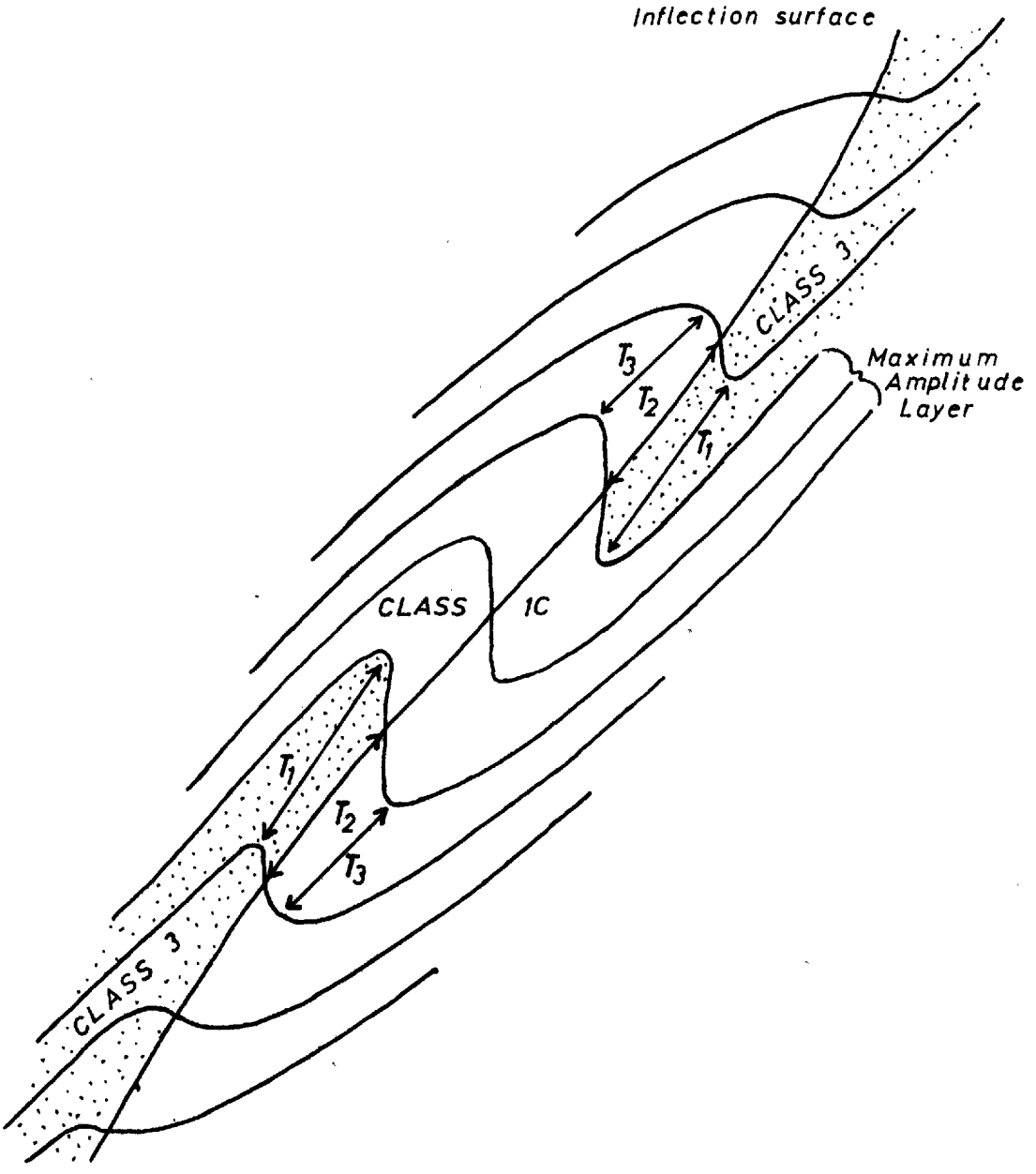
Inflection surface
CLASS 3
Maximum Amplitude Layer
T_3
T_2
T_1
CLASS 1C
T_1
T_2
T_3
CLASS 3

Fig. 3·49

Fig. 3.50. a Idealized concentric or parallel fold. The dotted layer shows concentric fold geometry whereas the layers on either side depart from this geometry (see text).

b Idealized fold modified by a component of homogeneous compressive strain superimposed at 45 degrees to the x and y coordinate axes. The amount of shortening at right angles to the plane of flattening is 50%. The isogon pattern is consistent with the geometry outlined in Fig. 3.49. It is also clear from this figure that the axial surface trace is curved.

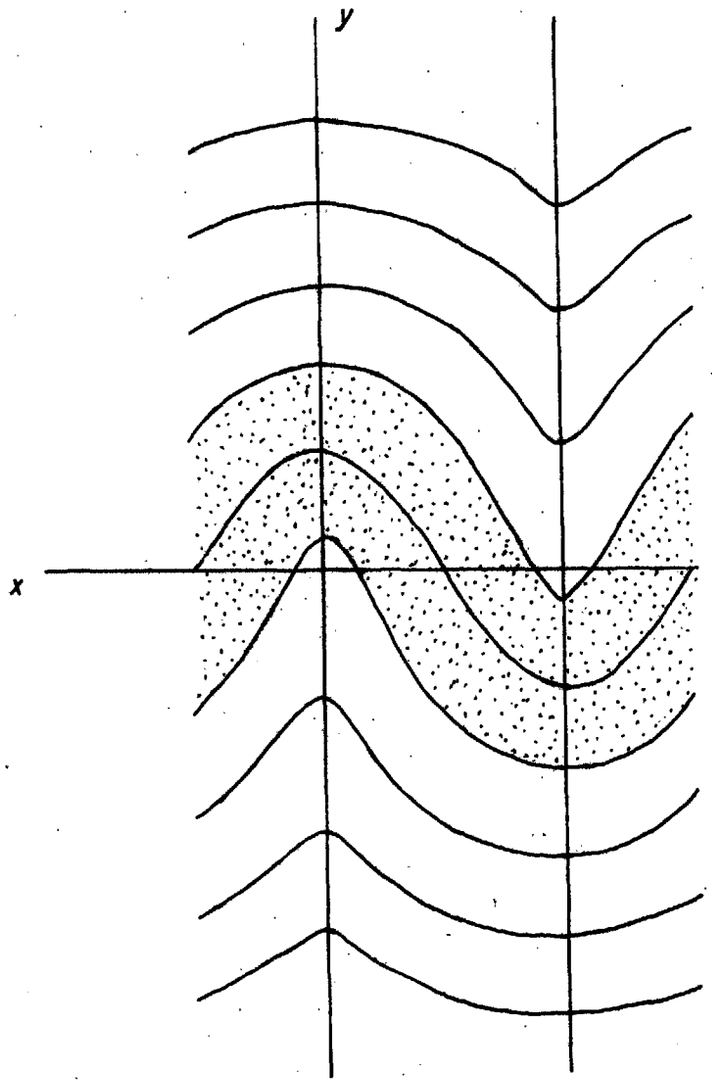
y
x

(a)

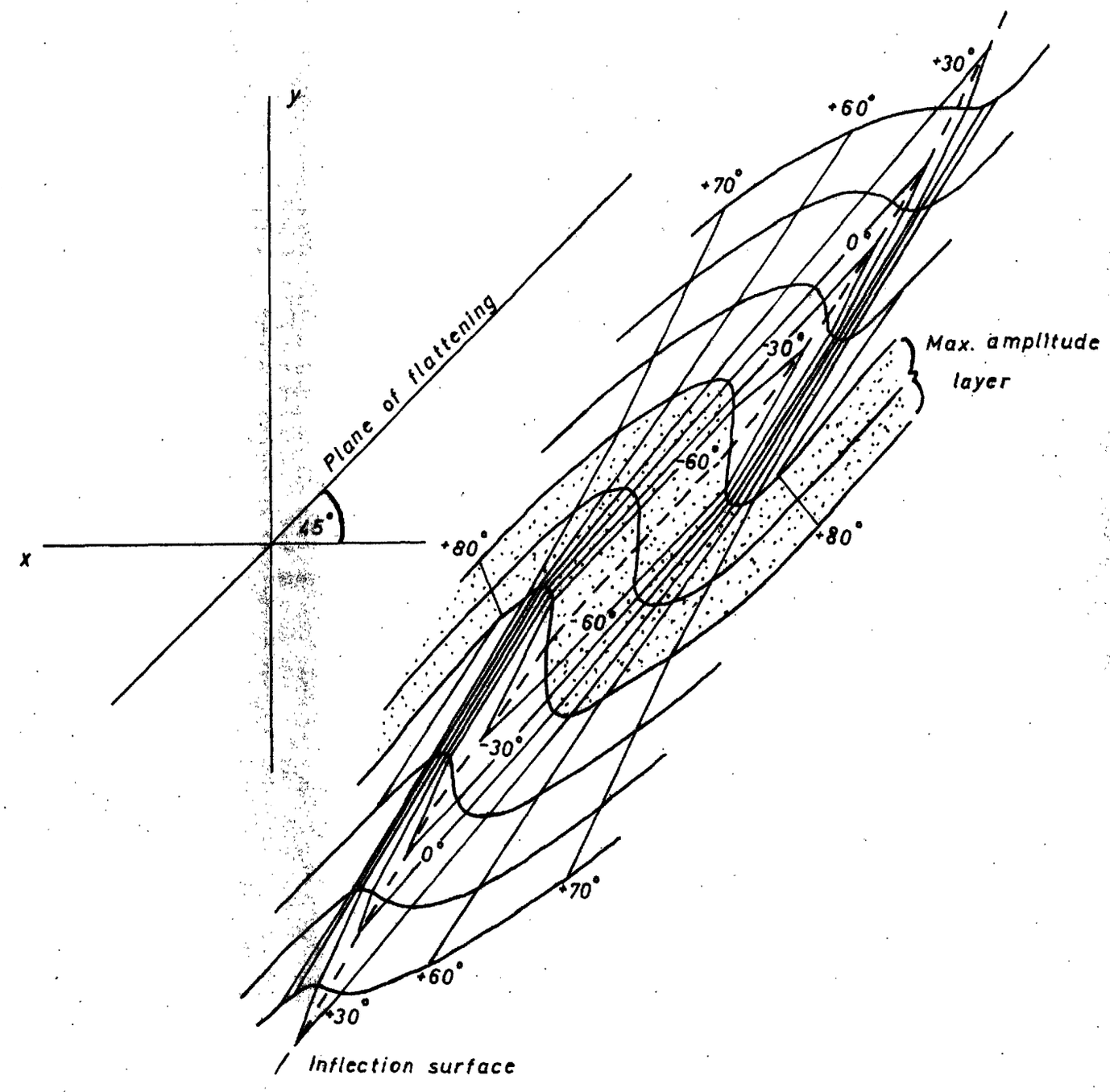
y
x
Plane of flattening
45°
I
+30°
+60°
+70°
0°
-30°
-60°
+80°
-60°
-30°
0°
+70°
+60°
+30°
Max. amplitude layer
/ Inflection surface

(b)

Fig. 3·50

of the type represented by the model, above, might be developed around regions of inhomogeneous finite strain. In this event there would be no immediate reason to expect any wavelength control of the folded layers. This is not the case for the three visible fold structures illustrated in Fig. 3.48, which appear to be equally spaced and apparently determined by a mechanism which involved buckling. Folds should die out fairly rapidly from the maximum amplitude layer if a buckling mechanism has operated, as the zone of contact strain around a single layer buckle is limited to a distance of less than one wavelength (wavelength of initial buckle) on either side of the buckled layer (Ramberg, 1960, 1961). It is appropriate to point out that in the instance above where the factors which determined the rheological differences between the maximum amplitude layer and the surrounding layers, which led to buckling, are unrecognisable, so also are the factors which determined the region of inhomogeneous strain where the inhomogeneous finite strain approach is considered.

The modification of a symmetrical buckle and its zone of contact strain or of an idealistic concentric fold, by an obliquely superimposed homogeneous strain* (Fig. 3.50b) leads to a fold with a curved axial trace. This arises because of the differing rates of curvature of the layers in the unmodified fold structure. Curvature of the axial traces of natural folds has been observed in the Val Piora area. The discussion of changing geometry above has been confined to considering profile sections of folds. It is invariably the case that geometry also changes along fold hinges. The hinges die out, converge or diverge, etc. Such variations possibly reflect the changing rheological properties of the layered system along the fold hinge.

It is apparent that some of the folds in the Val Piora area probably owe their changing geometry to the pattern of contact strain around a single layer buckle. Where two or more harmonically buckled

---

* The asymmetric superposition of a homogeneous strain component is a likely consequence, where the structures can be considered as 'drag' folds developing about a larger wavelength structure (Ramberg, 1963a, 1964).

layers are involved the pattern is obviously more complex and the fold persistent over a greater distance. A common factor however is that these folds will also be characterised by changing geometry and will also eventually die out.

3.7) Complexity of structure

It has been aptly pointed out (Flinn, 1962, pp. 426-427; Ramsay, 1967, pp. 174-175) that where the concepts of homogeneous progressive deformation are applied to inhomogeneous layered systems, in the instance in which the layering has no particular relationship to the strain axes (in fact in the general case) the resultant structures can be expected to be complex. However, in many areas the structural patterns are such as to suggest a special relationship between layering and strain axes. The Val Piora area must be regarded as an area of this type in view of the specific relationships, demanded by third and fourth episode structures, between the layering and strain axes during the third and fourth episodes of Alpine deformation (Sections 3.23, 3.24).

Flinn has suggested that the inhomogeneity of layering may lead to a simplification of structural pattern, through strengthening of structural directions by folding and through rotation of stress and strain axes into more symmetrical positions in relation to layering. One might on this basis question the application of the concepts of homogeneous progressive deformation to inhomogeneous layered systems and the resultant conclusions. However, in doing so one also questions the validity of the only tool which is generally available to the structural field geologist for the analysis of the deformational history.

3.8) Correlations with other workers

In the following pages the structural history deduced in the previous sections is correlated with the interpretations of other workers (Table 3.3) both in the Val Piora area and in adjacent areas.

In his structural analysis of the Val Piora area Krige (1918, pp. 525-529) recognised that the Mesozoic rocks in Val Piora formed a complex synclinal structure between two blocks of dissimilar basement (the authochthonous Gotthard Massif and the allochthonous Lukmanier Massif). He interpreted the southern part of this structure (Fongio-syncline) as a series of small synclines in the basement and possibly as schuppen. He discussed (pp. 597-599) the significance of the lineated micas which cross cut the schistosity and suggested (p. 529) that their fabric indicated the action of an east-west directed pressure after the north-south directed pressure which gave rise to the schistosity. There are obvious parallels which may be drawn between Krige's analysis and that outlined in the preceding sections.

Wunderlich (1958) discussed some of the structures apparent in the Mesozoic rocks of Val Piora as part of a regional tectonic appraisal of the Mesozoic cover rocks surrounding the Gotthard Massif. He recognised two linear elements in these rocks, Linear I and Linear II, equivalent to structures described in this thesis as the third episode linear mineral fabrics and the fourth generation fold axis, respectively (Table 3.3). Wunderlich (1963) has produced maps indicating that these linear elements occur throughout a large part of the Alpine mountain chain. Wunderlich (1958, p. 131 and Fig. 11) interpreted the second generation folds as B1 B' structures, related to the formation of Linear I. In discussion of the syntectonic or snowball garnets he suggested (1958, p. 139) that these grew and rotated during the formation of Linear II and not Linear I (i.e. during D_4, not D_3 (Sections 3.23, 4.2)).

Steiger (1962, pp. 461-467 and Tabelle 17) (Table 3.3) described six episodes of Alpine deformation in the gneisses forming the southern margin of the Gotthard Massif between the Lukmanier and Gotthard Passes. From his detailed account of the structures formed during these episodes

it is apparent that the structures discussed in Section 3.3 are closely comparable. The essential differences in their interpretation are as follows (cf. Table 3.3).

1) Steiger considers schistosity (first foliation) and the penetrative mineral lineation to be largely the product of the principal Alpine phase of deformation (Phase II). (Though he recognises the schistosity to be Alpine Steiger infers (Table V) that "grobe Faltenachsen" in the Corandoni zone and Prato series and the quartz-felspar rodding in the Streifengneiss, which lie in the plane of the schistosity, are of pre-Alpine age !)
2) The north-south trending "Kleinfältelung" which parallel the mineral lineations he suggests developed after the imprint of the main linear fabric, in response to a weak east-west compression (Phase III). The girdle biotite fabric (Querbiotite fabric) formed at a late stage in the operation of the Phase III stress system.

Kvale (1957, 1966), as a result of fabric studies in the Gotthard Massif and the adjacent Mesozoic cover, finds evidence in these rocks for six tectonic events of which two are pre-Alpine (one of these events is the intrusion of the Hercynian granites) (Table 3.3). Mica fabrics described by Kvale are similar to those observed in the Val Piora area. A difference in their interpretation exists however, as Kvale considers the total tectonic mica fabric (excepting the Querbiotite fabric) to be the product of a single deformation act. In this analysis it has been suggested (Section 3.23) that the total tectonic mica fabric is made up of a number of part fabrics formed during different episodes of deformation and modified but not always destroyed by later episodes of deformation.

Kvale (1957, 1966) has pointed to the similarity in the pattern of structures in the Mesozoic synclines south of the Gotthard Massif. In the Nufenenpass region to the southwest of Val Piora (Chatterjee (1961) and Higgins (1964b) have carried out more detailed investigations. Chatterjee recognises three ages of linear structures in the Nufenen area, B_0, B_1 and B_2; where B_0 represents the axes of large

easterly plunging folds, considered to be the earliest Alpine folds, B_1 is a prominent mineral lineation representing the extension axis of a post B_0 flattening deformation and B_2 is a gently plunging to horizontal crenulation fold axis. These linear structures have their obvious equivalents in those produced during D_2, D_3 and D_4 in the Val Piora area (Table 3.3).

Passing southwards into the Pennine region it seems likely that Chatterjee (cf. Plate 2) has confused the B_2 folds of the Nufenen region with earlier generations of fold structures. Thus in the Albrunpass area where two generations of post nappe folds exist (Sibbald, 1965) his B_2 folds conform with the earlier of these. Higgins (1964b, p. 162), on the basis of his observations in the Pennine region, makes a similar criticism.

Higgins (1964b) records Chatterjee's three sets of structures but his interpretation of their age relations is slightly different (Table 3.3). He suggests (p. 114) that the mineral lineation in the Nufenen rocks was formed during the development of the large scale B_0 folds and is not to be considered as the product of a separate deformation.

Schuppen are present in the Nufenen as in the Val Piora area. Higgins (p. 100) suggests that these are related to the large scale B_0 folds as they are oriented approximately in the axial surfaces of these structures. They were probably initiated in pre-B_0 times in response to block movements in the basement. (The Corno-Schuppe (Oberholzer, 1955) is thought to be of this age). Further movements may have accompanied fold development. In the Gotthard Massif Higgins recognises these same structures but interprets the dominant early schistosity as a pre-Alpine structure. The contact of the Gotthard Massif with the cover is suggested to be tectonic and of B_0 age (cf. Oberholzer, 1955; Hafner, 1958).

In the context of the Alpine deformation as a whole the structures so far discussed belong to the third ($F_3 = B_0$ and B_1) and fourth ($F_4 = B_2$) episodes of deformation in Higgins's deformation sequence (Table 3.3). Structures formed during the two earlier episodes of

deformation are found in the Pennine region to the south, but are in general absent in the Nufenen rocks (only one example of folds predating F_3 structures has been recorded (Higgins, 1964b, pp. 132-133)). For this reason it has been suggested that the Gotthard Massif and the Nufenen zone did not become involved in the Alpine movements until late F_2 times.

Although Higgins interprets the major (B_0) fold structures in the Nufenen region as F_3 structures, there seems to be no evidence against the interpretation of these as F_2 folds. In this event the absence of folds of F_3 age in the Nufenen region is comparable to the absence of folds of D_3 age (other than crenulations parallel to the mineral lineation) in the Val Piora and Lukmanier areas.

The region to the east of Val Piora has been the subject of a number of recent investigations. Of these two are of particular interest, that of Chadwick (1965, 1968), because it represents a detailed structural and metamorphic analysis of the area immediately to the east of Val Piora, and that of Frey (1967), because in association with his investigation of the Greina area he synthesises the recent work in the cover rocks of the eastern Gotthard Massif of the Zürich school of geologists.

In the Lukmanier area, Chadwick recognises two episodes of Alpine deformation, Phases B and V, both of which postdate the Pennine nappe forming movements. Structures produced during Phase B (major and minor folds and associated penetrative axial plane cleavage in the cover rocks, tectonic slides at the basement cover contacts and the linear mineral fabrics) conform with structures formed during D_2 and D_3. Those produced during Phase V conform with structures formed during D_4 in the Val Piora area (Table 3.3). Thus Chadwick, in company with Higgins and in contrast to the opinion cited here (Section 3.23), considers the linear mineral fabric to be related to the formation of the Phase B folds and slides and to indicate the direction of movement on these slides.

Chadwick's suggestion that the schistosity (first foliation) in the gneisses of the Gotthard Massif is of Phase B age and hence Alpine

and that the rodding in the Streifengneiss may also be Alpine differs from the interpretation proposed in this thesis (Sections 3.3, 3.31). The Phase B age of the schistosity in the Hercynian intrusions in the Lukmanier area is not disputed, however, a similar age for the schistosity in many if not all of the pre-Hercynian gneisses of the Gotthard Massif is questioned. Because of the parallelism of Alpine and pre-Alpine structures, and the partial reworking of pre-Alpine structures during Alpine times (Section 3.32) some confusion over the ages of the structures is to be expected.

Frey (1967) on the basis of his mapping in the Greina area and of a synthesis of recent work in surrounding areas (e.g. Jung, 1963; Baumer, 1964; Chadwick, 1965), finds evidence for a phase of deformation which predates Chadwick's Phases B and V (Table 3.3). The tectonic events which took place during this early, B_0, deformation, as shown by Frey (1967, pp. 99-100) are summarised below.

1) The Mesozoic sediments of the Gotthard Massif above the Lias were removed, most probably tectonically, in response to movements in the Pennine region.
2) The Liassic sediments which remained behind on the Gotthard Massif (the Scopi Zone and Peidener Schuppenzone rocks) were folded. The Scopi Zone (parauthochthonous cover) was inverted on the residual Triassic and Lower Liassic sediments of the Gotthard Massif (authochthonous cover). (Nabholz and Voll (1963) conclude that the Mesozoic sedimentary pile is the right way up. Frey (1967, pp. 96-97) gives convincing stratigraphic and other reasons for refuting their conclusion.)
3) Movements took place in the Gotthard basement along the line Piz Miez, Lago Retico, Ri. di Prusfa (the northern contact of the Scopi syncline with the Gotthard basement), and led to shearing of the relict authochthonous cover.
4) The Pennine sediments were thrust over the authochthonous and parauthochthonous cover elements. It is not known whether this thrusting was earlier or later than event (3).

The following comments may be made with respect to the tectonic events outlined above. Firstly, as pointed out by Frey himself (p. 100) the early phase of Alpine deformation left no recognisable imprint in the form of minor structures in the Gotthard basement (Section 3.3). Secondly, in contrast to Chadwick, Frey considers movement to have taken place at the northern contact of the Scopi syncline with the Gotthard basement, in part at least before Phase B. It is difficult to reconcile the first of these observations with the second as presumably the Gotthard basement was deformed by the movements described in (3). Thirdly, it is suggested, (2), that the parauthochthonous sediments of the Scopi Zone lie with discontinuity on the authochthonous sediments of the Gotthard Massif. The Scopi syncline, which has been interpreted as a simple syncline with a strongly attenuated northern limb (Huber, 1943, p. 87), or as a syncline with its northern limb largely removed by tectonic sliding (Chadwick, 1965, 1968), is therefore a more complex structure. In the section through the Scopi Zone exposed along the new Lukmanier Pass road (see also Nabholz and Voll (1963, Fig. 10)) Frey (1967, pp. 38-39 and 82-83) illustrates the evidence for this discontinuity.

A part of Frey's area has recently been remapped (Cobbold, 1969) and the history of deformation deduced substantially agrees with that outlined by Frey. Cobbold recognises Frey's B_0, B, V phases of deformation and in addition a Phase T, which postdates Phase B, but is earlier than Phase V (Table 3.3). The possible significance of Cobbold's Phase T structures is considered in the concluding discussion.

The Pizzo Molare area to the south of Lukmanier has been the subject of a recent investigation (Thakur, 1971). Both structures and structural sequence outlined by Thakur can be equated with those found in the Val Piora area. A major northward closing synformal fold is recognised to occur between the Val Piora and Molare areas. Planar structures which are northward dipping in Val Piora become turned over into a southward dipping orientation on Pizzo Molare. The geometry and age of this major fold is discussed below (Section 3.9).

There is little basis for correlation of the structures observed in Val Piora with those described in the Sambuco-Massari area by Hasler (1949). A detailed study of minor folds in the Alpe Massari, Alpe Sheggia region, (Hudleston, 1969) has shown that at least three generations of fold structures exist there. These are possibly to be correlated with those produced during D_1, D_2 and D_4 in the Val Piora area. With respect to the large scale structures, the gneisses of the Sambuco lobe of the Maggia nappe, may form the core of a major second generation synform, which is the southern complement of the Lukmanier antiform and is continuous in the east with the Molare synform.

Table 3.3 Correlations with other workers.

Wunderlich (1958) (Cover)	Correlation*	Chatterjee (1961) (Cover, Nufenenpass)	Correlation
Linear I		B_o Phase	
N.S. mineral lineation.	D_3	Major folds in Nufenenpass area	D_2
B ⊥ B' folds.	D_2		
Linear II		B_1 Phase	
Folding on E.W. axes	D_4	N.S. mineral lineation	D_3
Syntectonic garnet rotation.	D_3		
		B_2 Phase	
		Folding on E.W. axes	D_4

*Correlations

D.p.A. - Structure formed by the pre-Alpine episode(s) of defm.
D_1 - Structure formed by the first episodes of Alpine defm.
D_2 - Structure formed by the second episodes of Alpine defm.
D_3 - Structure formed by the third episodes of Alpine defm.
D_4 - Structure formed by the fourth episodes of Alpine defm.
L.A. - Structure formed by the Late-Alpine episodes of defm.

Steiger (1962) (Gotthard Massif)	Correlation	Kvale (1966) (Gotthard Massif and Cover)	Correlation
Pre-alpine		Pre alpine	
Rodding in Streifengneiss.	D.p.A.		
Folds in Prato series and Corandoni Zone (Grobefalten).	D.p.A.	Phase 1. Rodding in Streifengneiss	D.p.A
Alpine		Phase 2 Intrusion of Medelser granite	D.p.A
Phase I Strong cataclaysis first outline of schistosity.	D.p.A.	Alpine	
Phase II (Chief Alpine phase) Development of schistosity	D.pA(D_2)	Phase 3 (Main Alpine movements) N.S. mineral lineation	D_3
and N.S. mineral lineation.	D_3	(and schistosity)	(D.p.A, D_2)
Syntectonic garnet rotation.	D_3	Phase 4 Development of N-N.W. trending	
Phase III Development of N.S. trending folds, (Kleinfältelung) and girdle biotite, (Querbiotite), fabric.	D_3	folds and girdle biotite (Querbiotite), fabric (Airolo-Nufenen area).	D_3
		Intrusion of Rotondo granite	?
Phase IV Weak cataclaysis.		Phase 5 Folding on E.W. axes (Wellung)	D_4
Phase V Folding on E.W. axes (Wellung)	D_4	Phase 6 Vertical upward movements on shear planes. Development of Gotthard Massif fan.	L.A. D_3D_4
Phase VI Weak cataclaysis.	L.A.		

Higgins (1964b) (Gotthard Massif and Cover) (Pennine Zone)	Correlation	Chadwick (1965, 1968) (Gotthard Massif and Cover) (Lukmanier Massif)	Correlation
Pre Alpine Early schistosity in Gotthard Massif	D.p.A.	Pre Alpine ? Rodding in Streifengneiss	D.p.A.
Alpine		Alpine	
F_1 Nappe emplacement and associated major and minor structures.	D_1	Phase B Schistosity in Gotthard Massif, Lukmanier Massif, and Cover.	)D.p.A., D_2)
		Major folds in Cover. (Scopi synclineetc)	D_1, D_2
F_2 Major folds in the Pennine Zone.		Slides at basement/cover contacts.	D_2
Initiation of block movements in Gotthard Massif basement.	D_2	Development of N.S. mineral lineation.	D_3
F_3 Major folds and Schuppen in Nufenenpass area	D_2	Phase V. Minor folding on E.W. axes.	D_4
Development of N.S. mineral lineation.	D_3		
F_4 Minor folding on E.W. axes.	D_4		

Frey (1967) (Cover)	Correlation	Cobbald (1969) (Gotthard Massif and Cover)	Correlation
Alpine		Pre-Alpine	
B_o Phase (See Text)	D_1	Early schistosity in Gotthard Massif.	D.p.A.
		Rodding in Streifengneiss	D.p.A.
Phase B (as Chadwick)		Alpine	
Phase V (as Chadwick)		B_o Phase (as Frey)	D_1
		Phase B Major and Minor folding of Gotthard Massif and Cover - (Marumo synform, Sassina antiform, (Greina-einmuldung)) Slaty cleavage in Cover. Second schistosity in Gotthard Massif.	D_2
		Phase T Major and minor folding on E.W. axes. Crenulation cleavage	D_3
		Phase V Minor folding on E.W. axes.	D_4

3.9) Discussion (a regional synthesis)

Some controversy exists over the correlation of structures in the Lukmanier area with those in the parauthochthonous cover of the eastern Gotthard Massif. Whereas the former region appears as an area affected by both folding and thrusting (Chadwick, 1965, 1968) the latter is dominated by thrust teotonics (Jung, 1963; Nabholz and Voll, 1963; Frey, 1967). Nabholz and Voll (1963, p. 773) and Chadwick (1965, p. 153) consider the second deformation folds and slides in the Lukmanier area (Phase B, of Chadwick; S_I, B_I, str.$_I$, of Nabholz and Voll) to be the same age as the flatter lying schuppen further east. The Zürich school find the schuppen to be of first deformation age, related to the inversion of the Scopi zone and intimately linked with the deformation which led to the thrusting of the Pennine metasediments over the authochthonous and parauthochthonous cover elements (B_0 Phase of Frey (Section 3.8)). When the individual schuppen are traced (Jung, 1963; Baumer, 1964; Frey, 1967) it is found, in support of the contention of the Zürich school, that not only do they show a general structural concordance with the Frontal Pennine Thrust, but also when followed into the region of major second folds and slides they become deformed by these structures (Frey, 1967, Figs. 23 and 24), (Figs. 3.51, 3.52).

Chadwick (1965, p. 153) in arguing for the contemporaneity of the schuppen and the Phase B structural zones in the Lukmanier area (Scopi Zone, Val di Campo Zone, Valle di Lucomagno Zone) points to how these zones turn over in the east to form gently dipping schuppen. For instance, the Trias of the Val di Campo anticline appears in the east as a Triassic slice separating the Forca and Pianca Zones of the Peidener Schuppen Zone (Fig. 3.51). As the schuppen are in fact first generation structures, by the same argument it can be suggested that the so called Phase B structural zones in the Lukmanier area are also first generation structures. The structural geometry of the Lukmanier area appears to require more than two deformation episodes to explain the distribution of rock types; a pre-Phase B deformation must be considered as an important part of the history of the cover deformation in this area as it is in Val Piora and the region to the east of Lukmanier.

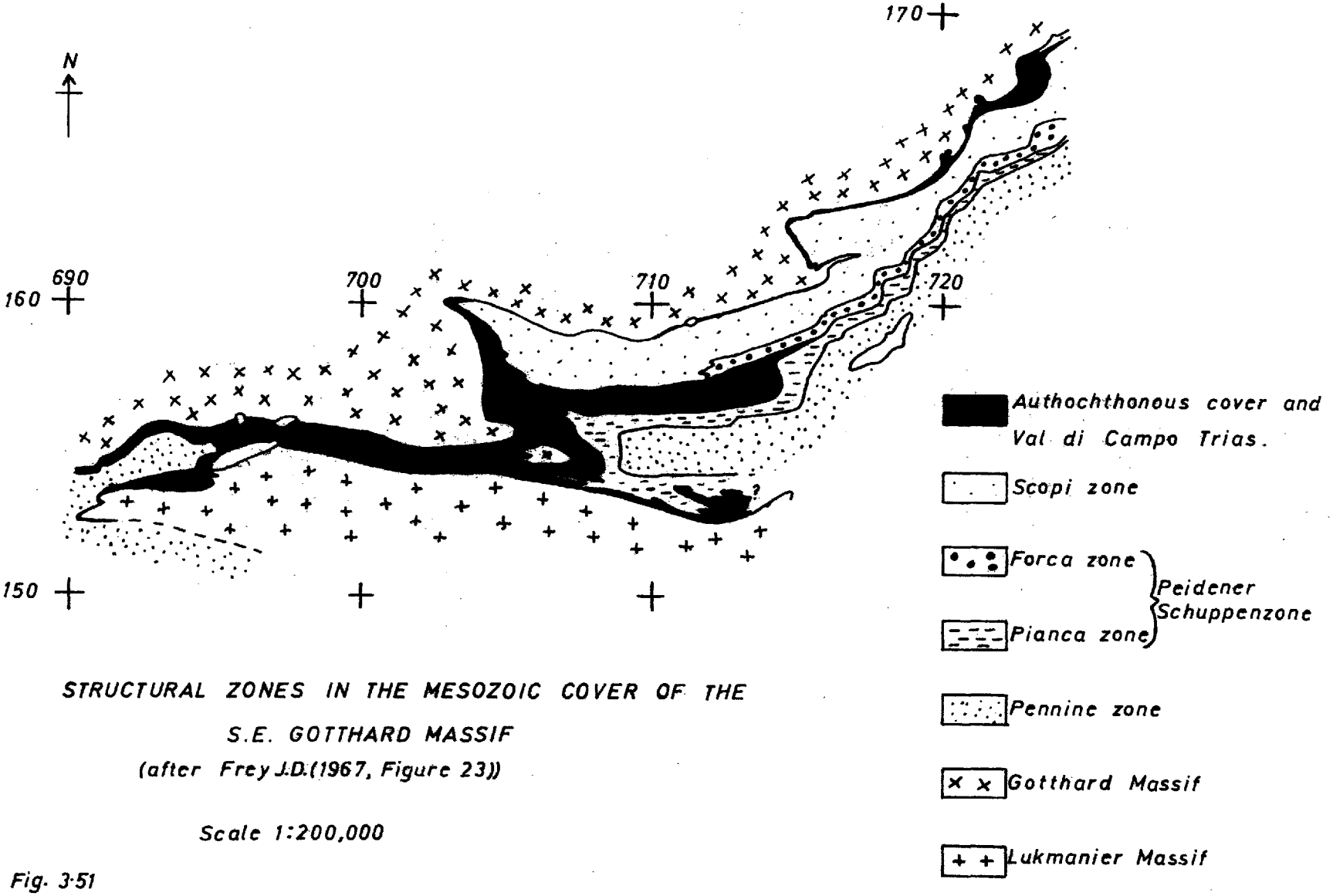

STRUCTURAL ZONES IN THE MESOZOIC COVER OF THE S.E. GOTTHARD MASSIF

(after Frey J.D.(1967, Figure 23))

Scale 1:200,000

Fig. 3·51

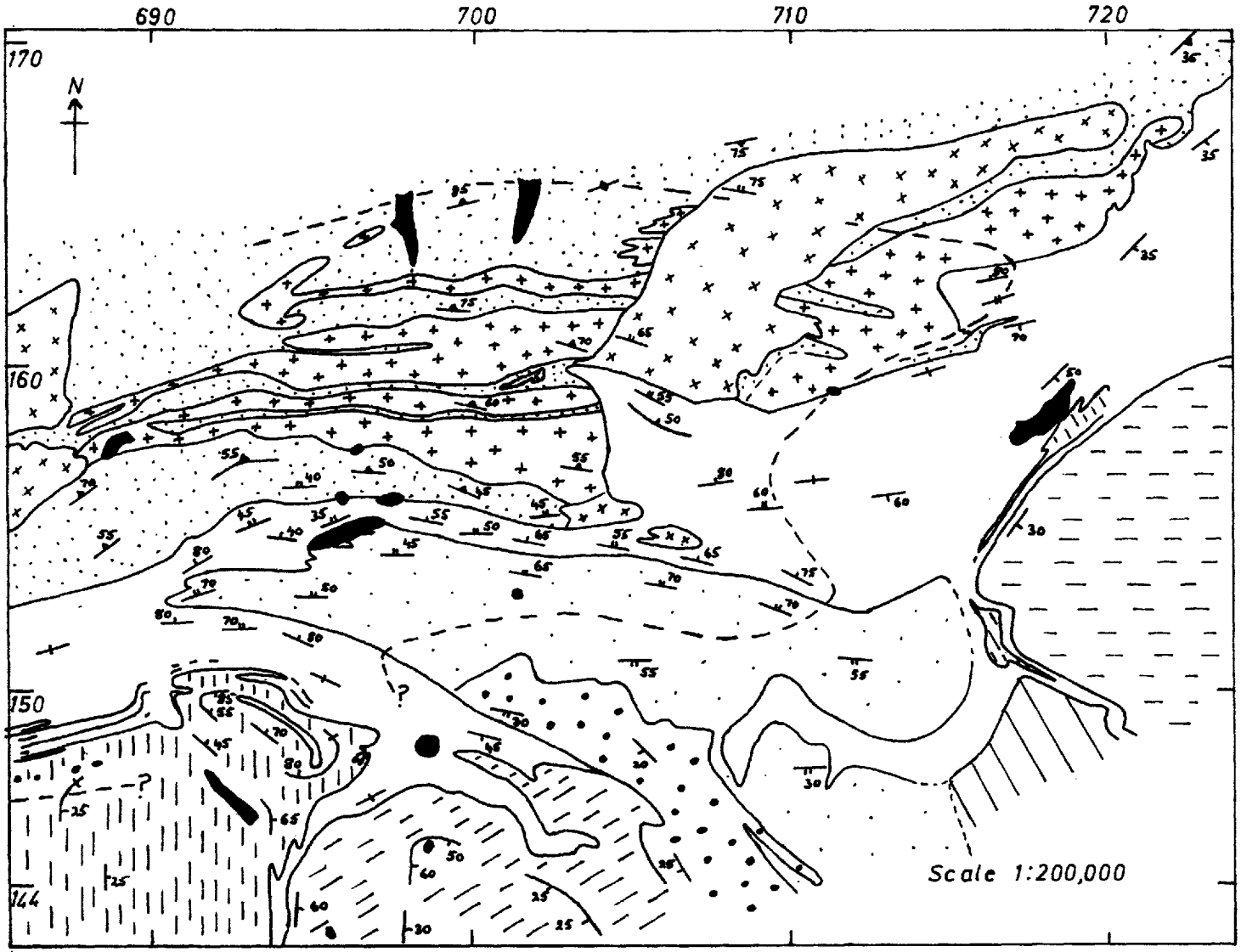

Fig. 3·52 GEOLOGICAL SKETCH MAP OF REGION SURROUNDING VAL PIORA

It can be concluded, following Frey (1967), that during the first episode of Alpine deformation most of the sediments of the Gotthard Massif cover were removed tectonically and probably slid northwards to form a part of the Helvetic nappe complex. The remaining Liassic sediments of the Scopi Zone and Peidener Schuppen Zone were folded and thrust to form a series of parauthochthonous slices (schuppen) on the residual authochthonous cover at the base of the Pennine nappe complex. The Pennine metasediments in Val Piora and on Nufenenpass appear to be in contact with the residual authochthonous cover, whereas in the east they are in contact with the Pianca Südschuppe of the Peidener Schuppen Zone (Fig. 3.51). From these observations it can be inferred that the Scopi and Peidener Schuppen Zones wedge out against the authochthonous cover towards Val Piora. A discordance must therefore exist between the authochthonous and parauthochthonous cover. In this context it can be suggested (cf. Frey, 1967, p. 33; Baumer, 1964, pp. 55-56) that the discordance between the parauthochthonous and sheared authochthonous cover at the northern contact of the Scopi Zone with the Gotthard basement has primarily originated in this way and is only secondarily the result of Phase B sliding at the basement-cover contact (Chadwick, 1968, p. 1130). The second cleavage, first foliation intersection relationships in the Val Camadra and Lukmanier areas are also inconsistent with Chadwick's conclusion that the major structural relationships in the cover are due to a single episode of deformation (Phase B). They are however consistent with the interpretation which has been outlined above (Fig. 3.53).

The Gotthard and Lukmanier Massifs were unaffected by the major translative movements in the cover rocks (Section 3.5), the residual authochthonous cover acting as a surface of décollement to the first episode of Alpine deformation. This observation has an important bearing on the origin of the Lukmanier Massif, which must be interpreted as a part of the relatively unmoved basement rather than as a basement nappe (Section 3.5).

The basement was activated during the second episode of Alpine deformation, deforming inhomogeneously, the zones of paragneiss

N. S.

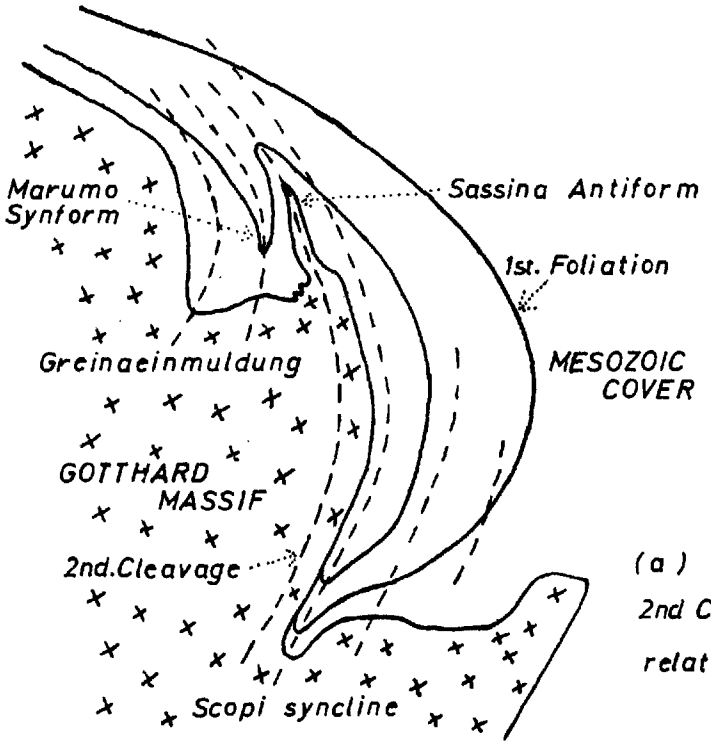

(a) Observed 1st. Foliation 2nd Cleavage intersection relationships.

(b) Intersection relationships suggested by Chadwick's interpretation of the structure of the Mesozoic Cover.

Fig. 3·53

forming regions of more intense deformation and determining the positions of second generation structures in the overlying Mesozoic cover. This is perhaps most clearly illustrated in the Gotthard Massif by the paragneisses of the Boreal Zone and the paragneisses at the southern margin of the Massif in the Val Camadra area (Frey, 1967; Cobbold, 1969) (Fig. 3.52). Thus, the pinched in nature of the cover rocks in Val Rondadura (Chadwick, 1968, Plate I), and the squeezed out aspect of paragneisses of the Sassina antiform (Frey, 1967, Tafel I; Cobbold, 1969) can be equated with a greater compressive strain in these paragneisses than in the adjacent blocks of granitic basement (Streifengneiss and Medelser granite). The relative elevation of the granitic basement to the north of the Boreal Zone with respect to that lying to the south indicates that the paragneiss horizons were also zones in which the differential movements between adjacent blocks of slightly deformed granitic basement were accommodated. The northern margin of the Scopi Zone has been interpreted as a slide (Chadwick, 1968, p. 1130).

Just as the Boreal zone determined the northern limit of the Scopi structure, the Tremola Zone is suggested to have influenced the position of the Valle di Lucomagno-Val Piora structure (Chadwick, 1968, p. 1134). The northern margin of the Val Piora structure is likewise bounded by a slide. East of Val Camadra the Greinaeinmuldung (Frey, 1967; Cobbold, 1969), though apparently comparable to the Scopi and Val Piora structures, is found in contrast to be a simple synform and not a slide determined structure. The basement surrounding this feature is however essentially homogeneous, Streifengneiss. Both large and small scale structures in the Gotthard Massif gneisses (Section 3.32) indicate that the pre-Alpine structures were reworked during the second episode of Alpine deformation.

The antiformal structure of the Lukmanier Massif suggests that in this case the basement behaved in a more uniformly ductile fashion than the Gotthard Massif basement, during the second episode of Alpine deformation. The present work has shown however that this deformation was concentrated in the paragneisses bounding the northern margin of the Massif and that this margin, like the southern margin of the

Gotthard Massif, has been affected by tectonic sliding.

The amount of movement on the individual second slides cannot be accurately determined but it seems probable that differential displacements may have reached several kilometres (Section 3.5). Frey (1967, p. 79) suggests a vertical displacement of 6000 metres along the northern margin of the Scopi structure. Baumer (1964, p. 55) has estimated the minimum displacement as 2000 metres. (Frey's figure of 6000 metres appears to have been derived by comparing the structural levels of the Greinaeinmuldung and the Scopi structure by a down plunge projection technique. A constantly oriented easterly plunging second fold axis is assumed. In view of the remarks which follow this figure should perhaps be treated with caution.)

The axes of folds formed during the second episode of Alpine deformation show a regional variation in attitude. In the Lukmanier area these fold axes appear generally to plunge gently east although individual fold hinge lines are curved (Chadwick, 1968, pp. 1130-1132). In the Nufenenpass (Higgins, 1964b, p. 100; Chatterjee, 1961, p. 11 and Fig. 4) and Molare (Thakur, personal communication) areas second fold axes also plunge gently east, whereas in the Val Piora area they plunge consistently north to northwest (Encl. 3). Chadwick's (1968, p. 1130) suggestion that the curvature of the hinge lines of second folds in the Lukmanier area is due to inhomogeneous strain provides a possible explanation for the observed regional variation in the attitude of second fold axes.

The hypothesis (Higgins, 1964b; Chadwick, 1965) that the linear mineral fabrics were produced during the second episode of Alpine deformation does not appear to explain the structural relationships observed in the Val Piora area. An alternative proposal has been made, namely that these linear fabrics were produced by a rotational strain superimposed on the second and earlier structures (Section 3.23). As the mineral linear fabrics and the second slides are therefore unrelated structures, there is no longer a basis for the conclusion (Chadwick, 1968, p. 1131) that the north-south trending mineral linear fabrics are parallel to the direction of movement on the second slides.

The direction of movement on these slides in the Val Piora area has been suggested to be northwest-southeast (Section 3.5).

Crystal rotation* about sub-horizontal east-west trending axes, which is consistent in sense throughout basement and cover, is a common phenomenon in Val Piora and probably over a much wider area as well (porphyroblasts in the Scopi Zone rocks on Lukmanier Pass show the same sense of rotation (Nabholz and Voll, 1963, Fig. 10)). Textural evidence suggests that rotation occurred after the second but largely before the fourth episode of Alpine deformation and was associated with the formation of the linear mineral fabrics (cf. Steiger, 1962, p. 462) (Sections 3.23, 4.2). The consistent sense of crystal rotation across second generation structures$^{\emptyset}$, together with the observation that this sense if due to slip on the second schistosity surfaces is opposed to that expected from the sense of movement on the second slides (upward movement of more northerly lying rocks), lends support to this viewpoint.

As the orientation of layering prior to the third episode of Alpine deformation and the strain path during this episode of deformation are unknown, the extent to which the differential crystal rotation is due to rotation of layering as opposed to rotation of the crystal itself (Section 5.8) is indeterminate. However, if it may be assumed that the layering rotated about the crystals, it is coincident with the sense of differential crystal rotation that the sub-vertical to southward facing structures along the southern margin of the Gotthard Massif initially showed a northward facing attitude which accorded with the general asymmetry of the Alpine mountain chain (cf. Steiger, 1962, p. 462; Kvale, 1966, p. 11).

Throughout the third episode of Alpine deformation in the Val Piora area the axis of rotation of layering appears to have been an axis of potential boudinage. The direction at right angles to this

---

* Differential rotation of the crystal and the matrix.

$^{\emptyset}$ Where crystal rotation can be related to fold forming movements it is commonly found that rotation sense differs on opposite limbs of the folds generated (e.g. Peacy, 1961; Zwart, 1960).

axis in plane of the layering is shown by the linear mineral fabrics (stretching fabrics) to be a direction of continuous elongation. The layering rotated towards and in the same sense as the extension axis of successive increments of the third episode rotational strain (Section 3.23) (Fig. 3.54a) In other areas, where the strain path was different or where the orientation of layering or of the extension axis of the first increment of the third episode strain initially differed from that in Val Piora, shortening of layering perpendicular to the axis of rotation might be envisaged at some stage during the third episode of Alpine deformation (Figs. 3.54b and c). The post-second, pre-fourth deformation folds in the Val Camadra area (Phase T folds (Cobbold, 1969)) may have originated through layer shortening in one of the ways outlined in Fig. 3.54.

The analysis of fourth episode structures in the Val Piora area indicates that the strain which gave rise to these structures was superimposed on a layering already overturned (back-folded) and of variable attitude (Sections 3.24, 3.55). In the Val Camadra area Cobbold (1969) arrives at a similar conclusion. For this reason the fourth episode of Alpine deformation is thought to have merely emphasised features already established during the earlier third episode. Although a distinction is made between the third and fourth deformation episodes the relationship deduced between the various strain parameters (ratio and orientation of the principal strain axes) suggests the deformations to be related and perhaps broadly continuous (Section 3.24). The deformation picture is comparable to that envisaged by Nabholz and Voll (1963) in the cover of the eastern Gotthard Massif; i.e. repeated folding during continuous rotational deformation in which the trend of the stretching direction remains constant, significantly in both cases sub-perpendicular to the axis of the mountain belt.

Although a detailed analysis is not yet possible, the limits of the region of overturned layering or back-folding south of the Gotthard Massif can be broadly established from existing work. In Fig. 3.52 this region has been delimited by constructing the 90 degree dip isogon for layering. A number of points arise from the analysis.

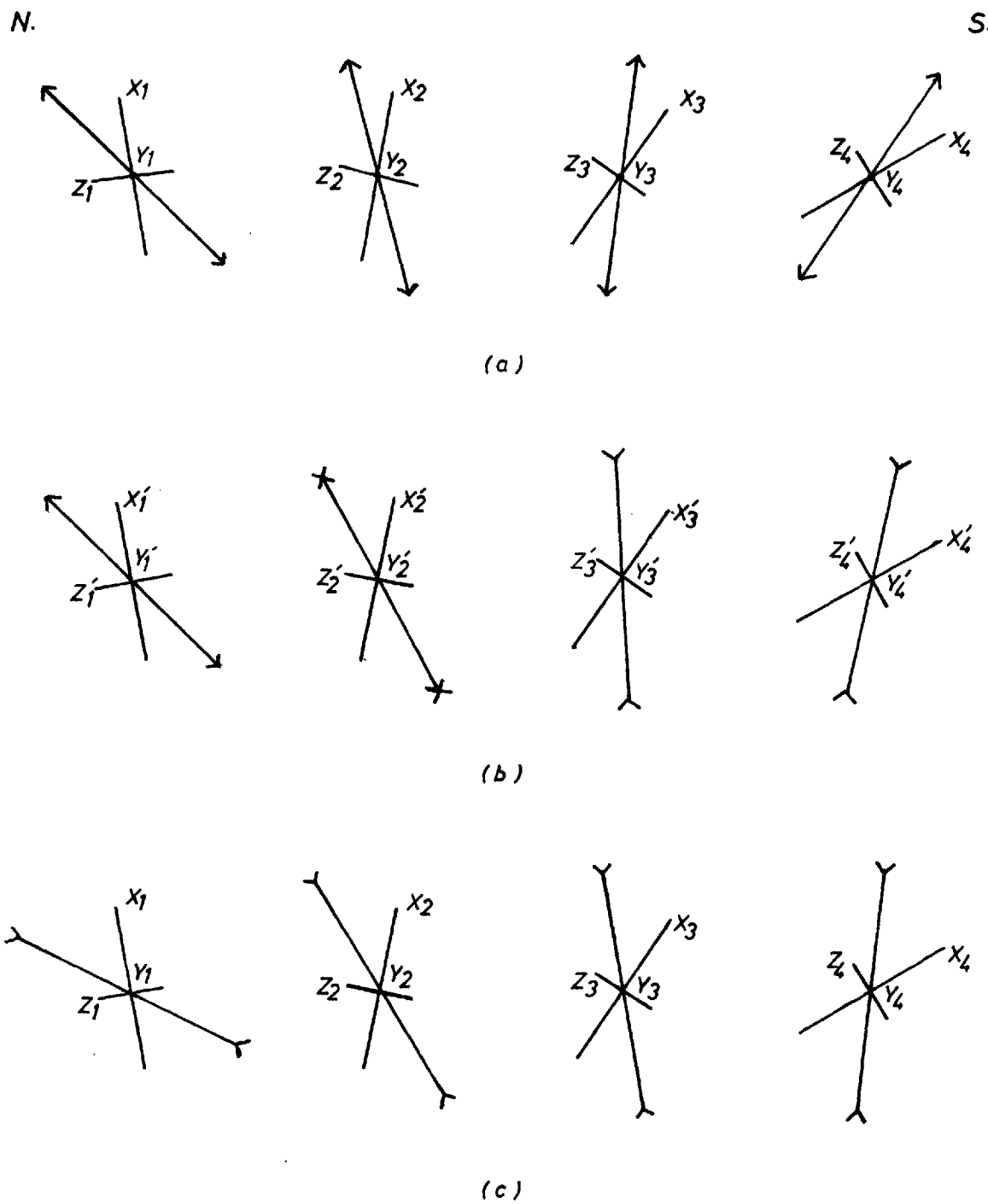

Fig. 3·54 Possible histories of layering during D_3. (a) Continuous boudinage. (Rotational strain increments $X_1 Y_1 Z_1, X_2 Y_2 Z_2$, etc.). (b) Initial boudinage and later folding. (Rotational strain increments $X_1' Y_1' Z_1', X_2' Y_2' Z_2'$, etc., different strain path to (a)). (c) Continuous folding. (Rotational strain increments as (a), but initial layering orientation differs). (Initial folding may also precede boudinage, where suitable strain path).

1) The back-folding or overturning is most severe in the Val Piora and Lukmanier areas.

2) The closure of the region of overturned layering towards the east indicates that the back-folding dies out in this direction (closed isogon patterns are a feature of folds with changing geometry). The rocks of the Simano and Adula nappes to the east of Val Blenio appear to be in structural continuity with the gently southeast dipping cover of the eastern Gotthard Massif.

3) The northern limit of the back-folded region is determined by the fan structure in the Gotthard Massif.

4) The southern limit of the back-folded region is determined by the major synformal fold closure, recognised by Thakur (Section 3.8), between the Pizzo Molare and Val Piora-Lukmanier areas. This latter structure has been traced as far west as Alpe di Chiera (Thakur, personal communication), but its continuity in the Sambuco-Massari area (Hasler, 1949) is less clear (Fig. 3.52).

From work in the region to the west of Airolo (Schmidt and Preiswerk, 1908; Burckhardt, 1942; Günthert 1954; Higgins, 1964b), a comparable region of steepened to overturned layering can be recognised almost as far west as the Simplon Pass.

The structural history of the region of steepened to overturned layering ('steep' zone) can be contrasted with that of the surrounding region of gently dipping planar structures ('flat' zone). Whereas layering in the 'steep' zone rotated and in some areas (e.g. Val Piora) underwent continuous north-south extension during the superimposition of the third episode strain increments, that of the 'flat' zone appears little changed from its pre-third deformation orientation and probably remained relatively static. As a consequence it can be expected to have suffered near continuous north-south shortening (Fig. 3.55). In the Nufenenpass-Basodino area (Higgins, 1964b) evidence can be found to support this hypothesis. In the 'steep' zone, the northern limb of Higgins's major F_3 synform where axial trace runs east-west from Lago Bianco to the Marchhorn, north-south stretching fabrics (linear mineral fabrics) are well developed. However, in the 'flat' limb to the south,

Fig. 3.55. Evolution of the major back-fold. (a) (b) (c) (d) and (e) show stages during the development of this structure. $X_1 Y_1 Z_1$, $X_2 Y_2 Z_2$, etc. represent incremental strain axes at these different stages. In (a) - (d) (the third episode of Alpine deformation) the steep limb ('steep' zone) undergoes continuous elongation and rotation (indicated by arrows) whereas the flat limb ('flat' zone) suffers continuous shortening and little finite rotation. Stage (e) corresponds to conditions during the fourth episode of Alpine deformation in which shortening of the steep limb and possibly refolding of the third generation structures on the flat limb took place.

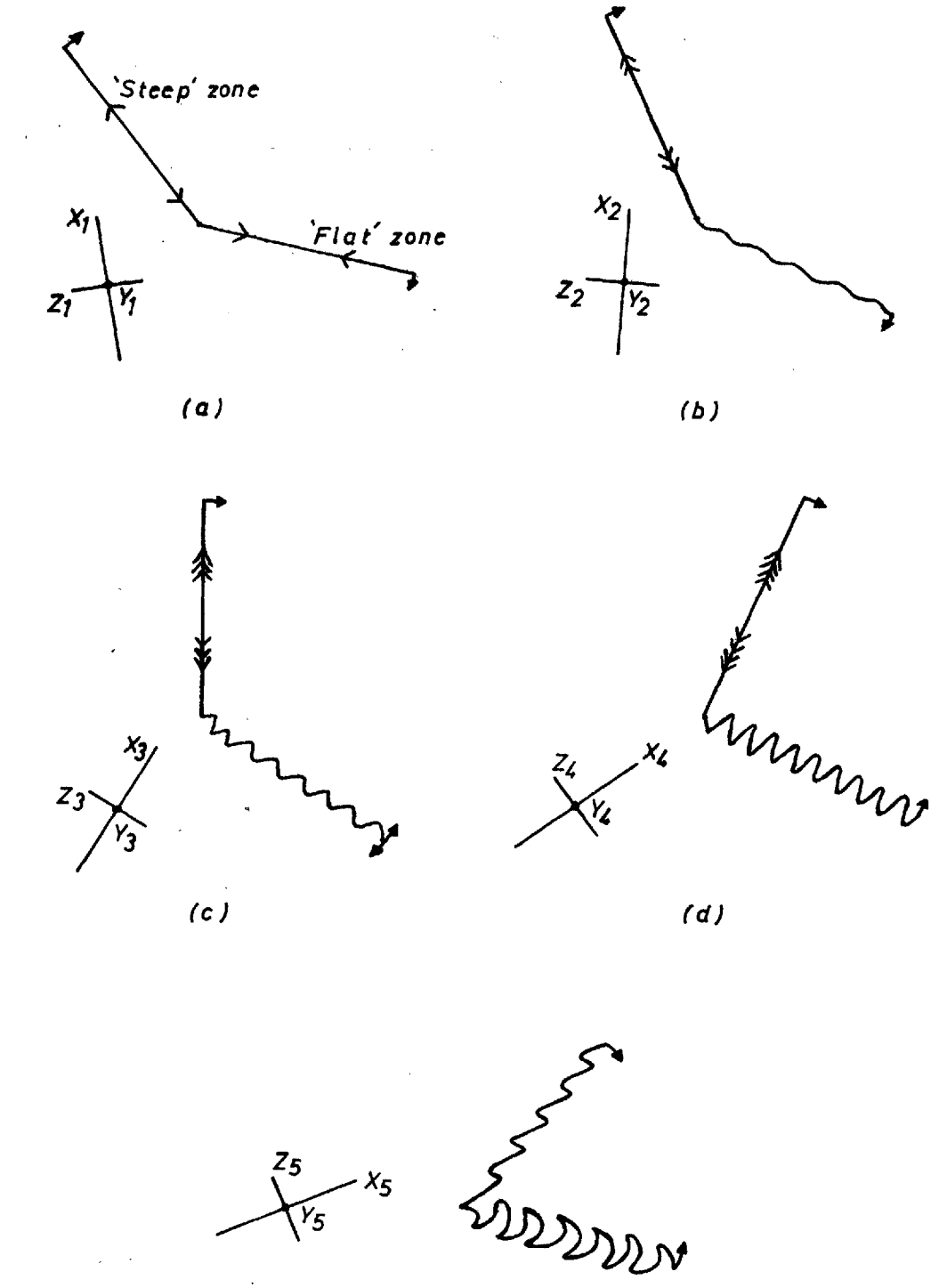
N.
S.
'Steep' zone
'Flat' zone
X1
Z1
Y1
(a)
X2
Z2
Y2
(b)
X3
Z3
Y3
(c)
Z4
X4
Y4
(d)
Z5
X5
Y5
(e)

Fig. 3·55

'flat' zone, these are absent. An east-west stretching fabric of an earlier generation is observed. A comparable observation is made by Chatterjee (1961, p. 12) in the region further to the west. He notes that the north-south trending linear mineral fabric (B_1) is found nowhere in the Pennine region to the south of the Gries valley (i.e. the 'flat' zone). The predicted north-south shortening of layering in the 'flat' zone is indicated by the presence of a set of fold structures with east-west trending axes and steeply dipping axial surfaces, Higgins's F_3 folds. (As pointed out in the previous section, it seems probable that the folds in the 'steep' zone suggested by Higgins to be F_3 folds are in fact F_2 structures.) Further to the west in the Albrunpass area (Sibbald, 1965) which lies to the south of the steep zone, a set of folds of similar orientation is observed and the north-south stretching fabrics are also absent.

In the gently dipping cover rocks of the eastern Gotthard Massif ('flat' zone), northeast of the region of back-folding, north-south to northwest-southeast trending stretching fabrics have been found (Jung, 1963, pp. 732-738). This observation appears to contradict the hypothesis outlined above, however the apparent contradiction is resolved when it is realised that these fabrics are related to the formation of the schuppen in this region (first episode of Alpine deformation) and are therefore of a different age to the stretching fabrics in the 'steep' zone. The conclusion (Nabholz and Voll, 1963), that stretching directions in these rocks had a similar trend during subsequent deformations, which led to folding of the early linear fabric, corresponds favourably with the evidence that the extension axes of the third and fourth episode strain ellipsoids in the Val Piora area were oriented north-south (Sections 3.23, 3.24).

The origin of the major back-folding presents a problem. If the fold structure is thought to have been initiated by buckling then layering within both fold limbs should have suffered an initial layer parallel compressive strain. The following suggestions can be made to explain the absence in parts of the overturned limb at least (e.g. Val Piora area) of fold structures indicative of such a strain component.

1) The initially formed minor folds were unfolded during subsequent development of the major fold limb (cf. Ramberg, 1963).
2) The initial compressive strain was resolved in such a way that folds with short wavelengths were inhibited.
3) An initial flexure was already present in the layering before the third episode of Alpine deformation. This flexure was merely developed by the third episode strain (cf. Fig. 3.55), parts of the overturned limb undergoing continuous stretching.

The possibility also exists, that back-folding was initiated by a mechanism other than buckling, such as differential rotation of layering due to regional strain inhomogeneity.

In conclusion it is appropriate to consider the origin of the rotational component and the constrictional nature of the third episode strain. As outlined earlier (Section 3.23) rotational strain is certainly an important factor in natural deformation, but is also in general an indeterminate component and hence often neglected. The existence of strain rate differences within an orogenic belt would give rise to rotational strain. In view of the dependence of strain rate on temperature and the likely orientation of the metamorphic isograds during the third episode of Alpine deformation, it is certain that such differences existed. The rocks at depth and in the south were hotter and deforming more rapidly than those at higher levels and in the north.

The constrictional nature of the third episode strain implies an east-west as well as a north-south shortening of the orogenic belt in the Val Piora region. Evidence of east-west shortening is provided by the large scale flexuring of the Gotthard Massif about a steep north plunging axis (Kvale 1966, pp. 71-2, Fig. 27). Kvale also notes that constrictional type fabrics and associated structures (Querbiotite fabrics and Kleinfältelung) are confined to the inner arc of this flexure. This suggests that it was here that the east-west compressive strain was most marked and hence that flexuring may have been accomplished by tangential longitudinal strain (Ramsay, 1967, pp. 397-403).

This explanation of the origin of the constrictional fabrics is in many respects comparable to that put forward to explain the "Schlingen" structure of the Maggia nappe to the south of the Val Piora area (Wenk in Wells, 1948; Günthert, 1954, p. 148).

CHAPTER IV
THE METAMORPHIC GEOLOGY

4.1) Introduction

Research work over the past decade has led to considerable advances in our understanding of the nature and age of the Alpine metamorphism in the Lower Pennine region. Regional studies (Niggli, 1960; Wenk, 1962; Niggli and Niggli, 1965; Tromsdorff, 1966; Wenk and Keller, 1969) have shown that the mineral zones and the metamorphic isograds cross cut the major structural units. This observation indicates that the main Alpine metamorphism took place after the emplacement of the major nappes, a conclusion supported by studies of the relationship between mineral growth and deformation. These have shown that the porphyroblast minerals which formed at the acme of regional metamorphism grew certainly after the nappe movements had taken place and in fact at a late stage during the Alpine deformation of this region (Wunderlich, 1958; Chatterjee, 1961; Steiger, 1962; Higgins, 1964b; Chadwick, 1965; Sibbald, 1965).

Several lines of evidence have been presented which indicate that the metamorphic peak occurred in the L. Oligocene (around 38 m.y. ago, the Eocene - Oligocene transition (Harland et al, 1964)), (Jäger et al, 1967; Milnes, 1969; Hunziker, 1970; Jäger, 1970). However in general radiometric age determinations of micas from the Lower Pennine region give much younger ages, biotite for instance, 15-18 m.y. in the area surrounding Val Piora and 11-30 m.y. throughout the region as a whole (Jäger et al, 1967). These young mica ages have been shown to be cooling ages, ages at which the mica cooled below the temperature at which its structure became isotopically closed (approx. 300°C for biotite, 500°C for muscovite). Muscovite ages are correspondingly somewhat greater than those of biotite (Jäger, 1965; Jäger et al, 1967). Steiger (1964) has determined the ages of hornblendes in gneisses from the southern Gotthard Massif. The hornblendes show a variety of growth fabrics (Section 4.3) representing various generations of crystal growth which Steiger has dated radiometrically.

Hornblendes with random growth fabrics have ages ranging from 23-30 m.y., those which are lineated, north-south, ages of 46 m.y. Steiger has suggested that the 46 m.y. lineated hornblendes date the nappe phase and that the 23-30 m.y. randomly oriented hornblendes coincide with the metamorphic peak. Jäger et al (1967, pp. 38-39) consider that the hornblende ages of less than 28 m.y. are cooling ages. The structural analysis of the Gotthard Massif presented in the previous chapter suggests that the ages obtained from the lineated hornblendes are not those of the nappe phase, but are possibly indicative of the third episode of Alpine deformation which occurred just before the metamorphic peak. The nappe phase, the first major episode of Alpine deformation, must be considerably older. Recently determined Rb/Sr whole rock isochrons in the range 110-125 m.y. from the fronts of the Pennine nappes possibly date the earliest of the Alpine movements (Hanson et al, 1967; Hunziker, 1970; Jäger, 1970).

To explain the concentric arrangement of the metamorphic isograds in the Lower Pennine region, Wenk (1962) postulated the presence of a heat dome associated with rising Alpine migmatites in the southern part of this region. Niggli (1960, 1970) and Niggli and Niggli (1965) however, question the necessity of assuming a rising migmatite front as the isograds are concentric about the deepest and hence hottest levels of the Alpine orogenic belt.

The almandine-amphibolite facies (Fyfe, Turner and Verhoogen, 1958) metamorphism which typifies the Lower Pennine region contrasts with a lower temperature, greenschist-glaucophane-lawsonite schist facies (Winkler, 1965, p. 144) metamorphism throughout the remainder of the Pennine Zone. Here, Bearth (1962, 1966) has distinguished two longitudinal metamorphic zones which parallel the tectonic trend, an outer lawsonite-pumpellyite zone and an inner garnet-chloritoid zone. Both zones contain glaucophane schists, but only those of the lawsonite-pumpellyite zone belong to the glaucophane-lawsonite schist facies. In both zones the glaucophane schists are in the process of replacement by assemblages of greenschist facies. Bearth (1958, 1962) has suggested that the almandine-amphibolite facies metamorphism of

the Lower Pennine region has been superimposed on the greenschist-glaucophone-lawsonite schist facies metamorphism. Elsewhere, for example in the Adula nappe (Van der Plas, 1959), evidence of Alpine polymetamorphism supporting Bearth's ideas has been found.

The Val Piora area lies towards the northern limit of the zone of younger almandine-amphibolite facies metamorphism (Wenk, 1962, Tafel I). Mineral assemblages are typical of those of the lower almandine-amphibolite facies, (almandine-staurolite subfacies).

The following sections are primarily concerned with descriptions of the microstructures of the metamorphic minerals, and determinations of the time relationships between mineral growth and deformation in the different structural units. The techniques used to decipher these relationships are as those discussed by various authors, for example, Read (1949), Zwart (1960) and Spry (1969). The significance of certain microstructures, snowball garnets, hornblende garbenschiefer and garnet crystal size distributions is described more fully in later chapters. Petrographic description of the various mineral phases recognised in the different structural units has been minimised, as such details are available elsewhere (Steiger, 1962; Krige, 1918).

4.2) The metamorphic minerals of the Mesozoic cover

The metamorphic minerals in the Mesozoic cover are indisputably the products of the Alpine metamorphism. They illustrate most clearly the time relationships between mineral growth and deformation (Table 4.1). For these reasons it is appropriate to discuss them first. The minerals listed below are recognised to have grown or recrystallised as a result of the Alpine metamorphism.

Quartz	Biotite	Epidote group	Kyanite
Calcite	Chlorite	Garnet	Hornblende
White Mica	Chloritoid	Staurolite	Plagioclase
	Ilmenite	Tourmaline	

Quartz

The shape fabrics of quartz grains suggest that static recrystallisation took place during the Alpine metamorphism after the third episode of Alpine deformation. Dimensional quartz grain orientations, developed during the first three episodes of Alpine deformation, are rare. Monomineralic quartz layers (Fig. 4.1) and segregations deformed by the first second and third episodes of Alpine deformation are often formed by grains whose shape fabrics compare with those produced by the annealing recrystallisation of experimentally deformed single phase metals and rock specimens, (i.e. aggregates of equidimensional polygonal grains with planar interfaces subtending angles of 120 degrees (Voll, 1960, 1961; Griggs et al, 1960)). When this occurs the grain boundary free energy of the aggregates, the driving energy for grain growth, is minimised (Burke and Turnbull, 1952). In polycrystalline systems the equilibrium grain boundary relationships are more complex. In the quartz mica system it is known that quartz-quartz grain boundaries adopt a position at 90 degrees to the basal planes of micas (Voll, 1960, 1961; Vernon, 1968). This relationship is often observed in mica schists in the Val Piora area and provides further evidence that the quartz fabric is an annealed fabric.

In contrast to the equidimensional grains of quartz in monomineralic quartz layers quartz grains in micaceous rocks showing a preferred orientation of micas are often dimensionally oriented. Where the

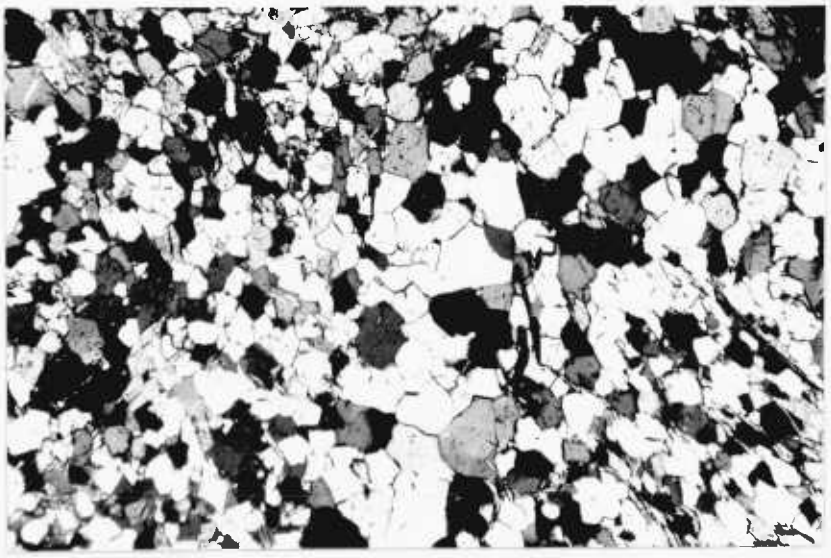

Fig. 4.1. Second generation folding of a quartz layer. On the inner arc of the fold chlorite and biotite show an axial planar orientation. The shape fabric of the quartz grains is comparable to that produced by annealing recrystallisation. Spec. 792, Quartenschiefer; M.R. 6962715570, W.S.W. of Motta. (x 30)

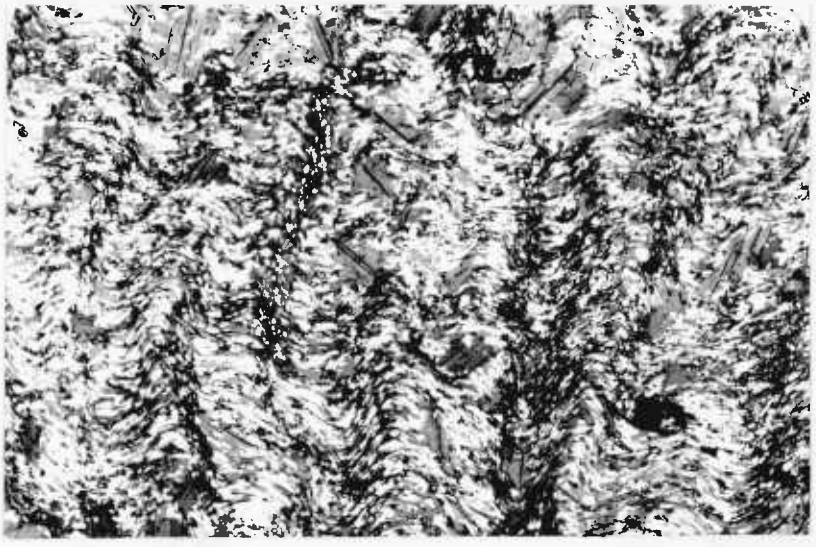

Fig. 4.2. Third generation folding of the first foliation (white mica and biotite). Biotite prophyroblasts forming the L. tectonite fabric (axis perpendicular to section) overgrow the folds. Concentrations of epidote are developed on some of the fold limbs. Spec. 66G, Quartenschiefer; M.R. 6944015571, Alpe di Lago. (x 8)

mica fabric is an S. tectonite fabric the quartz grains appear "flattened" in the plane of the schistosity, where it is an L. tectonite fabric the grains are elongated parallel to the fabric axis, (the pole to the plane containing the normals to the mica basal planes), but equidimensional in the plane at right angles to it (Section 3.23). These dimensional orientations arise because of the strong tendency for mica to always develop and impose an adjacent grains its faces of lowest surface energy, (i.e. its {001} faces, (Vernon, 1968, and Section 6.2)), and because quartz-quartz grain boundaries tend to adopt an equilibrium position at 90 degrees to these faces. The symmetry of the annealed quartz shape fabric thus reflects the symmetry of the mica fabric. It may therefore be emphasised that the quartz grain dimensional orientations observed in many micaceous rocks in the Val Piora area, and probably in other areas as well, have arisen through annealing recrystallisation and not through recrystallisation under directed stress during any of the episodes of deformation (cf. Spry, 1969; pp. 225-226).

There is no clear cut time relationship between quartz recrystallisation and the fourth episode of Alpine deformation. The solution, migration and selective deposition of quartz has been suggested to be a process which accompanies the formation of strain slip cleavage, sometimes developed parallel to the axial surfaces of fourth generation folds (Section 3.24). Thus, quartz grains in the cores of some crenulations of this age appear to be recrystallised. In the cores of others, there is evidence for only partial recrystallisation; grains bent across the apices of folds are subdivided into strain free sectors or subgrains (i.e. polygonised, (Cahn, 1950)). Quartz grains in the hinge zones of yet other folds of this age show features indicative of plastic deformation; undulose extinction, deformation bands and Boehm lamellae (Carter et al, 1964). Quartz generally forms a major constituent of the mineral fillings in the necks of fourth episode boudins, and it also occurs, often as euhedral crystals growing on the faces of late Alpine tensile fractures.

Calcite

Calcite appears to have suffered annealing recrystallisation during the Alpine metamorphism. Grain shape fabrics are similar to those shown by quartz, as are the time relationships between deformation and recrystallisation. In a few cases however, syntectonic fabrics have survived annealing. Calcite grains which are strongly "flattened" in the plane of the first foliation have been observed in some marbles (Section 3.21).

Micas, (white mica and biotite)

Unlike the other metamorphic minerals in the rocks of the Val Piora area micas have a history of crystallisation which can be shown to span the whole period of Alpine deformation. Early formed micas do not always appear to have recrystallised during later episodes of deformation and continuing metamorphism. The mica fabrics formed at different stages during the deformation history provide a record and often an indication of the nature of the deformation episodes (Sections 3.21, 3.22, 3.23).

White Mica

White mica is a prominent constituent in many of the cover rocks. It occurs most commonly as aggregates of fibrous crystals, (syntectonic?), or as larger discrete crystals (post-tectonic, mimetic?), oriented in the plane of the first foliation (Section 3.21). Less commonly it grows parallel to the axial surfaces of second generation folds (Section 3.22). The mica crystals are dimensionally oriented and hence lineated within their respective planar structures. The white micas which grow across the first and second generations of planar structures tend to show a complete girdle or L. tectonite fabric, (Section 3.23). From these observations it can be inferred that white mica grew during or after the first and second episodes of Alpine deformation. The girdle mica fabric is not clearly interpreted as the result of mechanical rotation of randomly oriented post second deformation micas, or of crystallisation, during the third episode of Alpine deformation. Local recrystallisation of white mica took place in late and post fourth deformation times, in the necks of fourth episode boudins and in late Alpine tensile fractures.

Biotite - Phlogopite

Biotites of varying pleochroic scheme appear in most of the cover rocks (Wenk et al, 1963, pp. 446-452). Pleochroic schemes vary within the limits:-

X = colourless - pale yellow

Y = Z = green - brown - red brown.

The green varieties are probably characterised by higher $Fe_2O_3/FeO + Fe_2O_3$ ratios (Hayama, 1959; Wenk et al, 1963, p. 453). Magnesium rich members of the biotite series, (phlogopites) are only found in calcareous schists and marbles.

Biotite tends to form porphyroblasts up to 6 mm. long. It occurs as dimensionally oriented crystals in the first and second foliation planes (Sections 3.21, 3.22) and also as large porphyroblasts which grow across both these generations of planar structures and which often show a complete girdle or L. tectonite fabric. These porphyroblasts are dimensionally oriented parallel to the girdle fabric axis (Section 3.23), (Krige, 1918, p. 597). Thus biotite appears to have grown after the first episode of Alpine deformation, (the crystals oriented in the first foliation plane are probably of mimetic origin), during the second episode and in the case of the biotites forming the L. tectonite fabric during the third episode of Alpine deformation. These latter crystals overgrow third generation folds (Fig. 4.2), and probably formed largely after the third episode of Alpine deformation from nuclei oriented during this episode of deformation. Nucleation appears to have outlasted deformation because biotite porphyroblasts with random orientations are observed in some cover rocks. In a few cases these crystals are seen to overgrow fourth generation folds (Figs. 4.3a, 4.3b). In general however they are deformed by the fourth folds (Figs. 4.4, 4.9). Evidence that the latest biotite growth took place under retrograde conditions is provided by the presence of biotite rims around garnet, staurolite and hornblende.

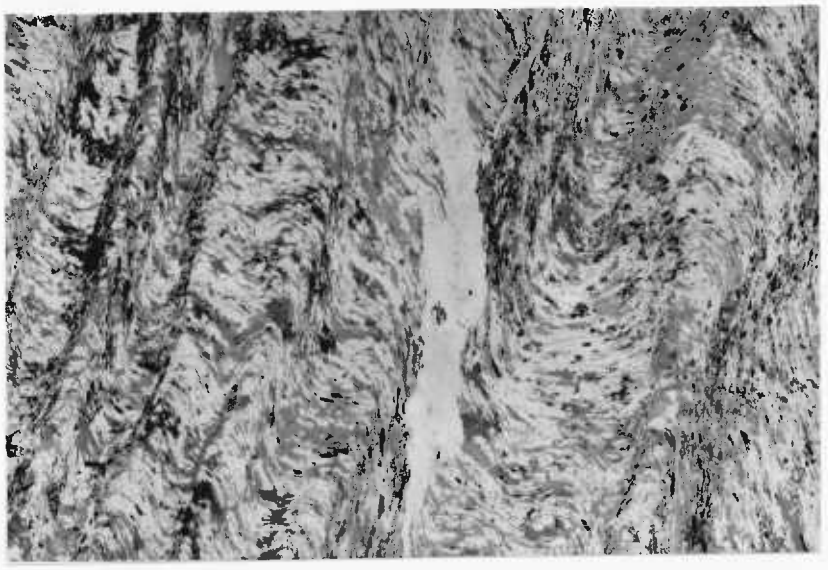

Fig. 4.3a. Asymmetric fourth generation crenulations folding the first foliation (biotite and white mica). Kyanite and epidote are concentrated on the steep limbs and quartz on the flat limbs of the crenulations. A later generation of biotite (porphyroblasts) which overgrow the folds is visible. (x 9)

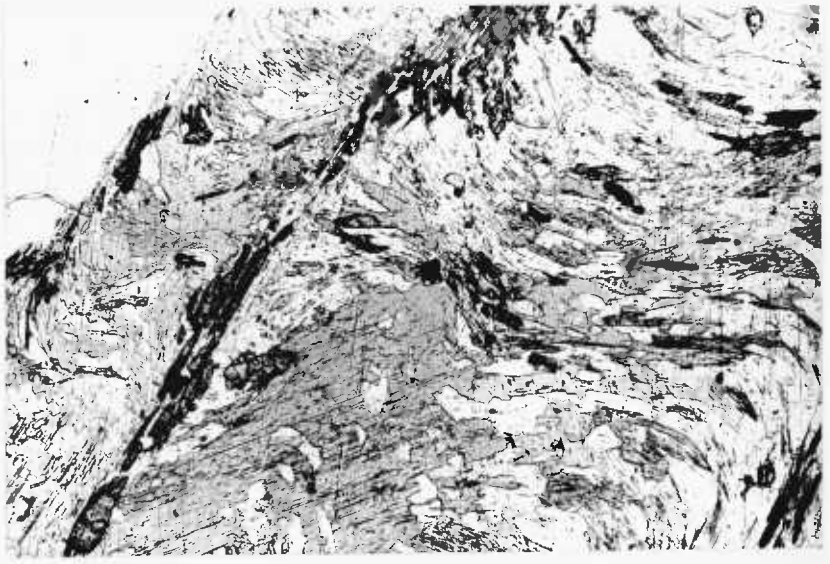

Fig. 4.3b. Detail from (a) showing kyanite and epidote concentrations on the steep limbs of the crenulations and the two generations of biotite. Spec. 688, Quartenschiefer; M.R. 6952715567, N.E. of Camoghe. (x 35)

Chlorite

Chlorite is not a common mineral in the cover rocks. It occurs chiefly as a retrograde phase replacing biotite or growing in the necks of fourth episode boudins (Section 3.24), and late Alpine tensile fractures (Section 3.56). Primary chlorite is rare and is present as small crystals oriented in the first and second foliation planes (Fig. 4.1), and as an intergrowth, (parallel{001}), with biotite porphyroblasts (cf.Chatterjee,1961, p. 25) which overgrow second generation folds.

Chloritoid

Chloritoid is found in some garnet-staurolite-kyanite-mica schists as small, (0.1 - 0.5 mm.), tabular inclusions in garnet prophyroblasts. This mode of occurrence suggests that the inclusions are unstable relicts which failed to react to the rising temperature. From textural evidence it appears that the mineral grew between the second and third episodes of Alpine deformation.

Epidote group

Epidote group minerals within the composition range clinozoisite-epidote are present in varying amounts in most of the cover rocks. The crystals are often zoned with epidote cores and clinozoisite rims. They tend to be elongate (up to 5 mm. long parallel to the crystallographic b axis). The crystals commonly lie with their longest axes in or near the plane of the first foliation and appear to have grown between the first and second episodes of Alpine deformation. They overgrow the first foliation but are deformed by second and later generations of structures (Fig. 4.5). In some kyanite-epidote-mica schists a later period of epidote porphyroblast growth appears to be broadly synchronous with the development of kyanite (Figs. 4.3a, 4.3b).

Garnet

The size of garnets (up to 1 cm. diameter) and the complexity of their inclusion patterns make these crystals the most spectacular of the prophyroblast minerals in the cover rocks of the Val Piora area.

Unit cell sizes ($a = 11.580 - 11.593$ Å) and $^{a}/_{R.I.}$ values (6.445 - 6.452) of garnets, (Appendix I), are typical of those of

Fig. 4.4. Fourth generation folding of the first foliation (compositional banding, white mica and biotite). The folds postdate the formation of the snowball garnet. (The curvature of the inclusion trails within the garnet is not due to the overgrowth of embryonic fourth generation folds.) Deformed biotite porphyroblasts are visible in the cores of the folds. Spec. B.5.V., Bünderschiefer; M.R. 6948015122, Val Leventina. (x 10)

Fig. 4.5. Second schistosity (N.E.-S.W.) formed by white mica and biotite. The first foliation has been transposed but relicts of this structure are seen as inclusion trails in the epidote crystal. Biotite porphyroblasts clearly overgrow the second schistosity. Spec. 404, Quartenschiefer; M.R. 6945515463, W. of Lago Ritom. (x 35)

almandine rich pyralspites formed in the lower almandine-amphibolite facies (Sturt, 1961; Nandi, 1967).

Both syntectonic snowball garnets and garnets which grew under static conditions have been observed. The statically formed crystals in particular are generally euhedral (rhombic dodecahedral). The formation of euhedral crystals, (accepting that the mineral possesses the required anisotropy of surface energy (Spry, 1969, p.147 and Section 6.2)), appears to depend on the chemical composition of the rock and the scale of the chemical inhomogeneities within it, (i.e. size of mineral grains and thickness of compositional banding). Thus euhedral crystals are common in finely crystalline rocks rich in garnet forming components, whereas skeletal crystals (Fig. 4.6) are typical of rocks which are poor in garnet forming components and coarsely crystalline. Where the rocks show a fine compositional banding garnet growth is restricted to those layers of appropriate composition and "flattened" crystals may result. Compositional variations often develop around the margins of crystals which are growing and rotating simultaneously and these variations may also lead to growth of irregular crystal shapes (Section 5.6).

Inclusions of quartz, epidote group minerals, ilmenite and opaque (possibly carbonaceous) material are ubiquitous and chloritoid, staurolite, tourmaline, calcite and white mica are also found. The inclusion patterns are sometimes related to the internal structure of the crystal. Thus some garnets show a tendency to develop sectors which are relatively inclusion free separated by other sectors in which inclusions are concentrated. The areas of inclusion concentration appear to conform with the internal dodecahedral planes of the crystal (cf. Rast and Sturt, 1957; Powell, 1966). These authors also found small rod shaped inclusions of undetermined composition lying normal to the crystal faces in the relatively inclusion free sectors. Wunderlich (1958, Fig. 18) figures a garnet from Val Piora which shows this feature. The inclusion free sectors are not always developed throughout the crystal, but are often separated from the crystal margin by a zone rich in inclusions whose spacial distribution

Fig. 4.6. Skeletal garnet formed by in situ replacement of micaceous areas. Inclusions in the garnet are of quartz. Note the equigranular annealed fabric of the quartz grains forming the matrix. Spec. 710, Black garnet schist series; M.R. 6957015545, Alpe Ritom. (x 35)

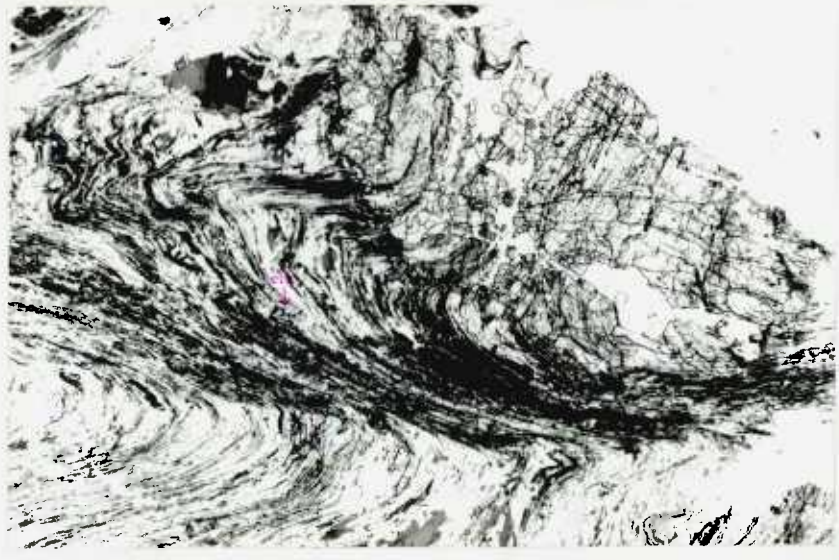

Fig. 4.7. Second generation folding of the first foliation (compositional banding, white mica, biotite and clinozoisite). The garnet porphyroblast and some of the biotite crystals overgrow the folds. Note the post-crystalline rotation of the clinozoisite crystal on the fold limb. Spec. B.5.B., Bünderschiefer; M.R. 6948015122, Val Leventina. (x 11)

is unrelated to the internal structure (cf. Rast and Sturt, 1957). The origin of the structurally related inclusion patterns in garnet is probably analogous to that of hourglass or maltese cross patterns in chloritoid and chiastolite (Spry, 1969, pp. 174-177).

The garnets generally contain clear inclusion trails which bear no relationship to the internal crystal structure, but represent relicts of an overgrown planar or folded foliation. Most commonly the trails are those which arise when crystal growth has taken place under static conditions, (inclusion trails are straight or depict an earlier folded foliation surface). Less commonly observed, are spiral or rotational inclusion trail textures typical of syntectonic crystal growth in which differential rotation of crystal and matrix has occurred.

The axes of rotation of the syntectonic or snowball garnets are subperpendicular to the third episode mineral lineation and the sense of (differential) crystal rotation is constant throughout the area (Section 3.23). The snowball garnets (Figs. 4.4, 5.4, 5.5) are found to overgrow first second and third but not fourth generation folds and fabrics (Fig. 4.4; see also Krige, 1918, Pl. XII, Fig. 2). From this observation it may be inferred that the snowball garnets grew during the third episode of Alpine deformation. Growth appears to have outlasted this episode of deformation, as in rocks unaffected by fourth generation folds inclusion trails in snowball garnets show no angular discontinuity at crystal margins when traced into the external foliation.

Maximum angular rotations (maximum angular differences between the internal and external foliation measured at the centre of the crystal in the plane at right angles to the rotation axis, (Section 5.4)) of different crystals vary widely in different specimens of garnet schist and even within the same hand specimen (Section 5.7). The maximum recorded angular rotation of a garnet crystal in the cover rocks was approximately 160 degrees. The majority of garnet crystals show no sign of rotation during growth. These crystals are also found to overgrow first, second and third but not fourth generation structures (Figs. 4.7, 4.8, 4.9).

Fig. 4.8. Second generation folding of the first foliation (white mica). Garnet staurolite, kyanite, biotite porphyroblasts overgrow the folds. Note also the tabular ilmenite crystals included by the porphyroblasts but spearing across the folds. Spec. 686, Quartenschiefer; M.R. 6951315556, N.E. of Camoghè. (x 11)

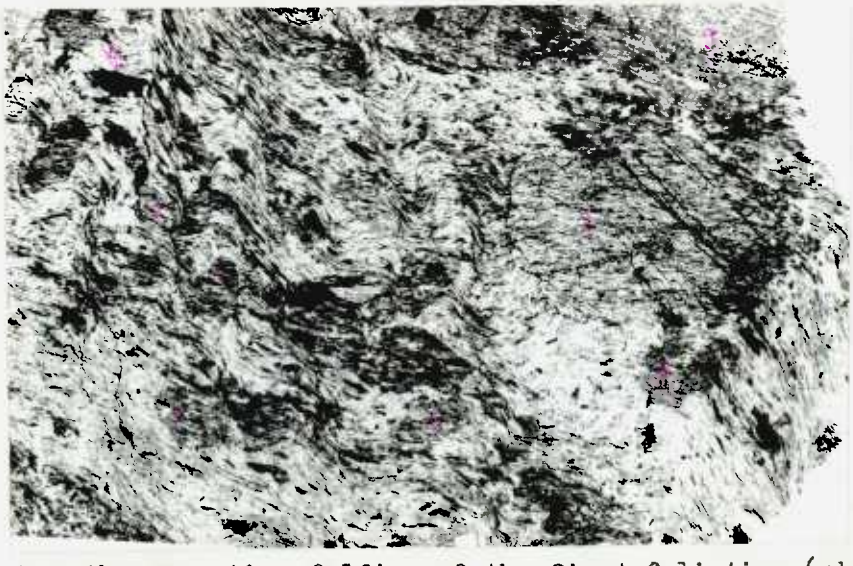

Fig. 4.9. Fourth generation folding of the first foliation (white mica). The garnet and staurolite porphyroblasts with straight inclusion trails clearly predate the folds. Biotite porphyroblasts are deformed by these structures and thus predate them. Spec. 588, Black garnet schist series, M.R. 6943515400, S. of Föisc. (x 7)

In view of the variation in maximum angular rotation displayed by different crystals it is considered probable that the garnet crystals did not all nucleate simultaneously. The first formed crystals nucleated at an unknown stage during the third episode of Alpine deformation, whereas the latest formed crystals nucleated after this episode of deformation. Growth terminated in all cases before the onset of the fourth episode of Alpine deformation.

Staurolite

Staurolite, like garnet, tends to occur as euhedral porphyroblasts. Lengths of crystals generally vary between 0.5 and 5.0 mm., though occasionally crystals up to 4 cm. long have been found. The porphyroblasts contain numerous inclusions commonly of quartz, epidote group minerals and opaque (possibly carbonaceous) material and less frequently of micas, tourmaline and kyanite.

Inclusion trails in staurolite crystals are usually either gently curved or straight and are sometimes discordant at crystal margins to the external foliation. Curvature of the inclusion trails suggests differential rotation of crystal and matrix during growth. Because this curvature is never very pronounced staurolite growth may be assumed to have been rapid in relation to the differential rotation rate. The rotation axes of staurolite crystals are oriented parallel to those of snowball garnets, and the sense of rotation of the crystals is constant and the same as that of the garnets. Angular differences between the inclusion trails and the external foliation, shown by crystals in sections cut at right angles to the rotation axes, vary between 0 and 40 degrees. Staurolite is found as inclusions in snowball garnets (Fig. 5.5) indicating that the mineral formed either before or at the same time as the garnets. Staurolite overgrows first, second and third generation folds and fabrics (Fig. 4.8), but is deformed by fourth generation folds (Fig. 4.9).

From these observations it may be inferred that staurolite grew during and after the third episode of Alpine deformation. As some staurolite crystals are rotated in relation to the matrix, whereas others are not, nucleation of staurolite, as of garnet, probably took

place over a period of time. It commenced at an unknown stage during, and ended after the third episode of Alpine deformation. Individual crystals, whose inclusion trails are discordant at crystal margins to the external foliation, may have finished growing before the end of the third episode of Alpine deformation, or they may have been further rotated during the fourth episode of Alpine deformation. Staurolite growth appears to have been completed by the onset of the fourth episode of Alpine deformation.

Kyanite

Subhedral to anhedral porphyroblasts of kyanite often several centimetres long are particularly common in the Quartenschiefer series. Random, planar (mimetic) and linear kyanite fabrics are found in rocks of differing composition. The crystallographic axes of kyanite crystals forming random fabrics show no preferred orientation, whereas the crystallographic c axes of crystals forming planar fabrics show a preferred orientation in the foliation plane, and the c axes of crystals forming linear fabrics show a preferred directional orientation within the rock. Random and planar fabrics are equally common, but linear fabrics are observed only occasionally. The linear kyanite fabrics are coincident in orientation with the third episode linear mica fabrics. Sheaf like aggregates of kyanite crystals, whose crystallographic c axes are arranged radially about a central point, are seen in many kyanite bearing rocks. The sheafs are usually randomly oriented, although instances are also found in which the c axes of crystals forming the sheafs are confined within the foliation plane, (as hornblende garben (Section 6.6)). Kyanite porphyroblasts contain inclusions of quartz, epidote, ilmenite, tourmaline and biotite.

The linear kyanite fabrics suggest that kyanite nucleated and possibly also grew during the third episode of Alpine deformation, and the random and planar,(mimetic), fabrics (fabrics typical of nucleation and growth under static conditions) that these processes continued after this episode of deformation. Structures and fabrics overgrown by kyanite crystals are those expected from this interpretation. Kyanite is generally deformed by fourth generation folds.

However in some crystals inclusion trails, which are straight in the centres of crystals, become sharply curved at the margins before passing discordantly into the folded matrix (Fig. 4.10). It may be deduced therefore that in some rocks kyanite growth continued into the period of the fourth episode of Alpine deformation. In a few rocks kyanite is found to overgrow fourth generation folds. Perhaps the most interesting illustration of this is provided by the restricted development of kyanite on the limbs of fourth generation crenulations (Figs. 4.3a, 4.3b), (Section 3.24).

Kyanite is also found forming segregations with quartz, chlorite and white mica. The kyanite crystals occur as large prismatic blades generally several centimetres long showing a colour zoning in which blue cores are surrounded by colourless margins. The segregations occur locally in the Quartenschiefer in the eastern part of Val Piora as mineral fillings in the necks of fourth episode boudins (Section 3.24). They are comparable to segregations described by Read (1933), Miyashiro (1951) and Keller (1968) and have arisen by a process of metamorphic differentiation in response to pressure gradients set up in the rocks during deformation. Chadwick (1965) has described similar segregations, in the Quartenschiefer of the Lukmanier area, which lie in the plane of the second foliation and which have been deformed by fourth generation folds (Chadwick's fold phase terminology has been converted to that used in this text, cf. Table 3.3). Chadwick's segregations are therefore earlier than those found in the Val Piora rocks.

Plagioclase

Plagioclase is the most widespread of the porphyroblast minerals and is present in the majority of the cover rocks in the Val Piora area. The porphyroblasts show no tendency to develop crystal faces and are often so rich in inclusions as to be almost indistinguishable from the matrix. The crystals are generally "flattened" in the plane of the compositional banding, their shape being determined by preferred growth within this plane. In finely banded rocks this affect is most marked. The maximum dimension of crystals measured in thin section is normally

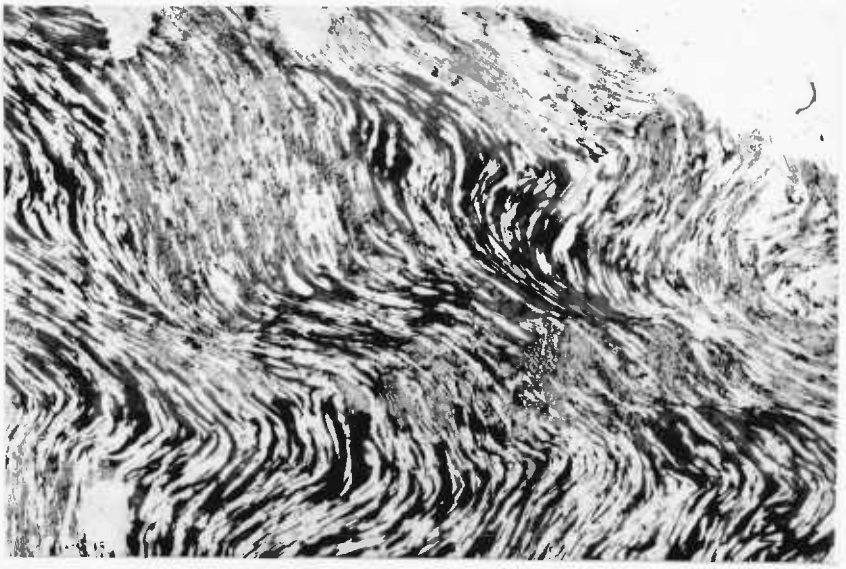

Fig. 4.10. Fourth generation folding of the first foliation (biotite and elongate quartz grains). Inclusion trails in the kyanite porphyroblasts are straight in the centres, but become sharply curved at the margins before passing discordantly into the external folded foliation. Cleavage traces show that some crystals have been bent by the fold forming movements. Spec. 950, Quartenschiefer; M.R. 7010215447, Alpe Carorescio. (x 11)

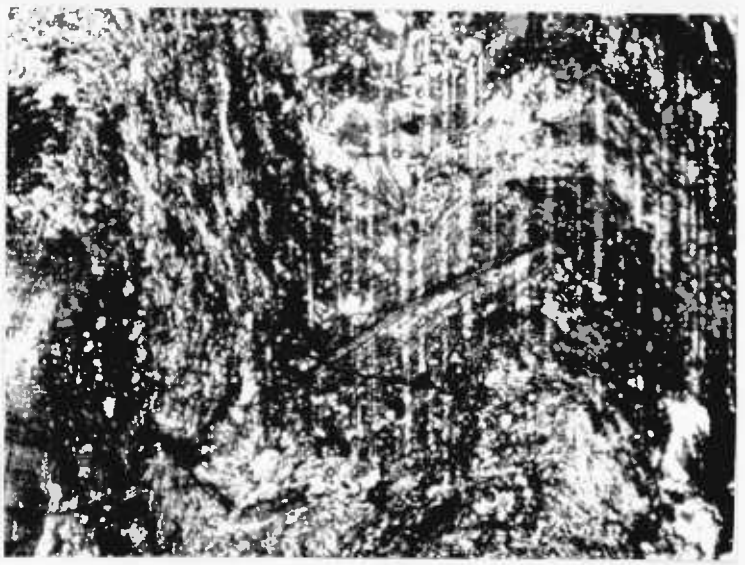

Fig. 4.11. Second generation folding of first foliation (compositional banding, white mica and clinozoisite). The folded surfaces are overgrown by a plagioclase porphyroblast (shown by albite twinning). Spec. 534, Bünderschiefer; M.R. 6943115500, Passo del Camoghe. (x 35)

in the range 2-5 mm. though some crystals are up to a centimetre long. Twinning is uncommon, but where observed is after the albite and pericline laws. The compositions of plagioclases in three specimens of calcareous mica schist from Val Leventina have been determined (U. stage) and found to fall within the composition limits, An_{40-60}, (cf. Wenk, 1962; Tafel I). Some crystals show reverse zoning suggesting crystallisation under conditions of rising temperature.

All the metamorphic minerals recognised in the cover rocks except chloritoid have been found as inclusions in plagioclase. It may be concluded therefore that plagioclase grew at the same time as or after the formation of these minerals. Studies of the relationship between deformation and plagioclase growth support this general conclusion as plagioclase porphyroblasts are found to grow across third and earlier generations of folds and fabrics (Fig. 4.11). Although plagioclase is generally deformed by fourth generation folds, like kyanite, there is sometimes evidence for growth during and more rarely after the fourth episode folding.

Hornblende

Hornblende occurs as large porphyroblasts up to several centimetres in length in the garnet-mica schists of the Quartenschiefer and occasionally in the Pennine Mesozoic metasediments. The porphyroblasts are either randomly oriented or form hornblende garben (Section 6.6, Fig. 6.2). The relationship of these crystals to the structures and fabrics indicates that growth took place between the third and fourth episodes of Alpine deformation. The porphyroblasts are generally rimmed or partially pseudomorphed by biotite.

Ilmenite*

Ilmenite forms crystals of platy habit up to 1 mm. long. These overgrow second folds but are deformed by third and fourth generation structures (Fig. 4.8). The ilmenite plates show complete girdle or L. tectonite fabrics (Section 3.23) comparable to those displayed by micas. The ilmenite fabrics appear to have developed during the third

---

* Although a positive identification has not been made crystals of similar habit in the Nufenenpass rocks have been shown to be ilmenite (Higgins, 1964b, p. 190).

episode of Alpine deformation by mechanical rotation of randomly oriented ilmenites grown under static conditions after the second episode of Alpine deformation. The mineral is often partially or completely altered to rutile.

Tourmaline

Tourmaline, (schorlite), is found in most cover rocks. The crystals are euhedral and usually less than 0.1 mm. in length. Zoning is characteristic. Tourmaline is thought to have grown in the interval of time between the second and third episodes of Alpine deformation.

Table 4.1. The history of growth of metamorphic minerals in the Mesozoic cover.

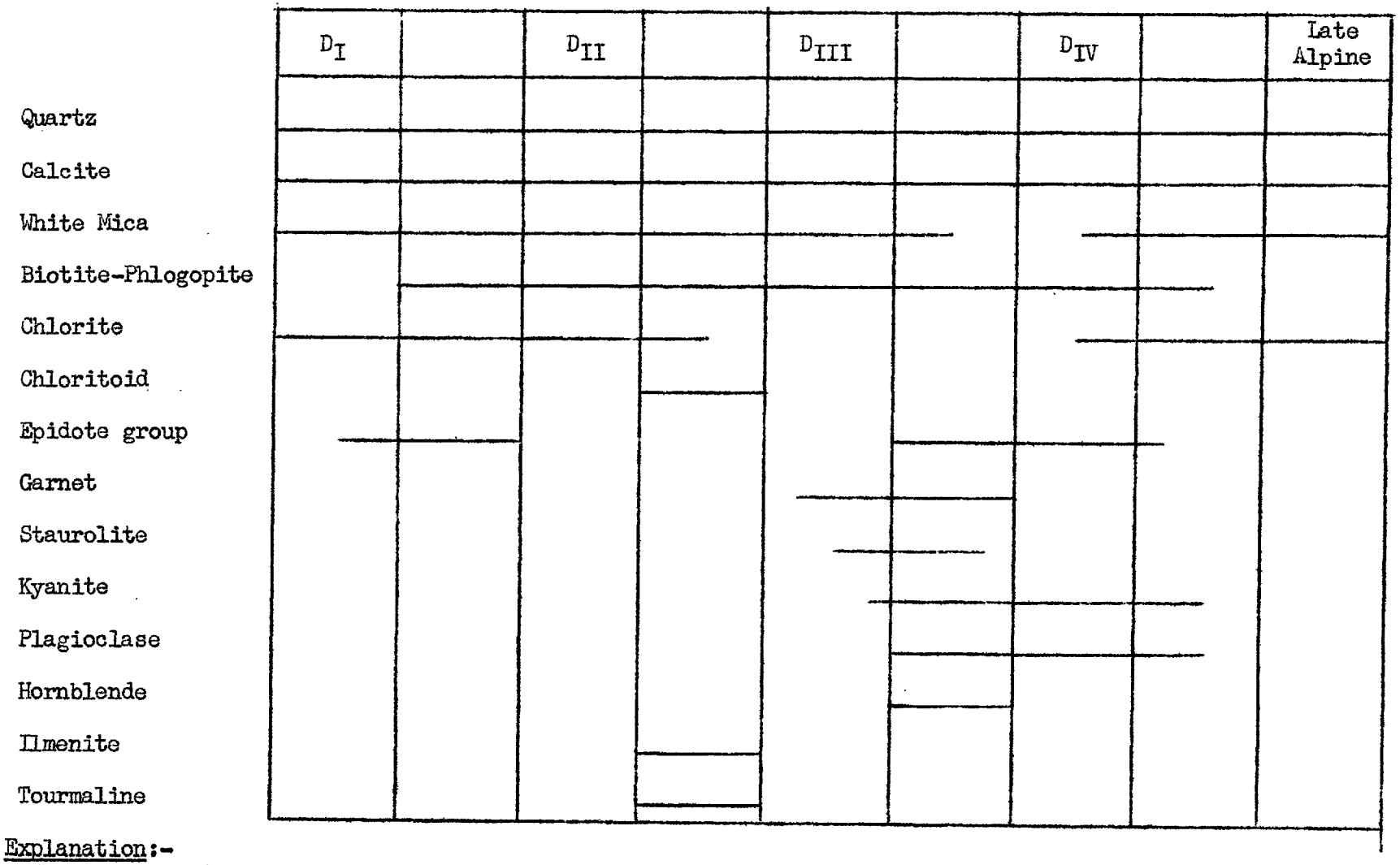

Explanation:-
The history of metamorphic mineral growth deduced from the relationships of minerals to structures and fabrics formed during the different episodes of Alpine deformation, (D_I, D_{II}, D_{III}, D_{IV} and late Alpine). The periods of time during which mineral growth or recrystallization took place are shown by the solid lines.

4.3) The metamorphic minerals of the Gotthard Massif

The history of mineral growth deduced in the gneisses of the Gotthard Massif (Table 4.2) compares closely with that observed in the Mesozoic cover (Section 4.2, Table 4.1) and accords well except in one respect with that outlined previously by Steiger (1962). Steiger has recognised six generations of crystals in the Gotthard Massif gneisses. The first two of these are:-

1) A fine-grained relict quartz-felspar cataclastic mosaic.
2) A fresh recrystallised texture of oriented mica, elongated quartz and finely nematoblastic hornblende.

These two generations of crystals are clearly illustrated in one of Steiger's microphotographs (Steiger, 1962; Tafel II, Fig. 2) and also in Fig. 4.12. Steiger has interpreted the first crystal generation as a pre-Alpine relict and the second as an Alpine fabric formed during the "chief phase of Alpine deformation" (Steiger, 1962, Tabelle 17; Table 3.3). I have placed a diametrically opposite interpretation on these same features (see explanation to Fig. 4.12). The fine grained quartz-felspar mosaic, which strongly resembles experimentally produced recrystallisation textures (Griggs et al, 1960; Hobbs, 1968) I have interpreted as a recrystallised fabric of Alpine age; the elongate quartz grains and some of the oriented micas which outline the first foliation (a pre-Alpine structure, Section 3.31), as pre-Alpine relicts. (Other micas oriented in the first foliation may have grown or recrystallised mimetically within this structure during Alpine times (Section 3.32).)

The most important minerals which grew or recrystallised during the Alpine metamorphism are:-

Quartz	Biotite	Garnet
Felspar	Chlorite	Kyanite
White Mica	Hornblende	Staurolite

Quartz

The shape fabrics of quartz grains suggest that static recrystallisation took place during the Alpine metamorphism, probably after the third episode of Alpine deformation. Fabrics are found which are

similar to those described in the cover rocks, but are generally less well developed. Quartz grains formed during earlier episodes of recrystallisation have survived in the final fabric; for example, large strained grains of quartz which are elongate in the plane of the first foliation (Fig. 4.12) or in the direction of the quartz-felspar rodding in the Streifengneiss, (pre-Alpine fabrics, Section 3.31). At other localities these are partially or completely replaced by aggregates of smaller grains, (Alpine fabric). The degree of quartz recrystallisation appears to have been variable from one locality to the next and often even on the scale of a thin section. Recrystallised quartz occurs in the necks of boudins formed during the fourth episode of Alpine deformation, in E-W trending quartz veins and in tensile fractures of late-Alpine age (Sections 3.34, 3.56).

Felspar

Recrystallisation of felspar took place during the Alpine metamorphism; the degree of recrystallisation, like that of quartz, is variable and relict felspars have locally survived.

The composition of recrystallised plagioclase crystals falls within the range, oligoclase - andesine. (As twinning is usually absent composition was determined mainly by refractive index comparisons with quartz and balsam.) In twinned crystals reverse zoning is often visible.

Micas, (White mica and biotite)

Mica fabrics were formed during the pre-Alpine, second and third episodes of Alpine deformation in the Gotthard gneisses of this area (Sections 3.31, 3.32, 3.33). Biotite porphyroblasts and white mica crystals which form the third episode girdle mica fabrics often appear to overgrow and hence postdate third generation fold structures (cf. Steiger, 1962; Tafel IV, Fig. 2), (Fig. 4.13). As these crystals are oriented they must have grown at a late stage in or after the third episode of Alpine deformation from nuclei formed during this deformation. Random growth fabrics shown by biotite porphyroblasts in rocks deformed by third generation folds indicate that nucleation and growth of this mineral locally outlasted this deformation. The replacement of

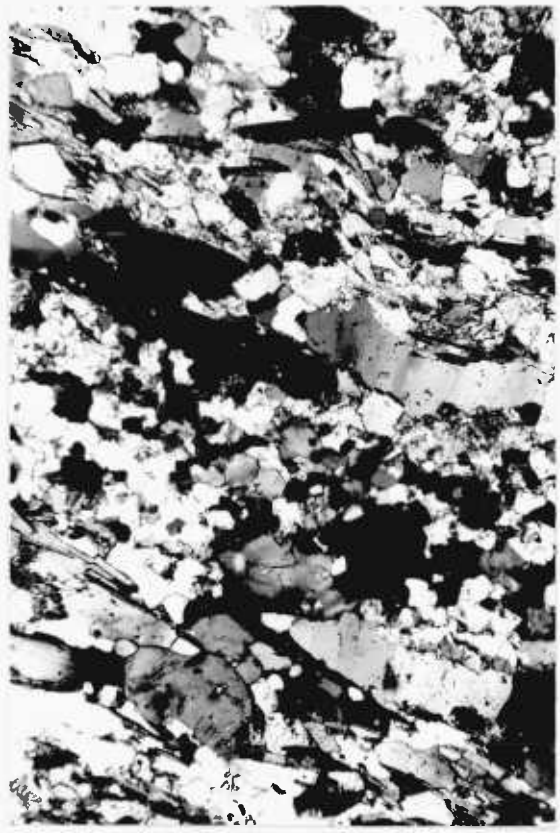

Fig. 4.12. Large strained grains of quartz elongate in the plane of the first (pre-Alpine) foliation. The equigranular quartz-felspar aggregate between successive trains of quartz grains is suggested to be a recrystallised Alpine fabric in relation to the elongate quartz grains which are interpreted as pre-Alpine relicts. Some of the large strained felspar crystals may also be pre-Alpine relicts. In places the relict quartz grains have been replaced by an aggregate of equidimensional grains. Spec. 1341, Sorescia gneiss; M.R. 6993515667, N.N.W. of Lago di Dentro. (x 30)

hornblende by biotite suggests that biotite growth also took place during the retrogressive stage of the Alpine metamorphism. Most of the biotite porphyroblasts are strained, some have suffered a post-crystalline rotation. These effects are possibly the result of movements during the fourth episode of Alpine deformation. White mica appears to have continued growing after biotite, as it is found in the necks of fourth episode boudins (Section 3.34) and in late Alpine tensile fractures.

Chlorite

Various ages of chlorite growth or recrystallisation may be distinguished. Chlorite is aligned in the first, second and third foliation planes and hence must have grown during or after, (mimetically), the pre-Alpine and second and third episodes of Alpine deformation. Chlorite is found intergrown, (parallel {001}), with biotite porphyroblasts which formed after the third episode of Alpine deformation. It also occurs as a retrograde mineral forming sheaf like crystal aggregates replacing biotite and is present in the necks of fourth episode boudins (Section 3.34) and in late Alpine tensile fractures.

Hornblende

Euhedral hornblende porphyroblasts are spectacular minerals produced by the Alpine metamorphism. Individual crystals are frequently several centimetres in length. Four types of hornblende fabric are recognised. Although individual rocks of homogeneous composition generally only show one of these fabrics sometimes (1) and (3) are observed together (Fig. 4.14).

1) A finely crystalline planar hornblende fabric.
   The crystals show a preferred orientation of c axes in the plane of the first foliation. The fabric is deformed by second and later generations of structures and is probably an inherited pre-Alpine fabric.

2) A finely crystalline linear hornblende fabric.
   The crystals show a preferred orientation of c axes parallel to the linear mica fabrics found in adjacent rocks (Section 3.33).

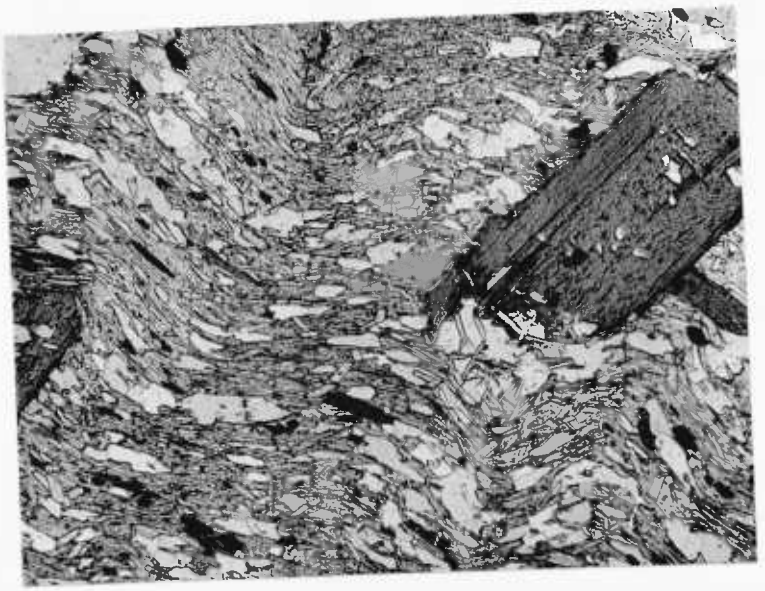

Fig. 4.13. Third generation folding of the first foliation (white mica and elongate quartz grains). Biotite porphyroblasts and smaller white mica crystals forming the L. tectonite mica fabric (axis perpendicular to section) appear to overgrow the folds. Spec. 1211, Tremola series; M.R. 6917915550, Val Canaria. (x 35)

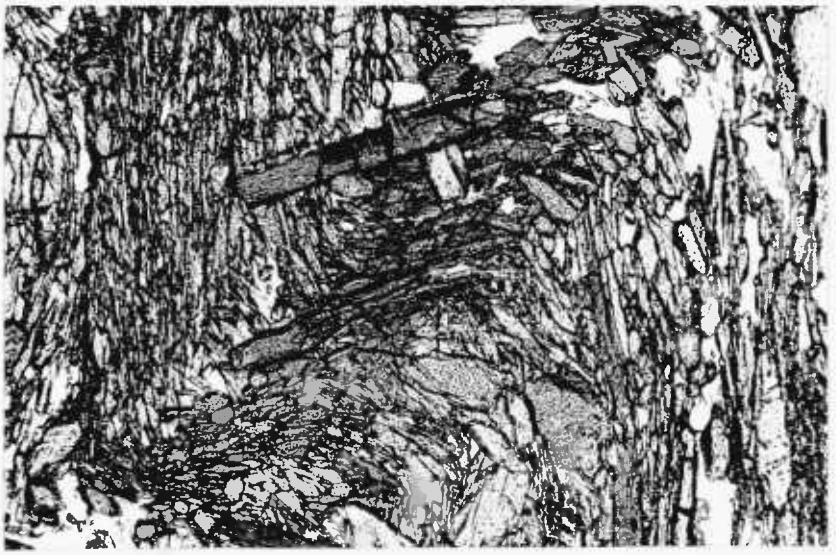

Fig. 4.14. Second generation folding of the first (pre-Alpine) foliation. Two generations of hornblende are visible; those oriented in the plane of the first foliation which are folded and the randomly oriented larger crystals which grow across the folds. Spec. 1104, Tremola series; M.R. 6962715645, N.W. of Lago Tom. (x 110)

This hornblende fabric probably developed during the third episode of Alpine deformation.

3) A random growth fabric.

Randomly oriented hornblende crystals, generally porphyroblasts, grow across third and earlier generations of structures and fabrics. This is the most common type of hornblende fabric. It formed after the third and probably before the fourth episode of Alpine deformation.

4) Hornblende garbenschiefer (Section 6.6).

The garben are large sheaf like aggregates of hornblende crystals whose a and c crystallographic axes are oriented in the foliation plane. They are often partially or completely pseudomorphed by biotite. The preferred orientation of the crystal aggregates is suggested to result from epitaxial nucleation (Chapter 6). The garben are thought to be coeval with the random hornblende fabrics found in other rocks.

Garnet

Garnet occurs as euhedral to subhedral porphyroblasts up to a centimetre in diameter. The earliest garnet growth appears to have taken place during the third episode of Alpine deformation, as snowball garnets with features (sense and axis of rotation) identical to those observed in the cover are found in the Tremola series (Becke, 1924, p. 196; Steiger, 1962, p. 462 and Tafel III, Fig. 1). Garnet crystals generally show no evidence of syntectonic growth and where these occur in rocks deformed by third generation folds they overgrow and hence postdate these folds (Fig. 4.15). The post-crystalline differential rotations exhibited by some crystals may be attributed to movements during the fourth episode of Alpine deformation, or where snowball garnets show this feature, to termination of crystal growth before the end of the third episode of Alpine deformation.

Inclusion fabrics, which are related to the internal crystal structure, and which are similar to those observed in garnet crystals in the cover rocks (Section 4.2) are also found in garnets from the Gotthard Massif.

Staurolite

Staurolite is not a common mineral in the Gotthard Massif gneisses of the Val Piora area. It is found rarely as euhedral to subhedral porphyroblasts up to a few millimetres in length. The porphyroblasts grew after the third episode of Alpine deformation (Fig. 4.15).

Kyanite

Kyanite occurs occasionally as anhedral porphyroblasts up to a centimetre in length in mica gneisses of the Tremola series. As kyanite crystals overgrow third generation folds (Fig. 4.15) growth must have taken place after the third episode of Alpine deformation. Crystals are commonly slightly deformed, possibly by movements during the fourth episode of Alpine deformation. Growth can be shown to have continued locally during this deformation as kyanite is occasionally found in the necks of fourth episode boudins and in E-W trending quartz veins (Section 3.34).

Fig. 4.15. Third generation crenulations folding the first foliation (white mica and biotite). The inclusion trails within and the shape of the garnet porphyroblast show that it post-dates the folding as do smaller porphyroblasts of staurolite, kyanite, and biotite. Spec. 1149, Tremola series; M.R. 6967215635, S. of Pne. Garioi. (x 15)

Fig. 4.16. Pre-Alpine albite porphyroclast. The schistosity in the matrix formed by oriented white mica and biotite is of second deformation (Alpine) age. The inclusion trails in the albite (quartz, epidote and micas) are relicts of an earlier (pre-Alpine) first foliation which has been obliterated in the matrix. Spec. 54, Orange Group gneiss; M.R. 6969215459, Canariscio di Campo. (x 35)

4.4) The metamorphic minerals of the Lukmanier Massif

In the gneisses of the Lukmanier Massif the following are the most important minerals which grew or recrystallised during the Alpine metamorphism.

Quartz	Biotite	Garnet
Felspar	Chlorite	Staurolite
White mica	Hornblende	Tourmaline

The history of mineral growth (Table 4.3) is similar to that deduced in the other two structural units. As in the Gotthard Massif pre-Alpine relicts (minerals formed before the second episode of Alpine deformation) have survived the Alpine metamorphism.

Quartz

Quartz grain shape fabrics suggest that static recrystallisation of quartz took place after the third and locally after the fourth episodes of Alpine deformation as in the rocks of the Mesozoic cover and Gotthard Massif. Relict pre-Alpine quartz grains are not observed, although occasionally syntectonically formed preferred dimensional orientations of quartz grains in the planes of second and fourth fold axial surfaces have survived static recrystallisation (Section 3.42, 3.44). Recrystallised quartz also appears associated with fourth episode structures (Section 3.44) and in late Alpine tensile fractures.

Felspar

Plagioclase is the dominant felspar phase present in the Lukmanier Massif gneisses in the Val Piora area. Composition varies within the range albite - andesine, the more calcic plagioclases occurring typically in amphibolites. (Wenk and Keller (1969, p. 163) reported plagioclases within the composition range An_{20-29} in amphibolites from this area.) Potassium felspar, chiefly in the form microcline, is found as discrete crystals or combined with plagioclase as perthite or antiperthite.

As plagioclase crystals are generally undeformed by fourth and earlier generations of fold structures, it may be deduced that plagioclase growth took place after the formation of these structures.

Locally however, albite crystals which are deformed by second generation structures (Fig. 4.16) and which represent possible pre-Alpine relicts have survived the Alpine metamorphism. Microcline appears also to have grown or recrystallised during the Alpine metamorphism probably coevally with plagioclase.

Mica (White mica and biotite)

Preferred orientations of mica formed during or after, (mimetic), the pre-Alpine and second, third and fourth episodes of Alpine deformation are recognised in the Lukmanier gneisses (Sections 3.41, 3.42, 3.43, 3.44), (Figs. 4.16, 4.17, 4.18). In some rocks randomly oriented biotite porphyroblasts and white mica crystals overgrow fourth generation folds (Fig. 4.17) suggesting that nucleation and growth of these minerals continued after the fourth episode of Alpine deformation. White mica is also found in the necks of fourth episode boudins and in late Alpine tensile fractures.

Chlorite

Chlorite occurs chiefly as an alteration product of hornblende, biotite and garnet. Alteration of these minerals is most marked adjacent to fourth episode boudin necks in which concentrations of chlorite are found. Chlorite is also present in late Alpine tensile fractures.

Hornblende

Hornblende forms euhedral porphyroblasts often several centimetres long. The different types of hornblende growth fabric which have been described in the Gotthard Massif gneisses (Section 4.3) are seen also in the Lukmanier Massif gneisses. Random growth fabrics are the most common. The crystals forming linear hornblende fabrics show a preferred orientation of crystallographic c axes parallel to the third episode linear mica fabrics found in adjacent rocks; those forming planar hornblende fabrics show a preferred orientation of c axes in the plane of the second schistosity. The second schistosity is overgrown by and therefore predates the crystals of all the fabric types. Hornblende garben are only rarely seen in the Lukmanier Massif gneisses.

The linear hornblende fabrics suggest that hornblende nucleated and possibly also grew during the third episode of Alpine deformation; the random and probably coeval planar (mimetic) fabrics suggest that these processes continued after this deformation. Hornblende crystals which are deformed by and others which overgrow fourth generation folds indicate that hornblende growth took place both before and after the formation of these structures.

Garnet

Euhedral to anhedral porphyroblasts up to 5 mm. in diameter are common in many of the Lukmanier Massif gneisses. Inclusion trails are generally poorly developed and age relationships between the structural sequence and crystal growth are often ambiguous. Various periods of garnet growth may be distinguished.

Garnet crystals are found which are clearly older than second generation folds (Fig. 3.17). This implies a period of garnet growth which predates the second episode of Alpine deformation and is probably of pre-Alpine age.

Snowball garnets with the same sense and axes of rotation as those in the cover rocks and with differential rotations of up to 200 degrees are also observed. From their occurrence syntectonic garnet growth during the third episode of Alpine deformation may be inferred.

Most of the garnet porphyroblasts show no evidence of growth during deformation and overgrow third and earlier generations of folds and fabrics (Fig. 4.18). These crystals grew after the third, but from the manner in which the matrix is deformed around them, apparently before the fourth episode of Alpine deformation (Fig. 4.17).

Staurolite

Staurolite occurs in some garnetiferous mica gneisses as euhedral prophyroblasts up to a centimetre in length (Fig. 4.18). Growth of the mineral appears to have been contemporaneous with the main period of garnet growth between the third and fourth episodes of Alpine deformation.

Tourmaline

Tourmaline,(schorlite), is a common accessory mineral in the

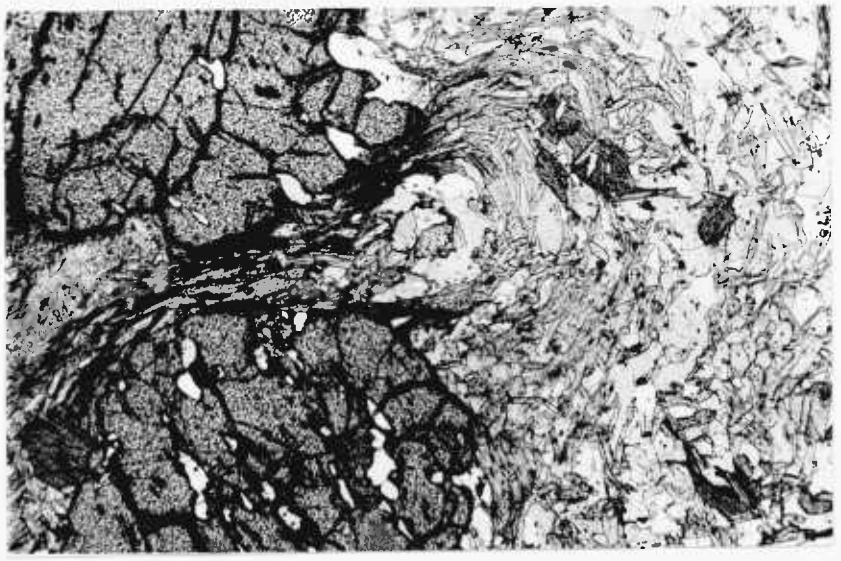

Fig. 4.17. Fourth generation fold pinched between two earlier garnet porphyroblasts. White mica crystals which grow across the folded second foliation show a weak preferred orientation parallel to the fourth fold axial surface. The larger biotite crystals are randomly oriented and postdate the folding. Spec. 493, Orange Group gneiss; MR. 6956315421, E.S.E. of Piora. (x 35)

Fig. 4.18. Second generation folding of the first foliation (white mica feltwork and carbonaceous trails). The folds are overgrown by garnet, staurolite and biotite porphyroblasts. Note also that there has been some recrystallisation of white mica after folding. Spec. X.16, Orange Group gneiss, M.R. 6925415341, Campoi. (x 10)

Lukmanier Massif gneisses. Crystals are usually euhedral, zoned and less than a millimetre long. Occasionally however crystals several centimetres in length are found growing mimetically on the second schistosity surfaces. Growth is thought to have taken place between the second and third episodes of Alpine deformation.

Table 4.2 The history of metamorphic mineral growth in the Gotthard Massif.

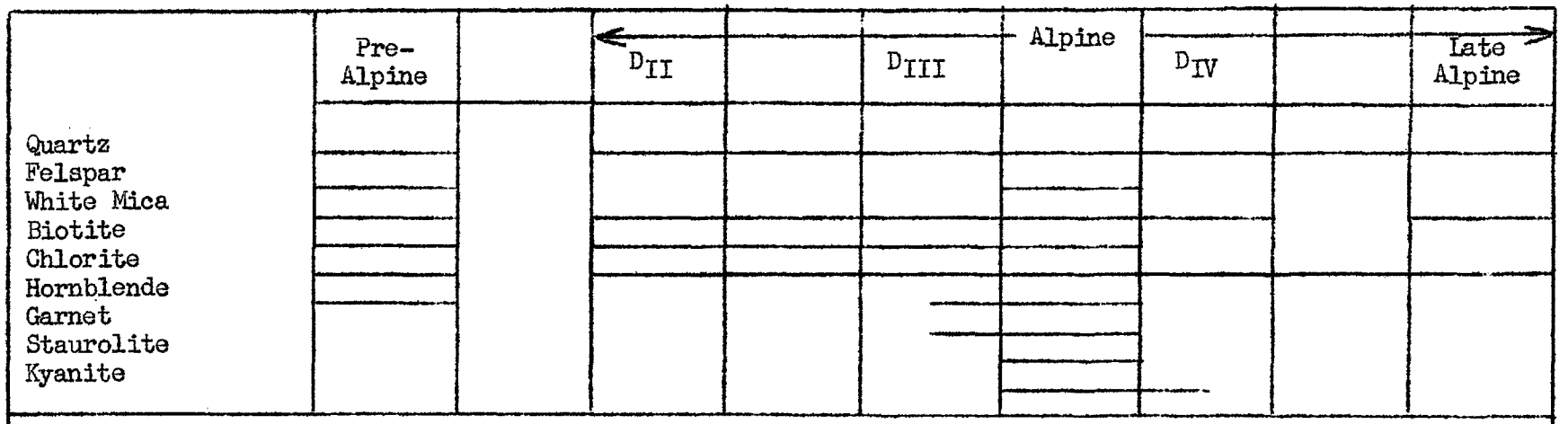

Table 4.3 The history of metamorphic mineral growth in the Lukmanier Massif.

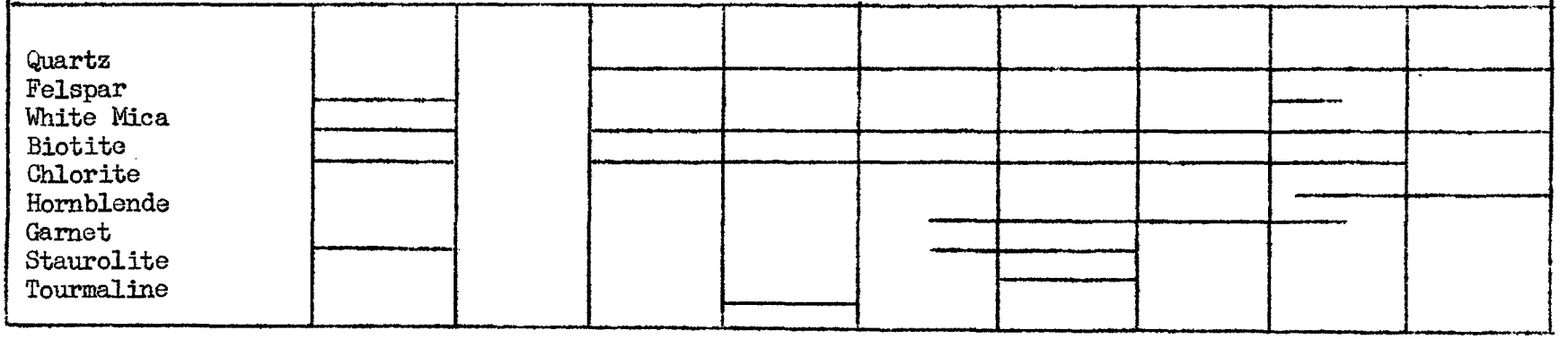

Explanation of Tables 4.2 and 4.3 :-

The history of metamorphic mineral growth deduced from the relationships of minerals to structures and fabrics formed during the pre-Alpine and Alpine, (D_{II}, D_{III}, D_{IV} and late Alpine), episodes of deformation. The periods of time during which mineral growth or recrystallization took place are shown by solid lines.

4.5) Discussion

From the tables summarising the history of metamorphic mineral growth in the different structural units, it is clear that the metamorphic peak was reached in the interval of time bounded by the end of the third and end of the fourth episodes of Alpine deformation, (i.e. at a late stage in the deformation history). This conclusion is generally agreed by workers throughout the Lower Pennine region (Section 4.1). Details of interpretation of metamorphic fabric do vary, but only in their finer points.

The evaluation of the paragenetic sequences of mineral growth has led to the conclusion that many of the porphyroblasts show different age relationships to the fourth generation folds. The growth of the porphyroblasts across fourth generation folds suggests that a much higher grade of regional metamorphism existed at the end of the fourth episode of Alpine deformation, than that which might be inferred from the frequent occurrence of deformed porphyroblasts. It is often assumed that during an episode of deformation the total strain is recorded in the form of visible deformation, generally fold development, and that this fold development is everywhere strictly isochronous. Such assumptions are probably unjustified and accordingly the strict treatment of a fold phase as an isochron is probably equally unjustified. The observation that the porphyroblasts in some cases grew after the fourth generation folds does not therefore imply that they grew after the fourth episode of Alpine deformation. It is probably significant that the rocks in which the porphyroblasts are found to postdate the folds are those in which the layering suffered early folding and later boudinage during the fourth episode of Alpine deformation (Section 3.24).

In the general context of the temporal relationship between deformation and regional metamorphism, mention should be made of the hypothesis of migrating deformation episodes put forward by Higgins (1964b) and Chadwick (1965). The hypothesis explains the apparent variation in the metamorphic peak with respect to the deformation episodes in both the Nufenenpass - Basodino (Higgins) and Lukmanier (Chadwick) areas.

In the Val Piora area I have found no evidence to support this hypothesis, in fact my observations have led me to suggest the following criticism.

In the Lukmanier area the basis for the hypothesis rests on the interpretation placed on the age of differential rotation of the porphyroblast minerals. Chadwick (1965) has suggested that rotation took place during Phase B (the second episode of Alpine deformation (Table 3.3)) in the north of the Lukmanier area, whereas in the south it occurred during Phase V (the fourth episode of Alpine deformation. Chadwick does not recognise a third episode of Alpine deformation (Table 3.3)). If porphyroblast growth took place essentially synchronously throughout the area then it follows that the equivalent deformation episodes must have been progressively later in the north than in the south of the area.

A Phase B age for the differential porphyroblast rotation in the north of the Lukmanier area may be questioned and hence so may the basis of the hypothesis. As in the Val Piora area the sense of the porphyroblast rotation appears to remain constant irrespective of the position of the porphyroblasts in relation to Phase B structures. It has been suggested (Section 3.9) for this and other reasons that rotation took place during the third and possibly fourth episodes of Alpine deformation.

An investigation of the age of mineral growth in terms of the temporal coordinates provided by the deformation episodes is of little value unless it leads to an understanding of the change of physical conditions with time.

In the Gotthard and Lukmanier Massifs the minerals interpreted as pre-Alpine relicts, (garnet, hornblende, micas, albite and quartz) suggest upper greenschist facies metamorphism of the basement in Hercynian times (cf. Steiger, 1962, p. 383).

The sequence of Alpine mineral growth in the Mesozoic cover and pre-Alpine basement corresponds with a general increase with time in the grade of Alpine metamorphism, from lower greenschist facies conditions during the first episode of Alpine deformation to lower

almandine-amphibolite facies conditions in late third to early fourth deformation times (Fig. 4.19). The increase in grade during the third episode of Alpine deformation may be accounted for primarily by a rise in temperature associated with a rise of the migmatite front into the S. Ticino region (Wenk, 1962).

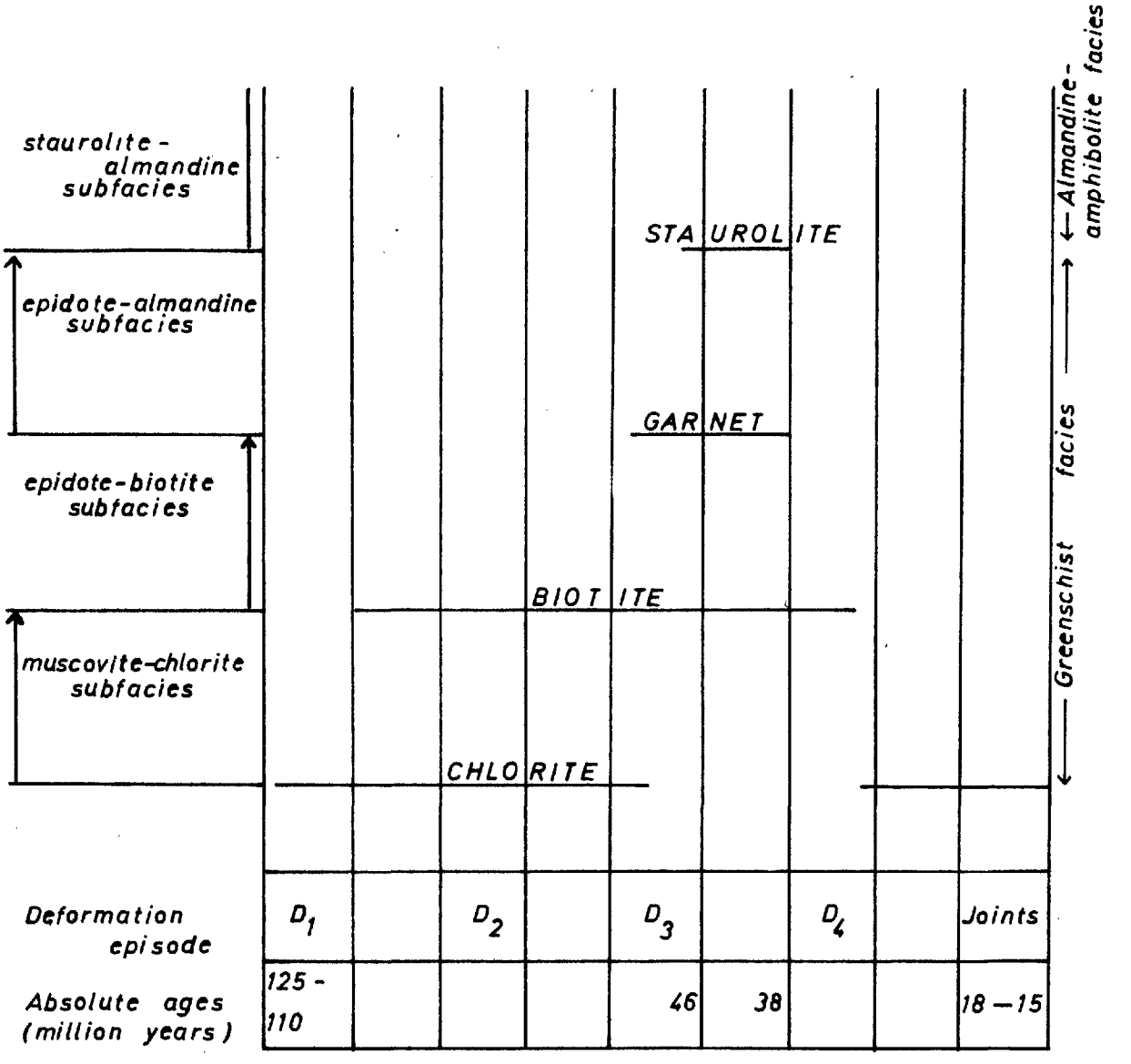

Fig. 4·19 *The change in metamorphic conditions with time suggested by the growth periods of chlorite, biotite, garnet and staurolite.*

CHAPTER V

SNOWBALL GARNETS

5.1) Introduction

Over fifty years ago Flett (1912) figured and described spiral rings of inclusions in garnets. These he interpreted as the products of rotation* during garnet growth; the garnet "was being rolled along and was growing larger like a snowball during the process". Since that time there have been numerous reports of snowball garnets, for example, from the Scottish Highlands, Rast (1958), Peacy (1961), the Alps, Krige (1918), Schmidt (1918), Becke (1924), Steiger (1962), and the Pyrenees, Zwart (1960).

The significance of the internal geometry of the inclusion trails as a strain marker was pointed out by Schmidt (1918), and has been discussed further by Mügge (1930), Ramsay (1962a) and Spry (1963), among others. However beyond the limited observations made from thin sections no attempt has been made until recently (Powell and Treagus, 1967, 1970) to study the three dimensional geometry of the inclusion trails. Furthermore the systematic measurement of strain from rotated garnets has not been considered. It was with this latter possibility in mind that investigation of the garnets of Val Piora was begun.

The conclusions arrived at in this chapter agree well with those of Powell and Treagus (1967, 1970), whose investigations took place concurrently with the following.

---

* Differential rotation of the crystal and the matrix surrounding it.

5.2) Material

The material used in this study was taken from three localities Nos. 110, 129 and 136 in Val Piora. These localities are exposures of the black garnet schist series in which the black garnet schists are interbanded with calcareous schists and occasional quartzites (Section 2.21). Localities 110 and 136 are situated on the north side of the shallow gorge cut by the Murinascia torrent, locality 110 (M.R. 6981515576) at a height of 1950 metres in the gorge below Capanna Cadagno and locality 136 (M.R. 6970415574) at 1860 metres a short distance from the point where the torrent flows into Lago Ritom. Locality 129 (M.R. 6967215576) is on the north side of the road from Piora to Alpe Piora a few metres below the chapel of San Carlo.

The garnets illustrated by Krige (1918, Plates XII and XIII, Figs. 1-5) are from the same black garnet schist series and from the same general, if not identical, localities. The petrography of these rocks has been described by him in some detail (pp. 606-608).

In hand specimen the garnets appear as porphyroblasts of around 5 mm. diameter, set in a dark, fine grained, schistose matrix. The crystals may sometimes be seen to be rotated because compositional banding is deflected where it passes through them and/or is offset across them. Generally however the deformation of the matrix surrounding the crystals indicates the rotation and its sense. The attitude of the rotation axis of the crystals may be determined by reference to the style of deformation in the matrix; whether the foliation wraps round the crystal symmetrically (Fig.5.1a) (section parallel to the axis) or asymmetrically (sections oblique to the axis) (Fig.5.1b). On the foliation surfaces of rocks in which rotated crystals are present a step-like structure reflecting the asymmetry of Fig.5.1b is developed across the crystals (Fig.5.1c). This structure is again a reflection of the deformation of the matrix surrounding the particle and is related to the rotation axis as illustrated. By observations such as these crystal rotation axes are found to be perpendicular or sub-perpendicular to the mineral lineation in the rocks.

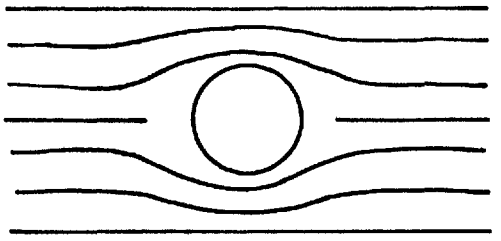

(a)

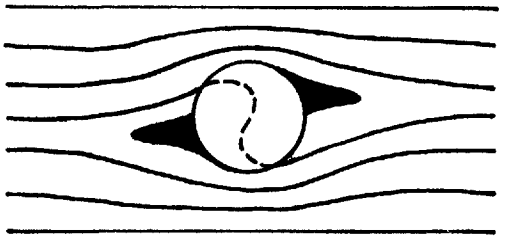

(b)

(Note asymmetry of pressure shadows)

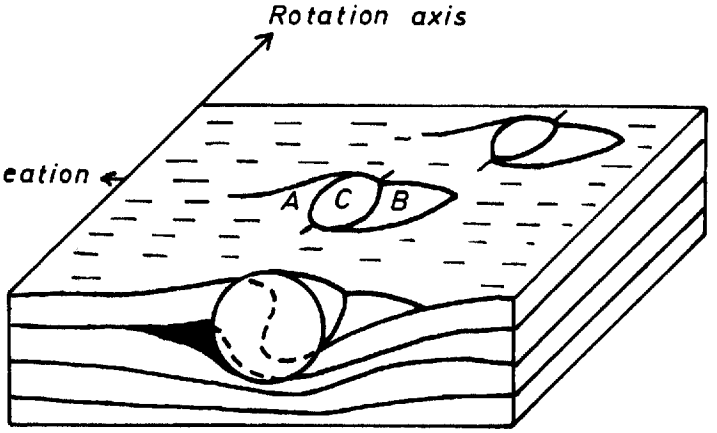

(c)

Fig. 5·1 Styles of deformation of the matrix surrounding snowball garnets. (a) Section perpendicular to external foliation and parallel to crystal rotation axis. (b) Section perpendicular to crystal rotation axis. (c) Block diagram showing the step like structure (C) which forms when the crystal is rotated. Regions of elevated (A) and depressed (B) external foliation are indicated.

As well as indicating the sense and axis of rotation of the crystals, the deformed matrix may also give some idea of the degree of rotation. All these observations can be carried out in the field and are thus valuable, in that they give evidence of the history and geometry of deformation.

5.3) Methods of analysis

Geometrical analysis, by plotting isogons, of the inclusion trails of random sections cut perpendicular to the crystal rotation axis (G I and G II Spec. 110, G I Spec. 129) was carried out on enlarged photomicrographs of the thin sectioned material (Section 5.51).

In the analysis of single crystals (Section 5.52), a serial grinding technique was employed to determine the three dimensional geometry of the inclusion trails. Within the field of palaeontology, serial grinding has long been recognised as a means of investigating the internal structure of organisms and some of the various methods employed have been described by Ager (1965). The apparatus used in the present study incorporated an electrically driven diamond lapping wheel to remove a fixed thickness from the face (2 x 3 sq. cm. approx.) of the specimen. Subsequent to this process the face was polished using fine grade carborundum powder to remove any scour marks and the total thickness ground away determined by difference.

The morphology of the face and in particular of the inclusion trails in any garnet section exposed could be recorded, at this instant, by first etching the surface by immersion in dilute hydrofluoric acid and then by taking a cellulose peel. For a discussion on the use of cellulose peels reference is made once again to Ager (1965). In practice some degree of experimentation with time of etching, thickness of cellulose sheet, etc., was required to produce the best results. The cellulose peel obtained was treated as a photographic negative and in this way a series of photographic enlargements of sections (perpendicular to the rotation axis) through an individual crystal was built up. Analysis of these sections using isogons allowed an interpretation of the internal geometry to be made.

The determination of the distribution of maximum rotation angles in specimens 136A and 136B (Section 5.7) involved the same sort of technique as above, but applied on a large scale. Surfaces of the order of 10 x 5 sq. cm. were serially ground using a large surface grinder, a fixed thickness being removed during each grinding operation. The surface was polished to remove scour marks, as before, and the position of every sectioned garnet crystal recorded by drawing its

outline on a sheet of cellophane placed over the surface. Each crystal was assigned a number. A binocular microscope incorporating a micrometer eyepiece and an eyepiece attachment for measuring angles was used to determine the size (maximum and minimum diameters) and rotation shown by each section. Thus it was possible to obtain a measure of the maximum rotation (rotation at the centre of the crystal (Section 5.4)) and size of the crystal.

5.4) The nature of the problem

The characteristic S. trails of inclusions found within some garnet crystals are presumed to arise by simultaneous growth and rotation of the crystals. This process can be represented by a sphere which grows and rotates successively by a series of incremental amounts. If it is accepted that during every growth increment the sphere includes an external foliation which is everywhere parallel, but is formed by discontinuous elements, then the locus of points of equal rotation, θ, of the now included foliation will represent a stage in the growth of the sphere. This is the basis of the model proposed by Spry (1963, pp. 213-214 and Fig. 2) and that constructed in Fig.5.2 a. The three dimensional implications of this model may be illustrated by reference to Fig.5.2 b, which shows part of a section, cut through the centre, O, of the model crystal, parallel to the external foliation and including the rotation axis. Successive growth stages are represented by successive circles, which in this section are the loci of points of equal dip of the included foliation. The diagram serves to illustrate a number of important points.

a) The maximum rotation a crystal has undergone can only be measured in the section cut at right angles to the rotation axis and through the centre of the crystal.
b) The included foliation surfaces are not cylindrical but complex.
c) The history of growth and rotation can generally only be analysed in the section cut at right angles to the rotation axis and through the centre of the crystal.

The first of the above points is self explanatory and has already been emphasised by Mügge (1930, p. 503). The second is an implication of the three dimensional geometry of this model and of the closely related models of Powell and Treagus (1967, Fig. 1) and Cox (1969, Fig. 1). Spry (1963, p. 212) stated incorrectly that the included foliation surfaces were cylindrical. The third point may require some clarification.

The absolute rates of growth and rotation of a crystal may not of course be determined, but it is possible to examine the history of

Fig. 5·2

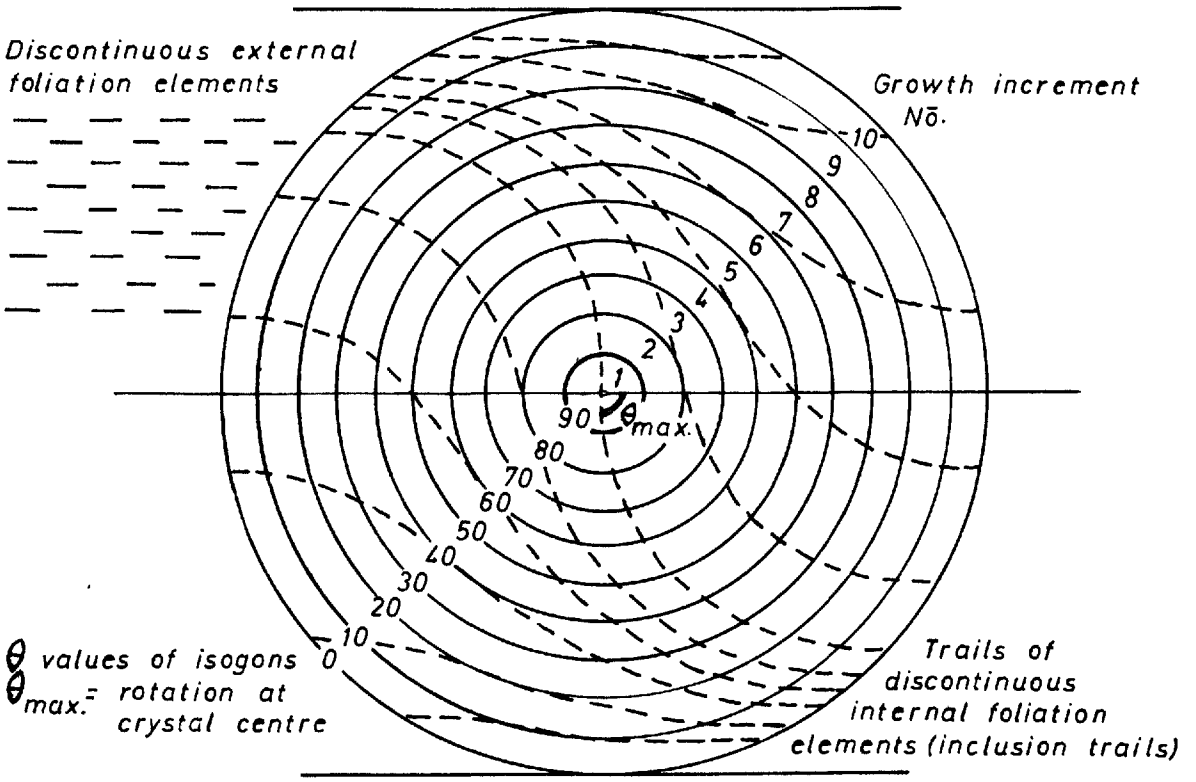

(a) Section perpendicular to rotation axis through model crystal centre.

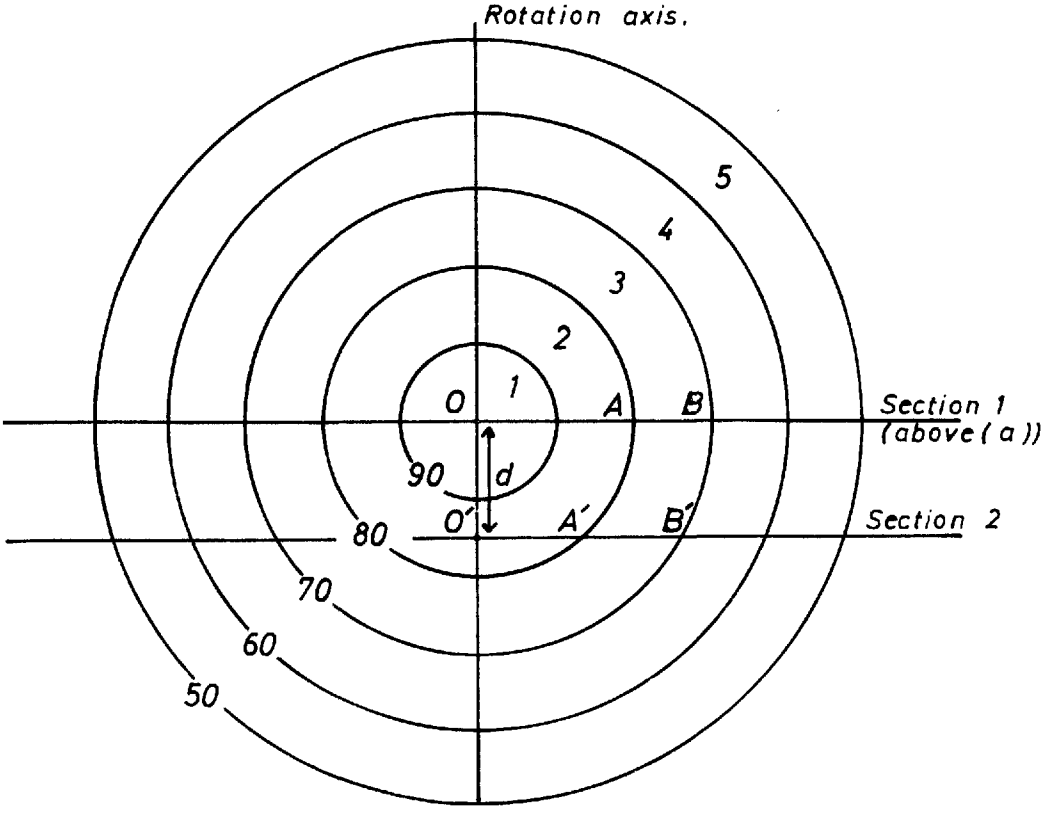

(b) Section parallel to rotation axis and external foliation plane.

growth in terms of rotation and vice versa. It has been shown in the above model that successive stages in the growth of a crystal may be represented by the loci of points of equal rotation of the included foliation (isogons). The distance apart of successive 10 degree isogons drawn in Fig5.2a shows the amount by which the crystal has increased its radius during each 10 degree increment of rotation. An analysis of this type has been used by Spry (1963, pp. 216-220) to determine the growth laws of crystals. Examples of simple growth laws are:-

a) Linear growth law.

The crystal increases its radius by an equal amount during each equal increment of rotation:

$$r = a\,\theta' \qquad (5.1)$$

where r = radius of the crystal, a = constant, $\theta' = \theta_{max} - \theta$ = maximum rotation angle - rotation value for isogon.

b) Cubic growth law.

The crystal grows by the addition of a constant volume of material during each equal increment of rotation.

$$r^3 = a\,\theta' \qquad (5.2)$$

Thus the geometry of the inclusion trails is a function of the growth law. The equal spacing of the 10 degree isogons in Fig.5.2a shows it to be constructed according to a linear growth law.

If an attempt to analyse the growth law is made from any section cut perpendicular to the rotation axis of the crystal at an unknown distance, d, from its centre (e.g. Section 2 in Fig.5 2b), the result may be shown to be invalid. In fact, this must generally apply to any analysis of a growth law from a thin section cut in the above orientation. The distance apart of adjacent isogons in Section 2, for instance A'B' is not equal to the increase in radius, AB ir Section 1, but is related to AB in the following manner.

$$\frac{A'B'}{AB} = \frac{(\sqrt{OB^2 - d^2} - \sqrt{OA^2 - d^2})}{(OB - OA)} \qquad (5.3)$$

A graph of $A'B'/AB$ / d may be drawn for each growth increment (Fig.5.3),

and illustrates the error introduced into the measurement of each growth increment by considering a section a distance, d, from the centre of the crystal. It is emphasised that this graph applies only to crystals which have a linear growth law. Where other growth laws have operated the relevant graphs may be constructed.

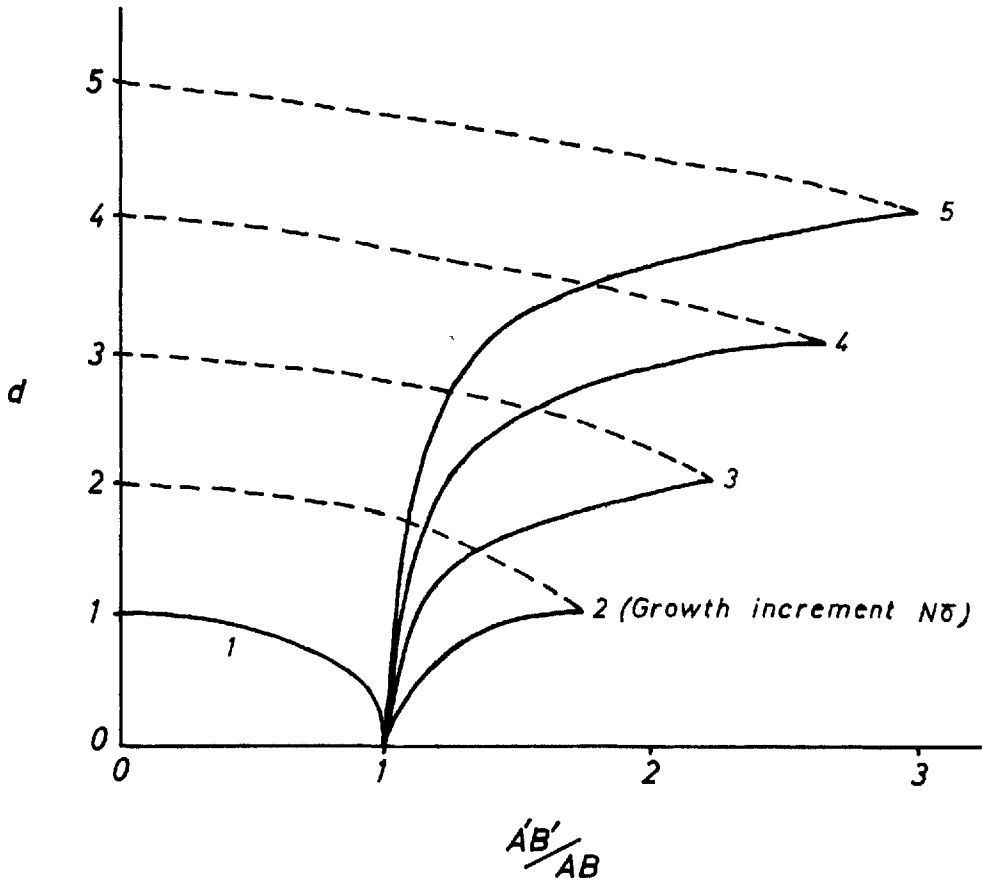

Fig. 5·3 Graph of $\frac{A'B'}{AB}/d$ *for growth increments 1-5 in Fig. 5·2*

5.5) Natural examples

A model has been proposed and some of its three dimensional implications examined. The degree to which natural crystals conform to the model has been studied by the use of two analytical methods:-

5.51) Geometrical analysis, using isogons, of the inclusion trails in sections perpendicular to the rotation axis and generally of unknown distance from the centre of the crystal.

5.52) Geometrical analysis, using isogons, of the inclusion trails in sections cut serially perpendicular to the rotation axis through single crystals.

The analytical techniques have been discussed (Section 5.3).

5.51) Figs. 5.4a and 5.4b show the isogon patterns constructed from the inclusion trails of two crystal sections GI and GII Spec. 110. In the general case, sections such as these are of unknown distance from the centres of their respective crystals and are thus unsuitable for determining growth laws (Section 5.4). In this instance however there is evidence to suggest that the sections pass through or near the centres of the crystals. The evidence is as follows. Prior to this analysis rotation angles were measured from garnet sections occurring on a number of surfaces cut perpendicular to the crystal rotation axes. Out of the 79 measured crystal sections none showed an angle of rotation greater than 150 degrees and it was concluded that this figure was the maximum amount of rotation to be expected in any crystal in the specimen. The values of rotation 145-150 degrees shown by GI and GII Spec. 110 are therefore maximum values and hence these sections probably contain the crystal centres.

Spry (1963, pp. 216-220) has discussed the method by which the growth law of a crystal may be deduced. Use of this method showed the growth laws to be: $r = a\theta'$ for GI and $r^2 = a\theta'$ for GII. In deriving the laws only those isogons which lie almost or wholly within the crystal section have been considered.

The model on which these determinations are based assumes the isogons to be circular and to represent successive outlines of the crystal during its growth. Although the shape of most garnets in

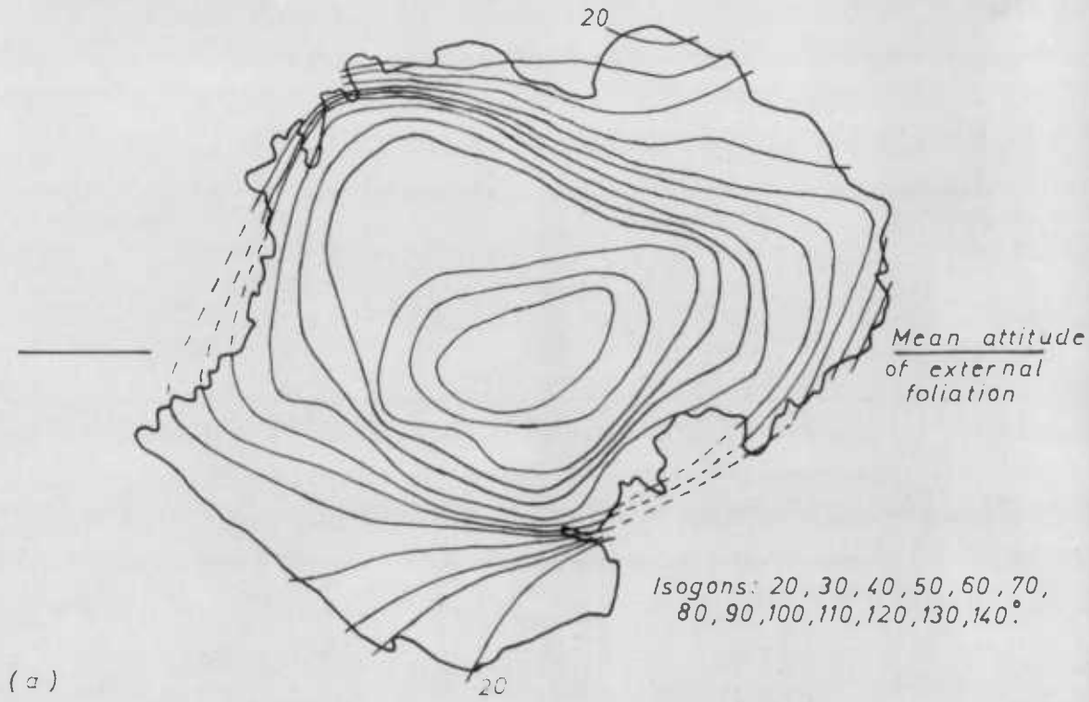

(a)

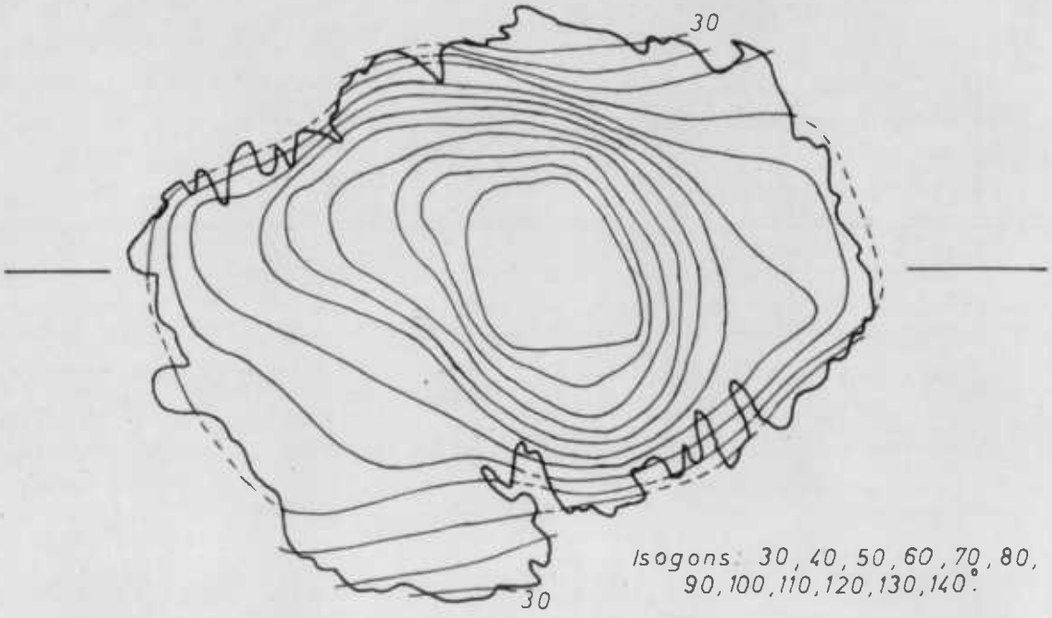

(b)

Fig. 5·4 Isogon patterns for garnet sections GI,(a), and GII,(b), Spec.110.

(c) GI and GII Spec.110.
Note the angular discordance between the internal and external foliation at the crystal margin in the pressure shadow region and the concordance elsewhere. (x10).

section approximates to a circle the isogons of GI and GII are very poor approximations. If the isogons are interpreted in this way then growth appears to have been extremely irregular. There is evidence of irregular growth of these crystals; the internal and external foliations are not everywhere in continuity with angular concordance at the crystal margins, so it appears that growth terminated prematurely in the discordant regions (Fig. 5.4c).

Fig. 5.5a illustrates the isogon pattern of a euhedral crystal (Fig. 5.5b), (GI Spec. 129) which has been rotated by 80-90 degrees. Although the final shape of the crystal is regular the isogons tend to be elliptical rather than circular, the long axis of the ellipse lying at a high angle to the inclusion trails and rotating in successive isogons in an opposite sense to the crystal. The same effect can be seen in Figs. 5.4a and 5.4b and has been found to be the general rule in other examples. The outer isogons of Fig. 5.5a cut across the crystal boundary. This situation can arise in two ways:-

(a) by irregular growth at the margin of the crystal.

(b) by the inclusion of external foliation which is not everywhere parallel.

If case (a) occurs, then there must be an angular discordance of the internal and external foliations at that part of the margin of the crystal where growth has been terminated, whereas in case (b) the internal and external foliations will be everywhere concordant at the margin. Reference to Fig. 5.5b shows the latter interpretation to be applicable to GI Spec. 129. In GI and GII Spec. 110 (Fig. 5.4c) a mixture of these two effects appears to be involved.

The proposed model assumed that during growth the included foliation was everywhere parallel. This situation is not realised in nature and the schistosity surrounding the crystal is of variable attitude because a zone of inhomogeneous or contact strain exists around the crystal. It will be shown (Section 5.6) how the inclusion of external foliation affected by contact strain can explain the observed isogon geometry.

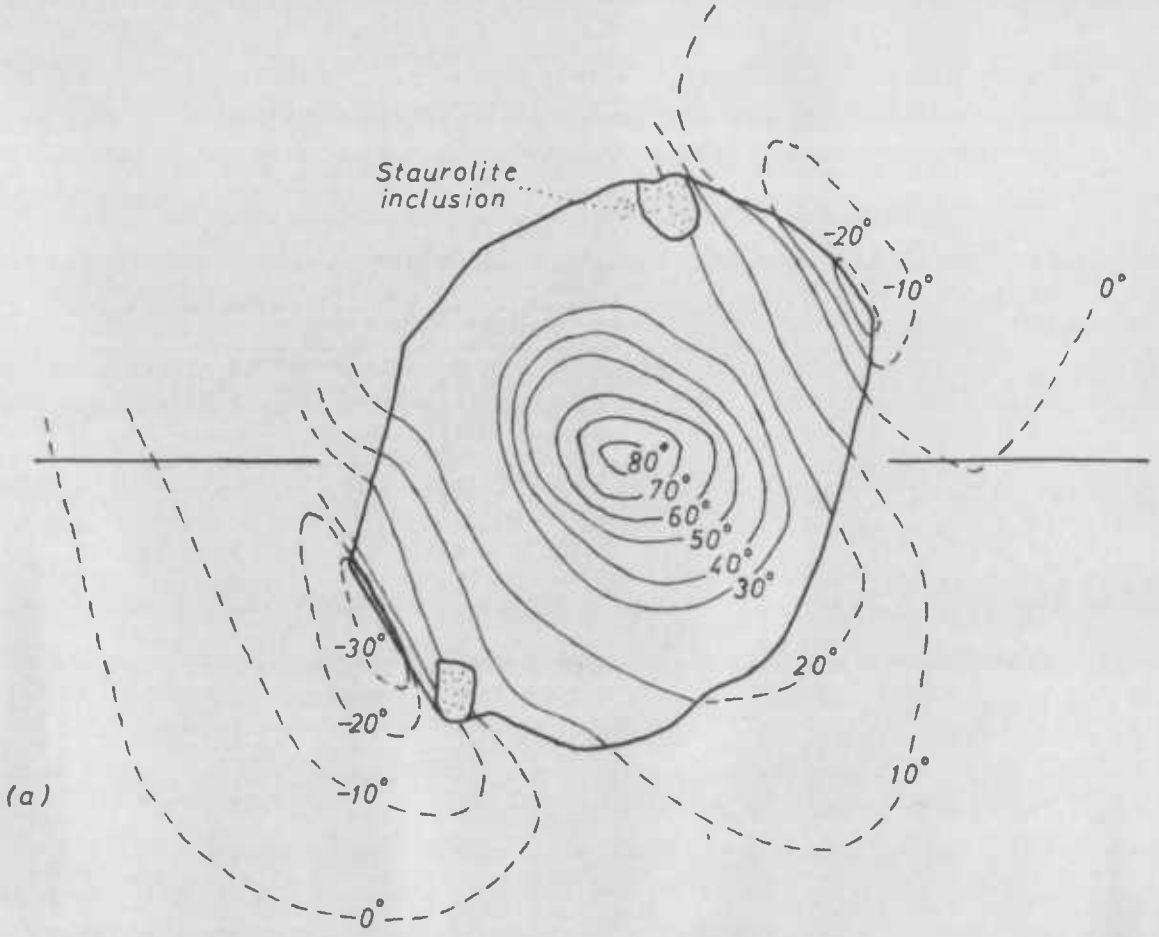

(b)

Fig. 5·5 (a) Isogon pattern for garnet section GI Spec.129. (b) GI Spec.129. Note the concordance of internal and external foliation at the crystal margin and the absence of pressure shadows. (x5).

5.52) The serial sections of single crystals from Spec. 136B (Figs. 5.6a and b) show how the attitude of the inclusion trails varies, in the plane perpendicular to the rotation axis, as the crystal is traversed. Figs. 5.6 a and b are the corresponding isogon plots. The isogon patterns in individual sections have the same characteristics as those described in Section 5.51 and as such do not require further discussion.

The model predicted that the maximum rotation shown by the inclusion trails, in sections perpendicular to the rotation axis, would change on passing through the crystal, varying from a minimum, zero, at the margins of the crystal to a maximum at the centre. Figs. 5.6a and b and 5.7a and b illustrate a comparable change, in maximum rotation angle, however the angle has a minimum finite value at the margin of the crystal. This finite rotation at the crystal margin may be shown to be caused by the zone of contact strain surrounding the crystal. Sections just beyond the crystal margin show a distortion of the external foliation, which has the same sense as the rotation of the crystal, indicating that the matrix has strained inhomogeneously. Somewhat further from the margin the external foliation resumes the attitude of the mean external foliation and the strain is assumed to be once more homogeneous.

It appears therefore, that the model proposed in Section 5.4 is inadequate to explain the geometry of the inclusion trails, and that a model which makes some allowance for a region of inhomogeous or contact strain, in the matrix surrouding the growing crystal, would perhaps be more applicable. A model of this type is not unreasonable in the light of the obvious ductility contrast which exists between the crystal and the matrix.

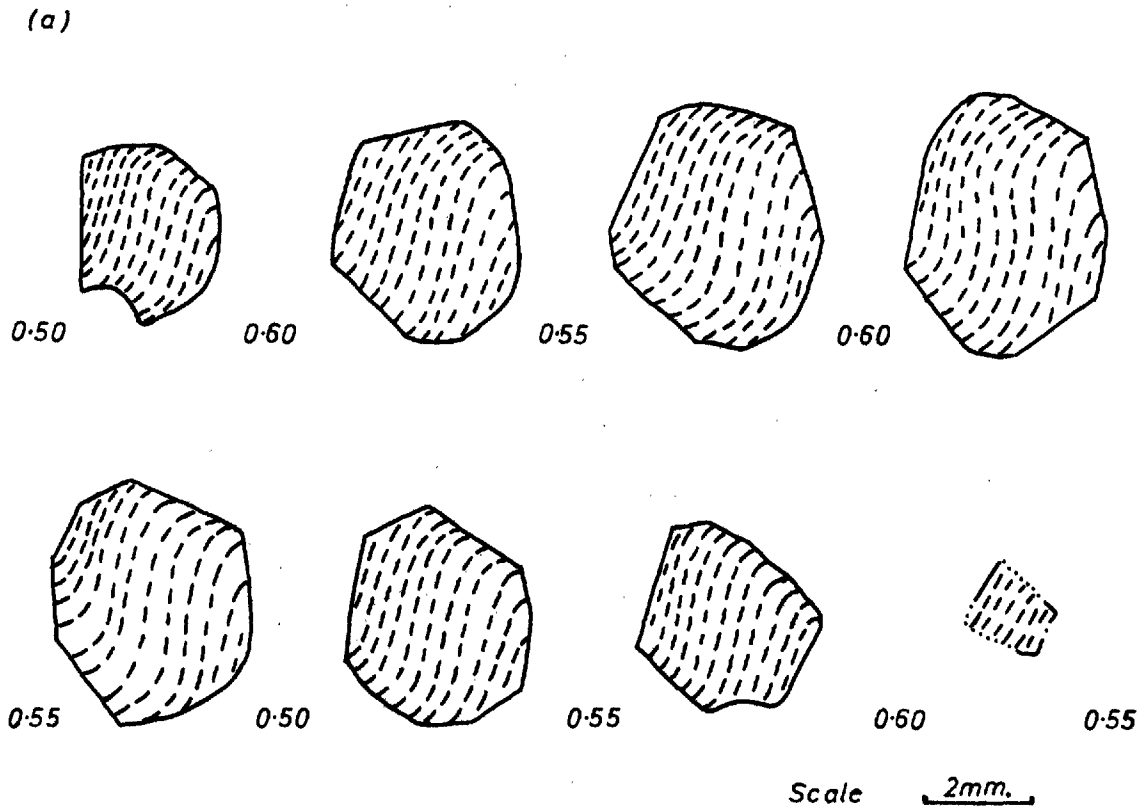

0·50 etc. = distance (mm.) between serial sections.

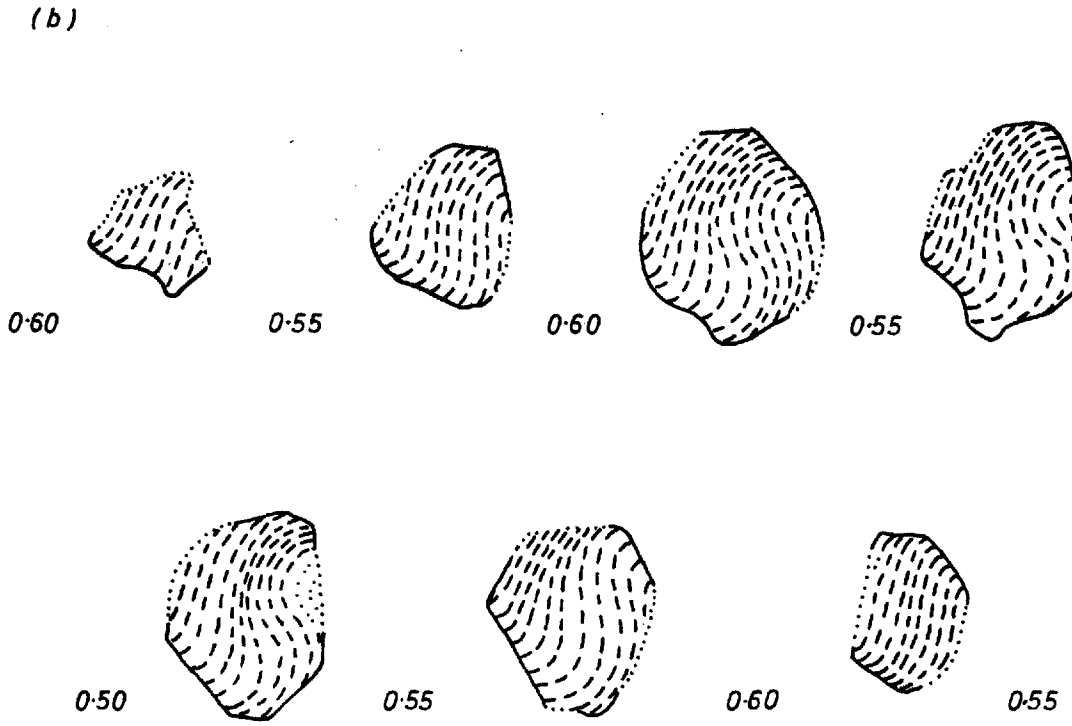

Fig. 5·6 Inclusion trails in serial sections of two garnets, (Spec. 136B).

(a)

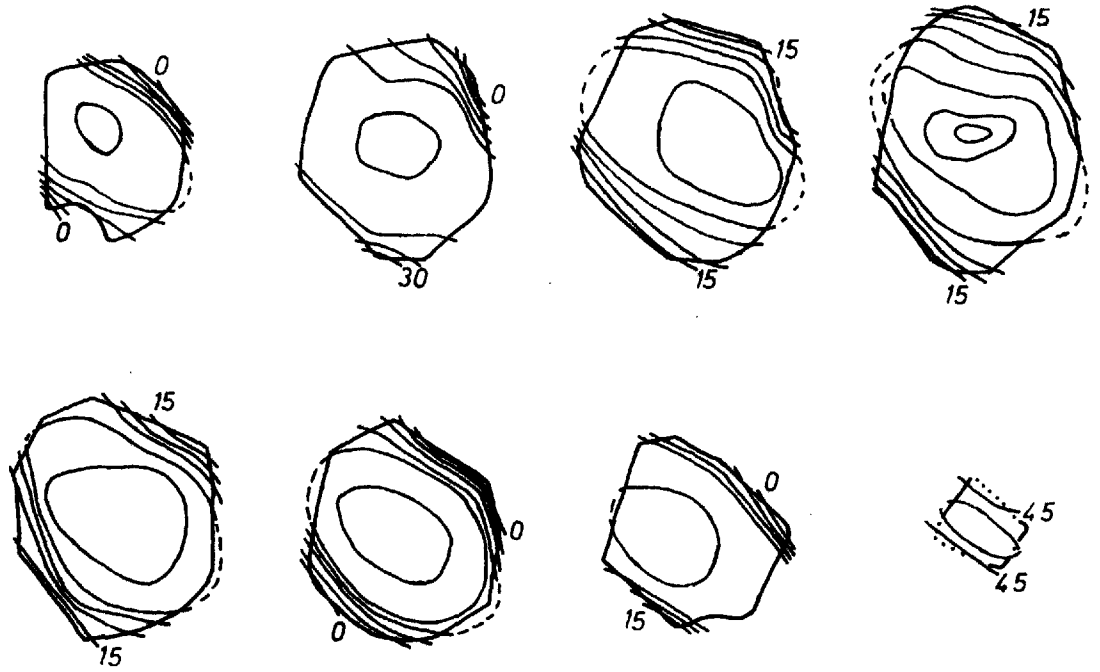

Isogons: 0, 15, 30, 45, 60, 75, 90, 105°. Scale 2mm.

(b)

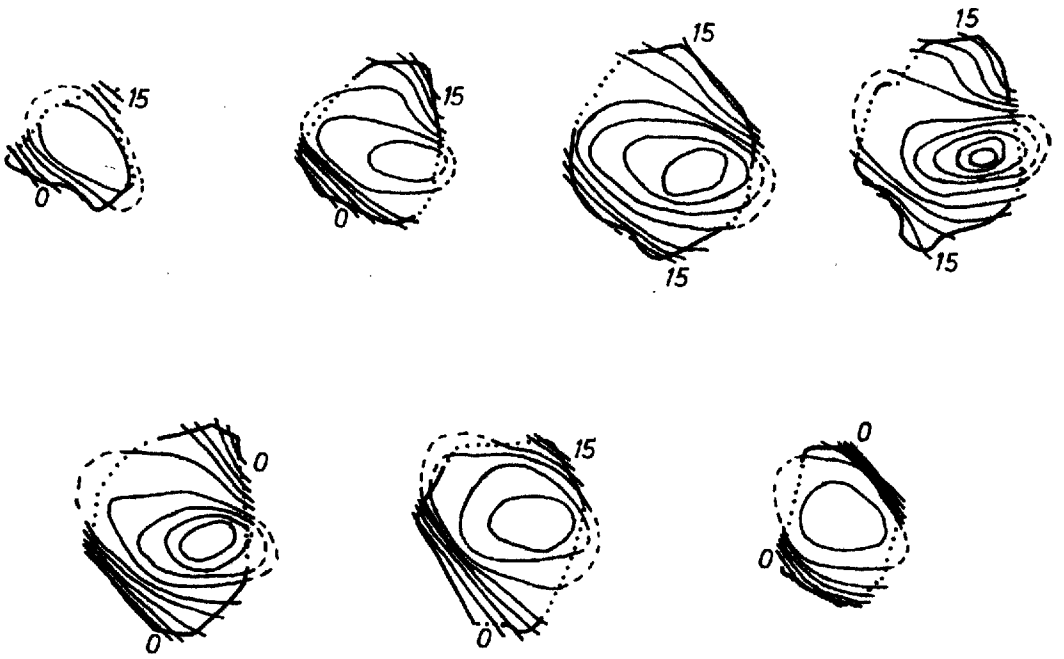

Isogons: 0, 15, 30, 45, 60, 75, 90, 105, 120, 135°.

Fig. 5·7 Isogon patterns for garnet serial sections in Fig. 5·6

5.6) A revised model

As in the previous model the garnet crystals are represented by rigid spheres, contained in a homogeneously deforming matrix, which grow and rotate successively by a series of equal incremental amounts. The growth law of the crystals is then linear. The strain mechanism causing the rotation is assumed to be simple shear, operating in such a way that the slip plane is parallel to the external foliation. The two planes of no strain will then be the slip plane and the plane at right angles to it, so that a number of equally spaced marker horizons parallel to the foliation in the homogeneously deforming matrix will always remain the same distance apart during deformation. In the neighbourhood of the rotating spheres the matrix deformation will no longer be homogeneous and it is in this respect that this model differs from the previous one. The effect of the inhomogeneously strained matrix on the geometry of the inclusion trails may be determined by examining a section perpendicular to the rotation axis through the centre of the sphere. Within this section the field of inhomogeneous or contact strain will be of finite extent. For the purposes of the model it may be delimited at each stage during the growth and rotation as a rectangle, of side 4r parallel and 3r perpendicular to the slip plane, centred on the circular section (r = radius of section). The choice of these values which is somewhat arbitrary arises from the observation of distortion around rotated garnet crystals. The values are however of a similar order to those observed (Gay, 1966, p. 144) for a rigid disc, contained by a viscous medium, rotating in a simple shear field. It is apparent that at the margin of the rotating section a displacement of the marker horizons within the plane of the section will take place. By joining the displaced positions of the marker horizons at the margin of the section to their undisplaced positions in the homogeneously strained matrix an approximate representation of the field of contact strain, after each increment of rotation, is obtained. Each subsequent growth increment will then include a portion of the matrix in which this contact strain is recorded by the marker horizons and in this way the internal geometry is determined.

Fig. 5.8 shows the internal geometry of a section, after a total rotation of 60 degrees, which has been built up by this method. The field of contaot strain is demonstrated by the attitude of the deformed marker horizons. The isogon pattern constructed on the section shows that the isogons are elliptical, that the long axis of the ellipse rotates in successive isogons in an opposite sense to the rotation of the section and that the outermost isogons cut across the section margin. All these features have been observed in the isogon patterns of garnet crystals. It is also apparent that the isogons do not coincide with successive outlines of the section at stages during its growth. Thus the determination of the growth law from the isogons using Spry's (1963, pp. 216-220) method is invalid.

Perhaps the most interesting feature of this model is that it predicts the positions of the pressure shadows that are often found accompanying rotated garnet crystals. It can be seen from Fig. 5.8 that the spacing of the marker horizons at the margin of the section is not equal. The regions of close spacing correspond to that part of the margin where the shear strain exerted on the matrix by the rotating section is additive to the simple shear deformation of the matrix and those of open spacing to where the strains are subtractive. Thus there are regions of high and low finite strain.

Although the matrix may be regarded on a sufficiently large scale as homogeneous in composition, it is infact a polymineralic, multi-component system. The response of individual minerals and chemical components to the processes of solution, diffusion and crystallisation which must take place during deformation will be different. The appearance in the regions of low finite strain, of quartz rich pressure shadows indicates that the solution of quartz and migration of silica to these regions occurs more readily than for the remainder of the matrix. This process is analogous to that involved in the formation of strain slip cleavage (Nicholson, 1966). In this way an inhomogeneous distribution of components may arise at the margin of the crystal, the garnet forming components being preferentially concentrated in the regions of high finite strain, so that here the growth

Fig. 5.8. Inclusion trail geometry resulting from the revised theoretical model of snowball garnet formation described in Section 5.6. Rotation is caused by a simple shear deformation (crystal rotates). In the construction of the model the field of contact strain at each stage in the growth and rotation was delimited as a rectangle, of side 4r parallel and 3r perpendicular to the slip plane, centred on the circular section (xxxx denotes the limits of the field of contact strain after the last increment of rotation). Increments of rotation = 10 degrees, Θ_{max} = 60 degrees.

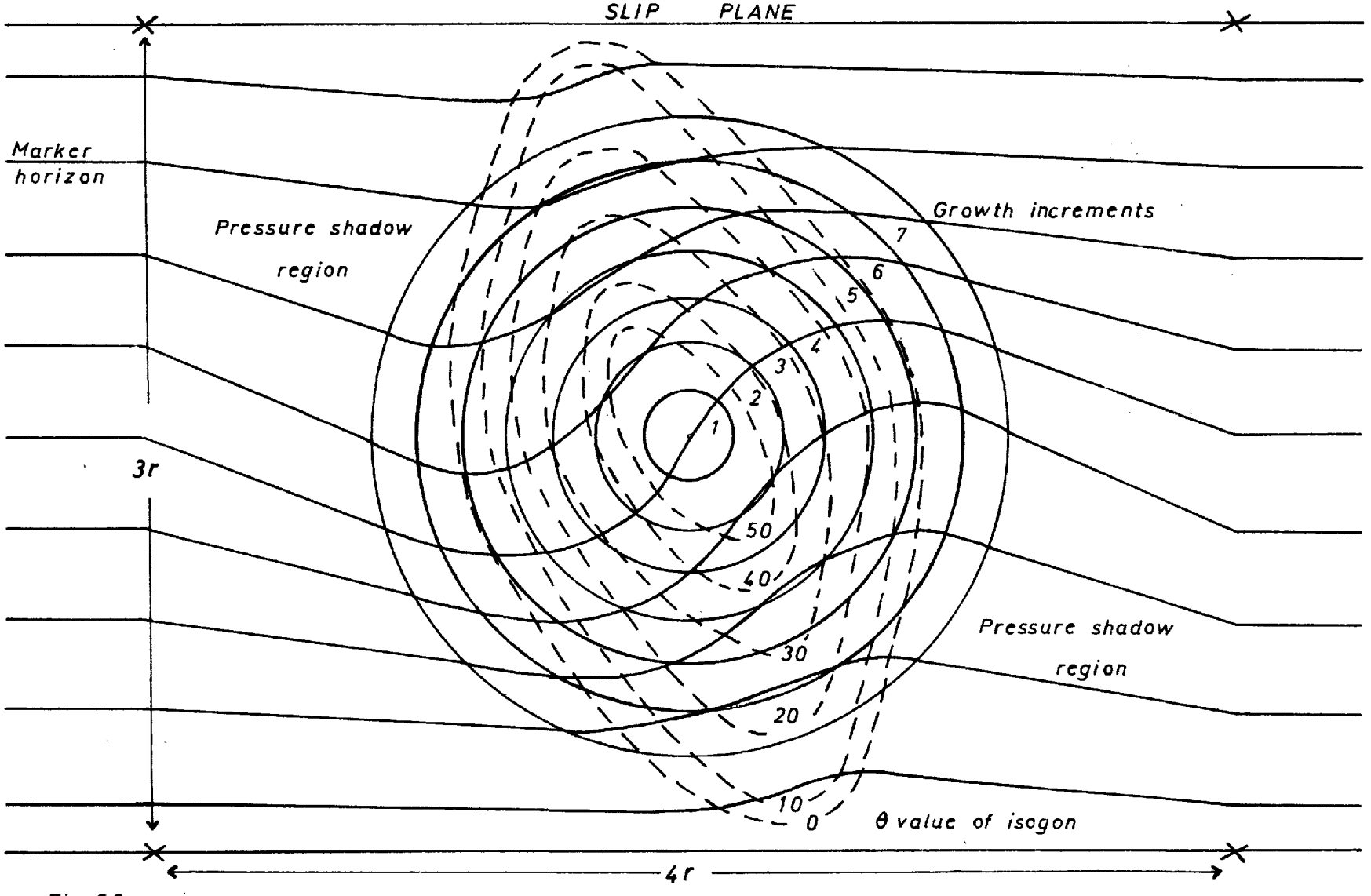
SLIP PLANE
Marker horizon
Pressure shadow region
Growth increments
7
6
5
4
3
2
1
3r
50
40
30
20
10
0
θ value of isogon
Pressure shadow region
4r

Fig. 5·8

of the crystal is enhanced, and in the region of the pressure shadow reduced or even terminated. Reference to Fig. 5.4c (GI and GII Spec. 110) and the corresponding isogon plots Figs. 5.4a and b illustrates this argument. The asymmetric distribution of the pressure shadow regions with respect to the external foliation of the model corresponds to that observed round rotated crystals.

The model is based on a number of assumptions previously listed in the discussion. It seems reasonable to represent the crystals as growing rigid spheres in a homogeneously deforming matrix and so to expect about them a field of inhomogeneous strain. Any assumptions as to the form and limits of this field, the growth law and the mechanism of strain causing rotation are subject to greater uncertainty. In view of this, the geometrical effect of changing the growth law has been examined and, using the same sort of technique as described above, the geometry of the inclusion trails of a sphere growing in a pure shear field, in the fashion discussed by Ramsay (1962a), investigated (Fig. 5.9).

Neither of these further investigations affect the conclusion drawn earlier, namely that in a model that takes into account contact strain, the isogons are elliptical and as such cannot be used to determine the growth law of the crystal. Nor do they predict a different orientation for the pressure shadow regions.

Throughout this analysis emphasis has been placed on the three dimensional nature of the problem. The model only considers a two dimensional section through the centre of the crystal, however, appreciation of the contact strain effect leads to the conclusion that a section cut perpendicular to the rotation axis at the margin of the crystal will show a finite rotation, a fact noted in the serial grinding of individual crystals.

In summary, a model has been suggested, which explains some of the features of internal geometry of the analysed garnet crystals. The model is not unique in that changes of strain mechanism and growth law do not lead to different results within the limits of the analysis.

Fig. 5.9. As Fig. 5.8. Rotation is caused by a pure shear deformation (matrix rotates). Initial and final orientations of the external foliation marker horizons and the orientation of the plane of flattening are indicated. The field of contact strain was delimited as a rectangle, of side 4r parallel and 3r perpendicular to the external foliation, centred on the circular section at each stage in the growth and rotation. (xxxx denotes the field of contact strain after the last increment of flattening). Increments of flattening = 20% (total flattening $\simeq$ 75%), Θ_{max} = 59 degrees.

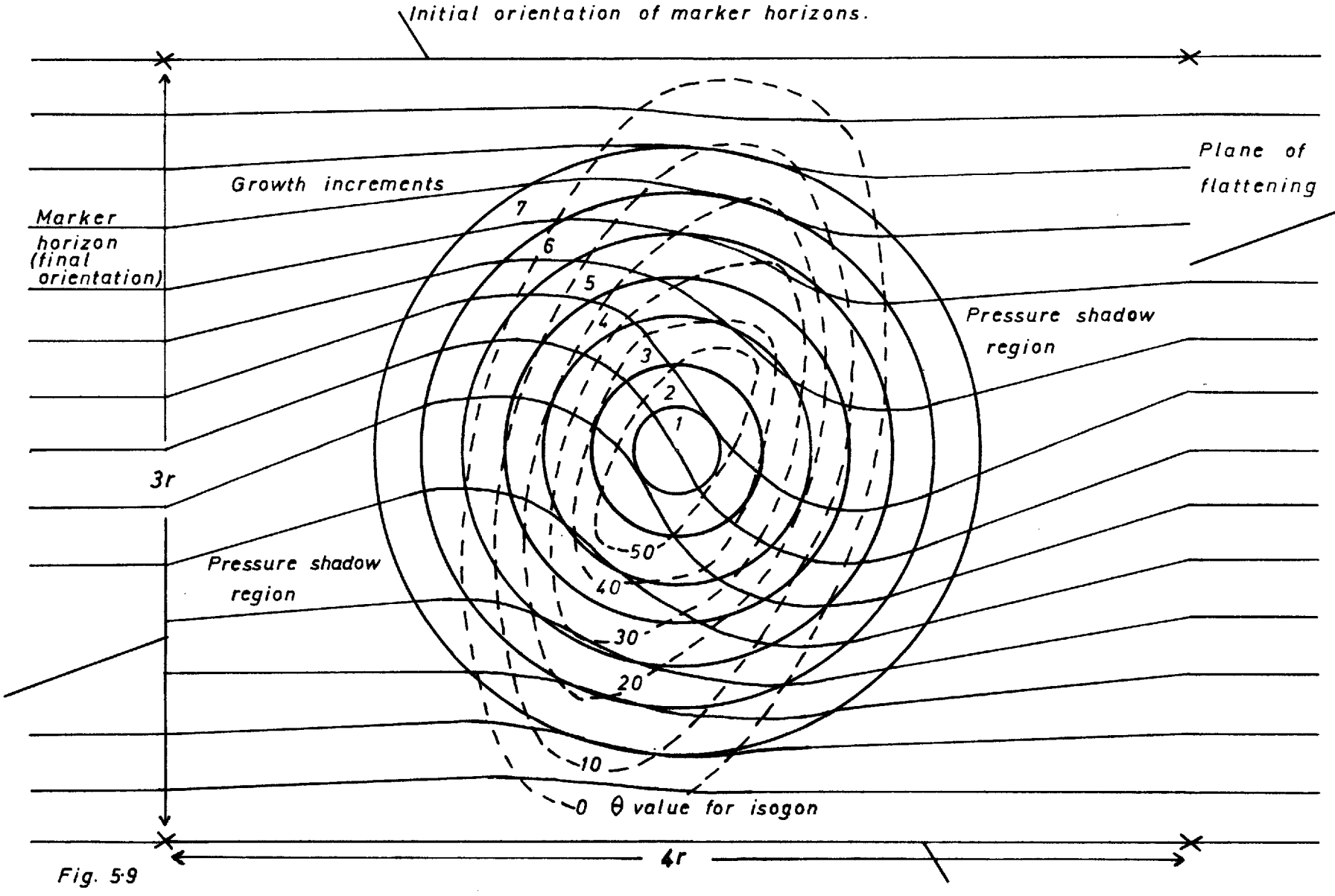
Initial orientation of marker horizons.
Growth increments
Marker horizon (final orientation)
Plane of flattening
Pressure shadow region
Pressure shadow region
7
6
5
4
3
2
1
50
40
30
20
10
0
θ value for isogon
3r
4r

Fig. 5·9

5.7) The distribution of rotation angles

The significance of the maximum rotation angle in recording the amount of strain a crystal has undergone has been discussed by many authors and is considered further (Section 5.8). Serial grinding techniques enable this angle to be measured approximately. A question which naturally presents itself is whether crystals from the same specimen show the same maximum rotation. In order to answer this question two large specimens, 136A and 136B were serially ground and the maximum rotation angles and sizes (maximum and minimum diameters of central section) of a large number of crystals recorded from each of these specimens. The analytical method has been discussed in Section 5.3. A variation in maximum rotation angle was observed as well as a distribution in the sizes of the crystals.

In attempting to explain this variation the possible processes of nucleation and growth of the crystals must be considered. Kretz (1966b) has reviewed various nucleation models for metamorphic minerals, and has suggested that the most realistic of these is a model which considers the crystals to have a time dependent nucleation rate, but a growth rate which is identical for each crystal provided the system is homogeneous. In chapters 6 and 7 the concepts of nucleation and mineral growth will be examined in greater detail. If this model is realised in these rocks, provided that all the crystals nucleated during the period of deformation, a variation in size and rotation is to be expected. However, as both the size and degree of rotation are parameters dependent on time there should also be a relationship between them.

Figs.5.10a and b show the data obtained in determining these parameters for the crystals of Specs.136A and 136B respectively. The size parameter is the mean diameter of the section containing the maximum observed rotation angle and a measure of the degree of ellipticity of this section is indicated by plotting the ratio of maximum and minimum diameter symbolically. The predicted dependence is poorly illustrated by the data, however it is suggested that a dependence

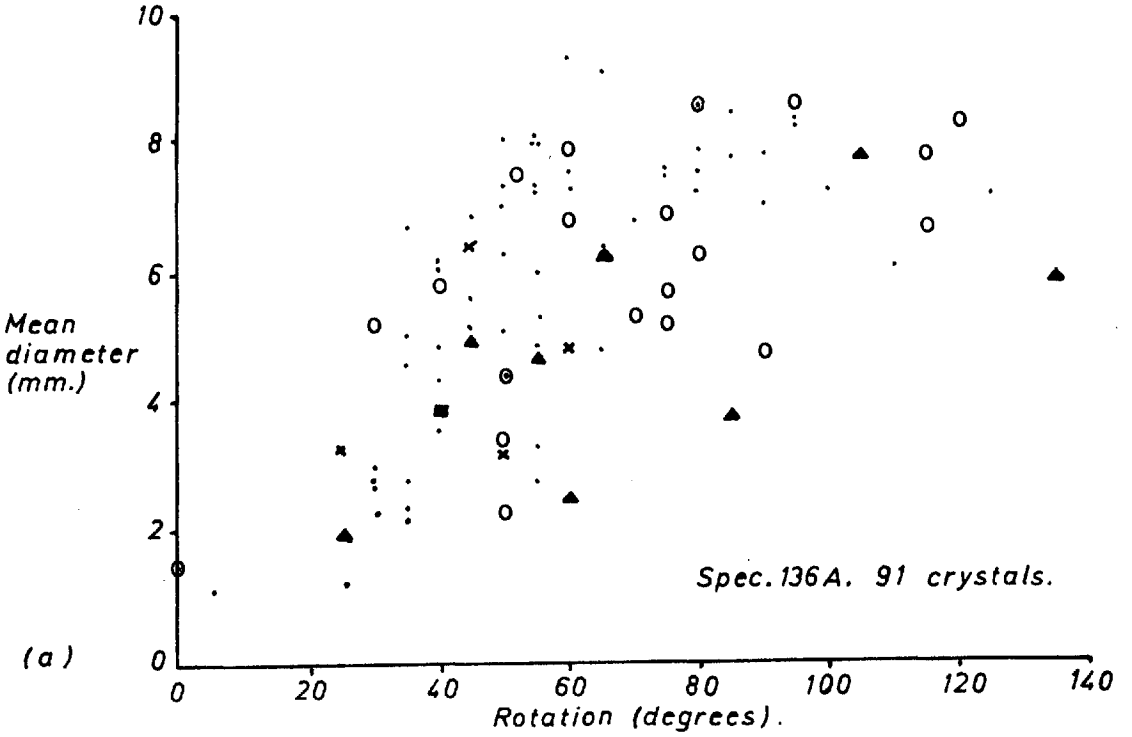

Axial ratios, (•) 1·00–1·25, (o) 1·25–1·50, (▲) 1·50–1·75, (■) 1·75–2·00, (×) > 2·00.

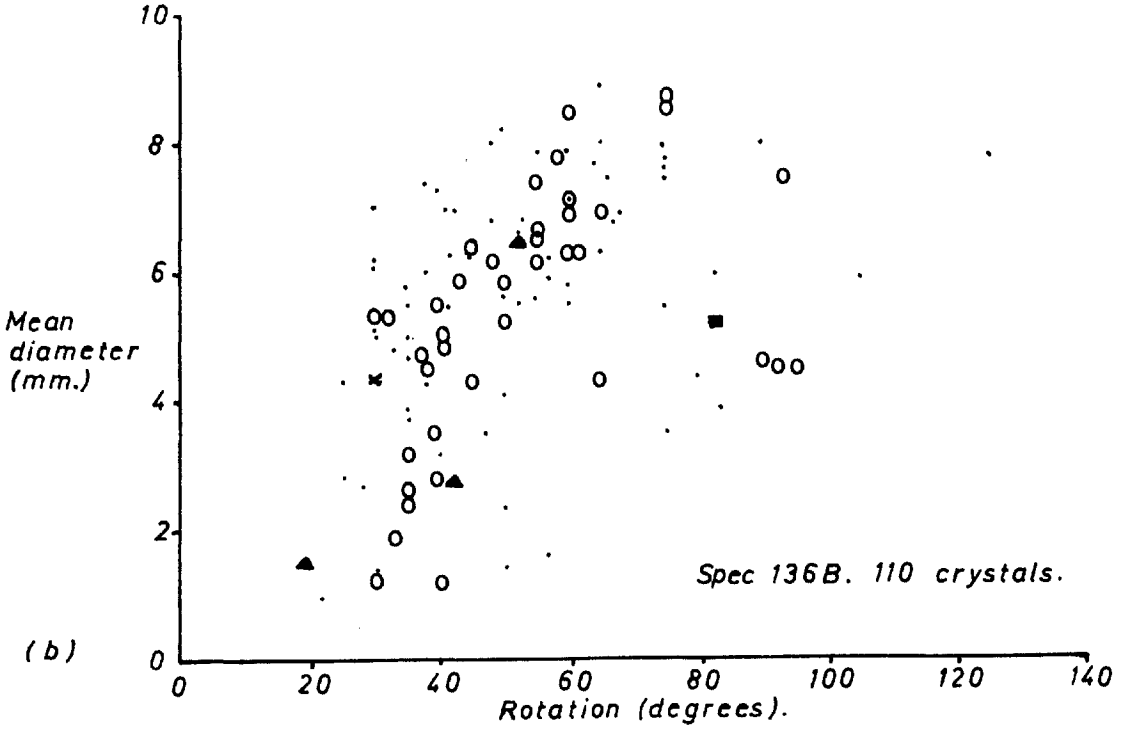

Fig. 5·10 Size / maximum rotation angle ($\theta_{max.}$) data for garnet crystals in Specs. 136A and B.

does exist as the data does fall in a field and not completely randomly. The extent of this field is nearly identical in both specimens, which were collected from the same locality and garnet schist horizon, supporting the conclusion that the shapes of these fields is significant.

Possible factors affecting the relationship between size and rotation are crystal shape, inhomogeneous growth and inhomogeneous strain. The first of these factors has been considered in the measurement of the axial ratio. If the crystals behave in the same way as particles rotating in a simple shear field, then the amount of shear γ_s required to produce a given rotation depends on the shape of the particle and is greater for an ellipsoidal particle than for a sphere (Gay, 1966) (Section 5.8, Equations 5.6 and 5.7). The data however fails to show the expected relationship, namely that for particles of the same mean size more elliptical sections show smaller rotation angles. The extent which the other two factors listed above play in affecting the amount of rotation is indeterminate.

The general conclusion, that there is a dependence of rotation on size, implies that the crystals did not all nucleate simultaneously and thus the quantitative determination of strain from any crystal is merely a measure of the deformation that has occurred since nucleation of the crystal took place, an unknown event in time.

In any given specimen showing rotated crystals it should however be possible, if sufficient crystals are measured, to obtain a figure for the maximum rotation that any crystal in the specimen has undergone. The comparison of this figure with that from another rock and the deduction on this basis that one rock has suffered a greater, lesser or equal strain is not justified as crystal nucleation is unlikely to have commenced simultaneously in both rocks.

The occurrence in Val Piora of garnet schist horizons in close proximity showing strongly rotated and unrotated crystals may not then be interpreted as a strain discontinuity, but is a reflection of the different times at which garnet growth commenced in these rocks. The value of synkinematic or snowball garnets as a quantitative measure of strain must then be strictly limited.

5.8) The determination of strain and strain mechanism

A method of determining strain from rotated garnet crystals was first presented by Schmidt (1918, pp. 300-302). He considered initially the rotation of pretectonic crystals, and drew the analogy of a ball in a ball-bearing. Schmidt's model, figured by Spry (1963, Fig. 3), assumes the crystals to be rigid spheres rotated by a simple shear strain mechanism, in which the slip plane is oriented parallel to the external foliation. The amount of slip occurring at the crystal margin is given by the equation:

$$S = 2r\Theta \qquad (5.4)$$

and the unit shear γ_s is therefore:

$$\gamma_s = \Theta \qquad (5.5)$$

where S = slip, r = radius of crystal and Θ = rotation angle measured in radians.

Schmidt (1918, pp. 302-303) points out that if growth and rotation are contemporaneous, which is the more common case in nature and is the case considered above, the same formula can be applied. Spry (1963, p. 220) however states incorrectly, that the Schmidt formula may not be applied to syntectonic or snowball garnets and that the amount of slip which occurs at the crystal margin is given by twice the length of the 'point of contact spiral'. As the calculation of this length is dependent on the growth law, the determination of which has been shown (Section 5.6) to be based on unsound principles, this concept can hardly be considered to be viable. Furthermore the formula for the length of the point of contact spiral is irrelevant in terms of the unit shear, the quantity which is of interest in the analysis of simple shear strain. In addition it has been shown by Gay (1966, Table V) that Spry (1963, p. 220) in comparing the slip calculated by his method with that derived by applying the Schmidt formula, has miscalculated in the latter case by a factor of two, and his conclusion that his formula gives a greater value of strain is therefore wrong.

Various authors who have used the Schmidt formula to estimate amounts of strain have emphasised the minimal nature of this estimate, as factors such as slip at the margin of the crystal will tend to retard the rotation. A model which largely overcomes this problem is the viscous model proposed by Gay (1966, p. 150). This model assumes the crystals to be rigid particles contained by a viscous fluid and has the additional advantage of taking into account non-spherical particles. Equations of motion of ellipsoidal particles immersed in a viscous fluid have been derived by Jeffrey (1922) and are discussed in detail by Gay (1966). The equations are approximated to fit a system with sufficiently slow motions or sufficiently small particles and assume that the motion of the fluid varies in space on a scale much larger than the particle dimensions. They thus appear to be applicable to the geological situation. The equations have been found to be impossible to solve for the general case of undisturbed motion but for the cases of simple shear (Jeffrey, 1922) and pure shear (Gay, 1968) solutions have been derived. The equations below apply to a two dimensional elliptical particle or an ellipsoidal particle oriented with one of the particle axes parallel to the intermediate strain axis.

The equation describing the particle rotation in a simple shear field is:

$$\tan\Theta_f = \tan\Theta_i + \frac{a}{b}\tan\left[\frac{ab\,\gamma_s}{(a^2 + b^2)}\right] \qquad (5.6)$$

where Θ_i and Θ_f are the initial and final angles between the minor axis of the particle and the slip plane and a and b are the semi-axial lengths of the major and minor axes of the particle.

In the case of circle or sphere ($a = b = 1$) the equation reduces to:

$$\gamma_s = 2\theta \qquad (5.7)$$

Thus for a given rotation this formula gives a value of γ_s twice that determined using Schmidt's formula.

In a pure shear field the equation becomes:

$$\ln \cot \Theta_f = \ln \cot \Theta_i + \left[\frac{(a^2 - b^2)}{(a^2 + b^2)}\right] \ln \sqrt{\frac{\lambda_2}{\lambda_1}} \qquad (5.8)$$

where Θ_i and Θ_f are the initial and final angles between the major axis of the particle and direction of shortening, $\sqrt{\lambda_1}, \sqrt{\lambda_2}$ are the major and minor semi-axial lengths of the strain ellipse.

In the case of a circle or sphere ($a = b = 1$) the equation reduces to:

$$\Theta_f = \Theta_i \qquad (5.9)$$

i.e. there is no rotation. It should also be noticed that in Equation 5.8 rotation cannot exceed 90 degrees.

An explanation for the apparent rotation of circular spherical particles in a pure shear field has been suggested by Ramsay (1962a). It has been shown above that because the particles are circular they do not rotate, but planar features in the matrix which are initially oblique to the principle strain axes will rotate passively during deformation giving rise to helicitic inclusion trails in growing crystals. The strain may be determined from the angular rotation of the matrix using Wettstein's (1886, p. 33) formula:

$$\tan \Theta_f = \tan \Theta_i \sqrt{\frac{\lambda_1}{\lambda_2}} \qquad (5.10)$$

where Θ_i and Θ_f are the initial and final angles between the planar features and the direction of extension. The application of this equation requires that the orientation of the principal strain axes be known. It should be noted that once again rotation cannot exceed 90 degrees.

Quantitative determination of strain from natural material may be carried out by making the relevant measurements and substituting in the above formulae, but in order to do this the strain mechanism must also be known. It has been shown that in pure shear rotations of greater than 90 degrees cannot be obtained and hence simple shear might seem to be a more probable natural strain mechanism. It must be emphasised that simple shear is a very specialised form of rotational strain and that any general rotational strain can give rise to rotations of greater than 90 degrees. The use of the above formulae therefore has severe limitations.

CHAPTER VI

HORNBLENDE GARBENSCHIEFER

6.1) Introduction

The investigation of certain microstructures in metamorphic rocks, (i.e. grain size, grain shape, etc.) has until recently (e.g. Voll, 1960, 1961; Kretz, 1966a and b; Vernon, 1968) received little attention from metamorphic petrologists. Metallurgists on the other hand, have gathered a wealth of information about these microstructures and the factors influencing them. The role of interfacial energy or interfacial tension is recognised to be of particular importance. The well known equilibrium microstructure in annealed single phase metals, equidimensional polygonal grains with planar interfaces subtending angles of 120 degrees, is due to the balance of interfacial tension at the junction of three interfaces and provides an example of how this energy determines grain geometry. Verhoogen (1948), De Vore (1959) and more recently McLean (1965) have all emphasised the dependence on interfacial energy of many processes occurring in the metamorphism of rocks. McLean discusses how this dependence is enhanced in cases where the driving energy for a reaction is low. This point can perhaps be clarified. The crystallisation of a phase from solution may be induced by cooling. The driving energy for crystallisation is dependent on the amount to which the phase has been cooled below its equilibrium crystallisation temperature.

In geological metamorphism rates of change of temperature, pressure and other physical parameters are slow and most phase changes takes place near to equilibrium and therefore under conditions of low driving free energy. This apart, the free energy changes involved in many metamorphic reactions are small.

In this chapter the concept of interfacial energy and the dependence of nucleation upon this energy is considered. It is shown how under certain circumstances the interfacial energy of a nucleating phase may be reduced and how a preferred orientation can arise as a consequence of this. Using these concepts a possible explanation of the origin of hornblende garbenschiefer or hornblende garben is put forward.

6.2) Interfacial energy

The energy of a particle at a surface or interface of a liquid or solid differs from that of a particle within the bulk material. For instance a particle at a free surface of a liquid or solid has no neighbours on one side and its energy is higher than that of an internal particle by approximately its missing share of bond energy, (bond energies are negative). The surface free energy may be defined:

$$F_s = E_s - TS_s \qquad (6.1)$$

F_s = surface free energy/unit area
E_s = surface energy/unit area
S_s = surface entropy/unit area
T = temperature.

6.21) Interfacial energy and interfacial tension

The surface or interfacial tension is defined (e.g. Mullins, 1962) as the reversible work required to create a unit area of new surface at constant temperature, volume and chemical potentials:

$$\gamma = \frac{dW}{dA} \qquad (6.2)$$

The relation to the surface free energy is given by the equation:

$$F_s = \gamma + \sum \mu_i \Gamma_i \qquad (6.3)$$

where μ_i = chemical potential of component i.
Γ = adsorption of component i/unit area of the surface.

The difference between surface free energy and surface tension is small and in the case of a one component system vanishes. This subject has been discussed in detail by Turner and Verhoogen (1960, pp. 460-465), Mullins (1962), Defay et al (1966) and Spry (1969).

6.22) Interfacial energy and crystal faces

It is well known that the energy of a plane surface will in general depend on the crystallographic orientation of the surface, other factors remaining constant (Turner and Verhoogen, 1960, pp. 595-596). It can be simply shown that the density of the atomic packing of a surface will affect the magnitude of the surface energy. As the energy is a function of the work required to create a unit of new surface, a close

packed surface will have a lower energy than an open packed surface as less atomic bonds are broken in the formation of new surface. The tendency for crystal faces to develop reflects this variation in surface energy. For example the ubiquitous development of the {001} faces of mica crystals is an indication of the anisotropy of surface energy of this mineral, whereas the tendency for quartz not to form well defined crystal faces reflects a relative isotropy of surface energy (Vernon, 1968).

6.23) The equilibrium shape of a crystal

The condition which minimises the free energy of a system is a condition of equilibrium and thus the shape of a crystal which minimises its surface free energy is its equilibrium shape. If the surface free energy is identical for all orientations, (isotropic), as is the case for a liquid, the equilibrium shape will be that which gives a maximum volume for a minimum surface area, i.e. a sphere.

In practice the equilibrium shape is seldom if ever attained in natural crystals, because of the important part played by crystal growth kinetics in determining shape (Cabrera and Coleman, 1963).

6.3) Nucleation

6.31) Homogeneous Nucleation

The dependence of the rate of nucleation on interfacial energy may be seen by considering the simplest theory of nucleation, the formation of droplets from a single component vapour. The Volmer-Weber theory of homogeneous nucleation (Holloman and Turnbull, 1953) has formed a basis for the study of nucleation in more complex systems.

The theory suggests that in a vapour statistical fluctuations occur in the density of small volumes of matter. Clusters form or dissolve by the sequential addition or subtraction of single molecules. The total free energy of any cluster is given by the equation:

$$\Delta G_T = 4\pi r^2 \gamma + \frac{4}{3}\pi r^3 \Delta G_v \qquad (6.4)(1)^{\beta}$$

where ΔG_T = total free energy
r = radius of cluster
γ = F_s = surface free energy/unit area
ΔG_v = volume free energy/unit volume.

In this equation an assumption is made in applying large scale thermodynamic properties to very small spherical clusters of atoms or molecules.

The relationship of ΔG_T to r is shown in Fig.6.1a, where it is seen that in the formation of a cluster the total free energy rises to a maximum ΔG_T^* at radius r^* and then decreases. Thus to form a stable nucleus a free energy barrier ΔG_T^* must be overcome. This barrier is given by finding the maximum values of ΔG_T in Equation 6.4:

$$\Delta G_T^* = \frac{16\pi}{3}\frac{\gamma^3}{\Delta G_v^2} \qquad (6.5)(5)$$

where the critical radius, r^*, is given by:

$$r^* = \frac{-2\gamma}{\Delta G_v} \qquad (6.6)(6)$$

The absolute frequency of nucleation/unit volume, I, may be derived by determining the number of critical nulei/unit volume, n^*, in equilibrium

$^{\beta}$ (1) refers to Holloman and Turnbull (1953, Equation 1) etc.

with vapour at given pressure, P, and temperature, T :

$$n^* = n \exp\left(-\frac{\Delta G_T^*}{KT}\right) \qquad (6.7)(8)$$

(where n = number of single molecules/unit volume)
and the collision frequency/unit area, z, of single vapour molecules with the surface of the critical nucleus. Then I is given by the equation:

$$I = z\, s^*\, n^* \qquad (6.8)(9)$$

where s^* is the surface area of the critical nucleus.
This equation is the basis of the Volmer-Weber equation for homogeneous nucleation.

The equations, as McLean (1965, p. 105) has shown, illustrate the special importance of interfacial free energy, γ, and of the driving free energy, ΔG_V, in determining the rate of nucleation, the rate being exponentially dependent on γ^3 and ΔG_V^2. As already mentioned, reactions taking place at equilibrium will give rise to minimal values for ΔG_V and hence emphasis is placed on the need for a small value for the interfacial free energy γ to aid nucleation. The interfacial free energy is lowered when heterogeneous nucleation takes place.

6.32) Heterogeneous nucleation

Most phase changes under natural conditions are heterogeneously nucleated because of the presence of foreign particles in the reacting system. The degree to which the rate of nucleation is increased depends on the nature of the interface between the foreign particle surface and the nucleating phase. The lower the interfacial energy of the interface, the lower will be the energy required for nucleation and hence the greater will be the rate of nucleation.

Heterogeneous nucleation has been discussed in many publications (e.g. Holloman and Turnbull, 1953; Hirth and Pound, 1963; Hirth and Moazed, 1967). Volmer's theory of heterogeneous nucleation (Holloman and Turnbull, 1953) investigates the conditions of formation from a vapour of a spherical liquid cap-nucleus on a solid planar substrate (Fig.6.1b). The free energy of formation of a critical size cap-nucleus

Fig. 6.1. a The free energy is shown as a function of, r, the radius of a droplet. A = surface free energy, B = volume free energy, C = total free energy. ΔG_T^* = the activation energy for the formation of a critical nucleus of radius r^*.

b The figure illustrates the equilibrium between cap-nucleus, (c), substrate, (s), and vapour, (v). Θ = the contact angle or angle of wetting. The balance of the interfacial tensions at equilibrium is given by the equation,

$$\gamma_{sv} = \gamma_{cs} + \gamma_{cv} \cos\Theta.$$

(a)

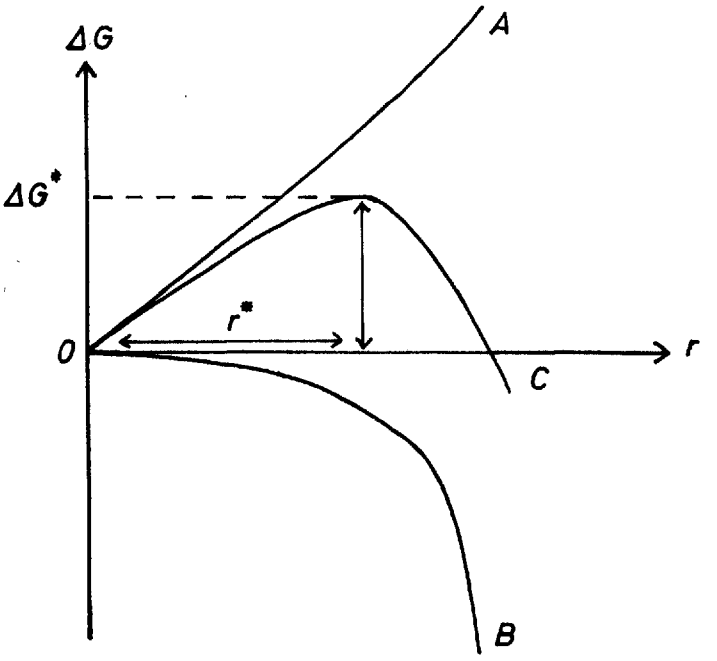

(b)

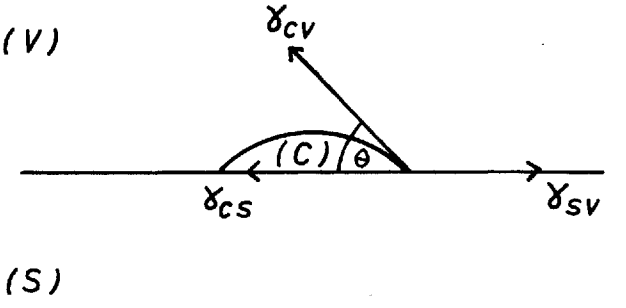

Fig. 6·1

is given by the equation:

$$\Delta G_T^* = 16\pi \frac{\gamma^3}{3\Delta G_v^2} f(\theta) \qquad (6.9)(17)$$

where $f(\theta) = \frac{1}{4}(2 + \cos\theta)(1 - \cos\theta)^2$ (6.10)

$f(\theta)$ expresses the relative values of the interfacial energies between substrate, cap-nucleus and vapour. θ is the contact angle between the cap-nucleus and substrate (Fig.6.1b) and is sometimes termed the angle of wetting. The other symbols have been defined previously.

From Equation 6.10 above it is seen that $f(\theta)$ is less than 1 for values of θ less than 180 degrees. Thus the free energy of formation of a cap-nucleus of critical size is less than that in the case of homogeneous nucleation. It is also evident that where θ is small this energy is greatly reduced and becomes zero when $\theta = 0$. Low values of θ occur when the nucleating phase wets the substrate surface (i.e. tends to spread itself along the surface). This situation can only be realised where the interfacial free energy between the nucleating phase and substrate surface is low. It is therefore pertinent to consider the nature of such low energy interfaces.

6.4) Low energy interfaces

In general for an interface to have a low energy, good atomic matching must occur between the materials on either side of the interface (McLean, 1965). If a boundary between two crystals of the same material is considered, then this condition is satisfied when there is a low angular difference between the lattice orientations of the two crystals. Chalmers (1952) has shown, for a number of metals, that the experimentally determined variation of interfacial energy is a function of angular difference between the lattices of adjacent crystals. Interfacial energy decreases rapidly when the angular difference is less than about 10 degrees (low angle boundaries), but shows in general little variation with increasing angular difference for values of greater than about 10 degrees (high angle boundaries).

The nature of the low angle boundary is well understood, for it is known that it can be considered as an array of dislocation and that the increase in interfacial energy with angular difference reflects a decrease in the dislocation spacing along the boundary.

There are however certain specific orientation relationships at high angle boundaries which give rise to low interfacial energy. These orientations are those in which the two crystals share a high proportion of atoms in the boundary plane; the most obvious of these is a twin boundary. Less obvious is the boundary which coincides with a high density atomic plane in each crystal.

Good atomic matching across interfaces is not restricted to crystals of the same material. For instance it is possible to have an interface between two crystals whose lattice parameters differ only slightly. Many cases of the oriented growth of one crystal on another, or epitaxy (Royer, 1928), are known and in these cases it is usually found that the plane of overgrowth is one across which there is good atomic matching.

The energies of such interfaces have been considered theoretically by Van der Merwe (1949, 1964). He analysed the condition in which the atomic spacing of atoms across an interface differed in one direction

only. The atomic mismatch, f, in this direction is given by:

$$f = \frac{(a - b)}{a} \qquad (6.11)$$

where a = atomic spacing in lattice A, (substrate)

b = atomic spacing in lattice B, (overgrowth).

The energy of the interface is found to be a function of the atomic mismatch; it decreases rapidly for misfits of less than about 15% but does not vary significantly for misfits of greater than about 15%. The energy/misfit curve is of the same form as the energy/angular difference relationship, between two similar lattices, discussed earlier.

An important conclusion which arises from this analysis is, that where a misfit exists, which cannot be accommodated by uniform elastic strain of the overgrowth crystal lattice, then the overall non-alignment of the atoms and hence the energy of the interface is reduced by the formation of zones of close atomic matching separated by narrow zones of atomic mismatch across the interface. The narrow zones of atomic mismatch may be interpreted as interfacial dislocations. Thus the theoretical structure of the interface is analogous to that of a low angle boundary between the lattices of two crystals of the same material.

6.5) Epitaxy

The subject of epitaxy has been reviewed by Seifert (1953), Pashley (1956, 1965) and Matthews (1967). The reviews of Pashley and Matthews are concerned with the formation and structure of oriented thin films. The techniques of thin film physics enable the actual formation, growth and coalescence of nuclei to be observed, and the theoretical and experimental conditions which favour epitaxy can be relatively well defined.

In general the surface on which deposition takes place should be at a high temperature and the rate of deposition of the new phase should be low. Under these conditions, as Cabrera (1959, p.527) points out, nucleation is a barrier to deposition and the surface energy is important in determining the orientation of nuclei, as well as the processes which occur after nucleation.

As the condition of low driving energy, which favours epitaxy in experimental systems, also exists when a new phase nucleates in geological metamorphism, it is reasonable to consider the possibility of epitaxial growth relationships between metamorphic minerals.

Chinner (1961) has suggested the epitaxial growth of sillimanite on biotite, but better documented is the case of garnet on muscovite or biotite. Frondel (1940) measured the attitudes of garnet inclusions in muscovite and found that the (110) of garnet was parallel to the (001) of muscovite in 85% of the crystals measured. It has been shown by Powell (1966), that inclusion trails within garnet porphyroblasts from regionally metamorphosed rocks lie (in some cases at least) parallel to the (110) of garnet. He suggested that this orientation relationship resulted from the epitaxial growth of the garnets on the now digested mica which lay originally with (001) in the plane of the schistosity. He further suggested that the oriented garnet inclusions in muscovite described by Frondel (1940) could be explained in a similar way.

The evidence for the epitaxial growth of garnet on mica is good. Powell has shown that the spatial arrangements of the potassium atoms in the (001) of mica and the aluminium atoms in the (110) of garnet

are very similar. Further evidence is given by Gresens (1966b) who noted that garnet inclusions in muscovite tended to be "flattened" in the (001) of muscovite. He concluded that, as the maximum area of surface contact between the garnet inclusions and the muscovite was parallel to the (001) of muscovite, the garnet-muscovite (001) interface was the interface of lowest free energy between the two crystals.

Oriented inclusions of other minerals have been found in muscovite (e.g. staurolite and zircon (Frondel, 1940) and tourmaline (Frondel, 1936)).

6.6) Hornblende garben

Bonney (1898) described the sheaf like growth forms or garben of hornblende, which are found quite commonly in the gneisses of the Tremola series along the southern margin of the Gotthard Massif. Some years later Krige (1918, pp. 557-562) examined the garben in greater detail. Observations (listed below) made, on the basis of field and thin section studies, in the present investigation agree well with Krige's, although the interpretation of them differs.

1) The rocks in which the garben occur usually contain a rather low content of hornblende, certainly less than 50% by volume and for the most part very much less. Krige gave the hornblende content as between 10% and 40% and Steiger (1962, p. 413) found the largest hornblende garben in rocks containing less than 5% hornblende. Fig. 6.2b give some idea of the concentration in a typical example.

2) The rocks have a well developed schistosity and the garben appear as fan-like arrangements of hornblende crystals on the schistosity surfaces. The angle between the outer most branches of the fan, α, is acute (Figs. 6.2a and b) and the individual branches are not always straight but may appear gently curved.

3) The garben are oriented with respect to the schistosity plane; the crystallographic a and c axes of the crystals forming the individual branches of the fan lie in or near the schistosity plane. As hornblende is monoclinic the a axis faces forward on one side but back on the other side of the c axis. It is found that the facing direction is the same for all crystals from the same garben suggesting that they developed from the same nucleus. These relationships are summarised in Fig. 6.3. There is no orientation of the long axes of the fans (i.e. the bisectors of the angle α) on the schistosity plane. This feature is well illustrated in Fig. 6.2b.

4. The axial dimensions measured parallel to the crystallographic axes of the branches of the fan always have the same relationship namely $c > b > a$; c may reach values of up to about 15 cm.

Fig. 6.2. a The figure summarises the crystallographic and dimensional relationships discussed in the text. a, b, and c are crystallographic axes. α is the angle between the outermost branches of the crystal fan.

b The appearance of garben on a schistosity surface is illustrated. Some idea of the concentration of hornblende in these garben bearing rocks can be gained. Note the random arrangement of the garben within the schistosity surface. Giubine series gneiss; Lago di Stabbio, M.R. 6975515749.

c Photomicrograph of garben forming hornblende crystals, illustrating the relationships shown in Fig. 6.2a. Section approximately at right angles to the crystal c axes. (x 35)

Fig. 6·2

(a)

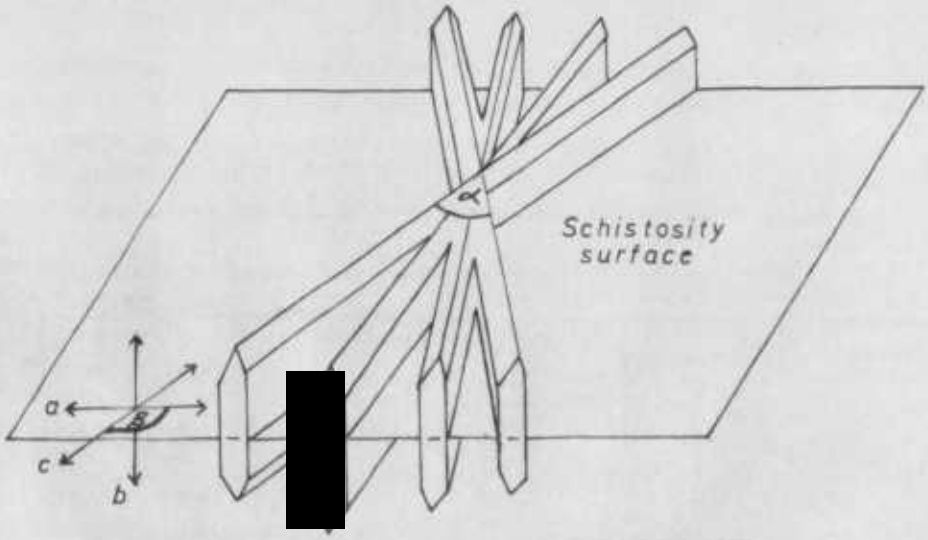

(b)

(c)

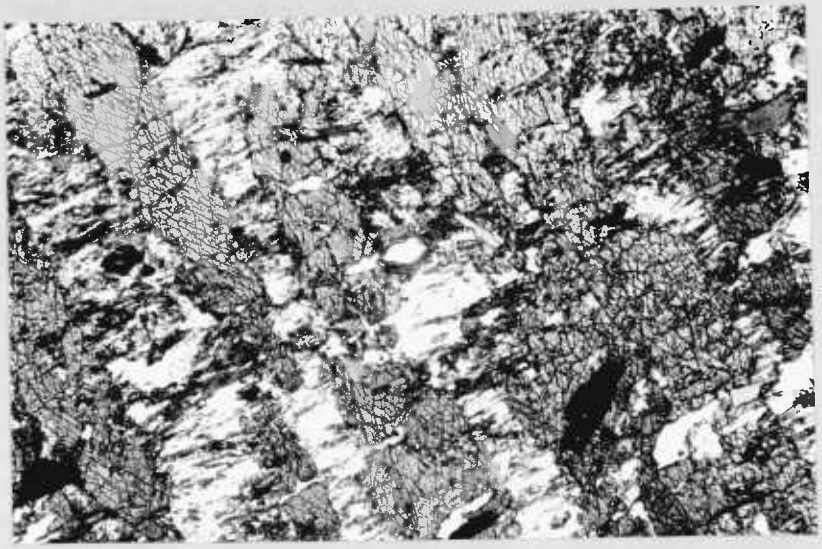

Fig. 6.3. The figure illustrates the crystallographic orientation of single garben in relation to the schistosity plane. The specimens are from two localities Nos. 1109 (M.R. 6964315658) and 1524 (M.R. 6948515618). The crystallographic a, b and c axes determined for crystals forming the branches of the same garben are plotted stereographically in relation to the schistosity plane (oriented N-S). It is readily seen, that for the six garben shown here, the a and c axes lie in or near the schistosity plane and that the facing direction of the a axis is the same for crystals from the same garben.

Spec. 1109

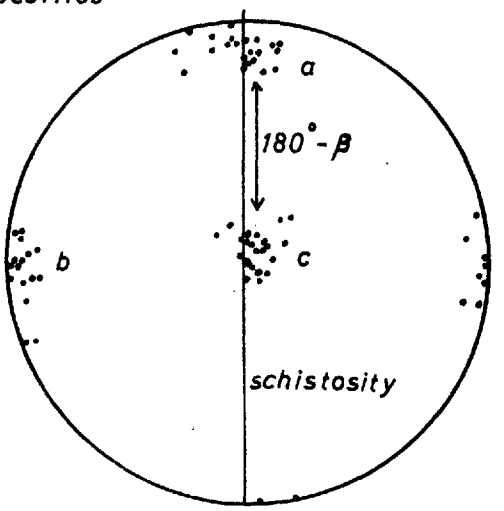

Spec. 1109A

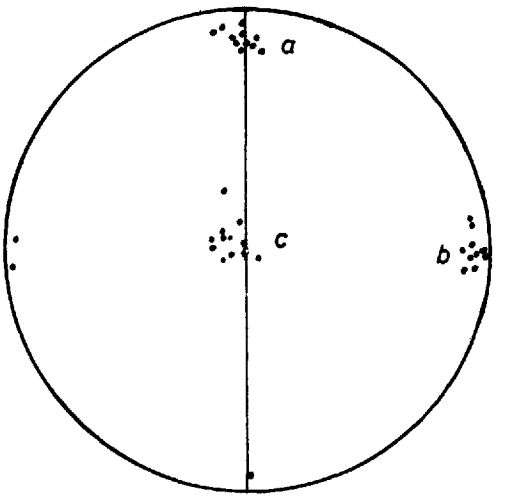

Spec 1109C

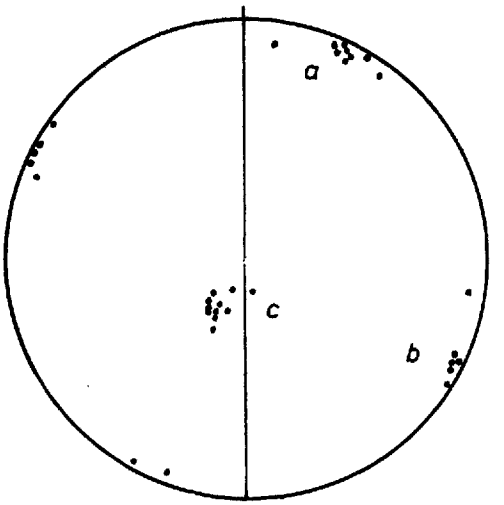

Spec 1109C

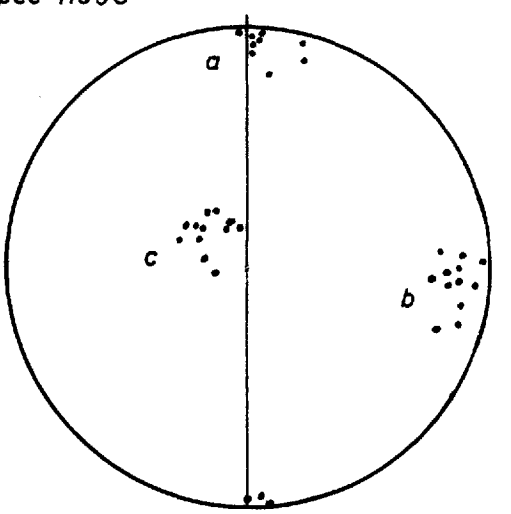

Spec 1524B

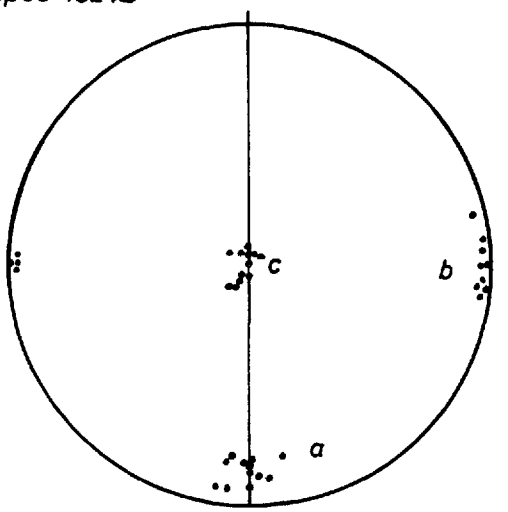

Spec 1524C

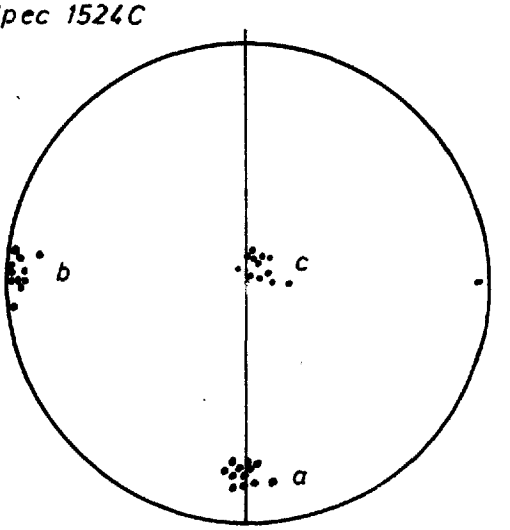

Fig. 6-3

but is generally in the range 5-10 cm. The ratio a:b:c is of the order 1 : 10 : 100.

The garben microstructure may be discussed in terms of the interfacial energy concepts outlined earlier in this chapter. The orientation relationship between hornblende garben and the schistosity plane could arise in the same way as that between garnet and schistosity, demonstrated by Powell (1966); namely by epitaxial growth on the micas, in this instance muscovite, forming the schistosity. For epitaxial growth to occur, the (001) muscovite (010) hornblende interface would necessarily be an interface of low energy, which in general implies good atomic matching of the two crystal lattices across the interface. Figs.6.4a, b and c show atomic arrangements in the (001) of muscovite and the (010) of hornblende. It is apparent that certain similarities in the arrangements exist. The interatomic spacing is of the same order, particularly parallel to the a axis (and other directions demanded by symmetry) of muscovite (5.19 Å) and the c axis of hornblende (5.3 Å), (misfit = 2.1%). The spacing of successive rows of atoms measured parallel to the b axis in muscovite and perpendicular to the (100) of hornblende is also close (misfit 6.4%). The main source of misfit is angular. Cases of epitaxy where there is angular misfit are known; the growth of halides on $CaCO_3$ and $NaNO_3$ is a well documented example (e g. Van der Merwe, 1949). In such cases Van der Merwe has shown that the mismatch can be represented by the parameters shown in Fig.6.4c. The values of these parameters for hornblende on muscovite are compared with those for various halides on $CaCO_3$ and $NaNO_3$, (Table 6.1).

How effective the mismatch relationships are in determining epitaxial growth of hornblende on muscovite is a question which cannot yet be answered. However certain other features which favour epitaxy in these rocks can be examined.

It has been stated (Section 6.5) that the theoretical and experimental conditions for epitaxial growth are those in which the driving energy for reaction is low. This arises when the rates of change of physical variables are slow (i.e. in geological metamorphism) and when

Fig. 6.4. a The arrangement of potassium atoms in the (001) of muscovite. The interatomic distances are given in Å.

b The arrangement of potassium and magnesium atoms in the (010) of hornblende. The interatomic distances are given in Å.

c The superposed hornblende and muscovite lattices. The mismatch in this orientation can be represented by a spatial mismatch (Equation 6.11), $f \simeq 2\%$ and an angular mismatch given by $\tan\Theta\ \% = t \simeq 27\%$ (cf. Table 6.1).

(a)

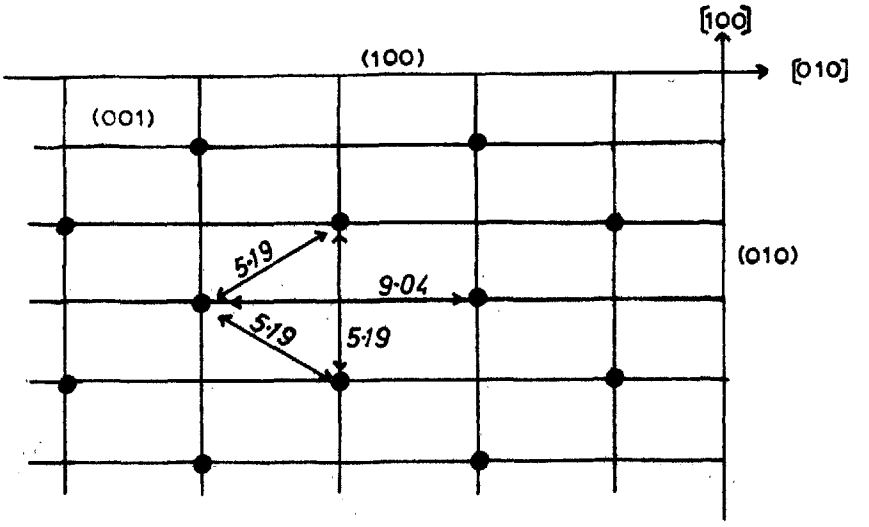
[100]
(100)
[010]
(001)
(010)
5·19
9·04
5·19
5·19

(b)

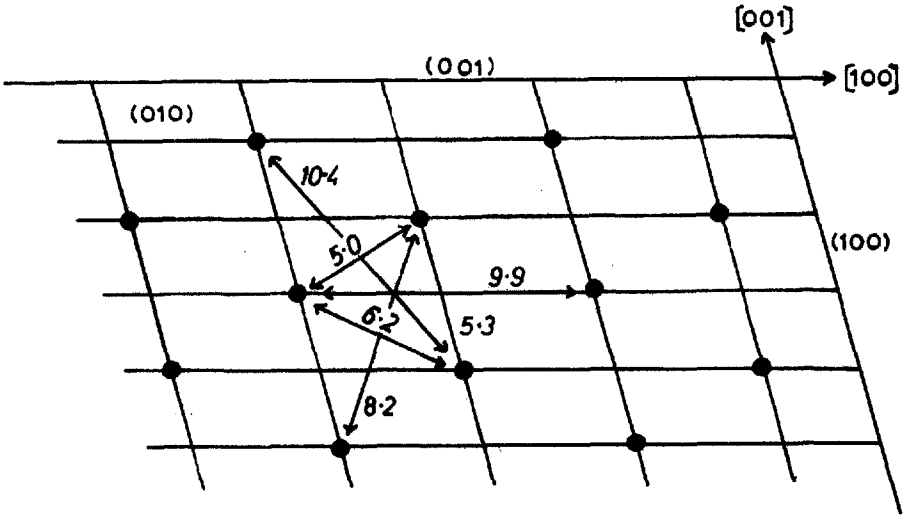
[001]
(001)
[100]
(010)
(100)
10·4
5·0
9·9
6·2
5·3
8·2

(c)

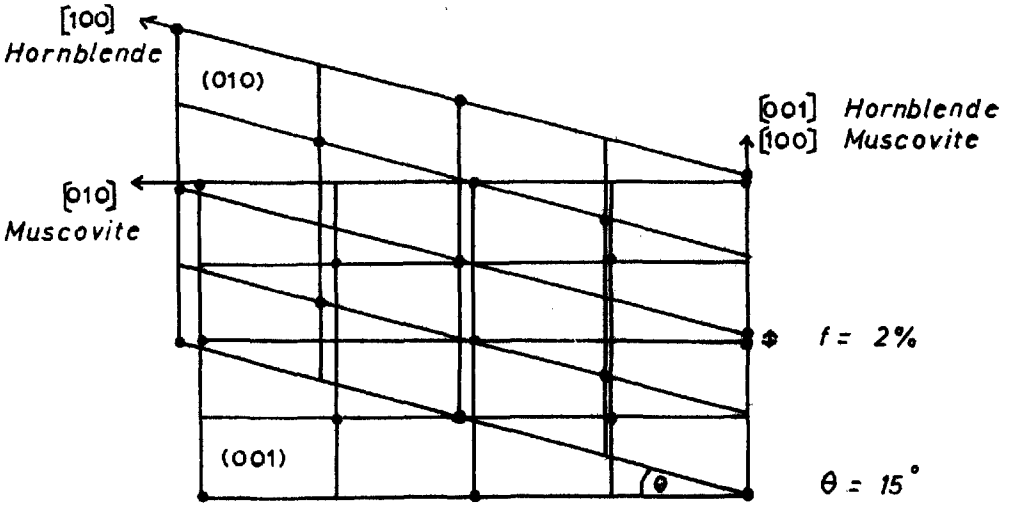
[100]
Hornblende
(010)
[001] Hornblende
[100] Muscovite
[010]
Muscovite
f = 2%
(001)
θ = 15°

Fig. 6·4

Table 6.1

Substrate mineral	Orientation	Overgrowth mineral	Orientation	Mismatch. %	
				Spatial	Angular
*Muscovite	(001) [100]	Hornblende	(010) [001]	+2	t = 27
"	(001) [010]	"	(010) [100]	+10	t = 27
$CaCO_3$	(100) [010]	NaCl	(100) [010]	-12	t = 21
"	"	RbI	"	+14	t = 21
$NaNO_3$	"	K I	"	+9	t = 23
"	"	LiCl	"	-13	t = 23

* The mismatch is defined for a particular orientation. For example in the first case listed above, hornblende on muscovite, the (010) hornblende is parallel to the (001) muscovite and within this plane the [001] hornblende is parallel to the [100] muscovite (cf. Fig.64c).

the concentration of reactants is low. In this situation nucleation becomes a barrier to growth and takes place only at preferred sites. The occurrence of hornblende garben in rocks in which the concentration of hornblende is low has already been noted. If the individual garben represent single nuclei as suggested above, then their large size and small number indicate that nucleation was indeed a barrier to growth. It is noticable that in rocks from this area which contain a high concentration of hornblende the crystals tend to be much smaller, greater in number, and do not form garben. This shows that at these higher concentrations nucleation took place more easily.

The discussion above gives a possible explanation for the crystallographic orientation of the garben with respect to the schistosity plane, but does not explain their fan-like structure. Because of this structure hornblende garben and crystal garben in general have been interpreted as dendrites (Voll, 1960, p. 531). These crystal forms are recognised to be the product of rapid non-equilibrium crystal growth. The formation of dendrites is favoured by a high

supersaturation of the crystallising phase, a situation which may arise when a concentrated solution is cooled rapidly (Saratovkin, 1959). At low concentrations high supersaturations cannot occur.

Thus the conditions which favour epitaxial growth are exactly opposed to those suitable for dendrite formation. Accordingly an alternative explanation must be sought for the sheaf like growth form of hornblende garben.

The growth of crystals from dilute solutions presents a special problem. It is known that before growth of a new layer on an atomically flat or singular surface can occur the layer must first be nuoleated. The probability of nucleation taking place is not great unless the degree of supersaturation is considerable. The fact that real crystals grow at low supersaturations appears to be an enigma. The nucleation problem is overcome in real crystals because they are never perfect; they contain imperfections, such as dislocations, which provide sites of good lodgement for the new material added to the crystal faces. Particularly important is the screw dislocation which provides a self perpetuating growth step on a crystal face. Traces of impurity added to the system can result in a poisoning of the growth process so that the crystal is constrained to grow parallel to the axis of the screw dislocation, giving rise to a whisker crystal form. Generation of new dislocations during growth may lead to branching. It is possible that the hornblende garben have arisen by a growth process such as this, rather than by the rapid growth of atomically rough or non-singular surfaces at high supersaturations.

CHAPTER VII

GARNET CRYSTAL SIZE DISTRIBUTIONS

7.1) Introduction

Although it is normal in the study of metamorphic minerals to make some assessment of their size, there is available little systematic data of crystal size distributions in metamorphic rocks. The work of Galwey and Jones (1963, 1966), Jones and Galwey (1964, 1966) and Kretz (1966b) appears to be unique in this field.

The thermodynamical approach to metamorphism is concerned with prediction, for a given set of physical conditions, of equilibrium mineral assemblages in a multicomponent system. As Galwey and Jones (1966) point out, it does not necessarily specify the state of subdivision and crystal size distribution of a mineral stable in the equilibrium assemblage. This is essentially a problem of reaction kinetics.

The kinetics of many isothermal phase transformations can be described in terms of the parameters N, the rate of nucleation and G, the rate of growth of the nuclei (Holloman and Turnbull, 1953). This is true of recrystallisation reactions (Burke and Turnbull, 1952) and slow decomposition reactions (Jacobs and Tompkins, 1955; Stone, 1961). In these reactions it is generally satisfactory to assume that the rate of growth is a constant, so that a graph showing the extent of reaction against time reflects the nucleation rate. The form of the crystal size distribution of a metamorphic mineral therefore also gives information about the nucleation rate, provided that the complex mineral forming reactions can be described in the same way as the simpler transformations considered above.

In the present study, garnet (almandine rich pyralspite) crystal size distributions from three specimens from Val Piora have been determined, and analysed in terms of the relative rates of nucleation and growth. Data for the spatial distribution of crystals is presented. This data is important in deciding which of the various hypothetical nucleation models best accounts for the formation of garnet in these rocks.

7.2) Material

The three specimens for which garnet crystal size distributions have been determined are black garnetiferous schists from localities Nos. 136, 757 and 781 in Val Piora. These localities are all exposures of black garnet schist series rocks in which the black garnetiferous schists are interbanded with calcareous schists and occasional quartzites, (Section 2.21). Locality 136 (M.R. 6970415574) is situated on the northern side of the Murinascia torrent a short distance above the point where the torrent enters Lago Ritom. Localities 757 (M.R. 6968815582) and 781 (M.R. 6967415576) are on the north side of the road from Piora to Alpe Piora.

The petrography of these garnets schists has been described in some detail previously (Krige, 1918, pp. 605-608) and will not be described again here. The specimens chosen for analysis were ones which appeared to be homogeneous in bulk composition and in which the garnet crystals showed good dodecahedral crystal form. In Specs. 757 and 781 the growth of garnet took place under static conditions, whereas in Spec. 136B the garnets are syntectonic. The garnet crystal size-rotation relationships for Spec. 136B have been analysed and are discussed separately (Section 5.7).

7.3) Methods of analysis

Garnets are particularly suitable for crystal size distribution analysis as their crystal form enables them to be represented approximately by spheres. In these specimens it was impossible to separate the garnets from the rock and consequently a serial grinding technique, similar to that used by Kretz (1966b) was employed to determine their size distribution.

The garnet crystal sections exposed on a flat surface cut through the specimen were recorded by tracing their outlines on a sheet of cellophane placed over the surface. Each garnet section was assigned a number and its average section diameter measured on the surface using a binocular microscope with a micrometer eyepiece. (The average section diameter was taken as the mean of four measurements at 45 degrees through the centre of the crystal). The crystals were assumed to be spherical and the true crystal diameter was determined geometrically from the average section diameter measurements of at least two sections of the same garnet crystal.

This method of analysis allowed the spatial coordinates of each crystal to be determined. An orthogonal x, y, z, coordinate system was set up, so that x and y lay in the plane of the section and z in the direction of sectioning. x and y were measured from the cellophane traces of the crystals and z from the geometric construction used to find the true crystal diameter. From the knowledge of the positions of the crystal centres, the distribution of the crystals in space and the distance apart of any two crystal centres were determined.

7.4) The crystal size distributions

Figs. 7.1a, b and c show the garnet crystal size distributions for Specs. 757, 781, and 136B respectively. The distributions are neither log-normal nor arithmetic normal, though they approximate more closely to the latter. The various data are summarised in Table 7.1 below.

Table 7.1

Spec. No.	No. of crystals measured	Crystal density/c.c.	Range mm.	Mean mm.	Standard Deviation mm.
757	318	3.4	0.6 - 8.8	4.1	1.90
781	285	1.8	0.6 - 8.8	4.1	2.09
136B	130	-	0.6 - 8.2	4.5	1.56

The crystal density, (number of crystals/c.c.) was calculated for Specs. 757 and 781 from the x, y, z coordinate data referred to in the previous section.

It is evident that the measurement of crystal size in a solid becomes rather difficult when the crystal cannot be removed from the solid. This problem is familiar to sedimentary petrologists and metallurgists. Krumbein (1935) has shown how the moments of a grain size distribution may be calculated from those of a two dimensional distribution. The calculation assumes the grains to be spherical. Greenman (1951) has extended Krumbein's method to calculate the complete grain size distribution from the two dimensional data, and has suggested that this method may also be applied where the particles are approximately ellipsoidal in shape.

A method of calculation which is essentially the same as that outlined by Greenman has been applied to the average diameter measurements of garnet sections (two dimensional distribution) collected in the determination of the crystal size distribution of Spec. 781. Fig. 7.2a shows the size distributions calculated from 277, 521 and 818 average section diameter measurements. These may be compared with the actual crystal size distribution, Fig. 7.2b. It is seen from these comparisons, that the calculated distributions differ consistently

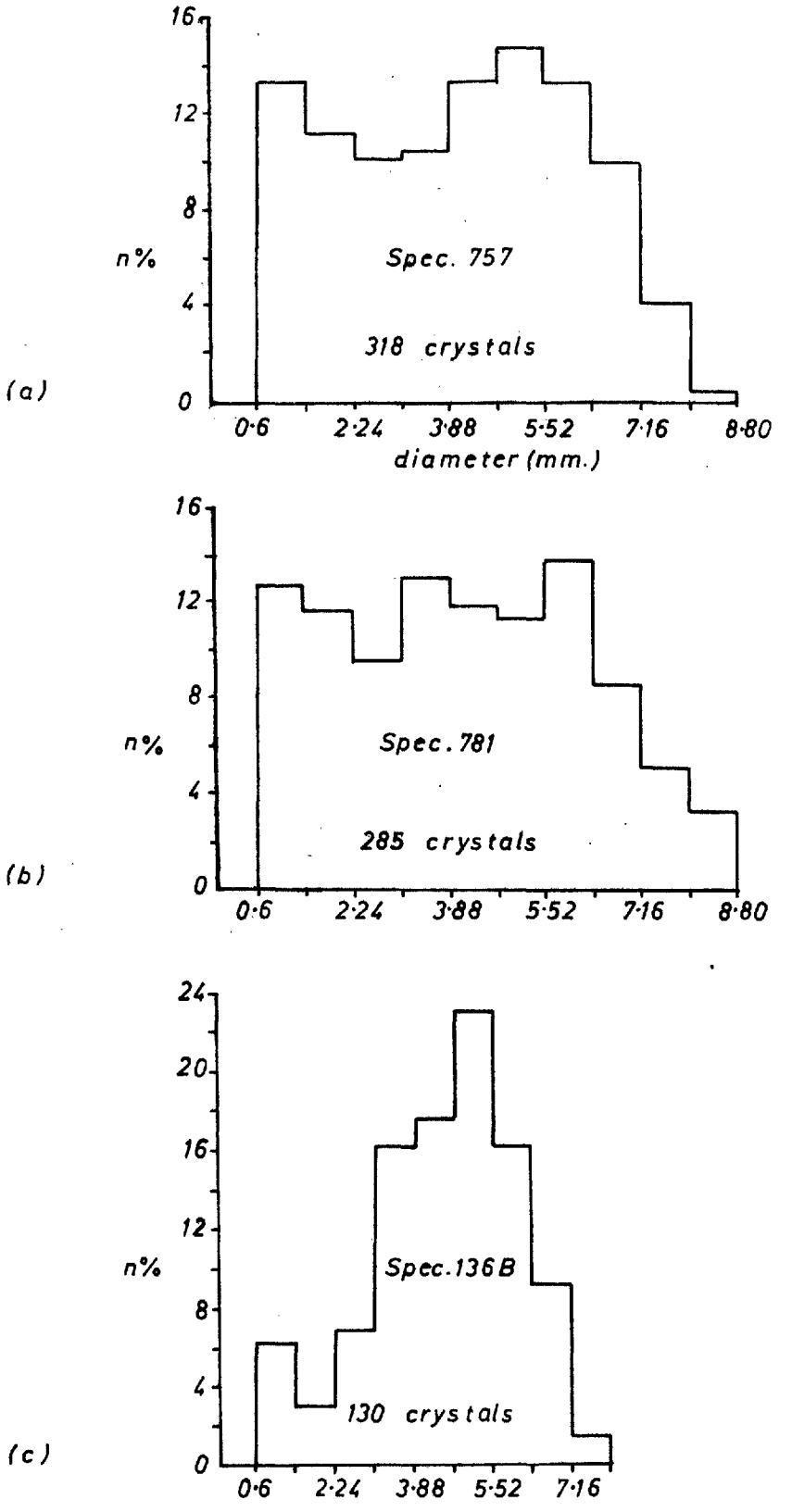

Fig. 7·1 Histograms illustrating garnet crystal size distributions

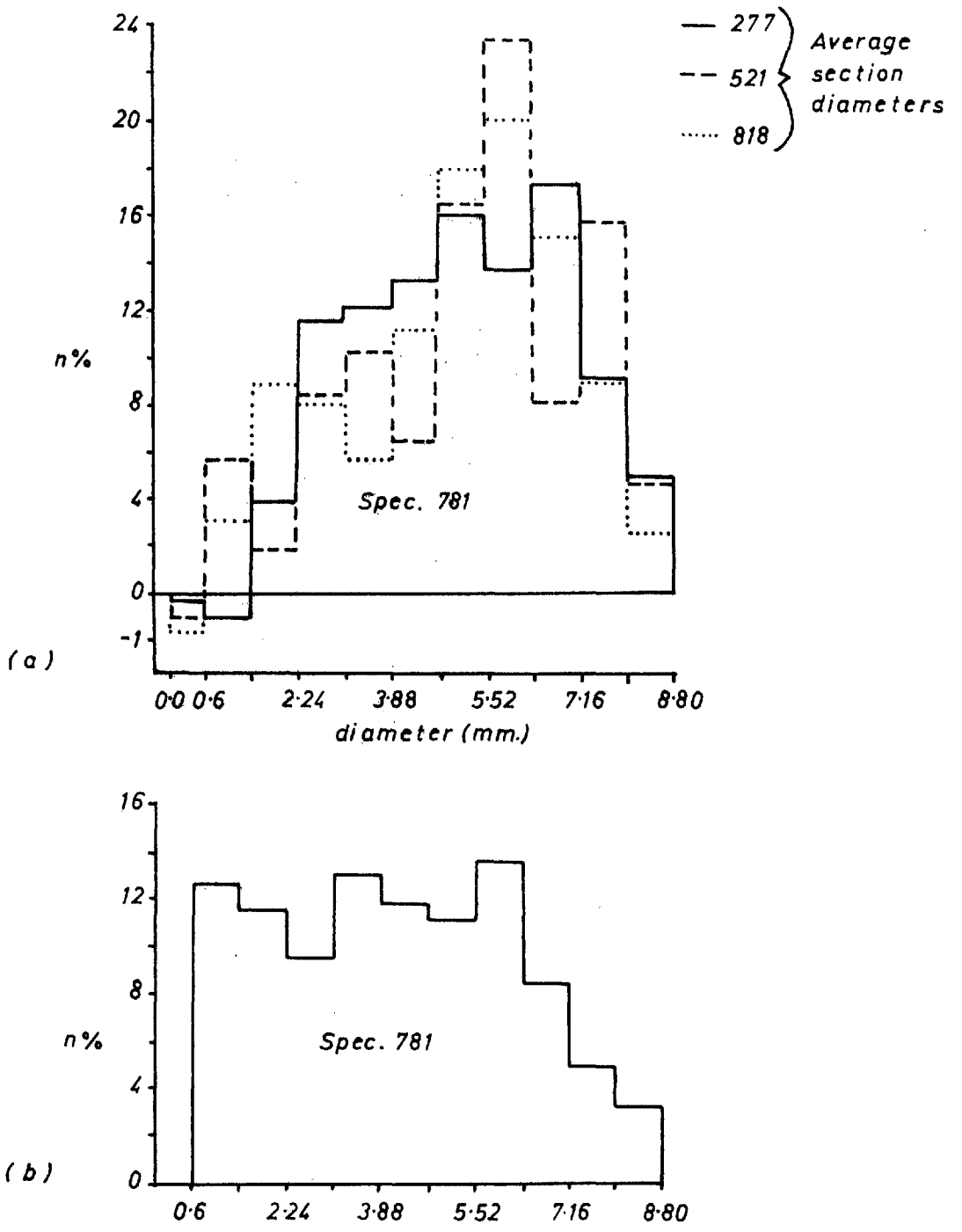

Fig 7·2 Relationship between garnet crystal size distribution calculated from 2D data (a) and observed distribution (b).

from the actual distribution in overestimating the number of large and underestimating the number of small crystals. As the correlation factors involved in the calculation are dependent on the curve which shows the probability of cutting a section of radius, r, through a sphere rather than a garnet crystal, they are only approximate in this instance. Similar curves for various polyhedra have been determined by Hull and Houk (1953), and found to differ from that for a sphere. However, the rhombic dodecahedron does not figure among the investigated polyhedra.

When crystals cannot be removed from a specimen there are obvious advantages, in terms of time, to applying a reliable two dimensional method of size distribution analysis. The purpose of the above calculations was to test a method which has been used in the grain size analysis of indurated sedimentary rocks (Greenman, 1951). The results of the calculations suggest that the method may not be applied to garnet crystals with any degree of accuracy. The reason for this is not because of an insufficiency of two dimensional data, (there is no systematic change in the calculated distribution with an increasing number of average section diameter measurements) but in the assumption of sphericity of garnet crystals.

7.5) The spatial distribution of crystals

The spatial distribution of nuclei in homogeneous nucleation is random. The same may be said of heterogeneous nucleation, where relative to the nuclei there exists a large number of preferred nucleation sites, which are randomly distributed in the system. In a rock it is possible to envisage the condition in which nucleation does not occur randomly. This will arise through a change of composition or through the existence of concentrations of preferred nucleation sites within the rock. These concentrations might be expected in regions of high strain, shear zones, or could be associated with the occurrence of a particular mineral with which the new phase has an epitaxial relationship. The analysis of the crystal size distribution from a system which is not homogeneous with respect to the concentration of nuclei, and hence the rate of nucleation, is meaningless. It is therefore important to establish that the crystals within the specimens examined are randomly distributed.

A spatial distribution analysis was carried out for some of the crystals measured in Spec. 781. The serial section method used in determining the crystal size distribution allowed the coordinates of the centres to be measured within the specimen. These known, the number of crystal centres in each small volume of specimen can easily be found. If the resulting distribution of centres between equal volumes is random, then the number of volumes with a particular number of centres will follow a Poisson distribution (Hald, 1952, Chapter 22). This hypothesis can be tested by the technique outlined by Hald (1952, Chapter 23.2), which is followed below.

Analysis of the spatial distribution of crystals.

Volume of size unit (c.c.)	= 1.0 x 1.7 x 0.5
No. of volume units	= 60
No. of crystal centres	= 90
Average no. of centres/unit volume	= 1.5
No. of crystals/c.c.	= 1.8

Table 7.2

No. of centres x	No. of Volume units a	Poisson Distribution $n\hat{\theta} = Np(x)$	Deviations $a - n\hat{\theta}$	$\frac{(\text{Deviations})^2}{Np(x)} = \chi^2$
0	13	13.38	+0.38	0.0108
1	19	20.05	+1.05	0.0510
2	17	15.02	-1.98	0.2600
3)	8)	7.52)	)	
4 } ≥3	2 } 11	2.82 } 11.19	} +0.19	0.0030
5)	1)	0.846)	)	
	60	59.64	-0.36	0.325

$n\theta$ should be greater than 5 for all classes.

No. of degrees of freedom = 2

As χ^2 = 0.325 is not significant (Lindley and Miller 1962), the observed distribution does not differ significantly from a Poisson distribution.

The distribution of crystal centres can then be inferred to be random. In other rocks, analyses of randomness (Kretz, 1966b; Jones and Galwey, 1964) led to a similar conclusion.

The relationship between the size of a crystal and the distance from its centre to that of its nearest neighbour has also been investigated. This investigation was carried out on the crystals from Spec. 781 whose spatial distribution has been examined above. The nearest neighbour was found, by inspection, from the coordinates of a crystal and those of the surrounding crystals. Crystals lying nearer to the margin of the specimen than to their nearest neighbour were rejected in the analysis. The data obtained is represented in Fig.7.3a. It can be inferred from the figure, that there is no apparent relationship between the size of a crystal and the distance to its nearest neighbour. Likewise it is shown in Fig.7.3b that there is no relationship between the size of a crystal and that of its nearest neighbour. This data is important in helping to decide between various nucleation models.

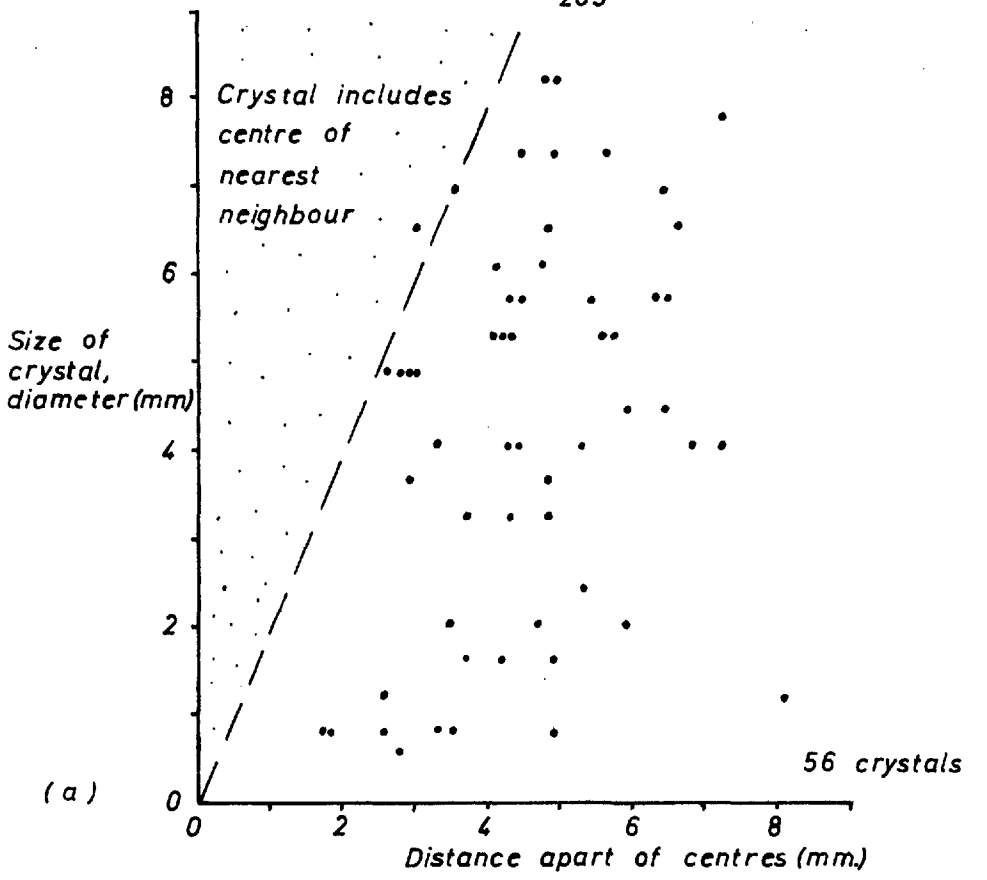

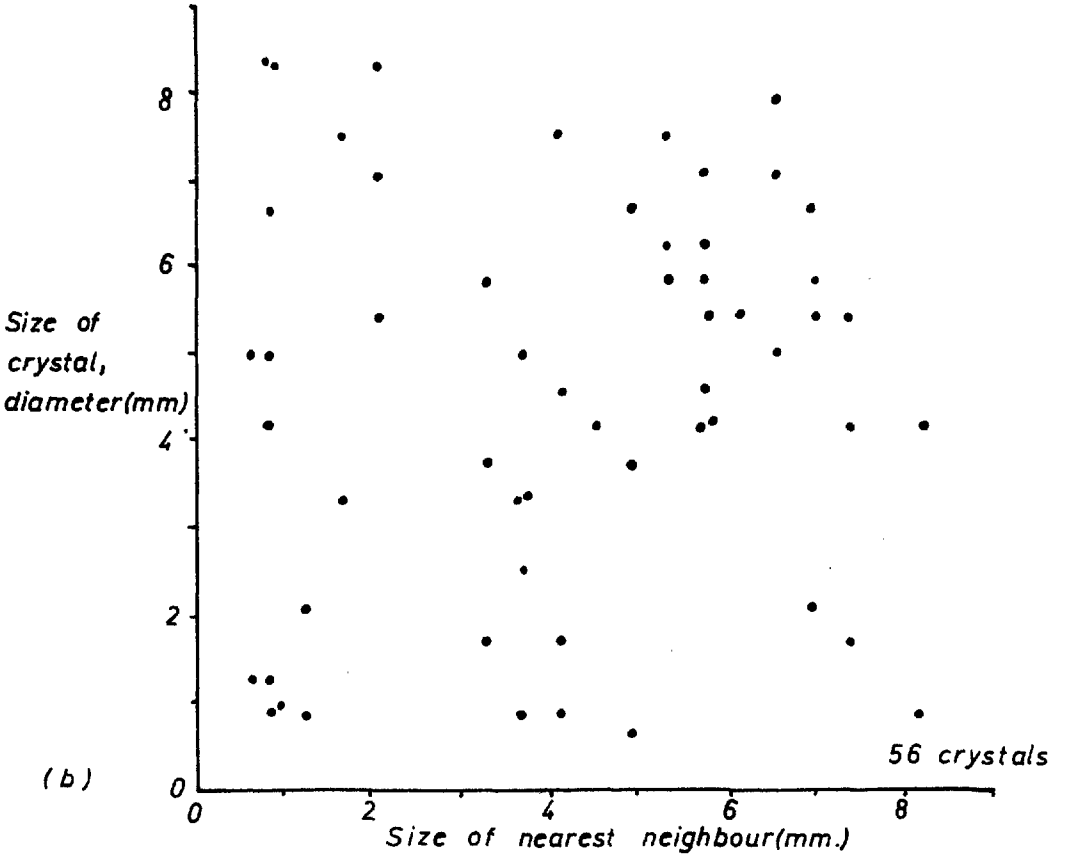

Fig. 7·3 *Size / distance to nearest neighbour and size / size of nearest neighbour data, Spec. 781.*

7.6) Nucleation models

Various models have been suggested to describe the nucleation and growth of metamorphic minerals. Kretz (1966 b, p. 162) considers three possibilities, outlined below.

1) All crystals nucleate at the same time. The nuclei are randomly distributed and extract growth matter from their surrounding volumes, the dimensions and shape of which are determined by the half distances to the crystals nearest neighbours. This model is essentially the same as the probability model of Galwey and Jones, (1963).
2) All crystals nucleate at the same time but some grow faster and to a greater size than others because of varying rates of diffusion in different zones within the rock.
3) All crystals grow at the same rate, but do not nucleate simultaneously. The form of the nucleation equation will control the size distribution.

If model (1) is viable then a relation might be expected between crystal size and distance to nearest neighbour, as well as between crystal size and size of nearest neighbour. The nearest neighbour data illustrated in the previous section (7.5) shows no such relationship. Similar data determined by Kretz (1966 b, p. 160, Table V) likewise shows no relationship.

In discussing their probability model, Galwey and Jones (1963, p. 5684) point out that the crystal size distributions predicted by the model will be normal distributions. The distributions determined here only approximate to normal and those analysed by Kretz (1966 b) appear to be closer to log-normal. Jones and Galwey (1966, p. 40) also find the model to be inadequate, in that the K values (Section 7.7) of the predicted distributions should be universally constant. Their data indicate that this is not the case.

The relationship observed between the amount of rotation and the size of a crystal, shown by the snowball garnets of Spec. 136B (Section 5.7) suggests that nucleation does not occur simultaneously for all crystals. It is known from experimental observation that for many

solid transformations nucleation is a time dependent process which may, for the acceleratory period of reaction at least, be expressed by an exponential or a power law (Burke and Turnbull, 1952; Jacobs and Tompkins, 1955; Stone, 1961). The rate of growth of the nuclei can in general be assumed to be constant. Thus the model which appears most appropriate to the evidence considered is model (3).

Accepting the assumption of a constant rate of linear crystal growth the form of the nucleation curves for the garnets of Specs. 757, 781 and 136B can be determined from the size distribution data. The diameter, D, of any garnet crystal in the distribution after time, t, may be expressed by the equation (c.f. Burke and Turnbull, 1952, Equation (1))

$$D = 2G.(t - \tau) \qquad (7.1)$$

where G = the rate of linear growth

t = the time

τ = the nucleation period of the garnet crystal.

Therefore, the diameter of the largest crystal in the distribution, which can be approximately represented by the limit of the upper class interval of the crystal size distribution, D_{max}, is:

$$D_{max} = 2G.(t - \tau_{max}) \qquad (7.2)$$

and the diameter of the smallest crystal in the distribution, represented by the lower limit of the smallest class interval, D_{min}, is:

$$D_{min} = 2G.(t - \tau_{min}) \qquad (7.3)$$

By subtraction:

$$\tau_{min} - \tau_{max} = \frac{D_{max} - D_{min}}{2G} \qquad (7.4)$$

where $\tau_{min} - \tau_{max}$ = the time interval between the nucleation of the first crystal and the last crystal.

Therefore, setting $\tau_{max} = 0$ and $\tau_{min} = 1$, a time scale for nucleation is erected such that the time of nucleation, T, of any crystal or group of crystals of diameter, D, is given by the

equation:

$$T = \frac{(D_{max} - D)}{(D_{max} - D_{min})} \qquad (7.5)$$

The nucleation curve is obtained by plotting the percentage number of crystals, n, nucleated after a time, T, against T. Table 7.3 shows the relationship between the garnet crystal size distribution, T and n for Spec. 757. The nucleation curves for Specs. 757, 781 and 136B are given in Fig. 7.4.

Table 7.3

Spec. 757

Diameter (D) mm.	No. of crystals %	T	n%	T'
0.00 - 0.60	0			
		1.0	99.9	1.00
0.60 - 1.42	13.2			
		0.9	86.7	0.98
1.42 - 2.24	11.0			
		0.8	75.7	0.94
2.24 - 3.06	10.0			
		0.7	65.7	0.88
3.06 - 3.88	10.4			
		0.6	55.3	0.81
3.88 - 4.70	13.2			
		0.5	42.1	0.72
4.70 - 5.52	14.7			
		0.4	27.4	0.61
5.52 - 6.34	13.2			
		0.3	14.2	0.49
6.34 - 7.16	9.8			
		0.2	4.4	0.34
7.16 - 7.98	4.1			
		0.1	0.3	0.18
7.98 - 8.80	0.3			
		0.0	0.0	0.00

It is found, by representing the data appropriately (Fig. 7.5), that the initial period of nucleation of the garnets of Specs. 757, 781 and 136B may be described within the limit of experimental error by power laws of the form:

$$\frac{dn}{dT} = CT^{\alpha} \qquad (7.6)$$

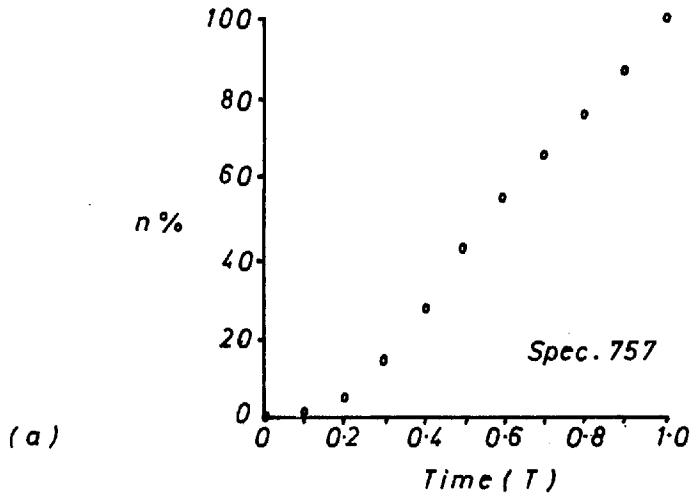

(a)

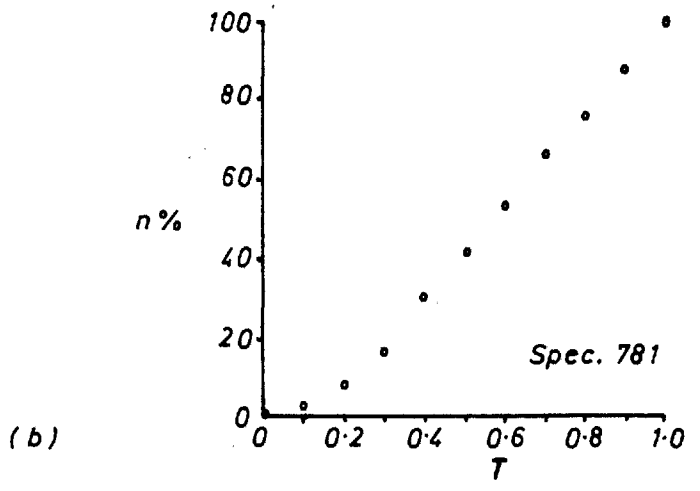

(b)

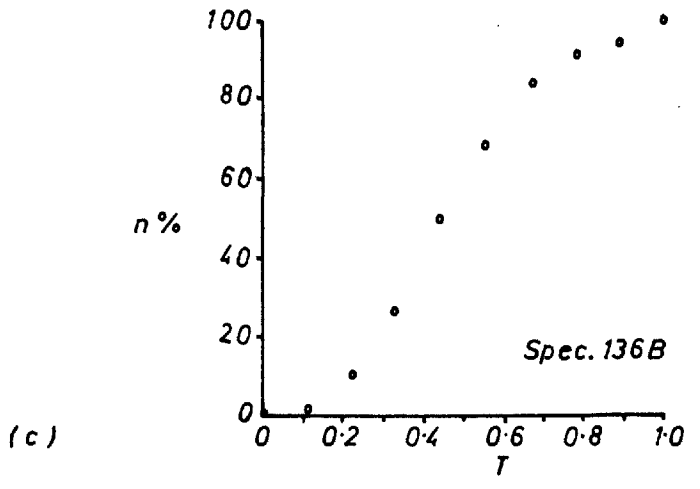

(c)

Fig. 7·4 Nucleation curves of garnet in Specs. 757, 781 and 136B, assuming a linear (Equation 7·1) crystal growth rate.

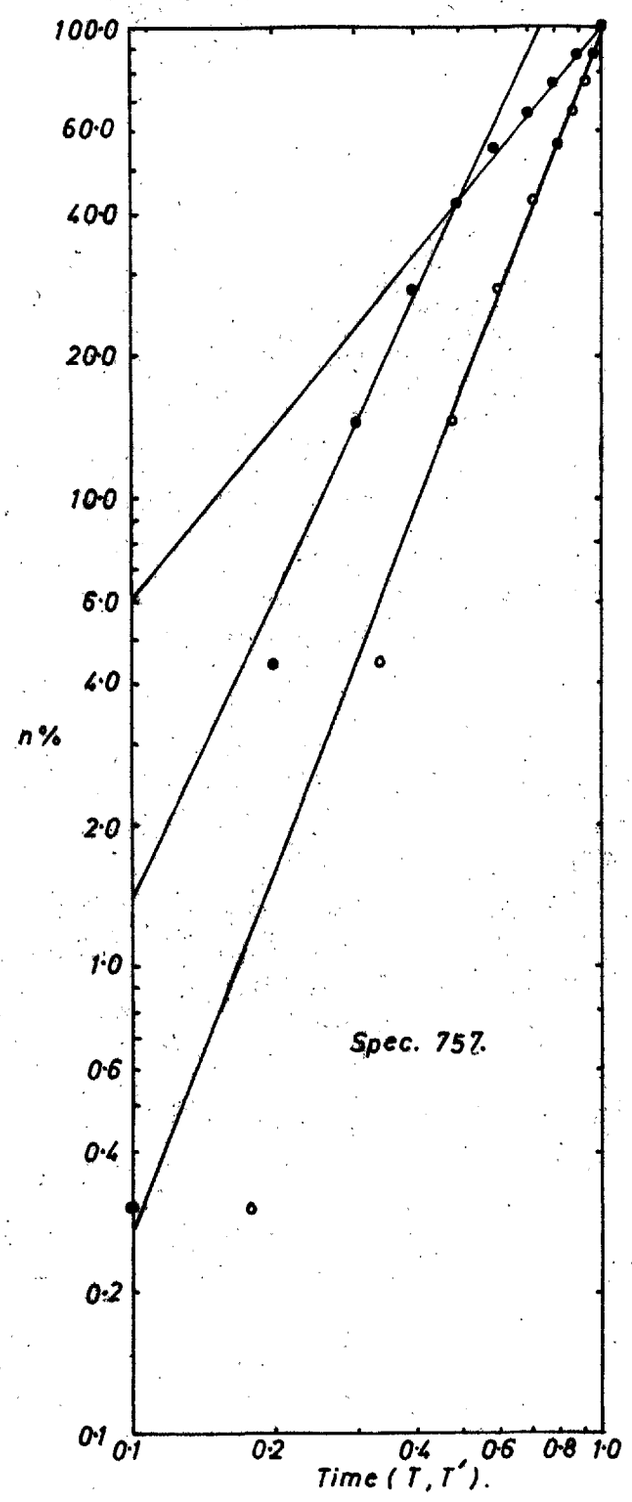

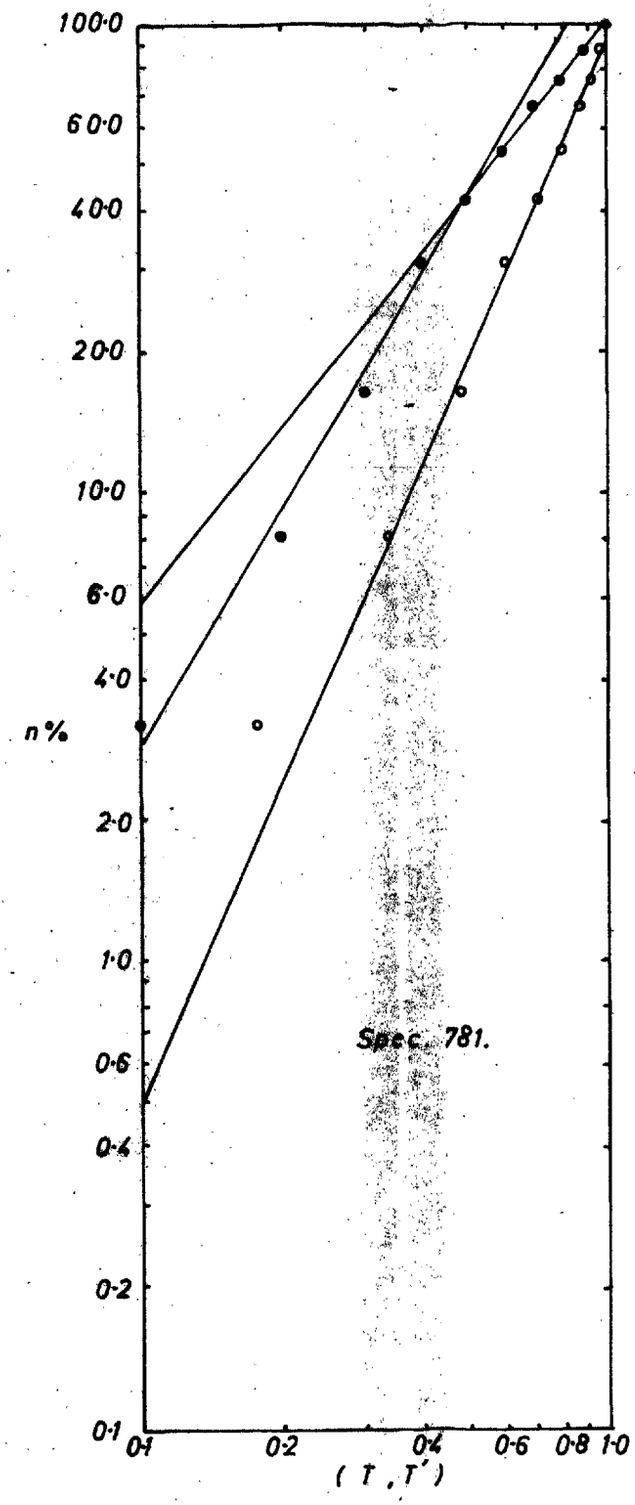

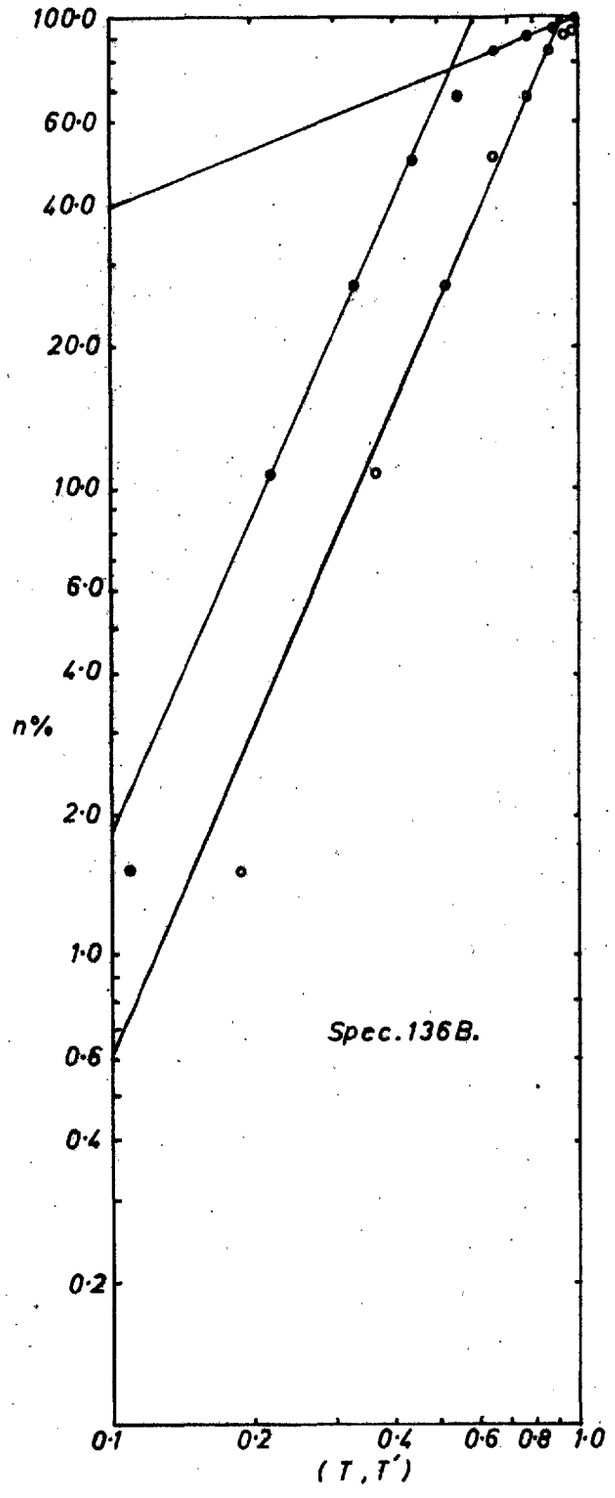

Fig. 7·5 Log-log plots of nucleation curves of garnet in Specs. 757, 781 and 136B, assuming linear (•)(Equation 7·1) and non-linear (○)(Equation 7·8) growth rates.

such that:

$$n = C\int_0^T T^{\alpha}\,dT$$

$$n = C'T^{\beta}$$

$$\log n = \beta \log T + \log C' \qquad (7.7)$$

where α, β, C and C' are constants.

It also appears (Fig. 7.5) that the latter half of nucleation may be expressed by power laws. A possible interpretation of this description of nucleation is that the first power law describes the acceleratory and the second power law the deceleratory period of the transformation.

The assumption of a constant rate of linear growth can be questioned. It is stated (Holloman and Turnbull, 1953), that for transformations in which a change of composition takes place, the growth of the new phase is often found to be diffusion limited. The size of the growing region of the new phase is given by the equation:

$$D = 2G^{\frac{1}{2}}.(t-\gamma)^{\frac{1}{2}} \qquad (7.8)$$

Under these conditions of growth Equation 7.5 becomes:

$$T' = \frac{(D^2_{max} - D^2)}{(D^2_{max} - D^2_{min})} \qquad (7.9)$$

As an example the values of T' for Spec. 757 are given (Table 7.3). The linear relationship shown by $\log n/\log T'$ (Fig. 7.5) suggests that in this case the major part of the nucleation process can be interpreted by a power law. The fit of values of n to this linear relationship is within the limit of $\pm$ 3% over the range n = 0 - 85% for all three specimens. In view of the possible error in determining n this interpretation would appear to be justified.

It is apparent that there are considerable difficulties in interpreting the size distribution data. The nucleation curves derived from the data have been shown to be dependent on the equation describing the growth of the crystals. Two simple equations have been considered, the second of which gives rise in all the specimens studied to a nucleation curve the major part of which may be described by a single power law.

7.7) The significance of crystal size distributions

Jones and Galwey (1966) have shown that, for all their determined garnet (andradite) crystal size distributions, a linear relationship exists between the function $\log (n/100-n)$ and d, where n = the percentage of crystals is a size interval of diameter, d, added to the percentage of crystals in all size intervals for which the mean diameter is less than d.

The slope, k, of the graph of $\log (n/100-n)$ against, d, multiplied by the median diameter, d_m, at which $d^2n/dd^2 = 0$, gives a dimensionless number, K, which they find to be approximately constant for distributions determined from the same area and/or similar environment. It is apparent that k is a quantity which bears an inverse relationship to the standard deviation of the distribution and hence K for any distribution is a measure of the median diameter divided by the standard deviation, Kretz (1966b, p. 169).

It should be noted that a linear relationship of $\log (n/100-n)$ against d implies that the distribution is symmetrical about the median diameter. Skewness of the distribution will lead to greater or lesser values of median diameter and hence K, and to a poorer fit to the relationship described above. In Spec. 136B the crystal size distribution is positively skewed whereas those of Specs. 757 and 781 are negatively skewed. Accordingly the K value of Spec. 136B is increased relative to those for Specs. 757 and 781 (cf. Table 7.4).

The significance of K can be appreciated by considering the rate of nucleation, N, in relation to the rate of growth, G, of the nuclei. Where N/G has a relatively small value the crystals nucleated early in the reaction will grow to a large size before nucleation is complete. There will be a large scatter of diameters about the median diameter, corresponding to a low value of K. Conversely where N/G has a relatively large value K will also be large. As N and G are dependent on the activation energies for nucleation and growth respectively, large values of K will be associated with a low $\Delta E_N/\Delta E_G$ value, where ΔE_N = activation energy for nucleation, ΔE_G = activation energy for growth. The observation that the K values

of garnet crystals adjacent to high temperature intrusions are greater than those close to low temperature intrusions (Jones and Galwey, 1966 pp. 39-42 and Fig. 4) suggests that:

$$\frac{\Delta E_N}{\Delta E_G} \text{ (high temp.)} < \frac{\Delta E_N}{\Delta E_G} \text{ (low temp.)}$$

This implies that the temperature dependence of the activation energies is different and that the nucleation rate increases more rapidly than the growth rate with temperature, and hence departure from the equilibrium reaction temperature. It has been assumed above, not unreasonably, that the activation energy for nucleation is greater than that for growth. Accordingly crystal growth will be expected to outlast nucleation, and the smallest crystals in the distribution can be expected to have a finite size. This conclusion is in agreement with the crystal size data described (Section 7.4).

As it leads to an increase in the median diameter, the extent to which crystal growth outlasts nucleation affects the value of K. This affect is not significant where the growth after nucleation, represented by the diameter of the smallest crystal in the distribution, is small in relation to that required to form a crystal of diameter equal to the median diameter of the distribution (e.g. in the specimens examined here). There is good reason to believe that this condition is generally obeyed, however this whole problem can be avoided by the choice of a suitable scale against which to plot log $(^{n}/_{100-n})$. For example:

$$\frac{d - d_{min}}{d_{max} - d_{min}}$$

where d is defined as above.

d_{max} = the diameter of the largest crystal in the distribution.

d_{min} = the diameter of the smallest crystal in the distribution.

K is now simply given by $\frac{1}{2}k$, where k = the slope of the graph.

Jones and Galwey (1966) have considered the affect of composition of the reacting matrix on K. They conclude, (p. 40), "that the value of K is not controlled to any great extent if at all by the composition of the reacting matrix". They also find that small changes in the composition of the garnet crystals do not seem to be related to changes in K.

The observed crystal density in Spec. 757 is twice that in 781, yet the crystal size distributions are shown to be almost identical (Table 7.1 and Figs. 7.1a and b). Their calculated K values, 1.46 and 1.56 respectively, reflect this similarity and also demonstrate the apparent lack of dependence of K on chemical composition.

This observation suggests that the value of $^{N}/_{G}$ is not significantly altered by changing chemical composition. In the manufacture of steels it is known that the addition of alloying elements can change N or G by several orders of magnitude, however in general this addition does not change the value of $^{N}/_{G}$ appreciably (Mehl and Dube, 1951). On the other hand in the iron-manganese-garnet system it has been noted that spessartine nucleates more easily than almandine (Hsu, 1968), and the field occurrence of manganese rich iron-garnet as smaller crystals than manganese poor iron garnet (Chinner, 1960), has been interpreted as $^{N}/_{G}$ (manganese rich iron-garnet) $>$ $^{N}/_{G}$ (manganese poor iron-garnet) (Kretz, 1966b, p. 172). Thus it would appear to be dangerous to generalise about the effect of chemical composition on K beyond the limits of actual observations.

It has been shown, for Specs. 757, 781 and 136B, that if the crystal growth is described by Equation 7.8, the dependence of nucleation on time can be expressed for 85% of the transformation by the equation:

$$\log n = \beta \log T' + \log C' \quad \text{(c.f. 7.7)}$$

where β = slope of graph

C' = n where $T' = 1$.

It is apparent (Fig. 7.5 and Table 7.4) that the slopes of the graphs for the different specimens are closely similar, indicating that nucleation can be described by the same power law in all three specimens. As the time scale for nucleation is a function of the growth rate, β is a function of $^{N}/_{G}$, which in turn has been shown to be related to K. β then provides an alternative description of the distributions. Values for β, C' and K are given (Table 7.4).

Table 7.4

Spec. No.	β	C'	K
757	2.45	92	1.46
781	2.27	90	1.56
136B	2.30	120	2.38

It can be concluded, that for the examined specimens $^{N}/_{G}$ is effectively constant. Jones and Galwey have shown a similar constancy of $^{N}/_{G}$ through their determination of K values. Values of K are found to vary with environment, but not to differ significantly with change in composition of the reacting matrix, or with small changes in composition of the product. It is found in certain systems (Mehl and Dube, 1951) that the temperature dependence of the activation energies for nucleation and growth differs. Thus the degree of departure of the temperature from the equilibrium reaction temperature during reaction affects the value of $^{N}/_{G}$. The observation that larger K and hence larger $^{N}/_{G}$ values are found adjacent to high temperature intrusions suggests that a greater degree of disequilibrium develops during reaction than adjacent to lower temperature intrusions. This greater degree of disequilibrium would be a natural consequence of a higher rate of heating. This conclusion is substantially the same as that of Jones and Galwey (1966).

ACKNOWLEDGMENTS

I am indebted to Professor J.G. Ramsay for the suggestion and supervision of this research topic and to Dr. A.G. Milnes for introducing me to Alpine geology. My thanks go to Dr. P. Hudelston, Dr. R.H. Graham, Dr. D. Dunnet, Dr. B.K. Tan and Dr. B. Chadwick for valuable discussion and correspondence, Mr. R. Curtis for the X ray analyses of garnet and Mr. J. Gee and his assistants for their help with photography.

For their kindness and hospitality I wish to thank the Ridolfi family, Mr. and Mrs. B. Petar and Mr. and Mrs. C. Mottini.

The receipt of a N.E.R.C. research studentship is gratefully acknowledged.

REFERENCES

AGER, D.V. 1965 Serial grinding techniques: in, Handbook of Palaeontological Techniques. Edit. B. Kummerlaand, D. Raup. W.H. Freeman, London.

AMBÜHL, E. 1929 Petrologie und Geologie des zentralen Gotthardmassivs südlich Andermatt. Schweiz. Min. Petr. Mitt. 9 pp. 265-441.

ARGAND, E. 1916 Sur l'arc des Alpes occidentales. Eclogae Gedl. Helv. 14 pp. 145-191.

BAILEY, E.B. 1935 Tectonic Essays - mainly Alpine. Clarendon Press, Oxford.

BAUMER, A. 1964 Geologie der Gotthardmassivisch-penninischen Grenzregion im oberem Bleniotal. Geologie der Blenio-Kraftwerke. Beitrage zur Geologie der Schweiz, Geotech. Serie, 39. Schweiz Geotech. Komission.

BAUMER, A., FREY, J.D., JUNG, W., and UHR, A. 1961 Die Sedimentbedeckung des Gotthardmassivs zwischen oberem Bleniotal und Lugnez. Eclogae Geol. Helv. 54 pp. 478-491.

BEARTH, P. 1958 Über einer Wechsel der Mineral Fazies in der Wurzelzone des Penninikums. Schweiz.Min. Petr. Mitt. 38 pp. 363-373.

---------- 1962 Versuch einer Gliederung alpinmetamorpher Serien der Westalpen. Schweiz.Min. Petr. Mitt. 42 pp. 127-137.

---------- 1966 Zur minerafaziell Stellung der Glaucophangesteine der Westalpen. Schweiz. Min. Petr. Mitt. 46 pp.13-23.

BECKE, F. 1924 Struktur und Klüftung. Fortschr. der Min., Krist. und Petr. 9 pp. 185-220.

BIANCONI, F. 1965 Resti fossili in rocce mesometamorfiche della regione del Campolugno. Schweiz.Min. Petr. Mitt. 45 pp. 571-596.

BOLLI, H.M. and NABHOLZ, W.K. 1959 Bündnerschiefer, ähnliche fossilarme Serien und ihr Gehalt an Microfossilen. Eclogae Geol. Helv. 52 pp. 237-270.

BONNEY, T.G. 1890 On the Crystalline Schists and their relationship to the Mesozoic rocks in the Lepontine Alps. Q.J.G.S. 46 pp. 187-240.

---------- 1894 Mesozoic Rocks and Crystalline Schists in the Lepontine Alps. Q.J.G.S. 50 pp. 285-302.

---------- 1898 The Garnet-actinolite schists on the southern side of the St. Gotthard Pass. Q.J.G.S. 54 pp. 357-373.

BOSSARD, L. 1929a Zur Petrographie der unterpenninischen Decken im Gebiet der Tessiner Kulmination. Schweiz. Min. Petr. Mitt. 9 pp. 47-106.

---------- 1929b Petrographie der mesozoischen Gesteine im Gebiet der Tessiner Kulmination. Schweiz. Min. Petr. Mitt. 9 pp. 107-159.

---------- 1936 (In Niggli et al, 1936.)

BURCKHARDT, C.E. 1942 Geologie und Petrographie des Basodino-Gebietes. Schweiz. Min. Petr. Mitt. 22 pp. 99-186.

BURKE, J.E. and TURNBULL, D. 1952 Recrystallisation and grain growth. Progress in Metal Physics. 3 pp. 220-292.

CABRERA, N. 1959 In panel discussion: in, The structure and properties of thin films. Edit. C.A. Neugebauer, J.B. Newkirk, D.A. Vermilyea. J. Wiley and Sons, New York. p. 527.

CABRERA, N. and COLEMAN, R.V. 1963 Theory of crystal growth from a vapour: in, The art and science of growing crystals. Edit. J.J. Gilman. J. Wiley and Sons, New York.

CADISCH, J. 1953 Geologie der Schweizer Alpen. Wepf and Co., Basel.

CAHN, R.W. 1950 Internal strains and recrystallisation. Progress in Metal Physics. 2.

CARMICHAEL, D.M. 1969 On the mechanism of Prograde Metamorphic Reactions in quartz-bearing pelitic rocks. Contrib. Mineral and Petrol. 20 pp. 244-267.

CARTER, N.L., CHRISTIE, J.M. and GRIGGS, D.T. 1964 Experimental deformation and recrystallisation of quartz. J. Geol. 72 pp. 687-733.

CHADWICK, B. 1965 The Structural and Metamorphic Geology of the Lukmanier Region, Ticino-Grisons, Switzerland. Ph.D. thesis. Univ. of London.

---------- 1968 Deformation and metamorphism in the Lukmanier region, central Switzerland. Bull. Geol. Soc. Amer. 79 pp. 1123-1150.

CHALMERS, B. 1952 Structure of crystal boundaries. Progress in Metal Physics. 3 pp. 293-318.

CHAPPLE, W.M. 1968 The analysis of strain in deformed rocks: a discussion. J. Geol. 76 pp. 491-494.

CHATTERJEE, N.D. 1961 The Alpine Metamorphism in the Simplon Area, Switzerland and Italy. Geol. Rund. 51 pp. 1-72.

CHINNER, G.A. 1960 Pelitic Gneisses with varying Ferrous/Ferric Ratios from Glen Clova, Angus, Scotland. J. Petr. 1 pp. 178-217.

CHINNER, G.A. 1961 The origin of sillimanite in Glen Clova, Angus. J. Petr. 2 pp. 312-323.

CLOOS, E. 1947 Oolite deformation in South Mountain Fold, Maryland. Bull. Geol. Soc. Amer. 58 pp. 843-918.

COBBOLD, P. 1969 Independent field work. Val Camadra, Greina area, Ticino, Switzerland. B.Sc. thesis. Univ. of London.

COE, K. 1959 Boudinage structures in West Cork, Ireland. Geol. Mag. 96 pp. 191-200.

COLLET, L.W. 1935 The Structure of the Alps. (2nd Edition) E. Arnold and Co. London.

COX, F.C. 1969 Inclusions in garnet: discussion and suggested mechanism of growth for syntectonic garnets. Geol. Mag. 106 pp. 57-62.

DAL VESCO, E. 1964 Die geologischen Verhältnisse im Bereich der Piora-Mulde. Eidg. Amt Strassen-und Flussbau. Eidg. Amt Verkehr.

DONATH, F.A. and PARKER, R.B. 1964 Folds and Folding. Bull. Geol. Soc. Amer. 75 pp. 45-62.

DAVIS, W.M. 1900 Glacial erosion in the valley of the Ticino. Appalachia 9 pp. 136-156.

DAVIES, F.B. 1971 The geology of the Alpe Sheggia, Ticino, Switzerland. B.Sc. thesis. Univ. of London.

DEFAY, R., PRIGOGINE, I., BELLOMANS, A. and EVERETT, D.H. 1966 Surface Tension and Absorption. Longmans, Green and Co. Ltd. London.

de SITTER, L.U. 1958 Boudins and Parasitic Folds in relation to Cleavage and Folding. Geol.Mijnbouw 20 pp. 277-286.

de VORE, G.W. 1969 The role of minimum interfacial free energy in determining the macroscopic features of mineral assemblages. 1. The Model. J. Geol. 67 pp. 211-227.

DEWEY, J.F. 1965 The Nature and Origin of Kink Bands. Tectonophysics. 1 pp. 459-493.

ELLIOT, D. 1965 The quantitative mapping of directional minor structures. J. Geol. 73 pp. 865-880.

EVANS, B.W. and LEAKE, B.E. 1960 The composition and origin of the striped amphibolites of Connemara, Ireland. J. Petr. 1 pp. 337-363.

FLETT, J.G. 1912 Geology of Ben Wyvis, etc. Mem. Geol. Survey. U.K.

FLEUTY, M.J. 1964a The description of folds. Proc. Geol. Assoc. London. 75 pp. 461-492.

---------- 1964b Tectonic Slides. Geol. Mag. 101 pp. 452-456.

FLINN, D. 1962 On Folding during 3-dimensional progressive deformation. Q.J.G.S. 118 pp. 385-433.

--------- 1965 On the symmetry principle and the deformation ellipsoid. Geol. Mag. 102 pp. 36-45.

FREY, J.D. 1967 Geologie des Greinagebeites. Beitr. Geol. Karte Schweiz. N.F. 131.

FRONDEL, C. 1936 Oriented inclusions of tourmaline in muscovite. Amer. Mineralogist, 21 pp. 777-799.

---------- 1940 Oriented inclusions of staurolite, zircon and garnet in muscovite. Skating crystals and their significance. Amer. Mineralogist. 25 pp. 69-87.

FYFE, W.S., TURNER, F.J. and VERHOOGEN, J. 1958 Metamorphic reactions and metamorphic facies. Mem. Geol. Soc. Amer. 73.

GALWEY, A.K. and JONES, K.A. 1963 An attempt to determine the mechanism of a natural mineral forming reaction from examination of the products. J. Chem. Soc. pp. 5681-5686.

---------- 1966 Crystal size frequency distribution of garnets in some analysed metamorphic rocks from Mallaig, Inverness, Scotland. Geol. Mag. 103 pp. 143-152.

GANSSER, A. and DAL VESCO, E., 1964 Bericht über die Exkursion B der Schweizerischen Geologischen Gesellschaft: S.E. Gotthardmassiv und Penninikum (Piora-Lukmanier-Bleniotal). Eclogae Geol. Helv. 57 pp. 619-628.

GARWOOD, E.J. 1902 The origin of some of the hanging valleys in the Alps and Himalayas. Q.J.G.S. 58 pp. 703-715.

---------- 1906 The tarns of the Canton Ticino. Q.J.G.S. 62 pp. 165-193.

---------- 1932 Speculation and research in Alpine glaciology: an historical review. Q.J.G.S. 88 pp. 50-118.

GAY, N.C. 1966 The deformation of inhomogeneous materials and consequent geological implications. Ph.D. thesis. Univ. of London.

--------- 1968 The motion of rigid particles embedded in a viscous fluid during pure shear deformation of the fluid. Tectonophysics. 5 pp. 81-88.

GREENMAN, N.N. 1951 The mechanical analysis of sediments from thin section data. J. Geol. 59 pp. 447-462.

GRESENS, R.L. 1966 a The effect of structurally produced gradients on diffusion in rocks. J. Geol. 74 pp. 307-321.

GRESENS, R.L. 1966 b Dimensional and compositional control of garnet growth by mineralogical environment. Amer. Mineralogist. 51 pp. 524-528.

GRIGGS, D.T. and HANDIN, J. 1960 Observations on fracture and a hypothesis of earthquakes. Mem. Geol. Soc. Amer. 79 pp. 347-364.

GRIGGS, D.T., PATERSON, M.S., HEARD, H.C. and TURNER, F.J. 1960 Annealing recrystallisation in calcite crystals and aggregates. Mem. Geol. Soc. Amer. 79 pp. 21-37.

GRÜBENMANN, U. 1888 Uber die Gesteine der sedimentaren Mulde von Airolo. Mitt. Turg. natf. Ges. 8.

GRÜNENFELDER, M. 1962 Mineralalter von Gesteinen aus dem Gotthardmassiv. Schweiz. Min. Petr. Mitt. 42 pp. 6-7.

GRÜNENFELDER, M. and HAFNER, S. 1962 Uber das Alter und die Entstehung des Rotondogranits. Schweiz. Min. Petr. Mitt. 42 pp. 169-208.

GÜNTHERT, A. 1954 Beiträge zur Petrographie und Geologie des Maggia-Lappens (NW-Tessin). Schweiz. Min. Petr. Mitt. 34 pp. 1-159.

HAFNER, S. 1958 Petrographie des südwestlichen Gotthardmassivs (zwischen St. Gotthardpass und Nufenenpass) Schweiz. Min. Petr. Mitt. 38 pp. 255-362.

HALD, A. 1952 Statistical Theory with Engineering Applications. J. Wiley and Sons, New York.

HANSON, G.N., GRÜNENFELDER, M. and SOPTRAYANOVA, G. 1969 The geochronology of a recrystallised tectonite in Switzerland - The Roffna-Gneiss. Earth and Planetary Sci. Lett. 5 pp. 413-422.

HARLAND, W.B., SMITH, A.G. and WILCOCK, B. 1964 The Phenerozoic time scale. Holmes Symposium. Geol. Soc. London.

HASLER, P. 1949 Geologie und Petrographie der Sambuco-Massari-Gebirgsgruppe zwischen der oberen Valle Leventina und Valle Maggia im nördlichen Tessin. Schweiz. Min. Petr. Mitt. 29 pp. 50-155.

HAYAMA, Y. 1959 Some considerations on the colour of biotite and its relation to metamorphism. Journ. Geol. Soc. Japan. 65 pp. 21-30.

HEIM, A. 1920 Geologie der Schweiz (3 Vols. 1919-1922) Bernhard Tauchnitz Verlag Gmbh. Leipzig.

HIGGINS, A.K. 1964a Fossil remains in staurolite kyanite schists of the Bedretto-Mulde Bünderschiefer. Eclogae Geol. Helv. 57.

HIGGINS, A.K. 1964b The structural and metamorphic geology of the area between Nufenen Pass and Basodino, Tessin, Switzerland. Ph.D. thesis. Univ. of London.

HILLS, E.S. 1953 Outlines of Structural Geology. Methuen and Co. London. J. Wiley and Sons, U.S.A.

HIRTH, J.P. and POUND, G.M. 1963 Condensation and Evaporation: nucleation and growth kinetics. Progress in Materials Science. 11.

HIRTH, J.P. and MOAZED, K.L. 1967 Nucleation processes in thin film formation. Physics of Thin Films. 4 pp. 97-134.

HOBBS, B.E. 1968 Recrystallisation of single crystals of quartz. Tectonophysics 6 pp. 353-401.

HOFMÄNNER, F.J. 1964 Petrographische Untersuchung der granitoiden Gesteine zwischen Gotthard-und Witenwasserenreuss. Inaugural Dissertation, Univ. of Zurich.

HOLLOMAN, J.H. and TURNBULL, D. 1953 Nucleation. Progress in Metal Physics. 4 pp. 333-388.

HSU, L.C. 1968 Selected phase relationships in the system Al. Mn. Fe. Si. OH. A model for garnet equilibria. J. Petr. 9 pp. 40-83.

HUBER, H.M. 1943 Physiographie und Genesis der Gesteine im sudostlichen Gotthardmassiv. Schweiz. Min. Petr. Mitt. 23 pp. 72-260.

HUDLESTON, P. 1969 The morphology and development of folds. Ph.D. thesis. Univ. of London.

HULL, F.C. and HOUK, W.J. 1953 Statistical grain structure studies. Plane distribution curves of regular polyhedrons. J. Metals. 195 pp. 565-572.

HUNZIKER, J.C. 1970 Polymetamorphism in the Monte Rosa, Western Alps. Ecologae Geol. Helv. 63 pp. 151-161.

JACOBS, P.W.M., and TOMPKINS, F.C. 1955 Classification and theory of solid reactions: in, Chemistry of the Solid State. Edit. W.E. Garner. Butterworths Scientific Publications, London.

JÄGER, E. 1965 Rb-Sr age determinations on minerals and rocks from the Alps. Sciences de la Terre. 10 pp. 395-406.

--------- 1970 Rb-Sr systems in different degrees of metamorphism. Eclogae Geol. Helv. 63 pp. 163-172.

JÄGER, E. and NIGGLI, E. 1964 Rb-Sr-Isotopenanalysen an Mineralien und Gesteinen des Rotondogranites und ihre geologische Interpretation. Schweiz. Min. Petr. Mitt. 44. pp. 61-81.

JÄGER, E., NIGGLI, E. and WENK, E. 1967 Rb-Sr Altersbestimmungen an Glimmern der Zentralalpen. Beitr. Geol. Karte Schweiz, N.F. 134.

JEFFREY, G.B. 1922 The motion of ellipsoidal particles immersed in a viscous fluid. Royal Soc. Lond. Proc. 102 pp. 161-179.

JONES, K.A. and GALWEY, A.K. 1964 A study of possible factors concerning garnet formation in rocks from Ardara, Co. Donegal, Ireland. Geol. Mag. 101 pp. 76-93.

---------- 1966 Size distribution, composition and growth kinetics of garnet crystals in some metamorphic rocks from the West of Ireland. Q.J.G.S. 122 pp. 29-44.

JUNG, W. 1963 Die mesozoischen Sedimente am Sudostrande des Gotthard-Massivs (zwischen Plaun la Greine und Versam). Eclogae Geol. Helv. 56 pp. 653-754.

KELLER, F. 1968 Mineralparagenesen und Geologie der Campo Tencia-Pizzo Forno-Gebirgsgruppe. Beitr. Geol. Karte Schweiz. N.F. 135.

KÖNIGSBERGER, J. 1909 Einige Folgerungen aus geologischen Beobachtungen im Aare- Gotthard- und Tessinermassiv. Eclogae Geol. Helv. 10.

KRETZ, R. 1966a Interpretation of the shape of mineral grains in metamorphic rocks. J. Petr. 7 pp. 68-94.

--------- 1966b Grain-size distribution for certain metamorphic minerals in relation to nucleation and growth. J. Geol. 74 pp. 147-173.

KRIGE, L. 1918 Petrographische Untersuchungen im Val Piora und Umbegung. Eclogae Geol. Helv. 14 pp. 519-654.

KRUMBEIN, W.C. 1935 Thin section mechanical analysis of indurated sediments. J. Geol. 43 pp. 482-496.

KVALE, A. 1957 Gefügestudien in Gotthardmassiv und den angrenzenden Gebieten. Schweiz. Min. Petr. Mitt. 37 pp. 398-434.

--------- 1966 Gefügestudien in Gotthardmassiv und den angrenzenden Gebieten. Sonderveröffentl. Schweiz. Geotechn. und Schweiz. Geol. Komm.

LEAKE, B.E. 1964 The chemical distinction between ortho- and para-amphibolites. J. Petr. 5 pp. 238-254.

LEWIS, P.F. 1970 A report on the geological mapping of the Valle della Prosa, Val Bedretto, Ticino, Switzerland. B.Sc. thesis. Univ. of London.

LINDLEY, D.V. and MILLER, J.C.P. 1962 Cambridge Elementary Statistical Tables. Camb. Univ. Press.

LISZKAY-NAGY, M. 1965 Geologie der Sedimentbedeckung des sudwestlichen Gotthard-Massivs im Oberwallis. Eclogae Geol. Helv. 58 pp. 901-965.

MATTHEWS, J.W. 1967 Evaporated single-crystal films. Physics of Thin Films. 4 pp. 137-187.

McLEAN, D. 1965 The science of metamorphism in metals: in, Controls of Metamorphism. Edit. W.S. Pitcher and G.W. Flinn. Oliver and Boyd, Edinburgh and London.

MEHL, R.F. and DUBÉ, A. 1951 The eutectoid reaction: in Phase Transformation in Solids. Edit. R. Smoluchowski. J. Wiley and Sons, New York.

MILNES, A.G. 1969 On the orogenic history of the Central Alps. J. Geol. 77 pp. 108-112.

MIYASHIRO, A. 1951 Kyanites in druses in kyanite-quartz veins from Saihori in the Fukushinzan District, Korea. J. Geol. Soc. Japan. 57 pp. 59-63.

MOUNTENAY, S.N. 1970 Report on the geology and structure of the Alpe Massari, Ticino, Switzerland. B.Sc. thesis. Univ. of London.

MÜGGE, O. 1930 Bewegungen von Porphyroblasten in Phylliten und ihre Messung. N.J.f. Min Beil.-Bd. 61A pp. 469-520.

MULLINS, W.W. 1962 Solid surface morphologies governed by capillarity: in, Metal Surfaces. Amer. Soc. for Metals. Ohio, U.S.A.

NABHOLZ, W.K. and VOLL, G. 1963 Bau und Bewegung im gotthardmassivischen Mesozoikum bei Ilanz (Graubunden). Eclogae Geol. Helv. 56 pp. 755-808.

NANDI, K. 1967 Garnets as indices of progressive regional metamorphism. Min. Mag. 36 pp. 89-93.

NICHOLSON, R. 1966 Metamorphic differentiation in crenulated schists. Nature. 209 pp. 68-69.

NIGGLI, E. 1960 Mineral-zonen der alpinen Metamorphose in den Schweizer Alpen. 21st Int. Geol. Congress, Pt. 13 pp. 132-138.

---------- 1970 Alpine Metamorphose und alpine Gebirgsbildung. Fortschr. Min. 47 pp. 16-26.

NIGGLI, E. and NIGGLI, C.R. 1965 Karten der Verbreitung einiger Mineralien der alpidischen Metamorphose in den schweizer Alpen (Stilpnomelan, Alkali-Amphibol, Chloritoid, Staurolit, Disthen, Sillimanit). Eclogae Geol. Helv. 58 pp. 335-368.

NIGGLI, P. 1929 Die chemisch-mineralogische Charakteristik der metamorphen Paragesteinprovinz am Südrande des Gotthardmassivs. Schweiz. Min. Petr. Mitt. 9 pp. 160-187.

NIGGLI, P., PREISWERK, H., GRUTTER, O., BOSSARD, L. and KUNDIG, E. 1936 Geologische Beschreibung der Tessiner Alpen zwischen Maggia und Bleniotal. Beitr. Geol. Karte Schweiz. N.F. 71.

OBERHOLZER, J. 1955 Geologie und Petrographie des westlichen Gotthardmassivs Schweiz. Min. Petr. Mitt. 35 pp. 320-409.

OROWAN, E. 1960 Mechanism of seismic faulting. Mem. Geol. Soc. Amer. 79 pp. 323-346.

OULIANOFF, N. 1934 Massifs hercyniens du Mont Blanc et des Aiguilles Rouges. Geol. Führer der Schweiz, Fasc. 11, pp. 121-129.

PASHLEY, D.W. 1956 The study of epitaxy in thin surface films. Advances in Physics. 5 pp. 173-240.

---------- 1965 The nucleation, growth, structure and epitaxy of thin surface films. Advances in Physics. 14 pp. 327-416.

PATTERSON, M.S. and WEISS, L.E. 1966 Experimental deformation and folding in phyllite. Bull. Geol. Soc. Amer. 77 pp. 343-374.

PEACEY, J.S. 1961 Rolled garnets from Morar, Inverness-shire. Geol. Mag. 98 pp. 77-80.

POWELL, D. 1966 On the preferred crystallographic orientation of garnet in some metamorphic rocks. Min. Mag. 35 pp. 1094-1109.

POWELL, D. and TREAGUS, J.E. 1967 On the geometry of S-shaped inclusion trails in garnet porphyroblasts. Min. Mag. 36 pp. 453-456.

---------- 1970 Rotational fabrics in metamorphic minerals. Min. Mag. 37 pp. 801-814.

PREISWERK, H., BOSSARD, L., GRÜTTER, O., NIGGLI, P., KUNDIG, E. and AMBÜHL, E. 1934 Geologische Karte der Tessineralpen zwischen Maggia- und Blenio-tal. Geol. Spez. Karte Schweiz, Nr. 116.

RAGAN, D.M. 1967 Planar and layered structures in glacial ice. J. Glaciology 6 pp. 565-567.

RAMBERG, H. 1955 Natural and experimental boudinage and pinch and swell structures. J. Geol. 63 pp. 512-526.

---------- 1960 Relationships between length of arc and thickness of ptymatically folded veins. A.J.Sc. 258 pp. 36-46.

RAMBERG, H. 1961 Contact strain and folding instability in a multilayered body. Geol. Rund. 51 pp. 405-439.

---------- 1963a Evolution of drag folds. Geol. Mag. 100 pp. 97-106.

---------- 1963b Strain distribution and geometry of folds. Bull. Geol. Inst. Univ. Uppsala 42 pp. 1-20.

---------- 1964 Selective buckling of composite layers with contrasted rheological properties; a theory for simultaneous formation of several orders of folds. Tectonophysics. 1 pp. 307-341.

RAMSAY, J.G. 1960 The deformation of early linear structures in areas of repeated folding. J. Geol. 68 pp. 75-93.

---------- 1962a The geometry and mechanics of similar type folds. J. Geol. 70 pp. 309-327.

---------- 1962b Interference patterns produced by the superposition of folds of "similar" type. J. Geol. 70 pp. 466-481.

---------- 1962c The geometry of conjugate fold systems. Geol. Mag. 99 pp. 516-526.

---------- 1963 Stratigraphy, structure and metamorphism in the Western Alps. Proc. Geol. Assoc. London. 74 pp. 357-391.

---------- 1967 Folding and Fracturing of Rocks. McGraw Hill, U.S.A.

RAST, N. 1956 The origin and significance of boudinage. Geol. Mag. 93 pp. 401-408.

-------- 1958 The metamorphic history of the Schichallion complex, Perthshire. Trans. Roy. Soc. Edin. 63 pp. 413-431.

RAST, N. and STURT, B. 1957 Crystallographic and geological factors in the growth of garnets in central Perthshire. Nature. 179 p. 215.

READ, H.H. 1933 On the quartz-kyanite rocks in Unst, Shetland Islands, and their bearing on metamorphic differentiation. Min. Mag. 23 pp. 317-328.

---------- 1949 A contemplation of time in plutonism. Q.J.G.S. 105 pp. 101-156.

RICKARD, M.J. 1961 A note on cleavages in crenulated rocks. Geol. Mag. 98 pp. 324-332.

ROSSETTI, P.M. 1970 Geological report on Alpe Massari, Val Maggia, Ticino, Switzerland. B.Sc. thesis. Univ. of London.

ROYER, L. 1928 Recherches expérimentales sur l'epitaxie ou orientation mutuelle des critaux d'espèces différentes. Bull. Soc. fr. Miner. Crystallogr. 51 p. 7.

SARATOVKIN, D.D. 1959 Dendritic Crystallisation (English translation). New York.

SCHMIDT, W. 1918 Bewegungspuren in Porphyroblasten Kristalliner Schiefer. S.B. Akad. Wiss. Wien. 1 pp. 293-310.

SCHMIDT, W. and PREISWERK, H. 1908. Geol. Karte der Simplongruppe, Spezialkarte Nr. 48 mit Erläuterung.

SEIFERT, H. 1953 Epitaxy: in, Structure and Properties of Solid Surfaces. Edit. R. Gomer and C. St. Smith. Univ. of Chicago Press. Chicago.

SIBBALD, T.I.I. 1965 The geology of the Albrunpass, Switzerland and Italy. B.Sc. thesis. Univ. of Edinburgh.

SONDER, R. 1921 Untersuchungen über den Differentiationsverlauf der spätpalaeozoischen Granitintrusionen im zentralen und westlichen Gotthardmassiv. Schweiz. Min. Petr. Mitt. 1 pp. 323-391.

SPRY, A. 1963 The origin and significance of snowball structures in garnet. J. Petr. 4 pp. 211-222.

-------- 1969 Metamorphic Textures. Pergamon Press.

STEIGER, R.H. 1962 Petrographie und Geologie des sudlichen Gotthard-massivs zwischen St. Gotthard- und Lukmanierpass. Schweiz. Min. Petr. Mitt. 42 pp. 381-578.

---------- 1963a Use of K-Ar ages of hornblende for dating phases of Alpine orogeny. Geol. Soc. Amer. Program Ann. Meeting 1963.

1963b K-Ar ages of hornblendes from the southern Gotthard Massif, Switzerland. Ann. Rep. Dir. Geophys. Lab., Carnegie Inst. 1962-1963 p. 227.

---------- 1964 Dating of orogenic phases in the Central Alps by K-Ar ages of hornblende. J. Geophys. Research. 69 No. 24 pp. 5407-5421.

STONE, F.S. 1961 The kinetics and mechanisms of the reactions of solids: in, Reactivity of Solids. Edit. J.H. DeBoer. Elsevier, Amsterdam.

STURT, B.A. 1961 The Geological Structure of the area south of Loch Tummel. Q.J.G.S. 117 pp. 131-156.

TROMSDORFF, V. 1966 Progressive Metamorphose kieseliger Karbonatgesteine in den Zentralalpen zwischen Bernina und Simplon. Schweiz. Min. Petr. Mitt. 46 pp. 431-460.

TRUMPY, R. 1960 Palaeotectonic evolution of the central and Western Alps. Bull. Geol. Soc. Amer. 71 pp. 843-908.

TURNER, F.J. and VERHOOGEN, J. 1960 Igneous and Metamorphic Petrology. McGraw Hill. U.S.A.

TURNER, F.J. and WEISS, L.E. 1963 Structural Analysis of Metamorphic Tectonites. McGraw Hill. U.S.A.

Van de KAMP, P.C. 1969 The origin of amphibolites in the Beartooth Mountains, Wyoming and Montana: New data and interpretation. Bull. Geol. Soc. Amer. 80 pp. 1127-1136.

Van der MERWE, J.H. 1949 Misfitting monolayers and oriented overgrowth. Discussions of the Faraday Society. 5 pp. 201-214.

---------- 1964 Interfacial misfit and bonding between oriented films and their substrates: in, Single Crystal Films. Edits. M.H. Francombe and H. Sato. Pergammon Press.

Van der PLAS, L. 1959 Petrology of the Northern Adula Region, Switzerland. L. Geol. Mededelingen 24 pp. 418-598.

VERHOOGEN, J. 1948 Geological significance of surface tension. J. Geol. 56 pp. 210-217.

VERNON, R.H. 1968 Microstructures of high grade metamorphic rocks. J. Petr. 9 pp. 1-22.

VOLL, G. 1960 New work on petrofabrics. L'pool and Manchr. Geol. Journ. 2 pp. 503-567.

-------- 1961 Zur Frage Stofftransport auf den Korngrenzen metamorpher Gesteine. Geol. Rund. 51 pp. 375-404.

Von FRITSCH, K. 1873 Das Gotthardgebiet. Beitr. Geol. Karte Schweiz. 15.

WELLS, M.K. 1948 An account of the long field meeting held in Switzerland. Proc. Geol. Assoc. London 59 p. 181.

WENK, E. 1955 Eine Strukturkarte der Tessineralpen. Schweiz. Min. Petr. Mitt. 35 pp. 311-319.

-------- 1962 Plagicklas als Indexmineral in den Zentralalpen. Schweiz. Min. Petr. Mitt. 42. pp. 139-152.

WENK, E., SCHWANDER, H., HUNZIKER, J. and STERN, W. 1963 Zur Mineralchemie von Biotit in den Tessineralpen. Schweiz. Min. Petr. Mitt. 43 pp. 435-463.

WENK, E. and KELLER, F. 1969 Isograde im Amphibolitserien der Zentralalpen. Schweiz. Min. Petr. Mitt. 49 pp.157-198.

WETTSTEIN, A. 1886 Uber die Fischfauna des tertiären Glarner Schiefers. Schweiz Paläont. Ges. Abh. 13 pp. 1-101.

WINKLER, H.G.F. 1965 Petrogenesis of Metamorphic Rocks. Springer-Verlag Inc. New York.

WINTERHALTER, R.U. 1930 Zur Petrographie und Geologie der Ostlichen Gotthardmassivs. Schweiz. Min. Petr. Mitt. 10 pp. 38-116.

WUNDERLICH, H.G. 1958 Ablauf und Alterverhältnis der Tektonik und Metamorphose - Vorgange in Bundnerschiefern. Nordtessins und Graubundens. Nach. Akad. Wiss. Gottingen, Math-Phys. Klasse, Nr. 7 pp. 115-151.

---------- 1963 Ablauf und Alterverhältnis der postvaristischen Tetonik und Metamorphose in Westalpenbogen. Geol. en Mijnbouw. 42 pp. 155-169.

ZWART, H.J. 1960 Relationships between folding and metamorphism in the Central Pyrenees, and their chronological succession. Geol. en Mijnbouw 39 pp. 163-180.

ADDITIONAL REFERENCE

THAKUR, V. 1971 The structural and metamorphic geology of Pizzo Molare, Ticino, Switzerland. Ph.D. thesis. Univ. of London.

APPENDIX I

Unit cell sizes and refractive indices of garnets from the black garnet schist series

Spec. No.	Location (M.R.)	Unit Cell Size = a Å($\pm$0.003)	R.I. ($\pm$0.005)	$^{a}/_{R.I.}$
121	6969015580	11.593	1.797	6.452
129	6967215576	11.580	1.797	6.445
131	6965815571	11.584	1.797	6.447
134	6967715570	11.582	1.797	6.446
136	6970415574	11.593	1.797	6.452

ENCLOSURE 1

A GEOLOGICAL MAP OF THE VAL PIORA REGION, TICINO, SWITZERLAND.

SCALE 1:10,000

MESOZOIC COVER.

(a) AUTHOCHTHONOUS COVER.

JURASSIC.

Black garnet schist series.

TRIASSIC.

Quartenschiefer.

Rauhwacke, Dolomite and Gypsum.

Quartzite.

(b) ALLOCHTHONOUS COVER.

JURASSIC.

Calcareous mica schist series.

TRIASSIC.

Rauhwacke, Dolomite and Gypsum.

GOTTHARD MASSIF.

HERCYIAN INTRUSIVE ROCKS.

Lamprophyre dykes.

PRE-HERCYNIAN GRANITE GNEISS (STREIFENGNEISS.)

PRE-HERCYNIAN SEDIMENTARY AND MIXED GNEISS.

Tremola series.

Soresecia gneiss.

Corandoni zone.

Giubine series.

LUKMANIER MASSIF.

Augen gneiss (Piora type)

Orange group gneiss.

Mixed group gneiss.

Amphibolite.

Outcrop boundary.

Observed / Inferred Lithological boundary.

Slumped and broken exposure.

Strike and dip of pre-Alpine foliation.

Strike and dip of first Alpine foliation.

X 2773 Height in metres.

2400 Contour — Interval = 200 m.

703 / 151 Kilometre grid (Landeskarte der Schweiz.)

ENCLOSURE 2
First foliation trend map.
(Lago Ritom area.)

SCALE 1:10,000

Stereogram sub-areas (J,K,L, etc) are shown in Enclosure 3.

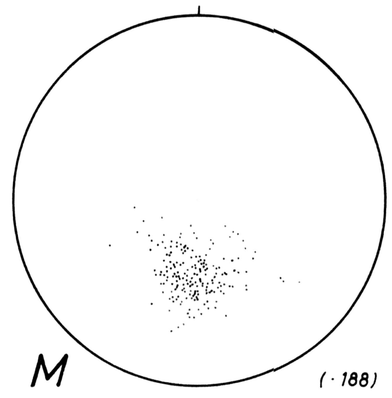

Camoghe, Alpe d'i Lago

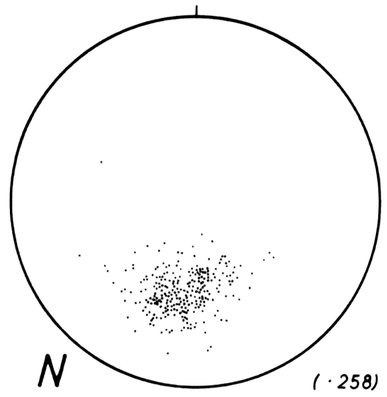

Alpe Ritom, Alpe Piora

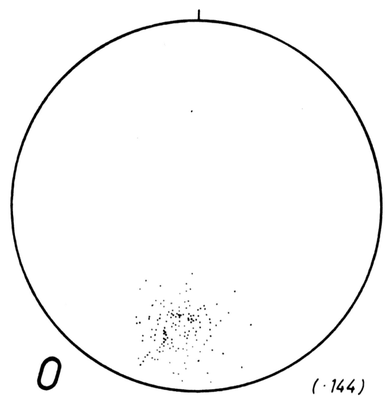

Costa Giubin, Alpe Carorescio

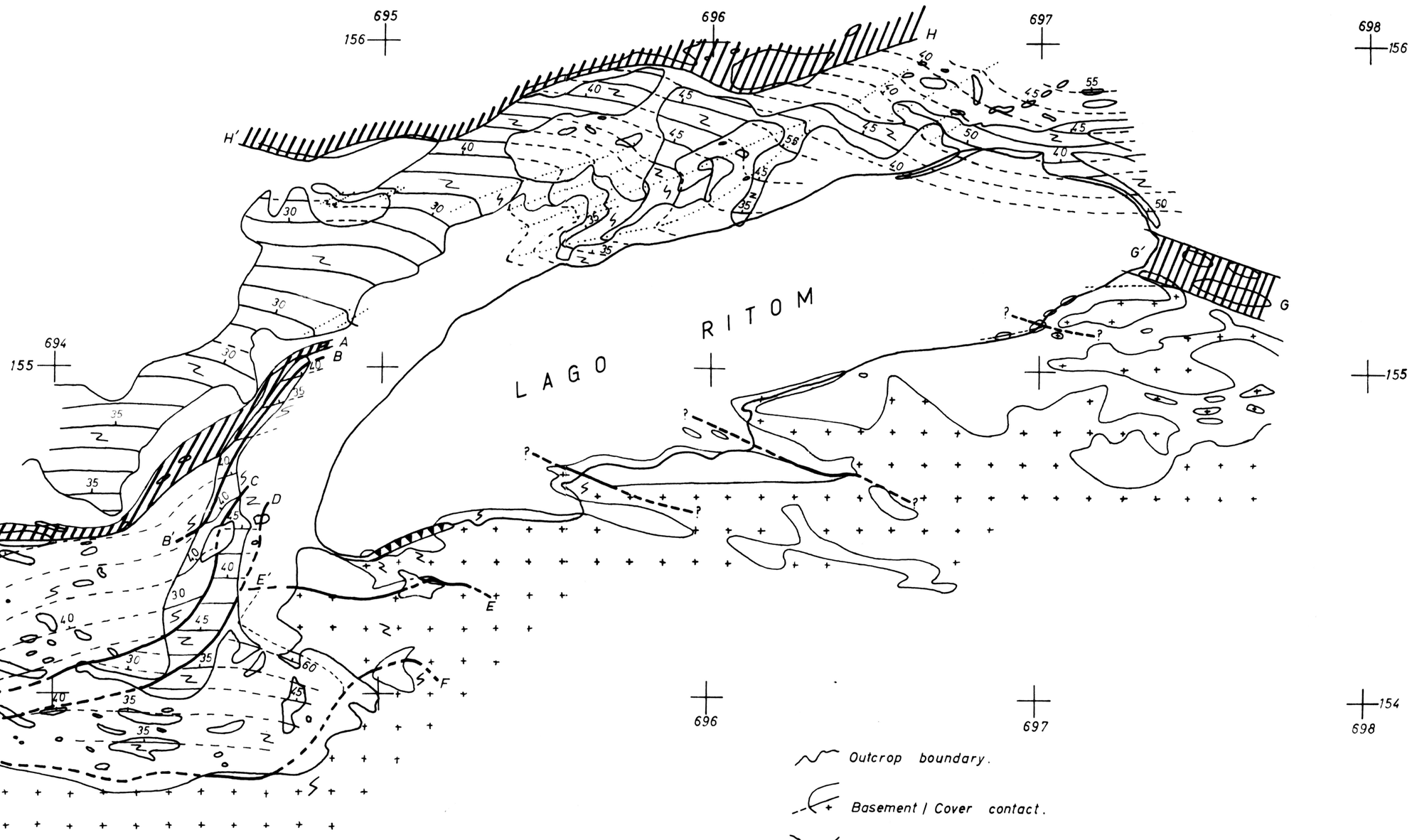

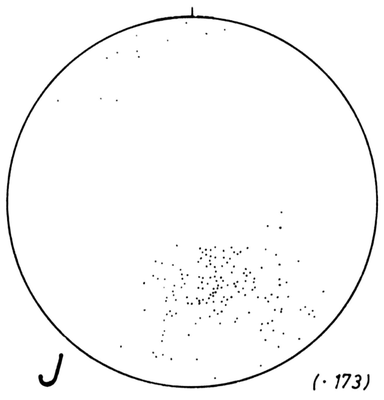

Val Canaria

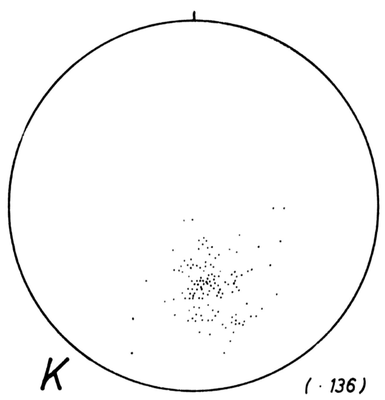

Föisc

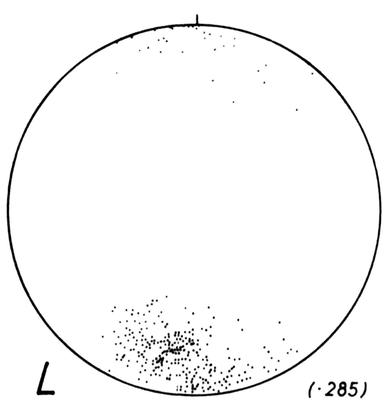

Val Leventina

Outcrop boundary.

Basement / Cover contact.

Strike and dip of first foliation.

Second fold axial trace. (S,Z, = sense of second folds.)

F Second slides.

G Second slides marked by Triassic marble horizons.

Pole to first foliation plane. (·156) Number of poles.

Mesozoic cover.

Lukmanier Massif.

SIBBALD T.I.I. 1971 D.I.C.

ENCLOSURE 3

Second foliation / second fold axial surface trend map.

SCALE 1:25,000

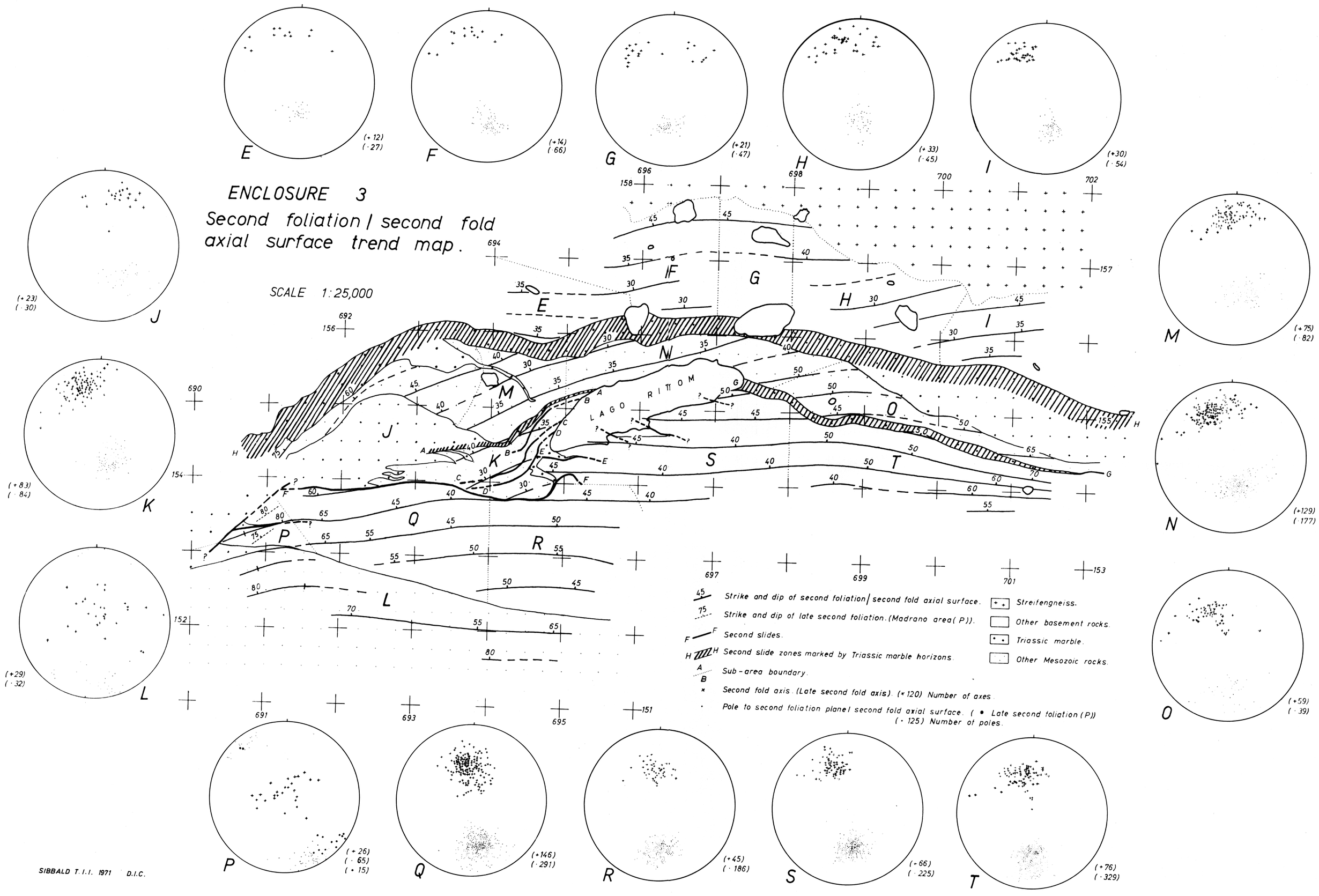

SIBBALD T.I.I. 1971 D.I.C.

ENCLOSURE 4

First generation structures in the Gotthard Massif.

SCALE 1:10,000.

Lithological boundaries.

+30 Rake isogon for quartz-felspar rodding in Streifengneiss.

Control station.

W. STRIKE E. +ve RAKE +30 -ve RAKE RODDING DIP(N.) 1st foliation surface

-34 Rake of first generation fold axis / intersection lineation.

45 Strike and dip of first foliation. (slumped)

A/B Sub-area boundary.

Pole to first foliation plane. (·135) Number of poles.

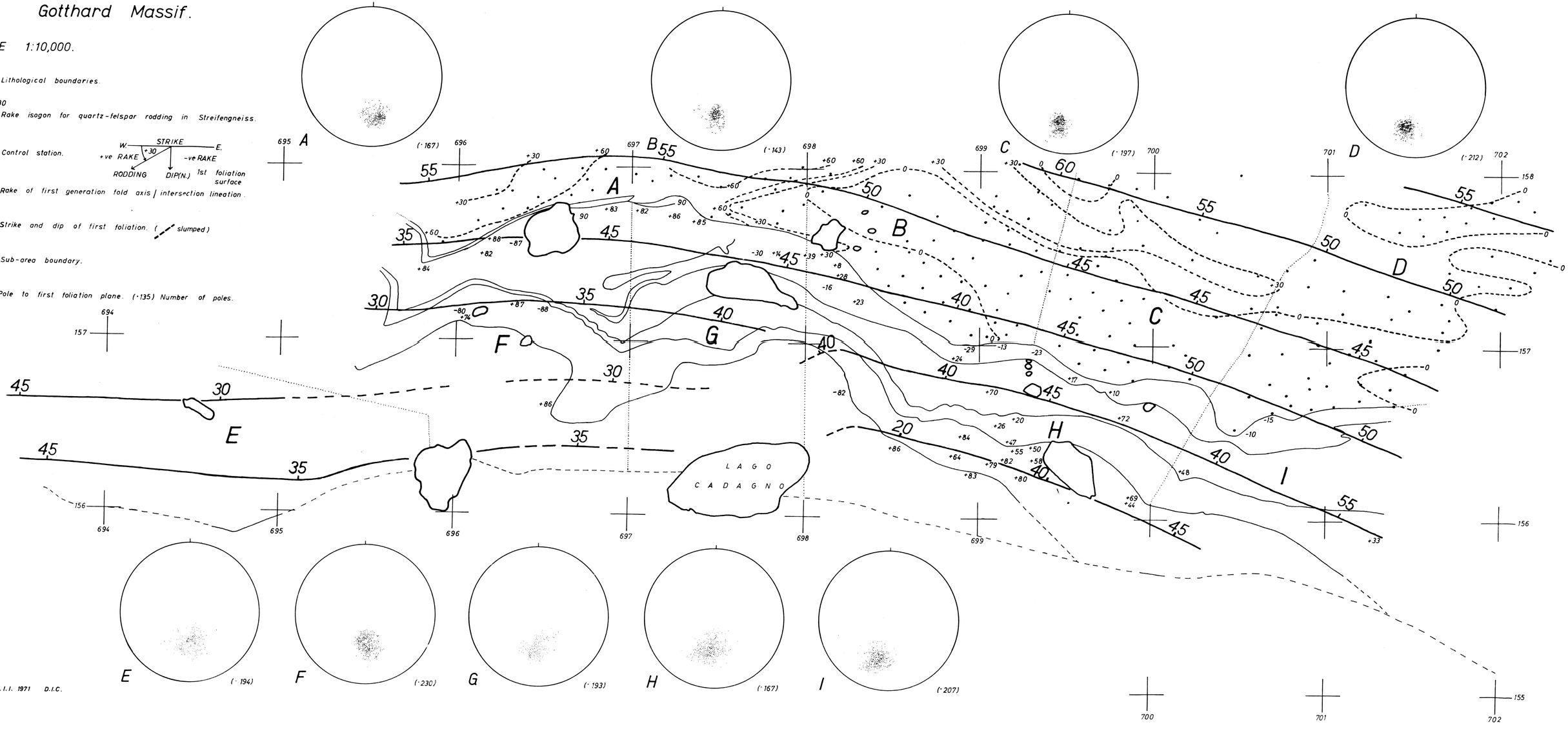

SIBBALD T.I.I. 1971 D.I.C.

ENCLOSURE 5

First (pre-Alpine) foliation trend map. (Western Lukmanier Massif.)

SCALE 1 : 10,000

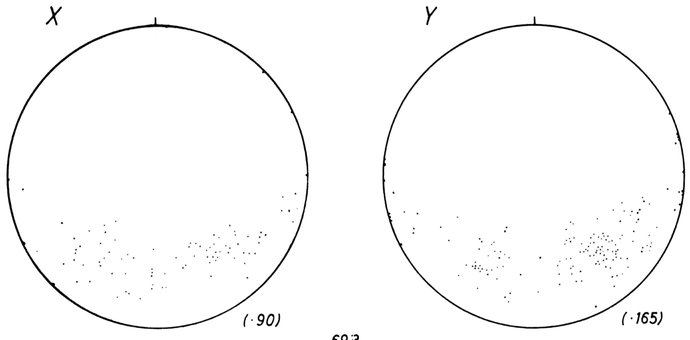

Outcrop boundary.

Basement / Cover contact.

Strike and dip of first (pre-Alpine) foliation.

Measured. Inferred (structure transposed by second foliation, or unexposed.)

Second fold axial trace. (S,Z = sense of second folds.)

Second slides.

Pole to first (pre-Alpine) foliation plane. (·160) Number of poles.

Mixed Group gneisses.

Orange Group gneisses.

Mesozoic cover.

STEREOGRAM SUB-AREAS
(West and east of co-ordinate 694)

SIBBALD T.I.I. 1971 D.I.C.

ENCLOSURE 6

Third and fourth generation structures in the Val Piora area.

Stereogram sub-areas are located on map.

- MINERAL LINEATION
+ FOURTH FOLD AXIS
● POLE TO FOURTH FOLD AXIAL SURFACE.
○ FOURTH GENERATION BOUDINAGE AXIS.
* FOURTH FOLD 'a' DIRECTION.

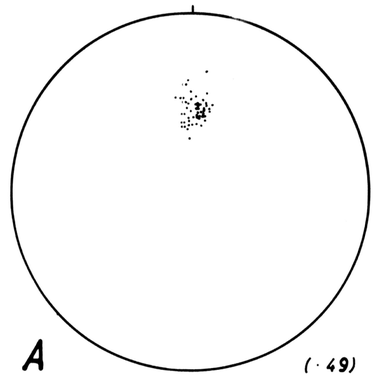
A (· 49)

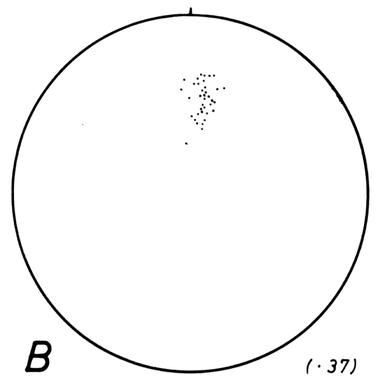
B (· 37)

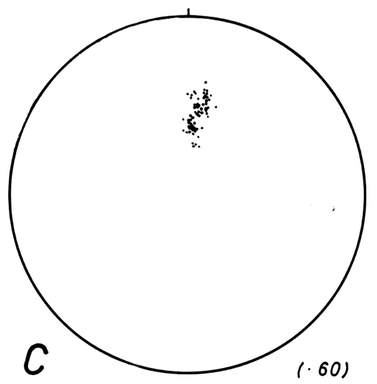
C (· 60)

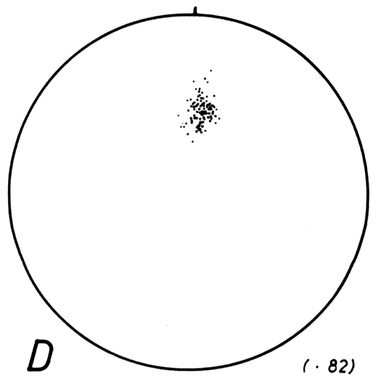
D (· 82)

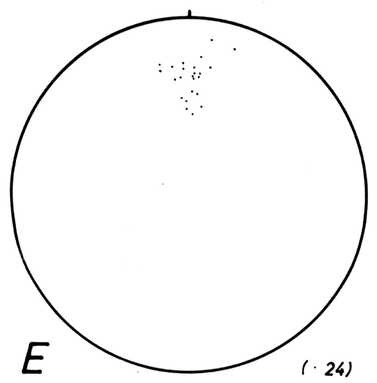
E (· 24)

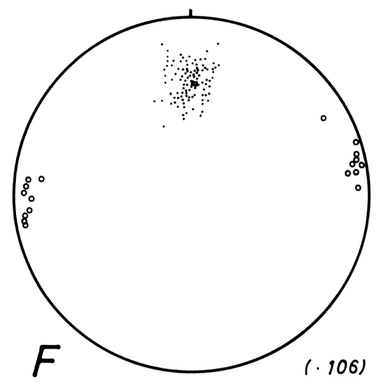
F (· 106) (∘ 18)

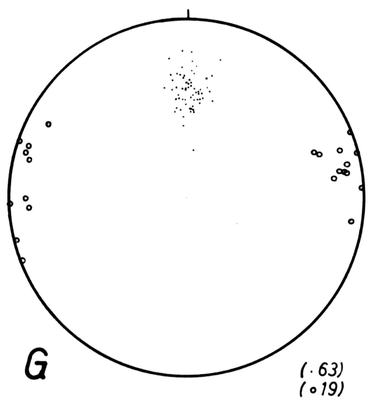
G (· 63) (∘ 19)

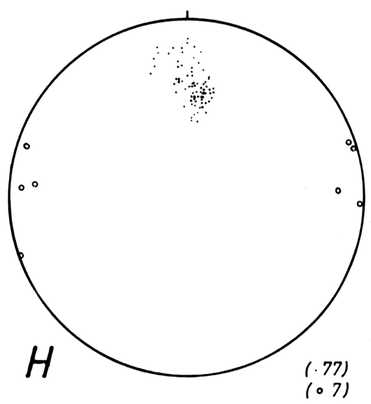
H (· 77) (∘ 7)

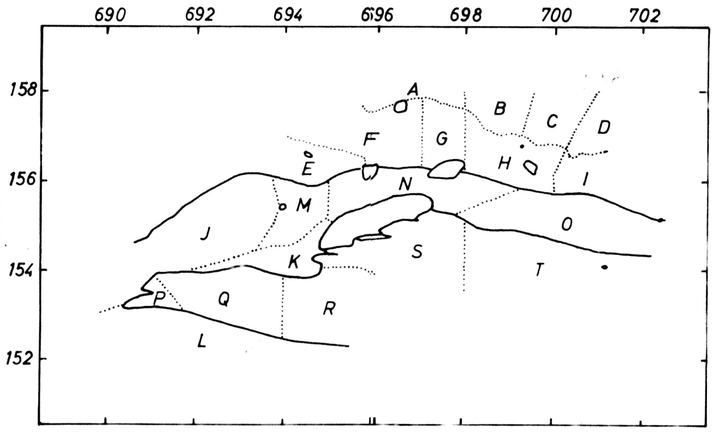

SCALE 1:100,000

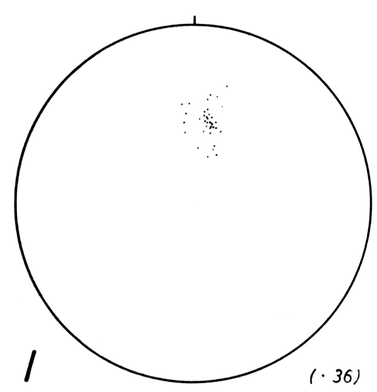
I (· 36)

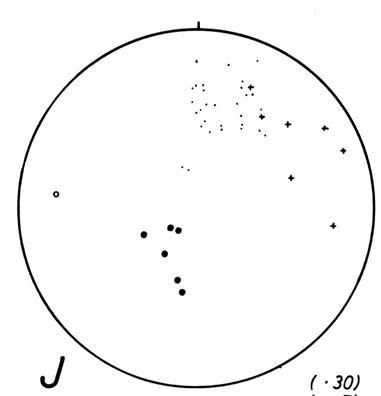
J (· 30) (+ 7) (● 6) (∘ 1)

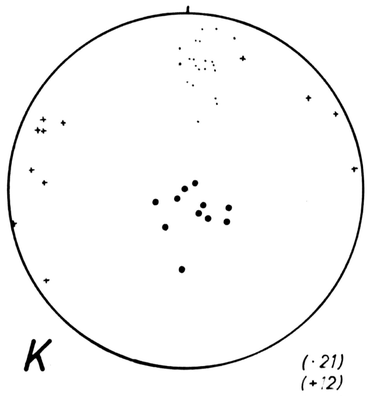
K (· 21) (+ 12) (● 11)

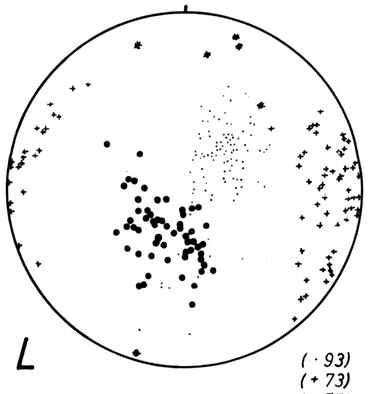
L (· 93) (+ 73) (● 57) (✱ 6)

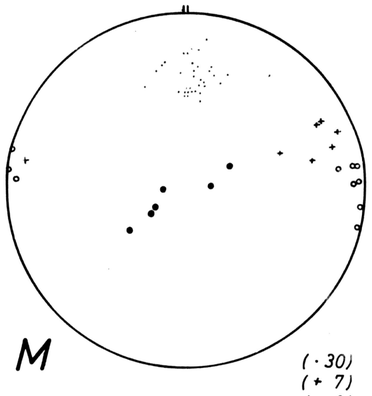
M (· 30) (+ 7) (● 6) (∘ 8)

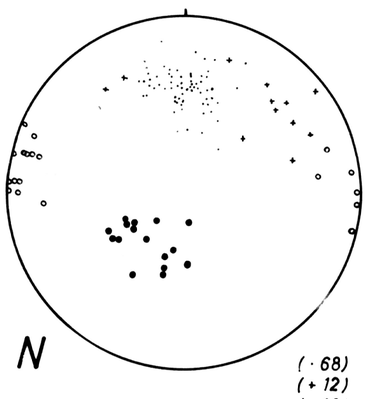
N (· 68) (+ 12) (● 16) (∘ 16)

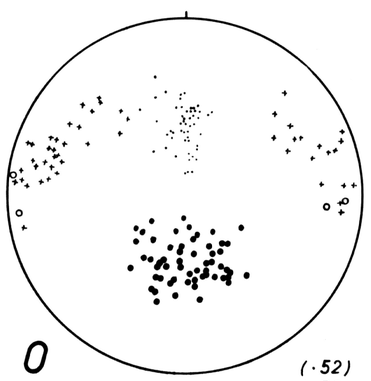
O (· 52) (+ 50) (● 58) (∘ 4)

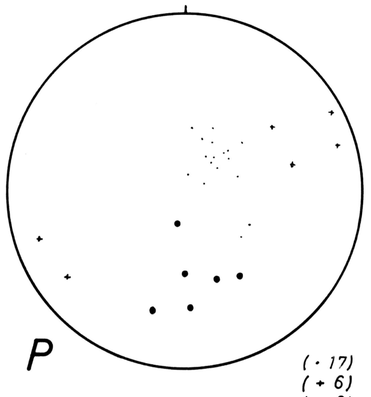
P (· 17) (+ 6) (● 6)

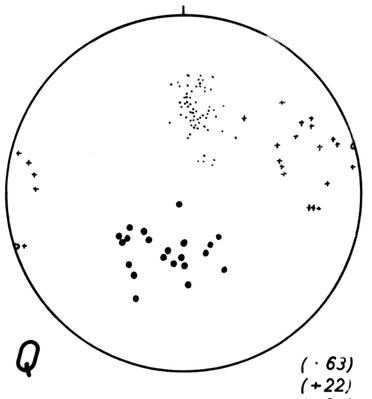
Q (· 63) (+ 22) (● 21) (∘ 1)

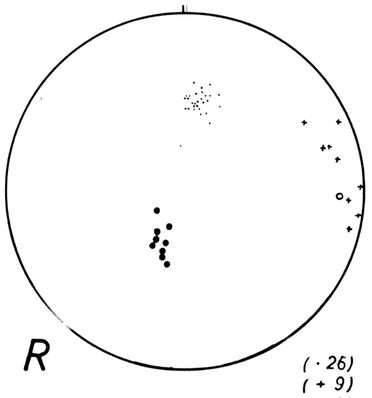
R (· 26) (+ 9) (● 9) (∘ 1)

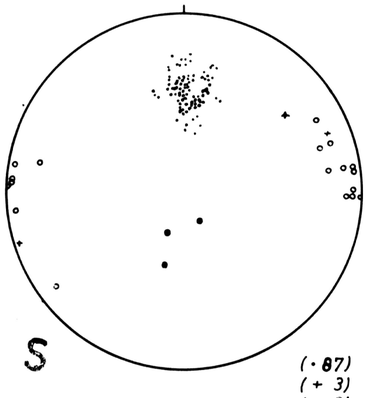
S (· 87) (+ 3) (● 3) (∘ 17)

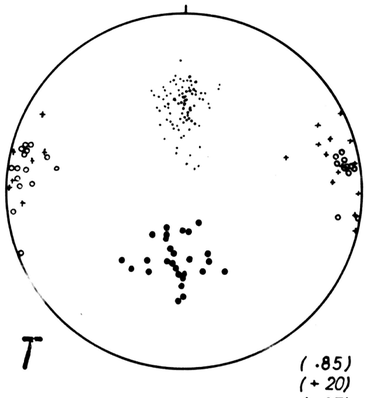
T (· 85) (+ 20) (● 27) (∘ 26)

SIBBALD T.I.I. 1971
D.I.C.